João Daniel da Silva Seixas

Development of CO-Releasing Molecules for the Treatment of Inflammatory Diseases

Dissertation presented to obtain a Ph.D. degree in Chemistry
at the Instituto de Tecnologia Química e Biológica da Universidade Nova de Lisboa

Instituto de Tecnologia Química e Biológica
Universidade Nova de Lisboa

João Daniel da Silva Seixas

Development of CO-Releasing Molecules for the Treatment of Inflammatory Diseases

Dissertation presented to obtain a Ph.D. degree (Doutoramento) in Chemistry at the Instituto de Tecnologia Química e Biológica da Universidade Nova de Lisboa

Academic Supervisor: Prof. Carlos C. Romão

Company Supervisor: Dr. Nuno Arantes e Oliveira

This Thesis was financially supported by Fundação para a Ciência e Tecnologia, European Social Fund grant number SFRH/BDE/15501/2004 and ALFAMA – Research and Development of Pharmaceutical Drugs Ltd.

FCT Fundação para a Ciência e a Tecnologia
MINISTÉRIO DA CIÊNCIA, TECNOLOGIA E ENSINO SUPERIOR

Instituto de Tecnologia Química e Biológica
Universidade Nova de Lisboa

First Edition: October 2010
Second Edition: January 2011

Cover Picture:

Design by Sérgio Costa.
Molybdenum hexacarbonyl crystals purified by sublimation. Crystals obtained by the author.
Compound ALF001 from ALFAMA"s portfolio

Agradecimentos

Em primeiro lugar queria expressar o meu profundo agradecimento à ALFAMA, por me ter dado a oportunidade de realizar o Doutoramento na empresa e por me ter apoiado e dado todas as condições para o efectuar.

Ao Nuno Arantes-Oliveira, CEO da Alfama, por ter acreditado em mim e me ter proporcionado as condições necessárias para o meu crescimento profissional e científico. Pela sua capacidade muito especial de gerir pessoas e conciliar opiniões diversas, fazendo-nos sentir que somos parte fundamental no desenvolvimento e crescimento da empresa.

Ao meu orientador, o Prof. Carlos Romão por ter sido o meu mentor desde o início da minha carreira cíentifica, por ter podido sempre contar com o seu apoio, incentivo, boa-disposição e pelas largas horas passadas em profícuas discussões cíentificas que não raras vezes ultrapassavam o âmbito da Ciência e se estendiam a outras areas de interesse, bem diversificadas.

À minha "família cíentifica" da Alfama. Aos colegas de laboratório, passados e presentes, Ana Gorgulho, Ana Margarida (Maggie), Ana Rita, Bruno Guerreiro, Catarina Rodrigues, Filipa Cruz, Gonçalo Bernardes, José Fernandes, Lukas Kromer, Marta Norton de Matos, Nuno Penacho, Sandra Rodrigues e Vasco Romão. Obrigado por terem contribuido para um ambiente de trabalho espectacular, com boa disposição e regado com doses q.b de maluqueira! Além de fazerem com que ir trabalhar todos os dias fosse um prazer, esta Tese tem um bocadinho de todos vocês por isso Muito Obrigado!

Ao nosso *team* do outro lado do Atlântico Leo Otterbein, Sherrie Otterbein, Dave Gallo and Rachel Ruggieri e sem esquecer o *Chairman* Stan Kugell, thank you all!

À Agnes Lopes (*Services Manager*) e Catarina Chaves (*Administrative Assistant)* que com o seu trabalho nos permitem fazer Ciência sem nos preocuparmos com toda a burocracia que a rodeia.

Aos cientistas "séniores" da Alfama – Werner Haas e Jan Andersson – que me fizeram olhar para a Biologia com outros olhos e perceber que a Química era muito mais interessante quando aliada a esta.

Ao Walter Blättler, que em pouco tempo conseguiu "revolucionar" a minha maneira de pensar e por ter contribuido para o meu crescimento como cientista.

No ITQB, um obrigado especial ao Prof. Miguel Teixeira pela ajuda com os estudos de EPR. Obrigado também aos restantes colegas, em especial aos "vizinhos" do 7º piso, que fazem deste Instituto um sítio onde dá gosto trabalhar.

Em especial à São, por nunca ter sido só um serviço (de análise elementar) mas sempre um ponto de apoio, fonte de boa disposição e amizade ao nosso dispor!

À Isabel Tomaz (que entretanto viajou do IST para a Faculdade de Ciências), pela grande ajuda e sugestões que deu na interpretação dos resultados de Dicroísmo Circular.

Aos meus amigos de sempre, que sempre souberam compreender e desculpar a minha ausência em períodos mais complicados. As verdadeiras amizades são assim, não precisam de explicações e tudo se resolve com um beijo e um abraço…

E por fim, o mais importante:

À minha namorada, a Sandra, por me ter sempre apoiado e pela paciência e compreensão inesgotável mesmo quando eu deixava a nossa casa de pernas para o ar com artigos e papelada espalhada em todo o lado!

À minha família "verdadeira" por todo o apoio e carinho e a quem devo aquilo que sou: à minha mãe e ao Luis Filipe, à Tia Aurora, Tio Luis, Ricardo e Carolina OBRIGADO por serem o meu suporte para tudo na vida.

Obrigado a todos!

Summary

Carbon Monoxide, CO, has been recognized as an endogenously produced, potent biological mediator involved in many defense mechanisms both in physiologic and pathologic situations. As a result of these signaling processes, CO possesses a strong therapeutic potential on a wide range of disease indications. However, the hardly avoidable safety and practical problems associated with therapeutic inhalation of toxic CO gas, led to the search for molecules capable of delivering CO to tissues in a living organism in a controlled and therapeutically useful manner. From all the areas of the chemical space where such CO-Releasing Molecules (CO-RMs) can be found, Metal Carbonyls Complexes (MCCs) seems to be the most versatile.

It is the purpose of this Thesis to provide an extensive characterization of the behavior of MCCs in the presence of biological molecules and media, in order to identify the chemical and structural parameters that are more relevant to define the profile of a therapeutically effective metal-based CO-RM drug.

In pharmacological terms, CO-RMs are prodrugs which carry and appropriately deliver molecular CO as the therapeutically active principle. This delivery requires the chemical decomposition of the CO-RM. Such decarbonylation is triggered by an interaction of the CO-RM with the biological entity or medium. Ideally, a CO-RM should be targeted to the diseased tissue or organ in order to minimize its effective dose and prevent toxicity issues resulting from the indiscriminate, non-specific release of CO in the organism. Therefore, targeting of the CO-RM is largely dependent on the matching between the chemistry of decarbonylation and the chemical properties of the tissue or organ where it should take place, to produce the desired therapeutic effect.

As mentioned above, MCCs were selected as the most versatile molecular structures that can provide controlled, targeted CO delivery because of their ease of decarbonylation compared to other organic functionalities. To give a meaning to the words “controlled, targeted CO delivery” it will be necessary to adjust and

tune the nature of both the inner coordination sphere of the MCC (wherefrom CO will have to be released), and the nature of the outer sphere made up by the distal substituents appended to the ligands which will mediate the interaction between the CO-RM and the biological environment.

However, the anticipated complexity of such a delivery process, together with the fact that at the outset of this work extremely little was known about the interaction between MCCs and biological molecules and systems, required a stepwise approach towards the understanding of the chemistry of MCCs in such biological media.

The starting point is the unavoidable need of establishing the "islands of stability" of MCCs in the aqueous, aerobic solutions that are needed for administration to living species. It is very loosely assumed by the chemical community that the vast majority of MCCs, that are metal complexes in low oxidation states, are unstable in air and water. In practice, very few such complexes have been manipulated in aqueous, oxic conditions and very little is indeed known about their actual stability under such conditions. Regardless of mechanistic details to be discussed later, CO release results from the decarbonylation of the MCC dissolved in the biological medium. Initially in solution, free molecular CO gas can later escape (diffuse) to the headspace of the *in vitro* experimental setup. Using a simple gas chromatography method, Chapter II describes the screening of the CO release profile (extension and rate) of a large variety of organometallic carbonyls dissolved in biologically relevant media/conditions. This mode of CO release is called *spontaneous* because it ensues after simple dissolution in the biological medium at 37°C under air and in the dark. Most compounds tested were octahedral carbonyl complexes and cyclopentadienyl containing carbonyl complexes all of which with 18-electron configurations. The compounds are based on Mo^0, Mo^{II}, Mn^I, Fe^{II} and Ru^{II} with classical, N, O, P and S-donor ligands or alkyl, acyl and halides. All the Mo^0 compounds, ionic or neutral, showed a high rate of CO dissociation unless a strong π acceptor like cyanide or phosphines is present as co-ligand. On the contrary, their Mn^I counterparts do not release CO

at high rates unless an halide (preferentially Cl^-) is coordinated to the metal. Most of the Fe^{II} and Ru^{II} compounds tested do not release CO in the conditions studied. The influence of pH and O_2 was also evaluated for a set of Mo^0 ionic compounds and it was established that O_2 is the main trigger to promote CO release from these complexes, leading to the formation of hydroxyl radical, which was detected by ESR. The most remarkable fact was that ca. 2/3 of the compounds tested only released between 0-9% of their total CO contents. Unexpectedly, the common idea that MCCs are unstable in air and water is largely wrong. The need to study the influence of pH derives from the need to see which CO-RMs are able to resist the acidic environment of the stomach which is a determinant piece of information for developing orally available CO-RMs. Moreover, acid sensitive CO release may be particularly useful when driven to happen in the cellular lyzosome following drug internalization through the cell membrane.

Since the most prominent biological activity of CO is anti-inflammatory, useful CO-RMs should be targeted to inflamed tissues. Such tissues are rich in reactive oxygen species (ROS), and therefore, the use of CO-RMs that are specifically activated by ROS inside cells or in the intercellular space seems a reasonable and promising strategy for targeting CO-RMs. Presently, very little is known about the reactivity of organometallic carbonyls under any of these conditions. Chapter III describes our studies on this type of CO release profile and concludes that: the concept of oxidatively triggered CO release is valid for the overwhelming majority of MCCs tested; this oxidation can be tuned by the choice of ancillary ligands and the nature of the particular ROS (H_2O_2 or ROOH), and that ROS can activate air stable MCCs turning them into active CO-RMs.

The specific mechanisms through which CO exerts its biological activity are still not fully understood but is generally accepted that heme-proteins are the main targets (if not the only) for the molecule in the organism. In Chapter III the rate of CO release from several MCCs to Myoglobin (Mb) is evaluated by incubating them with deoxy-Mb and following the rise of carboxy-myoglobin (CO-Mb). The $Ru^{II}(CO)_3Cl(X)L$ complexes present the fastest rates of formation of CO-Mb

although they do not release CO to the headspace of their solutions. This effect was named *CO donation*. Since MCCs are rather reduced, electron-rich species, they may engage in electron transfer processes with redox active proteins, namely Myoglobin or Cytochrome C. A selected group of MCCs was also used to survey this issue. Most of the compounds tested do not interfere with the redox state of heme-proteins but almost all the Mo(0) complexes are strongly reducing agents and this reduction is accompanied by CO transfer to the reduced Myoglobin to give CO-Mb. This activity extends to Hemoglobin (Hb). Since animals have a natural protection against high levels of CO, hemoglobin, the efficiency of the CO delivery process requires that the CO-RM remains intact in the blood circulation. Otherwise, Hb will scavenge free CO from the blood stream and transport it to the lungs where it will be exhaled. The first studies of the behavior of MCCs and CO-RMs in blood that we know of, revealed that most CO-RMs do not release CO to the erythrocytes, but those that do, are fully decarbonylated within a few minutes. In fact, CO release from most Mo^0 CO-RMs is much, much faster in blood than in any other medium tested, including ROS rich media. We conclude that kinetic stability towards CO substitution is necessary to achieve stability of CO-RMs in blood. Ease of oxidation can be additive to substitutional lability but is not the key factor to determine stability of transition metal CO-RMs in blood.

At the time this Thesis was initiated, very little work had been published on the therapeutic activity of CO-RMs. The most promising results were obtained with two Ruthenium complexes – CORM-2 and CORM-3. Chapter V focus the attention on the development of a new series of Ru-based CO-RMs of the general formula $Ru(CO)_3Cl_2L$, where L is a ligand with a N-, O-, P- or S- donor atom. None of the compounds releases CO to the headspace of the GC apparatus but all are able to transfer CO to deoxy-Mb. Interestingly, it was possible to show that the amount of CO transferred can be tuned by the nature of L: from 0.2 equiv. (when L is a strong ligand) to 1 equiv. CO (when L is a weak ligand).

The interaction between drugs and plasma proteins is one of the key aspects that determine their pharmacological activity. The metabolic stability, half-life and

pharmacokinetic profile are just some of the parameters that may be determined by the degree of interaction of a given drug with the several proteins. Essentially nothing was known at the outset of this work with regard to the interaction of plasma proteins with MCCs. In Chapter VI some exploratory studies using Circular Dichroism and Absorbance Spectroscopy techniques are presented, which aim to that determine the interaction between CO-RMs and the plasma proteins Albumin and Transferrin. Although observed for all complexes with substitutionally labile ancillary ligands it is not possible to ascertain the molecular aspects of such interactions from the data available.

From all this work it can be concluded that MCCs are a suitable source of CO-RMs because they can be tuned to resist attack by water, air and blood and, therefore, may be equipped with the necessary properties to be administered to a living animal to deliver CO in a controlled, targeted fashion.

Resumo

O Monóxido de Carbono, CO, tem sido reconhecido como potente mediador biológico produzido endogenamente e envolvido em diversos mecanismos de defesa tanto em situações fisiológicas como patológicas. Como resultado destes processos de sinalização o CO possui um forte potencial terapêutico numa vasta gama de doenças. No entanto, é dificil contornar os problemas de segurança e questões práticas associadas à administração por inalação deste gás tóxico, o que desencadeou a procura de moléculas capazes de distribuir CO aos tecidos de um organismo vivo de um modo controlado e terapêutico. De todas as áreas do espaço químico onde tais Moléculas Libertadoras de CO (ML-CO) podem ser encontradas, os Complexos Metálicos de Carbonilos (CMCs) parecem ser os mais versáteis.

O objectivo desta Tese é fornecer uma caracterização extensiva do comportamento dos CMCs na presença de moléculas e meios biológicos, de modo a identificar os parâmetros químicos e estruturais mais relevantes para definir o perfil de uma droga tipo ML-CO com acção terapêutica.

Em termos farmacológicos, as ML-CO são pró-drogas que carregam e distribuem CO molecular como o princípio activo terapêutico. Esta distribuição requer a decomposição química da ML-CO. Tal descarbonilação é despoletada por uma interacção da ML-CO com a entidade ou meio biológico. Idealmente, uma ML-CO deve ser dirigida para um tecido ou orgão doente de modo a minimizar a sua dose efectiva e prevenir a toxicidade resultante de uma libertação de CO indiscriminada e não específica no organismo. Portanto, o direccionamento da ML-CO depende da semelhança entre as condições em que ocorre a química da descarbonilação e as propriedades químicas do tecido ou orgão onde deve ocorrer para produzir o desejado efeito terapêutico.

Como mencionado acima, os CMC foram escolhidos como as estruturas moleculares mais versáteis que permitem distribuir CO de forma controlada e direccionada devido à sua facilidade de descarbonilação quando comparada com

outras funcionalidades orgânicas. Para dar um significado à expressão "distribuição controlada e direccionada de CO" é necessário ajustar e afinar ,tanto a esfera de coordenação interna do CMC (de onde o CO irá ser libertado) como a natureza da esfera externa, constituída pelos substituintes nos ligandos que irão mediar a interacção entre a ML-CO e o ambiente biológico.

No entanto, a complexidade de tal processo de distribuição, juntamente com o facto de no início deste trabalho, muito pouco ser conhecido sobre a interacção entre CMCs e moléculas e sistemas biológicos, forçou a que se efectuasse uma abordagem faseada de modo a entender a química dos CMCs em meio biológico.

O ponto de partida é a inevitável necessidade de identificar "ilhas de estabilidade" dos CMCs em soluções aquosas, aeróbias necessárias para a administração a seres vivos. É vagamente assumido pela comunidade química que a grande maioria dos CMCs, que são complexos metálicos em baixos estados de oxidação, são instáveis ao ar e na água. Na prática, muito poucos desses complexos foram manuseados em condições aquosas, oxigenadas e muito pouco se sabe de facto sobre a sua verdadeira estabilidade nas referidas situações. Independentemente de detalhes mecanísticos que serão discutidos à frente, a libertação de CO resulta da descarbonilação do CMC dissolvido no meio biológico. Inicialmente em solução, o CO gás livre pode escapar (difundir) para a fase gasosa do *apparatus* experimental *in vitro*. Usando um método simples de cromatografia gasosa, (CG) o capítulo II descreve o escrutínio dos perfis de libertação de CO (quantidade e velocidade) de uma grande variedade de complexos de carbonilos organometálicos dissolvidos em meio/condições biológicas relevantes. Este modo de libertação de CO é denominado *espontâneo* pois ocorre após dissolução no meio biológico a 37ºC, ao ar e no escuro. A maioria dos compostos testados são complexos carbonílicos octaédricos e complexos carbonílicos contendo o ligando ciclopentadienilo, todos com configuração electrónica de 18 electrões de valência. Os compostos são baseados em Mo^{0}, Mo^{II}, Mn^{I}, Fe^{II} e Ru^{II} com ligandos clássicos com átomos doadores N, O, P e S ou ligandos alquilo, acilo e halogenetos. Todos os compostos de Mo^{0}, iónicos ou neutros, mostraram uma grande taxa de

dissociação de CO, a não ser que os co-ligandos sejam fortes aceitadores π como cianeto ou fosfinas. Pelo contrário, os compostos de Mn^{I} não libertam CO em grande quantidade a não ser que um halogeneto (preferencialmente Cl^{-}) esteja coordenado ao metal. A maior parte dos compostos de Fe^{II} e Ru^{II} testados não libertam CO nas condições estudadas.

A influência do pH e O_2 também foi avaliada para um grupo de compostos iónicos de Mo^{0} e foi concluído que o O_2 é o principal estímulo para promover libertação de CO destes complexos, levando à formação do radical hidroxilo, que foi detectado por Ressonância Electrónica Paramagnética.

O facto mais impressionante é que ca. de 2/3 dos compostos testados apenas libertaram 0-9% do total de CO possível. Inesperadamente, a ideia comum de que os CMC são instáveis ao ar e água parece estar errada. A necessidade do estudo da influência do pH advém da necessidade de perceber que ML-CO são capazes de resistir ao ambiente acídico do estômago, que é uma informação vital para o desenvolvimento de ML-CO para administração oral. Mais ainda, a libertação de CO catalizada em meio acído pode ser útil se acontecer no lisossoma após internalização da droga através da membrana celular.

Uma vez que o efeito biológico mais proeminente do CO é a sua acção anti-inflamatória, ML-CO úteis devem ser direccionadas para tecidos inflamados. Tais tecidos são ricos em espécies reactivas de oxigénio (ERO) e portanto o uso de ML-CO que sejam especificamente activadas por ERO dentro das células ou no espaço intercelular parece ser uma estratégia razoável e promissora para direccionamento das ML-CO. Presentemente, muito pouco se sabe acerca da reactividade dos complexos organometálicos contendo carbonilos, nestas condições. No Capítulo III descrevem-se os estudos deste tipo de perfil de libertação de CO e conclui-se que o conceito de libertação de CO por estímulo oxidativo é válido para a grande maioria dos CMC testados; esta oxidação pode ser afinada pela escolha dos ligandos auxiliares e pela natureza da ERO (H_2O_2 ou ROOH), e ainda que as ERO podem activar CMCs estáveis ao ar tornando-os ML-CO activas.

Os mecanismos específicos pelos quais o CO exerce a sua actividade biológica ainda não estão totalmente compreendidos, mas é geralmente aceite que as proteinas hémicas são o principal alvo (se não o único) para o CO no organismo. No Capítulo IV a taxa de libertação de CO de diversos CMCs para a Mioglobina (Mb) é avaliada por incubação destes com deoxi-Mb e seguindo a formação de carboxi-mioglobina (CO-Mb).

Os complexos $Ru^{II}(CO)_3Cl(X)L$ apresentam as mais rápidas taxas de formação de CO-Mb apesar de não libertarem CO para a fase gasosa das suas soluções. Este efeito foi denominado de *doacção* de CO. Uma vez que os CMCs são espécies reduzidas, ricas em electrões, podem participar em processos de transferência electrónica com proteínas com actividade redox, nomeadamente Mb ou Citocromo C. Um grupo selecccionado de CMCs foi também usado para abordar este processo. A maioria dos compostos testados não interfere com o estado redox das proteinas hémicas mas quase todos os complexos de Mo^0 são fortes agentes redutores e esta redução é acompanhada pela transferência de CO para a Mioglobina reduzida originando CO-Mb. Esta actividade é extensivel à Hemoglobina. Uma vez que os animais têm uma protecção natural contra níveis elevados de CO, a hemoglobina, a eficácia do processo de distribuição de CO necessita que a ML-CO permaneça intacta na circulação sanguínea. De outro modo a hemoglobina irá capturar o CO livre na corrente sanguínea e transportá-lo ao pulmões onde será expelido.

Ao efectuar os primeiros estudos conhecidos sobre o comportamento de ML-CO no sangue, mostrou-se que a maioria das ML-CO não libertam CO para os eritrócitos mas os que o fazem, são completamente descarbonilados em poucos minutos. De facto, a libertação de CO da maioria das ML-CO de Mo^0 é muito mais rápida no sangue do que em qualquer outro meio testado, incluindo meios ricos em ERO. Conclui-se que a estabilidade cinética em torno da substituição de CO é necessária para obter estabilidade das ML-CO no sangue. A oxidação pode ser um processo adicional à labilidade substitucional, mas não é o factor-chave para determinar a estabilidade da ML-CO no sangue.

À altura do início desta Tese, muito pouco trabalho tinha sido publicado sobre a actividade terapêutica das ML-CO. Os resultados mais promissores tinham sido obtidos com 2 complexos de Ruténio – CORM-2 e CORM-3. No Capítulo V, foca-se a atenção no desenvolvimento de uma nova série de ML-CO baseadas em Ruténio, de forma geral $Ru(CO)_3Cl_2L$ em que L é um ligando com átomo doador N-, O-, P- ou S. Nenhum dos compostos liberta CO para a fase gasosa do *apparatus* experimental de CG, mas todos são capazes de o transferir para a deoxi-Mb. Curiosamente, foi possível demonstrar que a quantidade de CO transferido pode ser ajustada pela natureza de L: desde 0.2 equiv. CO (quando L é um ligando forte) até 1 equiv. CO (quando L é um ligando fraco).

A interacção entre drogas e proteínas do plasma é um aspecto-chave que determina a sua acção farmacológica. A estabilidade metabólica, tempo de meia-vida e perfil de fármaco-cinética são apenas alguns dos parâmetros que podem ser modelados pelo grau de interacção de uma determinada droga com diversas proteínas. No início deste trabalho muito pouco era conhecido a respeito da interacção de proteínas do plasma com CMCs. No capítulo VI, são apresentados alguns estudos exploratórios recorrendo a técnicas de Dicroísmo Circular e Espectroscopia de Absorção que pretendem determinar a interacção entre ML-CO e as proteínas do plasma Albumina e Transferrina. Apesar de tais interacções terem sido observadas para todos os complexos com co-ligandos lábeis, não foi possível determinar os aspectos moleculares envolvidos a partir dos dados disponíveis.

De todo este trabalho pode-se concluir que os CMCs são uma fonte viável de ML-CO pois podem ser modificadas para resistir a àgua, ar e sangue e portanto, capazes de serem munidos das propriedades necessárias para serem administrados a um ser vivo, de modo a distribuir CO de forma controlada e direccionada.

List of Abbreviations:

Ac	acetyl
acac	acetylacetonate
ADME	absorption, distribution, metabolism and excretion
AIP	Alfama's Intelectual Property
AUC	area under curve
bipy	bipyridyl
BMPO	5-*tert*-butoxycarbonyl 5-methyl-1-pyrroline N-oxide
bpa	N-(*p*-carboxy-benzyl)bis(2-picolyl)amine
Bu	butyl
BSA	Bovine Serum Albumin
bw	body weight
CD	Circular Dichroism
CDs	cyclodextrins
choline	*N,N,N* – trimethylammonium cation
CHT	1,3,5-cycloheptatriene
cit	Citrate
CMT	cyclopentadienyl manganese tricarbonyl
CO	carbon monoxide
CO-Hb	carboxy-hemoglobin
CO-RM	CO releasing molecule
Cp	cyclopentadienyl
Cp*	pentamethylcyclopentadienyl
Cp'	general abbreviation for a substituted Cp ring
Cy	cyclohexyl
Cyst	Cysteine
Cyt	Cytochrome
DAB	1,4 – diazabutadiene
DAPTA	3,7-diacetyl-1,3,7-triaza-5-phosphabicyclo[3.3.1]nonane
detpa	diethylenetriaminepentaacetate

DMSO	dimethylsulfoxide
E.A.	elemental analysis
Equiv.	equivalent
ESI-MS	electrospray ionization Mass Spectrometry
ESR	Electron Spin Resonance (Spectroscopy)
Et	ethyl
fac	facial
FBS	Fetal Bovine Serum
FID	Flame Ionization Detector
GABA	γ-aminobutyric acid
Gal-S-Me	methyl-β-D-thiogalactoside
GC	Gas Chromatography
GRM	Gas Release Machine
GSH	Glutathione
H_2O_2	hydrogen peroxide
Hb	Hemoglobin
hist	Histidinate
HO	Heme-Oxygenase
HOMO	Highest Occupied Molecular Orbital
HPLC	High Performance Liquid Chromatography
HRP	Horseradish Peroxidase
h-Tf	Human *apo*-Transferrin
ICP-AES	Inductively coupled plasma atomic emission spectroscopy
Im	Imidazole
Ind	Indazole
IR	Infrared
Kg	kilogram
LD_{50}	lethal dose 50%
LUMO	Lowest Unoccupied Molecular Orbital
Mb	Myoglobin

MCC	Metal Carbonyl Complex
Me	methyl
mg	milligram
MMT	Methylcyclopentadienyl manganese tricarbonyl
morph	morpholine
MTD	Maximum Tolerated Dose
MTO	methyltrioxorhenium
NAC	N-acetyl cysteine
NAD(P)H	nicotinamide adenine dinucleotide (phosphate)
nita	nitrilotriacetate
NMR	Nuclear Magnetic Ressonance Spectroscopy
PBS	phosphate buffered saline
PDA	Photodiode Array
PEG	polyethyleneglycol
Ph	phenyl
pip	piperazine
PPB	plasma protein binding
ppm	parts per million
PTA	1,3,5 - Triaza-7-phosphaadamantane
PTFE	Polytetrafluoroethylene
p-tolyl	3–methyl toluene
py	pyridine
RBC	red blood cell
RCP	Reducing Compound Photometer
ROS	reactive oxygen species
RPMI	RPMI-1630 supplemented with 10% FBS: culture medium rich in aminoacids, inorganic salts, vitamins and proteins
RT	retention time
sp	sparingly
TACN	1,4,7-Triazacyclononane

TBHP	*tert*-butylhydroperoxide
TCD	Thermal Conductivity Detector
TRIMEB	2,3,6-tri-*O*-methyl-β-cyclodextrin
TTCN	1,4,7-Trithiocyclononane
WGSR	water-gas shift reaction

Table of Contents

Chapter I: Introduction

1. The biological activity of Carbon Monoxide

Carbon monoxide (CO) is a colorless, odorless and tasteless gas that has always been tagged as a noxious and dangerous molecule. It is a product of incomplete combustion of organic compounds and the most common sources are car exhaust fumes, smoke from fires, gas-powered engines and wood-burning fireplaces.[1]

Historically, this poisonous reputation was built upon countless episodes of CO exposure with fatal outcome; since CO binds to hemoglobin with more affinity than O_2 it drastically decreases the oxygen transport capacity of the cardiovascular system. Moreover, when CO is bound to hemoglobin the oxy-hemoglobin dissociation curve changes. If CO is bound to two heme sites in the hemoglobin molecule, oxygen affinity increases and therefore it is no longer available to be released in the tissues.[2]

Nevertheless, the binding between CO and hemoglobin is reversible and CO can be replaced with oxygen applying common methodology like substitution hyperbaric chambers[3] since the ratio between oxy-hemoglobin and CO-Hb is determined by the relative partial pressure of CO and O_2. This is not a straightforward process and the same partial pressures of CO and O_2 give different results in different species and individuals, as demonstrated in the extensive work of Haldane and co-workers.[4] Thus, the toxic effects are largely dependent on CO concentration and duration of the exposure.

The current methodology to assess CO levels in the body is the measurement of the percentage of carboxy-hemoglobin (CO-Hb) in the blood. Table 1 lists examples of several CO concentrations, the calculated CO-Hb levels and related human health effects.

Table 1: Ambient CO concentration, % CO-Hb and human health symptoms associated (adapted from references [5] and [6]).

%CO-Hb in blood	Concentration/ ppm	Symptoms
2	10	Asymptomatic
10	70	Exhaustion in healthy people and headaches
20	120	Dizziness, nausea, dyspnea
30	220	Visual disturbance
40-40	350-520	Confusion, syncope, seizures and coma
60-80	1950	Cardiopulmonary dysfunction and death
	10 000	Lethal in minutes

Human levels of CO-Hb differ depending on the external source they have been exposed to, and, obviously, different individuals may experience different symptoms. For instance, regular smokers present CO-Hb baseline levels significantly higher (up to 9%) than non-smokers (typically below 2%).[7]

Despite being common sense that CO is a harmful poison for the organism[8, 9] several scientific discoveries forced scientists to look at this molecule from a different angle. It was already in the middle of the 20th century that Sjöstrand made a discovery that was one of the most important milestones in CO history, when he reported the *Endogenous production of carbon monoxide in man under normal and pathological conditions*.[10]

Sjöstrand, and later Coburn[11, 12] found that CO is endogenously generated in the body through the degradation of senescent red blood cells. It was only 30 years after Sjöstrand's original paper that Tenhunen and co-workers[13-15] characterized the enzyme responsible for breaking down the hemoglobin with concomitant CO release – Heme Oxygenase (HO).

The heme degradation is a concerted action catalyzed by HO with NADPH-cytochrome c (P-450) reductase and oxygen. During the heme degradative process, CO formation is accompanied by the liberation of ferrous ion and

biliverdin-IX α (blue-green pigment) that is rapidly converted into bilirubin-IX α (yellow pigment) by biliverdin reductase.[16-19]

This process is usually observed in bruises. During the injury, a dark red/purple is observed, which arises from deoxygenated hemoglobin released from lysed red blood cells. The released heme is then oxidized with formation of biliverdin, which is responsible for a green tinge. Later, biliverdin is reduced into bilirubin and a yellow coloration typical of this molecule is observed.

What at the first sight could look as a pure catabolic process results in the production of biological active elements.[20-22] Iron regulates several genes expression, including HO as well as transferrin receptors, ferritin (Fe homeostasis) and NO synthase. Bilirubin and biliverdin are antioxidants and are essential for the maintenance of the redox imbalance inflicted on cells and tissues by oxidative and nitrosative stress.[23]

Therefore, HO has both anabolic and catabolic functions inside the cell. In its catabolic functions it reduces the levels of intracellular heme concentration and hemeprotein and therefore inactivates the most potent catalyst for free radicals formation, the heme. In its anabolic functions HO produces the bilic pigments, CO and iron, all biological active elements.

So far three isoforms of HO were identified but only two were studied in detail[24] (reviewed in reference [25]). HO-2 is constitutively expressed in tissues such as brain, liver and endothelium and regulates the basal levels of free heme, acting as a neurotransmitter and regulator of vascular tone. HO-1 is an inducible isoform that represents a pivotal defense against stressful stimuli like ischemia-reperfusion damage, endotoxic shock, UVA radiations and other stressful insults derived from oxidative and nitrosative stress.

HO-3 is so far a very poorly studied isoform, whose functions are not clearly understood.[19] It has been found in the brain, heart, kidney, liver and spleen of rats but it does not possess any heme degrading activity.

Characterization of constitutive HO-2 and inducible HO-1 isoforms of heme oxygenase as well as studies on the kinetics and tissue distribution of these

enzymes revealed the importance of this pathway in the physiological degradation of heme and this production, under some pathophysiological conditions could even be enhanced.[26-28]

Indeed, oxidation of heme by HO accounts for ca. 86% of the total CO production in the body, ca. 79% directly from RBC breakdown[27, 29] and the remaining 21% from the turnover of other hemeproteins like myoglobin, cytochromes and others.[14] The remaining CO comes from other non-heme sources like lipid peroxidation (e.g. NADPH-dependent oxidation of microssomal lipids[30]) photo-oxidation, Fe^{3+}-ascorbate catalyzed oxidation of microssomes,[31] bacterial activity[32, 33] and xenobiotics.

For instance, methylene chloride which is often inhaled from paint strippers, mixtures used for degreasing machinery and pesticide products, is converted to CO by hepatic enzymes in the liver.[34]

Under normal physiological conditions, the rate of CO production in human body is 16.4 $\mu mol.h^{-1}$[35] but these basal levels may increase under stress or pathological conditions. Activation of HO-1 can lead to a local increase of CO in a determined tissue and this is evidenced by the increase levels of CO in exhaled breath of sick individuals.[36-41]

Taken altogether these results challenged CO toxic reputation and the scientific community became more interested in its physiological profile rather than the widely described toxic effects.

The discovery that CO activates soluble guanylyl cyclase (sGC)[42] was one of the first evidences that this molecule could act as an intracellular messenger.[43, 44]

Currently, a wide range of biological effects attributed to CO are already well documented showing anti-inflammatory, anti-apoptotic and anti-proliferative properties both *in vitro* and *in vivo* (reviewed in references [5, 20, 45, 46]). Also, the protective effects of exogenously applied CO have been demonstrated in several models such as organ ischemia/reperfusion injury, hepatitis, vascular injury, inflammatory lung disease and organ transplantation (for reviews see references [45] and [47]). The positive results obtained with inhalation of CO

levels between 10-250 ppm led the pharmaceutical company IKARIA® to test CO gas as a therapeutical molecule in on-going clinical trials in humans (http://clinicaltrials.gov/ct2/results?term=carbon+monoxide).

With CO inhalation therapy stable CO-Hb levels (typically 12-20%) are maintained during a desired period of time (usually 1h). However, the need for a controlled hospital environment and appropriate machinery favor the quest for better alternatives. CO-releasing molecules emerge as a suitable alternative to deliver CO to tissues in a living organism in a controlled and therapeutically useful manner, without increasing CO-Hb levels to dangerous limits.

2. CO and Heme Proteins

Endogenously produced CO as well as exogenously administered CO (as a gas) both depend on hemoglobin transportation to reach the cellular targets. CO binds hemoglobin in the heme center[48, 49] and is transported across the body until it reaches the tissues. The affinity for heme is the driving force that leads to formation of CO complexes with other hemeproteins. Plenty of evidence exists for the formation of such adducts with myoglobin, soluble guanylyl cyclase, inducible nitric oxide synthase, cytochrome P-450, cytochrome-c oxidase, NADPH oxidase and the heme-oxygenase complex[43, 50-56] which leads hemeproteins to be considered the most likely (if not the only) target for CO in biology.[47, 57] As a consequence of heme binding, intracellular CO potentially influences the activity of these hemeproteins and these changes in activity may result either in activation or inhibition of the metabolic functions. Indeed, the most well-known and documented effect is undoubtedly CO "poisoning" that arises from CO competition against O_2 for binding to the four heme iron centers of hemoglobin and producing carboxy-hemoglobin the formation of which is favored by the 245 times higher affinity of CO over O_2.

Binding to other heme centers such as cyt P450 and cyt *c* oxidase has important effects on the respiratory chain and the contribution of this effect to toxicity is

still under debate. For instance, coordination of CO to cyt *c* oxidase may prevent oxygen activation giving protection to reperfusion injury.

Myoglobin is a heme protein mainly found in muscle tissues whose primary function is to buffer the oxygen concentration in these tissues.[58] The protein is a monomer, containing a single five-coordinate heme center (iron protoporphyrin IX) that reversibly binds O_2, without auto-oxidation. It stores O_2 in muscles and allows the consumption of the stored O_2 in aerobic metabolism, providing "extra O_2" to small metabolic bursts, which wouldn't be possible if only the circulating O_2 in hemoglobin was available. The crystal structure of Myoglobin was the first protein structure to be revealed at atomic level. It was determined in the late 1950s by Kendrew and co-workers[59, 60] and since then new resolution structures were published in several ligation states.[61, 62]

Like other iron-based heme proteins, Mb also binds a broad range of ligands depending on the redox state of the metal. The ferric form reacts readily with water and anions like F, Cl, CN, N_3 and OH. The ferrous form, in addition to dioxygen also binds CO, NO, several alkyl isocyanides and nitroso aromatic compounds.[63]

The heme site is "lodged" between two helices and the spatial design of the environment (steric effect) as well as the pocket polarity determines several important functions such as an effective discrimination of CO over O_2 and the prevention of irreversible aerobic auto-oxidation. This prevention is achieved by enhancing stability of the oxy-heme form, favored by globins, against heterolytic cleavage of the Fe-O bond, formed in peroxo-bridged hemes that would result in the release of superoxide.

These complicated heme ligand affinities are regulated by polar, hydrophobic and steric interactions between heme, ligands and distal aminoacid residues. The high number of variables involved makes the kinetics of ligand binding a complex process that involves multiple stereochemical constrained steps, that include (O_2 is presented as an example): 1) displacement of a non-coordinated water molecule from the distal pocket; 2) entry of O_2 into the empty distal pocket; 3) non-

covalent binding of O_2 in the distal pocket and hydrophobic internal pockets; 4) covalent bond formation through the in-plane movement of the iron atom forming the hexacoordinate species; 5) relaxation of the protein and formation of a new electrostatic interaction with the distal pocket, typically hydrogen bonding.[56]

Despite sharing the same general "architectural displacement", some differences are observed between O_2 and CO binding forms. Similar iron-to-ligand bond lengths are observed (around 1.8 Å) but CO binds normal to the heme plane while the O_2 adduct is intrinsically bent. This results in a higher localization of the negative charge at the distal O of oxy-heme (often viewed as ferriheme-superoxide adduct) contrary to the little charge separation in the heme-CO adduct. Also the distal groups, through steric, electrostatic and H-bonding effects contribute to the CO *vs* O_2 discrimination.

These binding differences and conformational changes are reflected in the spectroscopic properties of the different states that strongly vary according to the ligand.

In the ferrous state the iron has six 3d electrons whereas in the ferric ion it has five. The tetrapyrrole ring of protoporphyrin-IX divides the d orbitals into three d_{eg} (d_{xy}, d_{yz} and d_{zx}) and two t_{2g} (d_{x2-y2}, d_{z2}) degenerated orbitals. In the ferrous liganded (O_2 and CO) forms, the energy difference between d_{eg} and t_{2g} orbitals is high so the three orbitals are filled with six electrons of opposite spin giving a low spin state of S=0.

In ferrous deoxy state, the energy difference between the two set of orbitals is low so that all the orbitals are filled with electrons according with Pauli's exclusion principle and Hund's rule. In result, a high-spin species with S=2 (½ + ½ + ½ + ½) is obtained.

Ferric met-Mb has five 3d electrons and the energy difference between the two energetic states will depend on the 6th ligand, giving rise to S = ½ or S = 5/2 species. These electronic differences are illustrated in Figure 1.

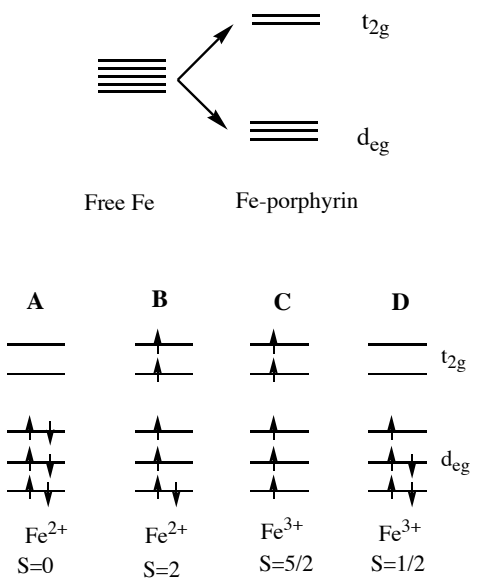

Figure 1: Electronic configuration and spin state of the iron metal in Hb: **Top**: Degenerescence of the 3d electrons in free Fe in the presence of the ligand field of the porphyrin ring into three d_{eg} (d_{xy}, d_{yz}, d_{zx}) and two t_{2g} (d_{x2-y2}, d_{z2}) orbitals. **Bottom**: A- Fe atom in ferrous low spin state (S=0), e.g. Oxygen and carbonmonoxy Hb; B- Fe atom in ferrous high spin state (S=2), e.g. deoxy Hb; C- Fe atom in ferric high spin state (S=5/2), e.g. fluoromet and aquomet Hb; D- Fe atom in ferric low spin state (S=1/2), e.g. cianomet and azidemet Hb.

These electronic properties are reflected in different spectroscopic profiles which allow the determination of different ligation states between "free" deoxygenated heme and CO adducts.

3. Plasma binding proteins and interactions with drugs

Most pharmaceutical drugs depend on bloodstream to reach the diseased tissues or organs. Different delivery routes like oral dosing (*per os*), intraperitoneal (IP), intravenous (IV), intramuscular (IM), subcutaneous (SC) or even transdermal rely on blood to transfer the drug to targets.

When drugs are administered to living systems there are several barriers that reduce the amount of dosed compound that reaches the target. The barriers encountered are diverse and include physicochemical and biochemical processes such as cell membranes, metabolic enzymes, local pH variations, efflux transporters and binding blood constituents.[64] The sequence of barrier events found by the molecules strongly depends on the route of administration and when such barriers are met the drugs' behavior is determined by the physicochemical properties of the molecules. Their binding and reactivity with specific enzymes, binding to transporters and plasma proteins as well as non-specific binding to macromolecules, affects their absorption, distribution, metabolism and excretion (ADME).[65-67] In the bloodstream, three barriers affect free drug availability: enzymatic hydrolysis, red blood cell binding and plasma protein binding.

The hydrolytic enzymes in bloodstream include diverse enzymes like lipase, acid and basic phosphatases, aldolase, dehydropeptidase, cholinesterase, glucuronidase, phenol phosphatase and dehydrogenase. The concentration of such enzymes and substrate specificity vary with factors like age, gender, race or disease state.

Red blood cell binding is another factor affecting free unchanged drug concentration since the cell membrane may bind drug molecules through lipophilic interactions. Nevertheless, the ratio of RBC binding observed is very small compared with plasma protein binding (PPB). Indeed, the major cause leading to a decrease of free drug concentration in solution is PPB. Approximately 6% to 8% of the plasma content are proteins, being the vast majority transporters for natural occurring compounds. Their concentration in plasma may vary with age or even disease states[68-70] but a more relevant fact is that drugs are also able to reversibly bind to these proteins. The affinity of binding determines the ratio of bound and unbound drug in solution and a stronger affinity will obviously decrease the amount of free drug in circulation.

Unless very high drug concentrations are used, the total protein binding is a constant fraction of bound and unbound drug over a wide total drug concentration

range due to the high capacity of drug binding in plasma which is never fully saturated. The high binding capacity is provided by three types of binding proteins: albumin, α_1-acid glycoprotein and lipoproteins.

Human serum albumin is the main carrier in the human organism and possesses six binding sites with high specificity which may carry different products such as fatty acids, bilirubin or drugs like warfarin and ibuprofen.[71]

The concentration of α_1-acid glycoprotein in blood (15 μM) is much lower than that of Human Serum Albumin (HSA) (500-800 μM). It has only one binding site and binds to basic drugs such steroids (e.g. disopyramide and lignocaine) essentially by non-specific hydrophobic interactions.[72, 73]

Lipoproteins (very-high-density lipoprotein [VHDL], high-density lipoprotein [HDL], low-density lipoprotein [LDL] and very-low-density lipoprotein [VLDL]) are particles constituted by non-polar lipids surrounded by more polar lipids and protein that work as natural transport for cholesterol and triacylglycerols. Drug binding to these proteins includes non-specific lipophilic interactions.

For most drugs, PPB has different effects some of which even contradictory. However, the interpretation of these effects for CO-RMs is not so straightforward. For most drugs binding prevents that the desired pharmaceutical effect is maximized since in order to reach a therapeutic concentration in the tissues, the drug must be unbound to permeate the membranes. In the case of CO-RMs, CO – the active principle – is able to permeate the membranes so binding to proteins may not have a deleterious effect, as the binding interaction itself may lead to disruption of metal-carbonyl bonds and favor the release of the therapeutic agent. On the other hand, half-life in circulation may also be increased since bound drugs do not permeate into the liver and kidney for clearance. This will depend on kinetics (on/off rates)[65] and affinity for the protein.

4. The Chemistry of CO release from Metal Carbonyl Complexes

Metal Carbonyl Complexes (MCCs) are coordination compounds of the general type $L_xM(CO)_y$ where M is a transition metal in various oxidation states, L_x represents a set of ancillary ligands and $y \geq 1$.

The vast majority of the MCCs have an 18-electron count in the valence shell of the central metal atom. This is called the Effective Atomic Number (EAN) or 18-electron rule, first stated by Nevil Sidgwick in 1927.[74] In this electronic situation, the bonding between ligands and metal is maximized by the involvement of all the s, p and d orbitals of the metal. The 18 electrons correspond to the full occupancy of the nine bonding molecular orbitals generated by the nine metal valence orbitals (one ns orbital; three np orbitals and five (n-1)d orbitals) and the appropriate ligand based orbitals. The nine corresponding anti-bonding orbitals remain empty. Exceeding the 18-electron count requires the occupation of an empty anti-bonding orbital which in metal carbonyl complexes lies usually at rather high energies, that is, they have high HOMO-LUMO gaps. Exceptions to the 18-electron rule are usually found at the earlier (Groups 3-5) and later groups (Groups 9-10) of the transition metal series in the periodic table, and in some particular cases like the [Fe(II)(porphyrin)] complexes of which hemes are an example. However, the exceedingly high reactivity of low-valent CO derivatives of group 3-5 metals on the one hand, and the high toxicity associated with the sulphophilic metals of groups 9-10 on the other hand, preclude their pharmacological use.

The carbonyl group is one the most studied ligands in organometallic transition metal chemistry due to its particular bonding mode.

The bonding of CO to a metal consists of two contributions: a σ bond is formed through a two-electron donation of the lone pair on carbon into a vacant and suitably directed d-orbital on the metal. This electron donation increases the electron density of the metal and to balance for this increased electron density, a

filled metal d-orbital backdonates electrons to an empty π* orbital on the carbonyl ligand. The second effect which delocalize electron density over the ligands is known as π-backdonation or π-backbonding.[75] The 2 components of M-CO bonding are illustrated in Figure 2.

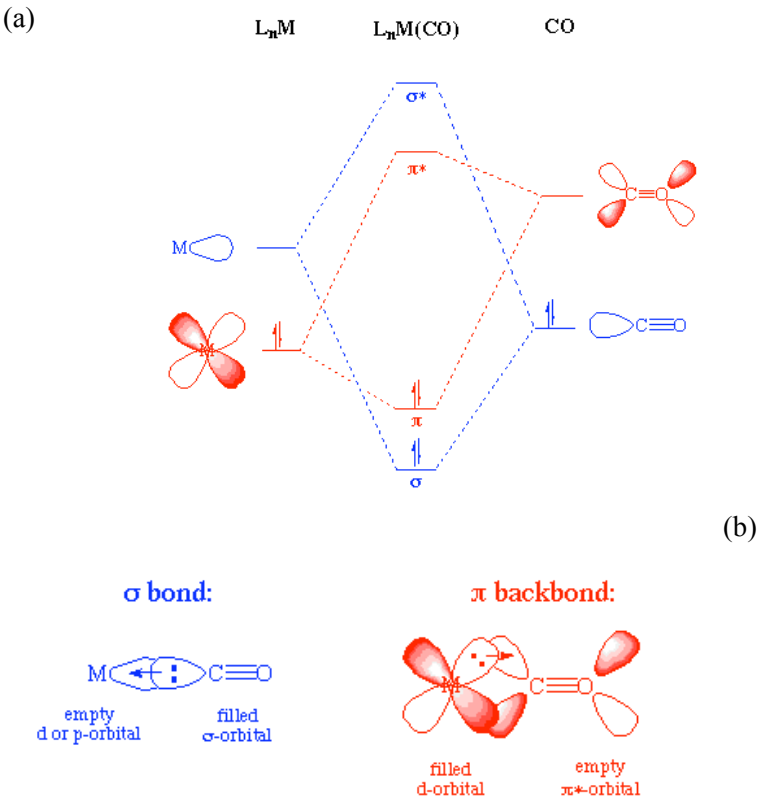

Figure 2: **(a)** Molecular orbital diagram of a $M(d^2)$-CO complex showing the σ and π components contribution to the bond formation. **(b)** Schematic representation of the orbitals overlap in M-CO bonding. Blue: σ overlap and donation from the lone-pair on C into a vacant (hybrid) metal orbital to form a σ M-C bond; Red: π overlap and donation from a filled d orbital on M into a vacant antibonding π* orbital on CO to form a π M-C bond.

CO is the archetypal π-acceptor ligand, a class that also includes C≡NR, N≡O and $C{\equiv}N^-$ all of which possess empty π* orbitals with suitable energies to accept π-backdonation from the metal. These 2 effects are synergistic and a stronger σ

donation from another ligand, immediately increases the π-backbonding to CO to alleviate the excess charge on the metal. An increase in backbonding leads to a decrease in C≡O bond order which is reflected in a slight increase of CO interatomic distance from 112.8 ppm in free CO to higher values in many complexes. The longer CO bond is also reflected in a lower stretching frequency in the IR spectra, changing from 2143 cm^{-1} in free CO to 2125-1850 cm^{-1} for terminal carbonyls in neutral metal carbonyl complexes. In fact, IR spectroscopy provides important information on the structural identity and geometry of carbonyl metal complexes, since carbonyl groups afford very distinct and intense bands, depending on their bonding mode. Carbon monoxide typically binds in an end-on fashion through carbon, although some extremely rare cases of coordination through oxygen have already been reported, namely for Aluminium[76] and Europium(III).[77] Apart from binding as a terminal ligand, CO may also act as a symmetrical or unsymmetrical bridging ligand between two (μ_2) or three (μ_3) metal centers. These are exemplified in Figure 3 and Table 2 reports their IR stretching frequencies.

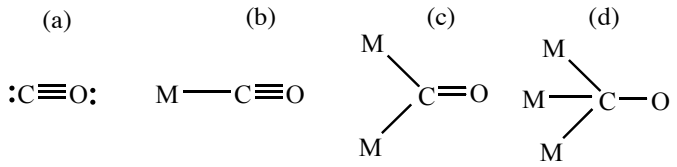

Figure 3: Typical CO bonding modes to metal center: a) "free" b) terminal; c) doubly bridging; d) triply bridging.

Table 2: Carbonyl group IR symmetric stretching frequencies and interatomic distances depending on the binding mode in neutral metal complexes.

Binding mode	**Typical IR stretching frequency / ν_{CO}**	**CO interatomic distance / d_{CO}**
"free" CO	2143 cm^{-1}	112.8 ppm
terminal M-CO	2125 to 1850 cm^{-1}	112-118 ppm
doubly bridging (μ_2-CO)	1850 to 1750 cm^{-1}	117-122 ppm
triply bridging (μ_3-CO)	1730 to 1620 cm^{-1}	117-122 ppm

As can be observed from Table 2, the position of the carbonyl bands in the IR spectrum depends mainly on the bonding mode of the CO (terminal, bridging) but also on the amount of electron density on the metal being backdonated to the CO. As the number (and intensity) of the carbonyl bands observed depend on the number of CO ligands present and the symmetry of the metal complex, introduction of a strong σ donor or a worse π acceptor will lead to a decrease in CO stretching frequency. Accordingly, Lewis base substituents, whose donor atoms are mainly phosphines or sulphides possess energetically accessible vacant d_π orbitals which can also enter into π bonding with the metal. However, almost all the ligands that replace CO in substitution reactions are poorer π acceptors, when compared to CO. Therefore, successive replacement of CO from $M(CO)_n$ by other types of incoming ligands leads to progressive lower CO stretching frequencies in the resulting complexes $M(CO)_{n-x}L_x$ since the carbonyls accept a grater share of the metal electronic density in comparison with the other substituents.

The rupture of one or more of the M-CO bonds of a MCC by physical or chemical processes leads to the liberation of CO and, therefore, CO release. The physical processes are heat and light. Warming a MCC will eventually provide enough energy to break one of the CO bonds and thermally induced CO release will take place. The classical example is the thermal decomposition of $Ni(CO)_4$ into metallic nickel and gaseous CO that takes place at 40°C or that of $Pd(CO)_4$ which

happens even below room temperature. Compounds of this kind cannot be considered for pharmacological uses because of the small gap that exists between the physiological temperature of living organisms (37°C) and room temperature. If they decompose at 37°C they surely have a very short shelf life at room temperature.

Interaction of a MCC with UV or more rarely with visible light causes the labilization of M-CO bonds, and promotes photo-induced CO release. This is a general characteristic of MCCs. However, with the exception of topical uses on the skin, or local photodynamic methods this kind of activation of CO release has no other practical pharmacological use.

Besides these two strictly physical processes that lead to M-CO bond breaking even in vacuum, ligand substitution reactions are the most common chemical pathway to CO release. Ligand substitution is a chemical process whereby one molecule reacts with a MCC and replaces CO within the coordination sphere of its central metal atom. CO is then liberated to the reaction medium from which it may escape to the atmosphere or enter into another chemical reaction. In the case of biological applications this free CO will be taken up by an appropriate target and initiate a biological cascade of events of therapeutic significance.

From the previous we have to conclude that in order to use MCCs as CO-RMs for biological/pharmacological applications, we need to control their reactions with the biological molecules in the medium, which will eventually replace CO in the coordination sphere of the metal in a reaction called ligand substitution.

The hundreds of studies published on the topic of ligand substitution in metal carbonyl complexes were carried out under inert atmosphere because most MCCs have low valent metal centers that are sensitive to oxidation by atmospheric oxygen.[78, 79] Moreover, with very few exceptions all these studies were carried out in organic solvents of low polarity (e.g. toluene, cyclohexane 1,2-dichloroethane) due to the lipophilic nature of most MCCs and the need to simplify the kinetic models of reactivity. Studies carried out in water or protic solvents are exceedingly rare.[80, 81]

Although air and water exclusion are obviously absent under biological conditions it is nevertheless instructive to recapitulate the fundamental aspects of ligand substitution in MCCs as they are described and interpreted in the literature. In this regard we call the attention to the importance of the monumental review made by Howell and Burkinshaw in 1983 where a large amount of information is reported that pertains mainly to the kind of complexes that are dealt within this Thesis.[78]

If we consider an octahedral complex L_5MCO, the substitution of CO by another ligand L' can occur by one of the four paradigmatic pathways (see Scheme 1): D or dissociative; A or associative; Id or intermediate dissociative and Ia or intermediate associative.

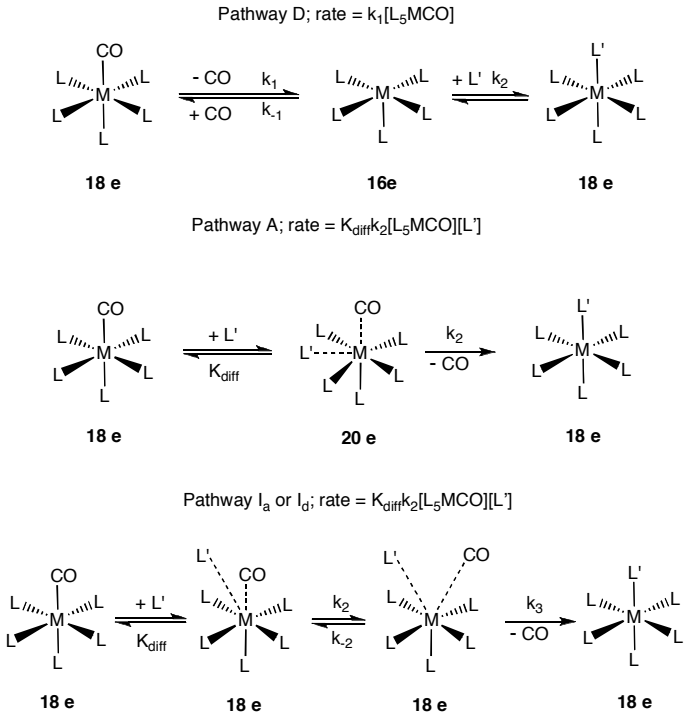

Scheme 1: Ligand substitution processes showing CO substitution by an incoming L' ligand. Pathway D is dissociative; Pathway A is associative; Pathway Ia is intermediate associative; Pathway Id is intermediate dissociative.

In the D pathway the rate limiting step is the complete breaking of the M-CO bond and the formation of a pentacoordinated transition state or intermediate. This one intercepts the incoming substituent L' yielding the final product. Since usually $k_2[L'] >> k_{-1}$ the final rate law reduces to the first order rate equation (Eq. 1)

$$\mathbf{rate = k_1[L_5M(CO)]} \qquad \textbf{Equation 1}$$

This pathway is essentially similar to the well known organic SN_1 paradigm and complies with the EAN rule which states that organometallic complexes of low valent metals exist only as 18- or 16-electron species and that their chemical transformations involve only 16- or 18-electron species.

For this reason, the associative pathway A does not exist for strict 18-electron complexes because the formation of the transition state leads to an energetically inaccessible 20-electron compound. On the other hand, this is a very common and actually the most followed kinetic pathway for 16-electron organometallic complexes which are not being considered for pharmacological applications (see above).

Of course, these remarks apply to the situation in which the incoming nucleophile attacks the central metal directly. However, associative kinetics will result when the nucleophile attacks the coordinated CO ligand in which case there is no elevation of the 18-electron count at the metal (scheme 2).

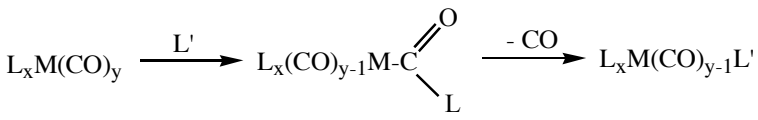

Scheme 2: Nucleophilic attack on coordinated carbonyl and concomitant decarbonylation without elevation of the 18-electron count.

Finally, both intermediate mechanisms I_d and I_a have a bimolecular rate law identical to that of pathway A (Eq. 2)

$$\textbf{rate} = K_{diff}k_2[L_5M(CO)][L'] \qquad \textbf{Equation 2}$$

but corresponding to a transition state where the formation of the M-L' occurs simultaneously with the M-L bond breaking. k_2 is assumed as the rate determining step. I_a corresponds to more advanced formation of the M-L' bond in the transition state and I_d to more advanced breaking of the M-L bond in the transition state. In both cases the 18-electron number is not actually exceeded because the total number of coordinated bonds remains at 6.

Another important case arises when the initial complex has the formula (L-L)$M(CO)_4$ where L-L is a chelating ligand (scheme 3).

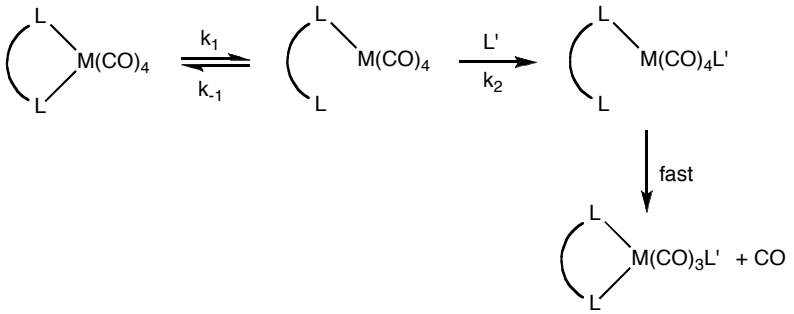

Scheme 3: Schematic representation of the ring-opening mechanism where complexes of the general formula (L-L)$M(CO)_4$ liberate CO upon opening the chelating ring, attack from an incoming ligand (L') and re-closing the ring, eliminating one carbonyl group.

Scheme 3 shows a situation where the chelate ring opens to give an unsaturated intermediate that reacts with the incoming ligand and then loses CO (or L') in a fast re-closing step. The rate law (Eq. 3)

$$\textbf{rate} = k_1k_2[(L\text{-}L)M(CO)_4][L']/k_{-1} + k_2[L'] \qquad \textbf{Equation 3}$$

will now be simplified according to the relative values of k_{-1} and $k_2[L']$. It will have a bimolecular dependence in the case where $k_{-1} >> k_2[L']$ and a first order

dependence on $[(L\text{-}L)M(CO)_4]$ when $k_2[L'] >> k_{-1}$. When $k_{-1} \approx k_2[L']$ the kinetics becomes more complex and plots of k_{obsd} against [L'] become non-linear.[78, 79]

These cases become quite interesting when the bidentate ligand has different coordinating atoms, e.g. P-N ligands.[82, 83] Systems of this type of bidentate P-N or P-O ligands, sometimes called hemilabile ligands, have been explored from the point of view of their catalytic activity.[84, 85]

These general substitutional patterns hold for the vast majority of the low valent metal carbonyl complexes encompassing the octahedral species $L_xM(CO)_y$ (x + y = 6), the trigonal bipyramidal species $L_xM(CO)_y$ (x + y = 5) as well as 18-electron complexes with CO and carbocyclic rings as arenes, cyclopentadienyl and polyolefins. As already mentioned with regard to the area of application of the 18-electron rule, such complexes are found mainly in groups 6-8 which are the most important ones in terms of actual and future applications in medicinal chemistry and in particular in CO-RM therapeutic development.

Interestingly, a very large number of the substitution reactions of these complexes obeys a rate law which is composed of two terms: one corresponds to the dissociative or ligand independent pathway and the other to the associative or interchange ligand dependent pathway, as in equation 4. In most cases where the solvents are nonpolar $k_1 > k_2$ and the reaction approaches limiting dissociative behavior. However, associative mechanisms may become dominant due to interactions like those in scheme 2 or when there are transition state interactions between reagents and solvent. The latter kind of situation is much more likely in polar and protic solvents and may become particularly decisive in water.[81]

$$\mathbf{rate = k_1[L_5M(CO)] + k_2[L_5M(CO)][Y]} \qquad \textbf{Equation 4}$$

Besides, reactions involving ring-opening may result in two-term rate laws with a ligand dependent term as mentioned above.[78, 79]

Early work on substitution reactions of metal carbonyls put a very strong emphasis on attempting to predict the favored sites of substitution in a

polycarbonyl complex as well as predicting relative reaction rates of CO substitution on the basis of parameters that describe the strength of the CO bonds in the intervening complexes.[79] Much of this effort was directed to establish CO substitution predictions based upon the values of the stretching frequencies of the CO ligands which are coupled to the strength of the corresponding M-CO bonds. As we stated above, higher values of νCO correspond to stronger C≡O bonds which, in turn, are found when the main component of the M-CO bond, π-backdonation, is weak. Since CO is also a weak σ donor high values of νCO signal a weakly coordinated CO ligand (weak σ + weak π bonds) with a low M-CO bond energy. Since most reactions are dissociatively activated their activation energy should correlate with M-CO bond energy, and when comparing two isoelectronic and isostructural complexes, higher νCO values should correlate with faster CO substitution (lower activation energy for CO dissociation).

In spite of being very simple, elegant and easily computable, this kind of prediction is very limited. One just needs to remember that the low π-acidity of most L ligands results in $M(CO)_5L$ complexes having lower values of ν(CO) than their $M(CO)_6$ parents. Yet, they all are much more reactive towards CO substitution. For instance, $[Mn(CO)_6]^+$ does not exchange with ^{14}CO at 60°C over a period of days. However, this exchange is fast in the halides $Mn(CO)_5X$.[86] This last fact also shows that some ligands (in this case the halides) are capable of activating CO substitution.

In 1965, Angelici presented an empirical rule that could predict the relative rate of substitution of CO in complexes with the same number of substituents and relative stereochemistry: hard base type ligands labilize carbonyls relative to soft base type ligands.[86] This very simple and early rule may raise several pro and con explanations as summarized by Dobson.[79] Nevertheless, it simply explains correctly the relative order of CO substitution in the family $Mn(CO)_5X$ to give $Mn(CO)_4LX$ which decreases in the order of decreasing halide hardness $Cl^- > Br^- > I^-$. Likewise, $Cr(CO)_4(bipy)$ reacts much faster with other ligands to give $Cr(CO)_3L(bipy)$ than $Cr(CO)_4(PR_3)_2$. More strikingly, it predicts that replacement

of bipiridyl (pK_a = 4.50) by the stronger base 4,4'-dimethyl-bipiridyl (pK_a = 5.45) accelerates the substitution from $Cr(CO)_4$(bipy) relative to $Cr(CO)_4$(4,4'-Me_2bipy).[86] As we will see, this rule is most useful to help understanding many of the results reported below. However, it must be noted that qualitative and quantitative studies on the nature of the substitution reactions showed that some exceptions may occur, and the rule is not always obeyed.

The $Mn(CO)_5X$ examples just mentioned call the attention to another important point: the stereochemistry of CO substitution in octahedral complexes of formula $LM(CO)_5$ or (L-L)$M(CO)_4$. Experiment reveals that the CO that is labilized and eventually replaced is almost invariably the one in *cis* position with regard to L or to (L-L). This can be assigned either to ground state factors that labilize the CO in *cis* position relative to the L ligand, or to site preferences of that L ligand in the pentacoordinated transition state that is formed after the initial dissociation step. Accordingly, *cis* labilization in $M(CO)_5L$ complexes will be stronger for good pi-donor ligands, e.g. halides. Very strong sigma donor ligands, e.g. H^-, still have a much lower preference for *cis* labilization but other weaker sigma donors may not labilize and may even inhibit *cis* labilization. Obviously, pi-acceptors stronger than CO are prone to labilize the *trans* CO ligand.

Many other examples of CO substitution reactions are reviewed and discussed in reference [78].

As mentioned, such reaction patterns have been found under anaerobic conditions. What differences can we expect if such reactions are carried out under atmospheric conditions with the normal partial pressure of molecular oxygen? The main differences will arise as the result of the oxidative action of O_2 on the MCCs. Not much has been reported on this topic but seminal studies by the groups of Poliakoff and Downs have revealed the mechanism of the reaction between $M(CO)_6$ (M = Cr, Mo, W) and O_2 under UV-vis irradiation in frozen Ar or CH_4 matrices at 10-20K (scheme 4).[87]

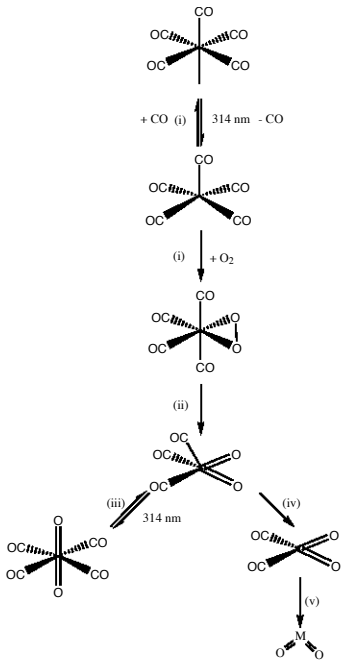

Scheme 4: (i) Cr, 554 nm; Mo, 403 nm; W, 435 nm. (ii) Cr, W, 367 nm; Mo, 314 nm. (iii) Mo and W *only*; Mo, 403 nm or anneal at 35 K. (iv) Cr, 314 nm or anneal at 35 K; Mo, W, 414 nm. (v) Cr, Mo, W (?), 314 nm; W tentative because bands due to WO_2 may be obscured.

The ultimate products are the oxides MO_2 (M = Cr, Mo, W) and MO_3 (for Mo and W only)[88] but relevant intermediate peroxo- and oxo-carbonyl complexes were identified. These mixed oxo-carbonyl species decompose readily not much above the matrix temperature of 20K releasing essentially CO with some CO_2 present in some cases as a side product. Of course, one may expect that the stability of this kind of complexes and their rate of CO release varies with the nature of the ancillary ligands that surround the central M atom. These studies are also relevant having in mind the large number of the Mo(0) complexes that were tested for biological CO release as described in chapter II.

The oxidative reactions described in scheme 4 are inner sphere redox reactions because the oxidant, O_2, initially binds to the metal occupying the vacant coordination position created upon light irradiation. One might also imagine that in the cases where such coordination position is not made readily available, either

no reaction occurs or a different course of events may take place. In fact, in the absence of irradiation, $M(CO)_6$ complexes (M = Cr, Mo, W) are indefinitely stable in air although they react very quickly with $M(CO)_5$ at the extremely low temperature of the frozen Ar or CH_4 matrices. In principle, when a vacant coordination position is not available for the entry of O_2 in the coordination sphere of the metal an outer sphere redox process might take place according to Equation 5.

$$[L_xM(CO)_y] + O_2 \rightleftharpoons [L_xM(CO)_y]^+ + O_2^{\bullet -} \qquad \textbf{Equation 5}$$

The 17-electron radical $[L_xM(CO)_y]^+$ formed in this process, together with superoxide anion, will undergo CO substitution at a much faster rate than its 18-electron precursor. This rate acceleration, which has been reported to be as high as 10^{10},[89, 90] may then result in a very fast CO release process from the initial MCC. In this case one could write the mechanism for CO release as depicted in scheme 5.

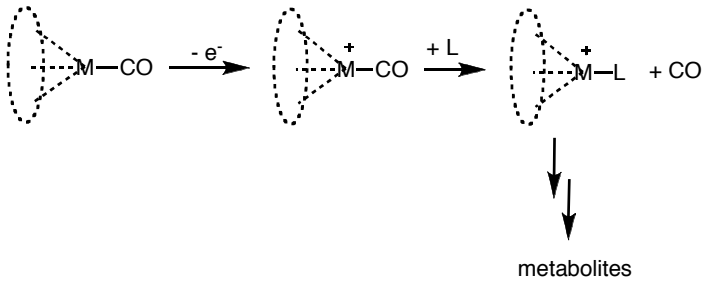

Scheme 5: CO substitution via 17-electron intermediate complex

Furthermore, the superoxide dismutation will generate H_2O_2 a stronger oxidant than O_2 quite likely to be an extra accelerator of the CO release process, as will be discussed in Chapter III.

One last important note refers to the fact that our studies are done in aqueous solution a medium that has been very seldom used for CO substitution chemistry.

In fact, in the early 1980s the first attempts to transpose organometallic chemistry reactions to the aqueous phase were reported.[84] By means of using phosphine ligands modified with water solubilizing groups, like sulfonates and quaternary ammonium ions, several important reactions were carried out in aqueous phase with remarkable success. Probably the most relevant example is the hydroformylation reaction which has been turned into an industrial process.[91] However, fundamental kinetic studies of CO substitution in aqueous solution are very scarce. In one seminal paper, Elias revealed the complex kinetic behavior taken by otherwise straightforward dissociatively activated substitution reactions of $Mo(CO)_4py_2$ with phenanthroline and related diimines, when they are performed in alcohols instead of toluene or hexane.[80] More closely to our case, Burgess has reported the only study we could find in the literature of a substitution of CO by amino acids in aqueous media.[81] In particular, the reaction of $Mn(CO)_5Br$ with glycine and β-alanine shows rather different rate constants for both amino acids that are not dependent on their concentration but are dependent on their nature. Furthermore, the activation parameters do not support the apparent and expected dissociative mechanism. It seems that solvation and other different interactions between the $Mn(CO)_5Br$ molecule and the amino acids govern the transition state of such substitutions, and according to the authors may render any forecast of the activation parameters impossible.[81]

Taken altogether, the factors that affect and control the rate of CO release under biological conditions are exceedingly complex and do not allow any accurate predictions. Therefore, our approach was just to carry out a simplified kinetic study of the liberation of CO from metal carbonyl complexes dissolved or suspended in biological media under air at 37°C and in the dark. Besides the temperature control and light exclusion all other factors that affect the possible mechanisms and rates of CO release (or CO substitution) are not controlled and remain largely unknown. Nevertheless, our expectation is that integrated over a rather large number of compounds the outcome of this exercise provides empiric means of identification of chemical and structural parameters that embody

preferred motifs for the obtention of CO releasers appropriate for therapeutic applications as CO-RM drugs.

5. The CO-RMs in the literature

Carbon Monoxide has now been recognized as an important therapeutical agent, however, the concept of CO-releasing molecule is slowly emerging as a viable alternative. CO-RMs have only been introduced into the scientific community in 2002, in a seminal paper by Motterlini *et al.*[92]

The first generation CO-RMs were lipophilic molecules like $Fe(CO)_5$, $Mn_2(CO)_{10}$ and $[Ru(CO)_3Cl_2]_2$ (CORM-2). While the iron and manganese compounds are activated by light, the ruthenium dimer is able to transfer CO to Mb upon dissolution in DMSO.

CORM-2 was the first example of a CO-RM exhibiting beneficial biological effects as observed with CO gas, such as vasodilatation of pre-contracted aortic rings or reducing acute hypertension *in vivo*.[92]

In order to facilitate their use in biological systems, water solubility was a requirement and an important step forward was taken with the first example of a water-soluble CO releaser: $Ru(CO)_3Cl$(glycinate) (CORM-3).[93] Its biological activity has been recognized in several *in vitro* and *in vivo* assays (reviewed in references [94] and [95]) and its chemistry has also been extensively studied in aqueous medium.[96]

Another water-soluble CO-RM is the boranocarbonate CORM-A1 ($Na_2[BH_3CO_2]$),[97] the only non-metal containing CO-RM described in the literature. Its family as recently been extended with new derivatives of the parent molecule.[98] It has a half-life of $t_{1/2}$ = 21 min which is a CO release profile completely contrary to CORM-3 that carbonylates deoxy-Mb within 1 min.[93]

Other complexes like $Na[Mo(CO)_3$(histidinate)][99] and $[Et_4N][Mo(CO)_5Br]$[100] have also shown pharmacological activity and served as proof-of-concept to use CO-RMs as therapeutical agents.

At the time this Thesis was initiated, only CORM-2 and CORM-3 were known by the scientific community. While performing the work described here, different CO-RMs have been produced with different metals, namely iron,[101-104] molybdenum,[104] chromium,[105] manganese[47, 105, 106] and cobalt.[107] However, most of these studies intended to evaluate mechanistic details concerning the CO release rate of different structures, or the toxicity profiles of these new structures and not their pharmacological activity.

Although several compounds present acceptable toxicological profiles and varied CO release rates they still lack good pharmacological properties like air-stability or water solubility, for instance.

Nevertheless, the published data helps orienting future research into new directions, looking for pharmacological properties like solubility and stability in water, viable CO release in the diseased tissues, with good therapeutical activity and ADME profile.

6. References

1. Burg, R.V., *J. Appl. Toxicol.* **1999**, 19, 379.
2. Roughton, F.J.W., Darling, R.C., *Am. J. Physiol.* **1944**, 141, 17.
3. Gorman, D., Drewry, A., Huang, Y.L., Sames, C., *Toxicology* **2003**, 187, 25.
4. Douglas, C.G., Haldane, J.S., Haldane, J.B., *J. Physiol.* **1912**, 44, 275.
5. Otterbein, L.E., *Respir. Care* **2009**, 54, 925.
6. Omaye, S.T., *Toxicology* **2002**, 180, 139.
7. Aker, J., *Aana J* **1987**, 55, 421.
8. Weaver, L.K., *Crit. Care Clin.* **1999**, 15, 297.
9. Piantadosi, C.A., *N. Engl. J. Med.* **2002**, 347, 1054.
10. Sjostrand, T., *Scand. J. Clin. Lab. Invest.* **1949**, 1, 201.
11. Coburn, R.F., *Prev. Med.* **1979**, 8, 310.
12. Coburn, R.F., Williams, W.J., White, P., Kahn, S.B., *J. Clin. Invest.* **1967**, 46, 346.
13. Tenhunen, R., Marver, H.S., Schmid, R., *J. Biol. Chem.* **1969**, 244, 6388.
14. Tenhunen, R., Marver, H.S., Schmid, R., *Proc. Natl. Acad. Sci. U S A* **1968**, 61, 748.
15. Tenhunen, R., Marver, H.S., Schmid, R., *Trans. Assoc. Am. Physicians* **1969**, 82, 363.
16. Abraham, N.G., Lin, J.H., Dunn, M.W., Schwartzman, M.L., *Invest. Ophthalmol. Vis. Sci.* **1987**, 28, 1464.
17. Maines, M.D., *FASEB J.* **1988**, 2, 2557.

18. Mccoubrey, W.K., Ewing, J.F., Maines, M.D., *Arch. Biochem. Biophys.* **1992**, 295, 13.
19. McCoubrey, W.K., Huang, T.J., Maines, M.D., *Eur. J. Biochem.* **1997**, 247, 725.
20. Otterbein, L.E., Soares, M.P., Yamashita, K., Bach, F.H., *Trends Immunol.* **2003**, 24, 449.
21. Maines, M.D., Gibbs, P.E., *Biochem. Biophys. Res. Commun.* **2005**, 338, 568.
22. Bilban, M., Haschemi, A., Wegiel, B., Chin, B.Y., Wagner, O., Otterbein, L.E., *J. Mol. Med.* **2008**, 86, 267.
23. Motterlini, R., Mann, B.E., Johnson, T.R., Clark, J.E., Foresti, R., Green, C.J., *Curr. Pharm. Des.* **2003**, 9, 2525.
24. Braggins, P.E., Trakshel, G.M., Kutty, R.K., Maines, M.D., *Biochem. Biophys. Res. Commun.* **1986**, 141, 528.
25. Otterbein, L.E., Choi, A.M., *Am. J. Physiol. Lung Cell Mol. Physiol.* **2000**, 279, L1029.
26. Coburn, R.F., Blakemore, W.S., Forster, R.E., *J. Clin. Invest.* **1963**, 42, 1172.
27. Coburn, R.F., Williams, W.J., Forster, R.E., *J. Clin. Invest.* **1964**, 43, 1098.
28. Coburn, R.F., Williams, W.J., Kahn, S.B., *J. Clin. Invest.* **1966**, 45, 460.
29. Berk, P.D., Rodkey, F.L., Blaschke, T.F., Collison, H.A., Waggoner, J.G., *J. Lab. Clin. Med.* **1974**, 83, 29.
30. Nishibayashi, H., Omura, T., Sato, R., Estabrook, R.W., *Structure and Function of Cytochromes,* (Eds.:K. Okunuki; M. Kamen; I. Sakuzu) University of Tokyo Press, Tokyo, **1968**.
31. Wolff, D.G., Bidlack, W.R., *Biochem. Biophys. Res. Commun.* **1976**, 73, 850.
32. Engel, R.R., Matsen, J.M., Chapman, S.S., Schwartz, S., *J. Bacteriol.* **1972**, 112, 1310.
33. Levine, A.S., Bond, J.H., Prentiss, R.A., Levitt, M.D., *Gastroenterology* **1982**, 83, 633.
34. Chauveau, C., Bouchet, D., Roussel, J.C., Mathieu, P., Braudeau, C., Renaudin, K., Tesson, L., Soulillou, J.P., Iyer, S., Buelow, R., Anegon, I., *Am. J. Transplant.* **2002**, 2, 581.
35. Wang, R., *Carbon Monoxide and Cardiovascular Functions,* (Eds.:R. Wang) CRC Press, Boca Raton, **2002**.
36. Paredi, P., Kharitonov, S.A., Barnes, P.J., *Eur. Respir. J.* **2003**, 21, 197.
37. Paredi, P., Kharitonov, S.A., Barnes, P.J., *Eur. Respir. J.* **2003**, 21, 195.
38. Zegdi, R., Perrin, D., Burdin, M., Boiteau, R., Tenaillon, A., *Int. Care Med.* **2002**, 28, 793.
39. Horvath, I., Loukides, S., Wodehouse, T., Kharitonov, S.A., Cole, P.J., Barnes, P.J., *Thorax* **1998**, 53, 867.
40. Antuni, J.D., Kharitonov, S.A., Hughes, D., Hodson, M.E., Barnes, P.J., *Thorax* **2000**, 55, 138.
41. Paredi, P., Kharitonov, S.A., Leak, D., Shah, P.L., Cramer, D., Hodson, M.E., Barnes, P.J., *Am. J. Respir. Crit. Care Med.* **2000**, 161, 1247.
42. Kharitonov, V.G., Sharma, V.S., Pilz, R.B., Magde, D., Koesling, D., *Proc Natl Acad Sci U S A* **1995**, 92, 2568.
43. Furchgott, R.F., Jothianandan, D., *Blood vessels* **1991**, 28, 52.
44. Verma, A., Hirsch, D.J., Glatt, C.E., Ronnett, G.V., Snyder, S.H., *Science* **1993**, 259, 381.
45. Ryter, S.W., Otterbein, L.E., *BioEssays* **2004**, 26, 270.
46. Ryter, S.W., Otterbein, L.E., Morse, D., Choi, A.M., *Mol. Cell. Biochem.* **2002**, 234-235, 249.

47. Mann, B.E., Motterlini, R., *Chem. Commun.* **2007**, 4197.
48. Maines, M.D., *Annu Rev Pharmacol Toxicol* **1997**, 37, 517.
49. Perutz, M.F., *Annu. Rev. Physiol.* **1990**, 52, 1.
50. Stone, J.R., Marletta, M.A., *Biochemistry* **1994**, 33, 5636.
51. Stevenson, T.H., Gutierrez, A.F., Alderton, W.K., Lian, L.Y., Scrutton, N.S., *Biochem. J.* **2001**, 358, 201.
52. Volpe, J.A., O'Toole, M.C., Caughey, W.S., *Biochem. Biophys. Res. Commun.* **1975**, 62, 48.
53. Guengerich, F.P., Ballou, D.P., Coon, M.J., *J. Biol. Chem.* **1975**, 250, 7405.
54. Cross, A.R., Higson, F.K., Jones, O.T., Harper, A.M., Segal, A.W., *Biochem. J.* **1982**, 204, 479.
55. Estabrook, R.W., Franklin, M.R., Hildebrandt, A.G., *Ann. N. Y. Acad. Sci.* **1970**, 174, 218.
56. Migita, C.T., Matera, K.M., Ikeda-Saito, M., Olson, J.S., Fujii, H., Yoshimura, T., Zhou, H., Yoshida, T., *J. Biol. Chem.* **1998**, 273, 945.
57. Roberts, G.P., Youn, H., Kerby, R.L., *Microbiol. Mol. Biol. Rev.* **2004**, 68, 453.
58. Jr, G.N.P. in *Myoglobin*.in *Handbook of metalloproteins*,Vol. 1, (Ed.:A. Messerschmidt; R. Huber; K. Wieghardt; T. Poulos) Wiley VCH, Chichester, **2001**; pp 5.
59. Kendrew, J.C., Bodo, G., Dintzis, H.M., Parrish, R.G., Wyckoff, H., Phillips, D.C., *Nature* **1958**, 181, 662.
60. Kendrew, J.C., Dickerson, R.E., Strandberg, B.E., Hart, R.G., Davies, D.R., Phillips, D.C., Shore, V.C., *Nature* **1960**, 185, 422.
61. Ostermann, A., Tanaka, I., Engler, N., Niimura, N., Parak, F.G., *Biophys. Chem.* **2002**, 95, 183.
62. Vojtechovsky, J., Chu, K., Berendzen, J., Sweet, R.M., Schlichting, I., *Biophys. J.* **1999**, 77, 2153.
63. Antonini, E., Brunori, M., *Hemoglobin and Myoglobin in their reactions with ligands,* (Eds.:A. Neuberger; E. L. Tatum) North-Holland Publishing Company, Amsterdam, **1971**; Vol. 21, p 436.
64. Smith, D.A., Van der Waterbeemd, H., Walker, D.K., *Pharmacokinetics and metabolism in drug design,* Wiley-VCH, Weinheim-Germany, **2001**.
65. Talbert, A.M., Tranter, G.E., Holmes, E., Francis, P.L., *Anal Chem* **2002**, 74, 446.
66. Weisiger, R.A., *Proc Natl Acad Sci U S A* **1985**, 82, 1563.
67. Robinson, P.J., Rapoport, S.I., *Am J Physiol* **1986**, 251, R1212.
68. Grandison, M.K., Boudinot, F.D., *Clin. Pharmacokinet.* **2000**, 38, 271.
69. Kosa, T., Maruyama, T., Otagiri, M., *Pharm. Res.* **1998**, 15, 449.
70. Kosa, T., Maruyama, T., Otagiri, M., *Pharm. Res.* **1997**, 14, 1607.
71. Ascenzi, P., Bocedi, A., Notari, S., Fanali, G., Fesce, R., Fasano, M., *Mini Rev. Med. Chem.* **2006**, 6, 483.
72. Fournier, T., Medjoubi-N, N., Porquet, D., *Biochim. Biophys. Acta* **2000**, 1482, 157.
73. Kremer, J.M., Wilting, J., Janssen, L.H., *Pharmacol. Rev.* **1988**, 40, 1.
74. Sidgwick, N.V., *The electronic theory of valence,* The Clarendon Press, Oxford, **1927**; p 310.
75. Greenwood, N.N., Earnshaw, A., *Chemistry of The Elements,* 2nd ed., Butterworth-Heinemann, Oxford, **1997**; p 926.
76. Nelson, N.J., Kime, N.E., Shriver, D.F., *J. Am. Chem. Soc.* **1969**, 91, 5173.

77. Marks, T.J., Kristoff, J.S., Alich, A., Shriver, D.F., *J. Organomet. Chem.* **1971**, 33, C35.
78. Howell, J.A.S., Burkinshaw, P.M., *Chem. Rev.* **1983**, 83, 557.
79. Dobson, G.R., *Acc. Chem. Res.* **1976**, 9, 300.
80. Elias, H., Macholdt, H.T., Wannowius, K.J., Blandamer, M.J., Burgess, J., Clark, B., *Inorg. Chem.* **1986**, 25, 3048.
81. Burgess, J., Duffield, A.J., *J. Organomet. Chem.* **1979**, 177, 435.
82. Knebel, W.J., Angelici, R.J., *Inorg. Chem.* **1974**, 13, 627.
83. Knebel, W.J., Angelici, R.J., *Inorg. Chem.* **1974**, 13, 632.
84. Smith, R.T., Ungar, R.K., Sanderson, L.J., Baird, M.C., *Organometallics* **1983**, 2, 1138.
85. Habtemariam, A., Watchman, B., Potter, B.S., Palmer, R., Parsons, S., Parkin, A., Sadler, P.J., *J. Chem. Soc.-Dalton Trans.* **2001**, 1306.
86. Angelici, R.J., Graham, J.R., *J. Am. Chem. Soc.* **1965**, 87, 5586.
87. Almond, M.J., Crayston, J.A., Downs, A.J., Poliakoff, M., Turner, J.J., *Inorg. Chem.* **1986**, 25, 19.
88. Almond, M.J., Downs, A.J., *J. Chem. Soc.-Dalton Trans.* **1988**, 809.
89. Lin, Z.Y., Hall, M.B., *Inorg. Chem.* **1992**, 31, 2791.
90. Lin, Z.Y., Hall, M.B., *J. Am. Chem. Soc.* **1992**, 114, 6574.
91. Herrmann, W.A., Kohlpaintner, C.W., *Angew. Chem. Int. Edit. Engl.* **1993**, 32, 1524.
92. Motterlini, R., Clark, J.E., Foresti, R., Sarathchandra, P., Mann, B.E., Green, C.J., *Circ. Res.* **2002**, 90, E17.
93. Clark, J.E., Naughton, P., Shurey, S., Green, C.J., Johnson, T.R., Mann, B.E., Foresti, R., Motterlini, R., *Circ. Res.* **2003**, 93, e2.
94. Johnson, T.R., Mann, B.E., Clark, J.E., Foresti, R., Green, C.J., Motterlini, R., *Angew. Chem. Int. Ed. Engl.* **2003**, 42, 3722.
95. Motterlini, R., Mann, B.E., Foresti, R., *Expert Opin. Investig. Drugs* **2005**, 14, 1305.
96. Johnson, T.R., Mann, B.E., Teasdale, I.P., Adams, H., Foresti, R., Green, C.J., Motterlini, R., *Dalton Trans.* **2007**, 1500.
97. Motterlini, R., Sawle, P., Hammad, J., Bains, S., Alberto, R., Foresti, R., Green, C.J., *FASEB J.* **2005**, 19, 284.
98. Pitchumony, T.S., Spingler, B., Motterlini, R., Alberto, R., *Org Biomol Chem* **2010**.
99. Rodrigues, S.S., Seixas, J.D.S., Guerreiro, B., Pereira, N.M.P., Romao, C., Haas, W., Goncalves, I.M.S. WO 2009/013612 (A1), 2009.
100. Haas, W., Romao, C.C., Rodrigues, S.S., Seixas, J.D.S., Pina, A.R.M., Royo, B., Fernandes, A.C., Goncalves, I.M.S. US 2007/207217 (A1), 2007.
101. Fairlamb, I.J., Duhme-Klair, A.K., Lynam, J.M., Moulton, B.E., O'Brien, C.T., Sawle, P., Hammad, J., Motterlini, R., *Bioorg Med Chem Lett* **2006**, 16, 995.
102. Sawle, P., Hammad, J., Fairlamb, I.J., Moulton, B., O'Brien C, T., Lynam, J.M., Duhme-Klair, A.K., Foresti, R., Motterlini, R., *J. Pharmacol. Exp. Ther.* **2006**, 318, 403.
103. Scapens, D., Adams, H., Johnson, T.R., Mann, B.E., Sawle, P., Aqil, R., Perrior, T., Motterlini, R., *Dalton Trans.* **2007**, 4962.
104. Fairlamb, I.J., Lynam, J.M., Moulton, B.E., Taylor, I.E., Duhme-Klair, A.K., Sawle, P., Motterlini, R., *Dalton Trans* **2007**, 3603.
105. Zhang, W.Q., Atkin, A.J., Thatcher, R.J., Whitwood, A.C., Fairlamb, I.J.S., Lynam, J.M., *Dalton Trans.* **2009**, 4351.

106. Niesel, J., Pinto, A., N'Dongo, H.W.P., Merz, K., Ott, I., Gust, R., Schatzschneider, U., *Chem. Commun.* **2008**, 1798.
107. Atkin, A.J., Williams, S., Sawle, P., Motterlini, R., Lynam, J.M., Fairlamb, I.J., *Dalton Trans* **2009**, 3653.

Chapter II: Evaluating spontaneous CO release from Metal Carbonyls by Gas Chromatography

1. Summary

CO release from several Metal Carbonyl Complexes (MCCs) in a biological relevant medium was evaluated by Gas Chromatography. The vast majority of compounds tested were octahedral or cyclopentadienyl piano-stool 18-electron carbonyl complexes based on Mo^0, Mo^{II}, Mn^I, Fe^{II} and Ru^{II} with classical N, O, P, S-donor ligands or alkyl, acyl and halides. All the Mo^0 compounds, ionic or neutral, showed a high rate of CO dissociation unless a strong π acceptor like cyanide or phosphines is present as co-ligand. On the contrary, their Mn^I counterparts do not release CO at high rates unless a halide (preferentially Cl^-) is coordinated to the metal. Most of the Fe^{II} compounds are $CpFe(CO)_2L$ derivatives which do not release CO at measurable rates, most probably due to insolubility in aqueous solution. Also, $CpMo(CO)_3L$ compounds present a similar profile of insolubility and low rate of CO release. The Ru^{II} compounds tested also do not release CO in the conditions studied.

The influence of pH and O_2 was also evaluated for a set of Mo^0 ionic compounds and it was observed that O_2 is the main trigger to promote CO release from these complexes, leading to the formation of hydroxyl radical, which was detected by ESR with the spin trap BMPO.

2. Introduction

Several analytical methods are available for the quantification of free carbon monoxide. Infrared absorption spectroscopy, colorimetric, volumetric or spectrophotometric methods[1, 2] and high-pressure ^{13}C NMR spectroscopy[3] are some of the possibilities. However, not all of them can be readily applied to routine measurements in small scale. Electrochemical methods based on CO specific electrodes would be ideally versatile judging from the performance of their congeners in the biological and biochemical quantitation of NO. Motterlini's group and others devoted some effort to the development of electrochemical detection of CO.[4, 5] We tried to apply this methodology to quantify the CO released from MCCs but unfortunately, such method fails in the presence of transition metal complexes due to the redox processes that take place alongside CO oxidation. This behavior was observed with the ruthenium complexes CORM-2 and CORM-3, where the Ru^{II} metal center was oxidized in the electrode, preventing the detection of any CO released.

On the other hand, Gas Chromatography (GC) has been widely used since the 1960s in forensic toxicology laboratories to determine CO in blood samples[6-10] using either Thermal Conductivity Detection (TCD) or Flame Ionization Detection (FID). Both methods give higher accuracy and often lower detection limits when compared with the spectroscopic methods. GC emerges therefore as an excellent screening tool since it is an easy and inexpensive way of measuring the amount of CO released by organometallic carbonyl compounds into the headspace of a closed system after their dissolution in biologically relevant media. Although the TCD needs larger volumes than the FID, its simplicity still makes it a very useful method to follow CO releasing processes in the millimolar range.

3. Experimental Section

3.1 Methodology

Table A1 in Annex I lists a selection of the compounds tested for CO release. Most compounds were prepared as reported in the literature unless indicated otherwise. The compounds were characterized by NMR, IR and CHN elemental analysis before use.

The analysis and quantification of CO by GC was performed with a TCD. The detection limit of this method is 6000 ppm and the quantification limit is 22000 ppm. In the experimental conditions of our set-up (Figure 1) this requires an amount of compound for each experiment which varies between 5 and 30 mg. However, for the rapid screening of simple, readily available or easily prepared metal carbonyl complexes these are affordable quantities which produce up to 2 mL of gaseous CO upon full decomposition. A Thermofinnigan Trace GC equipped with a CTR1 column from Alltech™ and a thermal conductivity detector was operated at 36°C using He as carrier gas. CO, CO_2, N_2 and O_2 were simultaneously detected but the normal measurements only quantified CO unless it was found necessary to quantify any of the other gases. The amount of CO liberated from these compounds to the headspace was measured at 2h, 4h and 6h in all cases and calculated from a calibration curve recorded prior to the reaction course. Sometimes shorter or longer periods of time (e.g. 0.5h or 24h) were necessary to study the behavior of some particular compounds in finer detail. Experiments were carried out at 37°C, under CO_2 free reconstituted air (Ar K) in the dark. Absence of light is important since the M-CO bond is often photosensitive. The experimental set-up is depicted in Figure 1.

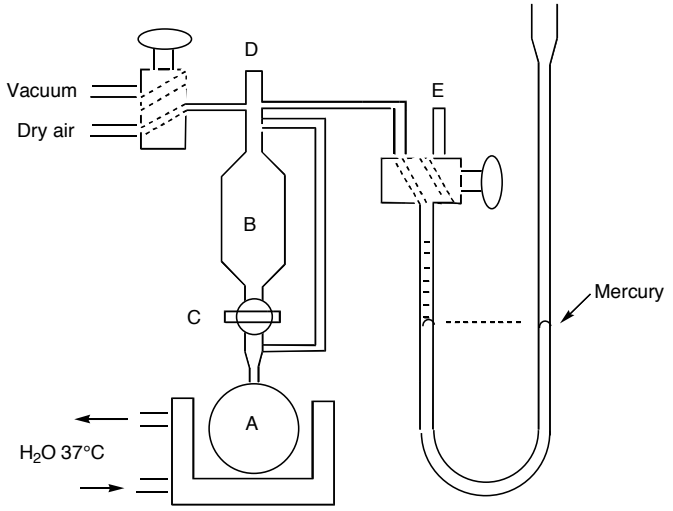

Figure 1: Gas Release Machine (*GRM*). Gas Burette used for measuring CO release from the metal carbonyls in different media and conditions. The compound is placed in flask A with a magnetic stirrer and the system degassed with the stopcock E closed. After being refilled with Ar K to atmospheric pressure, the medium is injected through the septum D into the cavity B. The stopcock C is then open letting the medium flow to flask A with the magnetic stirrer spinning. As CO is released, the gas diffuses through the system raising the mercury level, since the stopcock E is now open. Gas samples for GC analysis are taken with a gastight syringe through rubber septum D.

The amount of compound used in each experiment was always pre-calculated in order to ensure that the liberation of all the carbonyls in the molecule wouldn't exceed the volume of CO contained within the limits of the calibration curve.

Later on, another simplified method was developed, the "vial method", which presents several advantages. The experiments were performed in 7.5 ml Roth® sample vials equipped with a magnetic stirrer inside and capped with PTFE rubber or silicone septa and an aluminum cap. The amount of compound used in each experiment is close to the amounts used in the GRM. This method allows several assays to be performed in parallel. The assays at 37ºC were performed inside an oven, equipped with an orbital stirrer to ensure continuous stirring of the samples.

Experimental details concerning both methods are given below.

In order to bring these tests as close as possible to biologically significant conditions we chose as solvent RPMI-1630 supplemented with 10% fetal bovine serum which will be abbreviated simply to RPMI in the following text. This is a tissue culture medium developed by Moore and his co-workers[11] at Roswell Park Memorial Institute which is rich in aminoacids, inorganic salts, vitamins and proteins. Therefore, upon dissolution in RPMI a given MCC will be exposed to the kinds of molecules that are found in biological conditions.

HPLC traces of several compounds in aqueous medium were obtained using a Thermo HPLC system with an automatic injection system and a PDA detector. A C18 reverse-phase column was used with a MeOH/water gradient. Experimental details about the method are given in the HPLC section.

Gas Chromatography:

Method description:

The CO release assays in the GRM system were performed in a biocompatible medium, RPMI (pH=7.4) at 37ºC under Ar K (reconstituted air; CO_2 free) without light from which 500 µL samples were taken with a Gastight Hamilton® syringe. These were injected in a Thermofinnigam Trace GC equipped with a CTR1 column from Alltech™ (double column; inner column 6 ft x 1/8" packed with porous polymer mixture and outer column 6 ft x 1/4" packed with molecular sieve) and a Thermal Conductivity Detector. The column was inside the oven at 36ºC and the GC was operated at a constant pressure mode (111 KPa) with He as a carrier and reference gas with a 30 mL/min flow. The detector was set at constant temperature (150ºC) and the filament temperature to 250ºC. The injections were made through a packed column injector (PKD) set at 47ºC and 111 KPa.

CO was quantified using a calibration curve recorded prior to the reaction course. This was done by injecting 25 µL increments of CO up to a final total amount of 2

mL of pure CO gas (Carbon Monoxide 4.7, purity ≥ 99.997%; from *Linde Sogas*) to the system and taking samples that were injected in the GC.

The concentrations used in each assay ranged from 1.5 mM to 45 mM depending on the molecular weight and number of carbonyl groups in the molecule.

The assays performed in calibrated vials were performed in the same way but the reactor vessel was a 7.5 ml Roth® sample vial equipped with a magnetic stirrer inside and capped with a PTFE rubber or silicone septa and an aluminum cap. PTFE rubber septa were acquired from Sigma Aldrich® and silicone septa from Roth®. The assays were performed at room temperature and normal atmospheric air was used instead of Ar K. 250 µL samples were taken to analysis and CO was quantified using a calibration curve recorded using the same methodology, but where the volume of CO injected ranged from 0 to 1.5 mL.

High-Pressure Liquid Chromatography:

Method description:

HPLC traces of several compounds in aqueous medium were obtained using a Thermo HPLC system (Thermo Fisher Scientific, Inc.) with an automatic injection system and a PDA detector. A C18 reversed phase column (Alltech® Prevail™ Reversed-Phase Columns from Grace Davison Discovery Sciences; 150×4.6 mm; 3 µm particle size) was used with a MeOH/water gradient (see Table 1). HPLC-gradient grade MeOH from *Panreac* and Milli-Q water were used as eluents in the HPLC system with 1 mL/min flow rate.

Table 1 – Gradient used in the HPLC analysis for 15min runs.

t / min	% H_2O	% MeOH
0	90	10
2	90	10
8	0	100
9	0	100
10	90	10
12	90	10

Electron Spin Resonance

The spin trap NWT-BMPO, >99% was purchased from *Northwest Life Sciences Specialties, LLC.*

Method description:

A stock solution of CO-RM was prepared by dissolving a few milligrams of compound in 1 mL of deoxygenated distilled water or MeOH under N_2. Another stock solution of BMPO was prepared with a final concentration of 250 mM. An aliquot was taken from the CO-RM solution and 100 µL from the BMPO solution to a closed vial under N_2 and deoxygenated distilled water added to perform 1 ml total volume.

Table 2: Solvents and concentrations

Compound	Stock Solution	Final Concentration	[BMPO]
$[Et_4N][Mo(CO)_5Br]$	MeOH (0.7%)	199.0 µM	25 mM
$Na[Mo(CO)_3(hist)]$	H_2O	203.0 µM	12.5 mM
$Na_3[Mo(CO)_3(cit)]$	H_2O	199.3 µM	25 mM
$[Mo(CO)_3(bpa)]$	MeOH (0.6%)	199.8 µM	25 mM

A sample was taken from this solution and a control spectrum was acquired before bubbling O_2. Oxygen was then bubbled in the solution for 3-4 min and another sample was taken and analyzed.

The experiment was performed on a quartz, planar, ESR cell, at room temperature, microwave power of 2 mW, modulation frequency 100 kHz, modulation amplitude 0.1 mT.

3.2 Technical Details:

General Considerations:

Elemental Analysis were performed at ITQB, Oeiras, by Engª Conceição Almeida. Infrared spectra were recorded on a Unicam Mattson 7000 FTIR spectrophotometer using KBr pellets. ^1H NMR and ^{13}C NMR spectra were

recorded on a Bruker AMX300 or Bruker Avance III 400mHz. Chemical shifts are quoted in parts per million from $SiMe_4$ (TMS).

UV-VIS spectra were acquired in a Shimadzu UV-3100 or a Perkin Elmer Lambda35 spectrophotometer.

Synthetic Work:

All the reactions were carried out under a nitrogen atmosphere, using common schlenk techniques. Solvents were dried by standard procedures, distilled under N_2 and kept over 4Å molecular sieves. $Mo(CO)_6$, $Cr(CO)_6$, $Mn_2(CO)_{10}$, $Fe_2(CO)_9$ and $CpMn(CO)_3$ were bought from Sigma Aldrich and used without further purification. $[Ru(CO)_3Cl_2]_2$ was bought from *Strem Chemicals*.

The compounds $Mn(CO)_5Br$@TRIMEB, $CpFe(CO)_2Cl$@TRIMEB, $CpFe(CO)_2Cl$@β-CD, $[(C_2H_5)_4N][Mo(CO)_5Br]$@TRIMEB, $CpMo(CO)_3Cl$@TRIMEB and $(\eta^5–C_5H_4COOCH_3)Mo(CO)_3Cl$@TRIMEB were encapsulated and characterized by the group of Prof. Isabel S. Gonçalves, in Universidade de Aveiro, Portugal.

$Mo(CO)_3(\eta^6\text{-}C_7H_8)$[12], $Mo(CO)_4(pip)_2$[13] and DAPTA[14] were prepared according to literature procedure as well as most of the complexes, as indicated in Table A1 (Annex I).

Some of the new compounds presented were prepared by other members of Alfama's chemistry department and are part of Alfama's portfolio of compounds. Their synthesis is referred as Alfama's Intelectual Property (AIP).

The synthesis and characterization of the remaining new complexes are presented next:

$Mo(CO)_4(3\text{-}COOH\text{-}py)_2$:

$Mo(CO)_6$ (1.37 g; 5.189 mmol; 264 g/mol) and nicotinic acid (1.278 g; 10.381 mmol; 123.11 g/mol) were heated to reflux in 60 ml of a 1:1 mixture of toluene/EtOH. After 21h the reaction was stopped and the red solution cooled to room temperature giving a red precipitate. This was filtered, washed with hexane

and recrystalized from dichloromethane/hexane. It was further dried in vacuum at 50ºC for 1 week to remove coordinated toluene and EtOH. **Yield:** 14%.

IR (KBr/cm^{-1}): 2014(w), 1940(sh), 1898(s), 1873(sh) (C≡O); 1615(br) (C=O);

E.A. Calc. for $MoN_2O_8C_{16}H_{10}$**:** %C:42.31, %H:2.21, %N:6.17; Found: %C:42.61, %H:2.53, %N:6.12;

^{1}H NMR (MeOD, 400MHz, rt, δ in ppm): δ = 9.02 (s,1H), 8.61 (d,1H), 8.30 (d,1H), 3.44 (t,1H)

$Mo(CO)_4(DAPTA)_2$:

$Mo(CO)_4(pip)_2$ (0.400 g; 1.06 mmol; 376.26 g/mol) and DAPTA (2 equiv.; 0.487 g; 2.126 mmol; 229.2188 g/mol) were suspended in 40 ml of CH_2Cl_2 and heated to reflux for 15min. While warming, the suspension became a clear solution. The yellow solution was cooled to room temperature and concentrated to approximatelly 1/3 of the initial volume. Hexane was added and a turbid suspension started to form. It was stirred and an orange oil was obtained mixed with some solid yellow product. The oily fraction was thoroughly washed with Et_2O. After washing, a yellow powder was obtained and dried in high-vacuum for 3 days. **Yield:** 87%.

IR (KBr/cm^{-1}): 2027(s), 1909(s) (C≡O); 1632(s) (C=O);

E.A. Calc. for $MoC_{22}H_{32}P_2N_6O_8$: %C:39.65, %H:4.84, %N:12.61; Found: %C:39.15, %H:4.84, %N:12.83;

^{1}H NMR ($CDCl_3$, 400MHz, rt, δ in ppm): δ = 5.87 (d,1H); 5.47 (d,1H), 5.01 (d,1H), 4.63 (d,1H), 4.46 (d,1H), 4.04 (d,1H), 3.94 (d,1H), 3.68 (s,2H), 3.47 (d,1H), 2.13 (s,3H), 2.16 (s,3H);

^{31}P NMR ($CDCl_3$, 162MHz, rt, δ in ppm): δ = -26.0.

$Mo(CO)_3(bpa)$:

The bpa (N-(*p*-carboxy-benzyl)bis(2-picolyl)amine) ligand was prepared as follows:

To a clear THF solution of methyl-4-(bromomethyl)benzoate (1.13 g, 4.85 mmol; 229.08 g/mol) was added at once the yellow di-2(-picolyl)amine (0.903 ml; 4.85 mmol; 1.107 g/ml; 199.25 g/mol) at room temperature. The solution turns light yellow. Triethylamine (675 μL; 4.85 mmol; 0.727 g/ml; 101.19 g/mol) is added and the solution turns immediately deep yellow. The mixture was allowed to reach room temperature and subsequently filtered to remove a white precipitate. After removal of the solvent under reduced pressure, the orange oily residue was dissolved in diethyl ether (40 ml) and filtered to remove some more precipitate. Evaporation of the solvent gives a dark orange oil which was used in the next step.

^{1}H NMR ($CDCl_3$, 400 MHz, rt, δ in ppm): δ = 8.49 (d,2H), 7.98 (d,2H), 7.64 (dt,2H), 7.53 (d,2H), 7.48 (d,2H), 7.12 (tt,2H), 3.89 (s,3H), 3.81 (s,4H), 3.75 (s,2H). Note: There is a 5% of the di-2(-picolyl)amine used in slight excess;

The orange oil was dissolved in methanol (20 ml) and a solution of aqueous NaOH (0.8 g in 5 ml H_2O; 20 mmol; 40 g/mol) was added. The solution gets immediately darker and is stirred for two hours at room temperature. The pH was adjusted to 7 by dropwise addition of 2M HCl (50 ml HCl 37% in 250 ml water solution) followed by removal of the solvent under reduced pressure. The sticky yellow residue was ground with $CHCl_3$ (200 ml) followed by filtration to remove NaCl. Removal of the solvent under reduced pressure afforded an orange sticky oil to which acetonitrile (30 ml) was added, followed by vigorous stirring to dissolve all compound. Precipitation is seen after 15 minutes. The solution was placed in the refrigerator to effect further precipitation. The white precipitate was filtered and dried under vacuum. **Yield**: < 20%.

E.A. Calc. for $N_3O_2C_{20}H_{19}$: %C:72.05, %H:5.74, %N:12.60; Found: %C:72.57, %H:5.98, %N:13.04;

^{1}H NMR ($CDCl_3$, 400 MHz, rt, δ in ppm): δ = 8.61 (d,2H), 8.01 (d,2H), 7.70 (dt, 2H), 7.60 (d,2H), 7.44 (d,2H), 7.12 (t,2H), 3.88 (s,4H), 3.77 (s,2H).

Synthesis of the complex:

$Mo(CO)_3(\eta^6\text{-}C_7H_8)$ (0.800 g; 2.94 mmol; 272.1117 g/mol) was dissolved in 40 ml of MeOH and added to $(C_5H_4CH_2)_2NCH_2C_6H_4COOH$ (0.980g; 2.94 mmol; 333.39 g/mol) in 25 ml of MeOH.

The red clear solution became turbid with an abundant insoluble precipitate after 5 minutes. The reaction was carried on for 2h at room temperature. The precipitate was allowed to rest and was filtered. It was washed with 25 ml of Et_2O and dried in vacuum giving a bright orange powder. **Yield:** 86%.

IR (KBr/cm^{-1}; C≡O): 1899(vs), 1759(s);

E.A. Calc. for $C_{23}H_{19}N_3MoO_5$: %C=53.81, %H=3.73, %N=8.19; Found: %C=54.01, %H=3.79, %N=7.79;

^{1}H NMR ($(CD_3)_2CO$, 400MHz, rt, δ in ppm): δ = 8.85 (d,2H); 8.14 (d,2H), 7.88 (d,2H), 7.61 (d,2H), 7.21 (d,2H), 7.11 (d,2H), 4.80 (s,2H), 4.73 (d,2H), 3.92 (d,2H).

$Mo(CO)_3(DAPTA)_3$:

$Mo(CO)_3(\eta^6\text{-}C_7H_8)$ (0.200 g; $7.350x10^{-4}$ moles; 272.1117 g/mol) was dissolved in 30 ml of MeOH to give a red solution. DAPTA (3 eq.; 0.502 g; 2.190 mmol; 229.29 g/mol) was added as a solid to the previous solution. The red solution immediately turned orange and gradually became lighter. After stirring at room temperature for 2 hours a small amount of a brownish powder precipitated. The mixture was filtered giving a very pale yellow solution. The filtrate was concentrated and Et_2O was added. A turbid suspension was formed and cooled to -30ºC during 6h and then filtered. An off-white powder was obtained and dried in vacuum. **Yield:** 43%.

IR (KBr/cm^{-1}):1950(s), 1859(s) (C≡O); 1645(s) (C=O);

E.A. Calc. for $MoC_{30}H_{48}P_3N_9O_9$: %C:41.53, %H:5.58, %N:14.53; Found: %C:41.40, %H:5.60, %N:14.60;

^{1}H NMR (D_2O, 400MHz, rt, δ in ppm): δ = 5.69 (d,1H), 5.25-5.15 (m,2H), 4.48 (d,1H), 4.28-4.18 (m,2H), 3.86 (m,2H), 3.57 (s,2H), 2.18 and 2.16 (ds,6H);

^{31}P NMR (D_2O, 162MHz, rt, δ in ppm): δ = -25.8.

The group of compounds $Na_3[Mo(CO)_3(citrate)]$, $[choline]_3[Mo(CO)_3(citrate)]$, $[Et_4N]_3[Mo(CO)_3(nitrilotriacetate)]$, $Na_3[Mo(CO)_3(nitrilotriacetate)]$, $Na_5[Mo(CO)_3(diethylenetriaminepentaacetate)]$ were prepared based on the published procedure for $[Et_4N]_3[Mo(CO)_3(citrate)]$.[15]

The general procedure is presented for $Na_3[Mo(CO)_3(citrate)]$:
Sodium citrate dihydrate (0.844 g; 2.801 mmol; 294.1 g/mol) and (η^6-C_7H_8)$Mo(CO)_3$ (0.780 g; 2.866 mmol; 272.12 g/mol) were suspended in 100 ml of dry MeOH and stirred for 24 hours at room temperature. The light orange solution was filtered and concentrated under vacuum. This was transferred to another schlenk, partially filled with a large amount of Et_2O. A flocculate precipitate was obtained and filtered. It was washed with Et_2O and dried in vacuum to afford a light brown powder. **Yield:** 74%.
IR (KBr/cm^{-1}): 1984(w), 1901(s) (C≡O); 1754(br), 1599(br); 1410(m) (C=O);
E.A. Calc. for $MoC_9H_5O_{10}Na_3.2(CH_3OH)$: %C:26.31, %H:2.61; Found: %C:26.49, %H:2.21;
^{1}H NMR (D_2O, 400MHz, rt, δ in ppm): δ = 2.67 (s,1H); 2.63 (s,1H), 2.57 (s,1H), 2.53 (s,1H).

$[choline]_3[Mo(CO)_3(citrate)]$
IR (KBr/cm^{-1}) 1985(w), 1901(s) (C≡O); 1867(br), 1735(br) (C=O);
E.A. Calc. for $MoC_{24}H_{47}NO_{13}N_3$: %C:42.29, %H:6.95; %N:6.17; Found: %C:41.52, %H:7.09, %N:6.13
^{1}H NMR (MeOD, 400MHz, rt, δ in ppm): δ = 4.02 (s,6H), 3.52 (s,6H), 3.2 and 3.31 (ds,27H), 2.8-2.2 (m,4H).

$[Et_4N]_3[Mo(CO)_3(nitrilotriacetate)]$
IR (KBr/cm^{-1}) 1985(w), 1901(s) (C≡O); 1867(br), 1735(br) (C=O);

E.A. Calc. for $MoC_{33}H_{66}O_9N_4$: %C:52.23, %H:8.77, %N:7.38; Found: %C:51.63; %H:8.92, %N:7.08;

^{1}H NMR (D_2O, 400MHz, rt, δ in ppm): δ = 3.73 (broad band), 3.29 (m,8H), 1.28 (t,12H).

$Na_3[Mo(CO)_3$(nitrilotriacetate)]

Yield: 90%;

IR (KBr/cm^{-1}) 1983(w), 1897(s) (C≡O); 1753(br), 1600(br), 1401(m) (C=O);

E.A. Calc. for $MoC_9H_6O_9NNa_3.(CH_3OH)$: %C:25.60, %H:2.15, %N:2.99; Found: %C:25.88, %H:2.44, %N:2.94;

^{1}H NMR (D_2O, 400MHz, rt, δ in ppm): δ = 3.73 (broad band).

$Na_5[Mo(CO)_3$(diethylenetriaminepentaacetate)]

Yield: 80%;

IR (KBr/cm^{-1}):1897(s) (C≡O); 1753(br), 1600(br), 1401(m) (C=O);

E.A. Calc. for $MoC_{17}H_{18}O_{13}N_3Na_5.(CH_3OH)$: %C=30.23, %H=3.10, %N=5.87; Found: %C=29.83, %H=3.66, %N=5.66;

^{1}H NMR (D_2O, 400MHz, rt, δ in ppm): δ = 2.8-3.9 (broad band)

4. Results and Discussion

All metal carbonyl complexes that were referenced as possibly useful CO releasing molecules (CO-RMs) were screened for CO release in RPMI. The number of compounds surpasses 300 and encompasses several transition metal complexes with an 18-electron shell, with different charges and a variety of ancillary ligands. With only a handful of exceptions, all compounds tested belong to metals of the groups 6-8. The reason for this is related to general metal toxicity and biocompatibility which discourage the use of metals at both ends of the periodic table (Groups 3-5 and 9-10). Late transition metals are normally considered toxic due to their strong tendency to react with sulfidryl groups and

hence accumulate in living tissues and cells. On the other hand, early transition metal carbonyls are usually highly reactive and oxygen sensitive species because their low d-electron count requires very low oxidation states to stabilize their M-CO bonds.

Figure 2 depicts the main structural types investigated which are divided in two broad groups: octahedral carbonyl complexes and cyclopentadienyl containing carbonyl complexes.

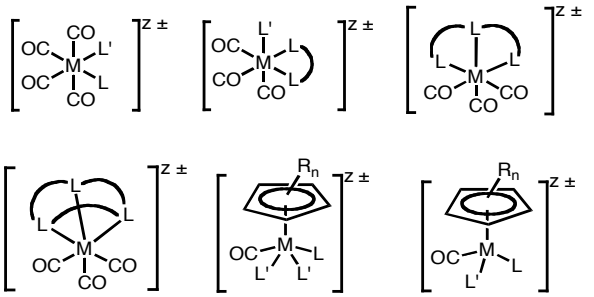

Figure 2: The main structural types of MCCs tested for CO release. L or L' mean C, N, O, P, S or halide ligands; R means an alkyl or functionalized alkyl bearing amine, alcohol, thiol, ether, thioether, or carboxylic functions (acid, ester, amide).

The octahedral complexes contain mainly classical N, O, P, S or halide donors. Only a few complexes have σ-C ligands (alkyl or acyl). A small group of 7-coordinated complexes was also studied (see Table A1 in Annex I).

Figure 3 represents the statistics of the results obtained for the amount of CO released after 6h, at 37ºC in RPMI and in the dark.

Since these tests were done under aerobic conditions using an aqueous medium very rich in biological molecules, and given the fact that biological molecules in aqueous solution are not expected to be very strong nucleophiles, one may only expect fast and extensive CO release to be found in compounds that behave close to one or both of the following limiting conditions:

i) high instability to oxidation by O_2

ii) high kinetic instability towards ligand substitution

The presence or absence of one or both of these conditions will certainly dictate which MCCs will lie at both the high and low ends of the CO release spectrum, respectively. Between such extremes, a variety of intermediate situations will be found.

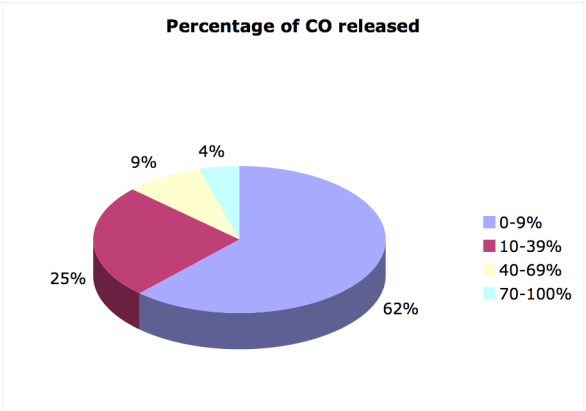

Figure 3: Distribution of MCCs according to the amount of CO released to the headspace of a closed system under standardized conditions: RPMI/10%FBS, under air at 37ºC in the dark after 6h. Measurements performed with compounds from ALFAMA's portfolio by GC with Thermal Conductivity Detection.

When looking at the results in Figure 3, one surprising observation stands out: the largest slice of MCCs tested are rather stable toward loss of CO (62% of the compounds release less than 10% of the total CO). These stable compounds cover all types of structural families and their stability may be attributed to the presence of one or both of the two previously mentioned conditions: oxidative and substitutional stability. However, this analysis is not entirely sound since we have identified another very important variable that interferes with and often masks the interpretation of the CO release results: solubility of the MCCs in aqueous media.
In fact, a closer look at the tests carried out with these compounds leads to the conclusion that a stringent link is often observed between solubility and CO release, and the vast majority of water-insoluble compounds do not spontaneously release CO or do so to a rather small extent. As a general example, zerovalent homoleptic metal carbonyls like $Mo(CO)_6$, $Cr(CO)_6$, $Mn_2(CO)_{10}$ or $Fe_2(CO)_9$, are

completely insoluble in water and do not release CO under the standardized conditions.

This behavior is independent of the metal and is observed in Molybdenum complexes e.g. $Mo(CO)_4$(bipy), $Mo(CO)_3$(TTCN), $CpMo(CO)_3CH_3$ and $Cp^*Mo(CO)_3Cl$; Iron compounds like $CpFe(CO)_2I$ and $CpFe(CO)_2(OCOC_6H_4OCOCH_3)$; Cobalt compounds like $[Co(CO)_3]_2(PhC{\equiv}CPh)$ and Ruthenium compounds like $CpRu(CO)_2Cl$ and $[Ru(CO)_3Cl_2]_2$. However, this connection between insolubility and low CO release isn't a blind rule since it was observed that some insoluble compounds were able to spontaneously release CO under our standardized conditions. Once more, this behavior wasn't limited to a specific structural family since a wide variety of compounds shared the same profile e.g. Mn(I) compounds such as $Mn(CO)_5Br$, $Mn(CO)_5CH_3$, $Mn(CO)_5OSO_2CF_3$; Fe(II) compounds such as $CpFe(CO)_2Cl$, $Fe(CO)_4I_2$, $CpFe(CO)_2(\eta^1\text{-}C_3H_5)$, $Fe(CO)_3Br(\eta^1\text{-}C_3H_5)$, $CpFe(CO)_2OCOC_5H_4NFe(CO)_2Cp$, $Fe(CO)_2(Cyst)_2$; Mo(0) compounds such as $[Bu_4N][Mo(CO)_5I]$, $[Me_4N]_2[(Mo(CO)_4(SPh)_2]$, $Mo(CO)_4$(4,4'-COOH-bipy), $Mo(CO)_4$(3-COOH-py)$_2$, $Mo(CO)_3(\eta^6\text{-}C_7H_8)$, $Mo(CO)_3$(bpa); Mo(II) compounds like $CpMo(CO)_3Cl$, $Mo(CO)_2(S_2CNMe_2)_2$, $Mo(CO)_3I_2(CH_3CN)_2$, $Mo(CO)_3I_2$(*p*-tolil-DAB), $Mo(CO)_3I_2$(Cy-DAB), $[Mo(CO)_4(SPh)]_2$, $CpMo(CO)_3OC_8H_6OBF_2$, $[(CO)_3Mo(C_5Ph_4O)]_2$, $CpMo(CO)_3CH_2COOH$.

From these examples it is clear that the prediction of the CO release profile of a given MCC is not a straightforward task, and the thorough screening that was carried out was necessary to identify possible CO-RM candidates. Once analyzed, the large amounts of data already obtained should allow the identification of the nature and importance of the main factors that condition the CO release profile of a given MCC.

To the best of our knowledge, the following discussion stands out as the widest existing screening of the stability of MCCs under biologically relevant media/conditions. The results are ordered mainly by structural groups and within

these by comparison of other factors such as oxidation state of the metal, complex charge and nature of the ancillary ligands.

4.1 CO release profiles of octahedral $[M(CO)_xL_{6-x}]^{\pm}$ complexes

Table 3 presents some selected examples of compounds of this very large and chemically flexible structural group, which allow insightful comparison and inferences with regard to the CO release profiles of this category of compounds. The compounds presented are based on Mo^0, Mo^{II}, Mn^I, Fe^{II} and Ru^{II}.

Table 3: Solubility in the medium and equivalents of CO released by several Mo, Mn, Fe and Ru MCCs in RPMI (10% FBS), at 37ºC after 6h in the dark.

Family of compounds $[M(CO)_xL_{6-x}]^{\pm}$	**L_n group/counter-ion**	**Solubility in RPMI**	**Equivalents of CO released in RPMI after 6h**
$Mn(CO)_5L$	Cl	insoluble	1.9
	Br	insoluble	1.6
	OSO_2CF_3	sp soluble	0.6
	CH_3	sp soluble	0.4
	$CH_2C(O)NH_2$	soluble	0.3
$Mn(CO)_4L_2]^{0/+/-}$	S_2CPh	insoluble	0.0
$[Mn(CO)_3L_3]^{n+}$	TACN/Br	soluble	0.0
$[Mo(CO)_5L]^-$	CN/Na^+	soluble	0.0
	Br/NEt_4^+	sp soluble	2.4
	I/NBu_4^+	insoluble	0.4
	$I/Na(15\text{-crown-5-ether})^+$	sp soluble *	0.5
	$I/Na(diglyme)_2^+$	sp soluble*	1.1
	$I/K(diglyme)_3^+$	sp soluble*	1.3
	$I/NH_4(diglyme)_3^+$	soluble*	0.8
	$I/½\ Ca(diglyme)_2^{2+}$	unstable	Not tested
	$I/½\ Mg(diglyme)_2^{2+}$	unstable	Not tested
$[Mo(CO)_5L]$	morph	insoluble	0.5
	$P(C_6H_4SO_3Na)_3$	soluble	0.0

	PTA	insoluble	0.0
	PTA.HCl	soluble	0.0
$[Mo(CO)_4L_2]$	bipy	insoluble	0
	4,4'-($NaO_3SCH_2CH_2OOC$)-bipy	sp soluble	2.7
	4,4'-(HOOC)-bipy	sp soluble	2.5
	Me-DAB	insoluble	0.0
	Me-pip-DAB	sp soluble	0.9
	3-(HOOC)-py	insoluble	0.4
	Me-pip	insoluble	0.5
	morph	sp soluble	2.3
	$OPPh_3$	insoluble	0.3
	PTA	insoluble	0.0
	PTA.2HCl	soluble	0.0
$[Mo(CO)_4L_2]^-/ Et_4N^+$	acac	soluble	1.7
	glycinate	soluble	1.5
$[Mo(CO)_3L_3]$	PTA	soluble	0.0
	TTCN	insoluble	0.0
	TACN	insoluble	1.5
	bpa	insoluble	2.5
$[Mo(CO)_3L_3]^{n-}/ nM+$	hist/Na^+	soluble	2.2
	hist/K^+	soluble	2.5
	nita/$3Na^+$	soluble	2.1
	nita/$3NEt_4^+$	soluble	2.0
	citrate/$3Na^+$	soluble	1.2
	citrate/$3NEt_4^+$	soluble	1.1
	citrate/3choline$^+$	soluble	1.7
	detpa/$5Na^+$	soluble	2.3
$MoI_2(CO)_3L_2$	CH_3CN	insoluble	1.1
	Cy-DAB	insoluble	0.9
	p-tolil-DAB	insoluble	1.0
$Fe(CO)_4L_2$	I	insoluble	1.4
$[Ru(CO)_3L_2]_2$	Cl	insoluble	0.0
$[Ru(CO)_3Cl_2L]$	DMSO	sp soluble	0.0

	methionine oxide	soluble	0.0
	methionine	soluble	0.0
	DAPTA	soluble	0.0
$[Ru(CO)_3ClL_2]$	glycinate	soluble	0.0

* highly unstable; CO release rate not properly determined

The family of the Mn^I complexes, $Mn(CO)_5L$, is a good starting point for this discussion because its substitution chemistry has been extensively studied in organic solvents and under anaerobic conditions. In spite of its low solubility $Mn(CO)_5Cl$ releases 2 equivalents of CO after 6 hr. This is in line with the typical substitution chemistry of the $M^I(CO)_5$ fragment of the group 7 metals that is well known to readily lose two *cis* CO ligands leading to a *fac*-$Mn^I(CO)_3$ fragment which is rather inert in terms of CO substitution as expected for a d^6 octahedral coordination. The substitutional inertness of the *fac*-$Mn^I(CO)_3$ fragment is very well exemplified by the complex $[Mn(CO)_3(TACN)]^+$ which is readily made from $Mn(CO)_5Br$ and neutral TACN. It is fully soluble in RPMI and yet does not release CO under our standardized conditions as already mentioned above.

All the other $Mn(CO)_5L$ complexes listed release less CO than $Mn(CO)_5Cl$ in the same time period. The order of decreasing CO release $Cl^- > Br^- > CF_3SO_3^- > CH_3^- > {}^-CH_2C(O)NH_2$ can be expected considering that the π-donor capability of the L ligands decreases in the order $Cl^- > Br^- > CF_3SO_3^- > CH_3^-$. Under anaerobic and non-protic conditions the predicted order of CO release should be exactly the same judging from published data.[16-18] This type of data was the basis for Angelici's rule of thumb:[19] harder bases are stronger labilizers. As it was already briefly mentioned in the introduction, strong σ-donors are also CO labilizers. The expected stronger σ-donor character of CH_3 compared to that of $CH_2C(O)NH_2$ is in agreement with the somewhat stronger labilization of the former. In any case, both alkyl substituents fall well below the labilizing power of the halides and triflate. The position of triflate in this series is an exception to Angelici's rule of thumb since in Pearson's sense[20] it is an harder base than halides.

Since these Mn^{I} complexes are all rather air stable, it seems that their CO release profile is being controlled by their kinetic CO lability. In organic, non-polar solvents these processes are dissociatively activated. However, our measurements do not allow confirming the substitution mechanism in these aqueous biological solutions because even the substituent or substituents that replace the broken M-CO bond are not identified and may vary from water solvent to proteins present in the FBS. Deviations from a strictly dissociative process as those reported by Burgess are most likely to take place.[21]

The second group of compounds is composed by Mo^{0} complexes with different numbers of CO ligands. Among these we can find the examples of the few compounds that release high amounts of CO after 6h, that is > 70% of total CO available, namely $[Et_4N][Mo(CO)_5Br]$, $Mo(CO)_4\{4,4'\text{-}(NaO_3SCH_2CH_2OOC)_2bipy\}$, $Na[Mo(CO)_3(hist)]$, $[Mo(CO)_3(\eta^6\text{-}C_7H_8)]$, $Na_3[Mo(CO)_3(nita)]$ and $(Mo(CO)_3(bpa)]$.

One of the fastest CO releasers in this group is the complex $[Et_4N][Mo(CO)_5Br]$ which is also one of the strongest CO releasers of all compounds tested and much stronger that its isoelectronic Mn^{I} counterpart. The compound is only sparingly soluble in water and all attempts to change its counter-ion to an alkaline metal cation failed due to instability of the final product. This was possible with the related iodide which is a much weaker CO releaser. The two other $[Mo^{0}(CO)_5L]$ compounds tested are the cyanide, $Na[Mo(CO)_5(CN)]$ and the phosphine derivatives all of which are completely stable and do not release CO under the standardized conditions. Many attempts to prepare mono-substituted complexes with amines and substituted pyridines invariably led to mixtures of the mono-, di- and tri-substituted complexes, all of which were too unstable to isolate in aqueous solutions where they decomposed upon dissolution liberating CO in an uncontrolled manner. Unlike the rather air stable cyano and phosphino complexes, $[Et_4N][Mo(CO)_5Br]$ is air sensitive.

The comparison between the complexes $[Mo(CO)_5X]^{-}$ among each other and with their $Mn(CO)_5X$ counterparts immediately raises the attention to some important

points. Among the three Mo pentacarbonyl anions $[Mo(CO)_5X]^-$, CO release decreases in the order $Br^- >> I^- >> NC^-$, the later being as stable as the neutral analogues with $P(C_6H_4SO_3Na)_3$ and PTA substituents. This parallels exactly the finding for the relative rates of the $Mn(CO)_5X$ congeners and is in agreement with the order of decrease of the π-donor labilization of these three ligands. In fact, the cyanide ligand, being a π-acceptor is expected and found to prevent CO release. However, the extent of CO release, which is limited to 2 equivalents of CO in the case of $Mn(CO)_5Cl$, is easily exceeded in the case of $[Mo(CO)_5Br]^-$. The CO labilization from Group 6 $[M(CO)_5X]^-$ species was investigated using density functional calculations by MacGregor and MacQueen[22] and was found that the CO labilization was affected by the balance between the energy of the ground state 18-electron $[M(CO)_5X]^-$ species and the relaxation effects of the 16-electron $[M(CO)_4X]^-$ derived species. The results showed that the trends in CO dissociation follow the series $NH_2^- > OH^- > F^- > Cl^- > Br^- > I^- > CH_3^- > H^-$. These are related not only with the ability of X to afford π stabilization of the 16-electron species formed but also with the π destabilization of the 18-electron ground state, which is equally important. The later arises as a direct consequence of the degree of donation from X, which enhances *trans* M-CO π backdonation but reduces *cis* M-CO π backdonation. Furthermore, strong π donation from X also induces *cis* M-CO σ antibonding interactions weakening the M-CO bond.

The further extent of the decarbonylation reaction of $[Mo(CO)_5Br]^-$ can only be explained by the air instability of the $Mo^0(CO)_3$ fragment. Oxidation of the Mo atom by O_2 will lead to the formation of Mo-oxides (ultimately molybdate or polyoxomolybdates) with total liberation of CO being achieved. This exhaustive CO release (5 equivalents released from $[Mo(CO)_5Br]^-$) has been observed both *in vitro* and *ex-vivo* in conditions that are more aggressive that those of the standardized conditions of Fig.1. In fact, with *tert*-butylhydroperoxide within 3h, 4 equivalents of CO are liberated and 1 CO is oxidized and liberated as CO_2 (see compound **17** in table 6 in Chapter III). Also, in sheep blood at 37ºC the 5

equivalents of CO are released to hemoglobin in 1h15min (see compound **2** in table 5 in Chapter IV).

In contrast, the $Mn^{I}(CO)_3$ fragment is stable to O_2 oxidation and resists CO release because the bond strength of the Mn-CO bonds achieves its highest stabilization in the *fac*-$Mn(CO)_3$ conformation. In fact, after replacing two CO ligands from $Mn(CO)_5X$, the three remaining M-CO bonds in the newly formed $Mn(CO)_3L_2X$ are reinforced whenever their *trans*-standing ligands are poorer π-acceptors than the two carbonyls that were replaced. When the substitutions are carried out in biological media, the incoming ligands are essentially O, N or S bound in which case their π-accepting capacity is either inexistent (for N, and O) or marginal for S. The excellent air and water stability of the *fac*-$M(CO)_3$ fragments in the group 7 metals (M = Mn, Tc, Re) is reflected in the extensive work of Alberto, Schibli, Schubiger and collaborators who have produced a very large variety of $[M^{I}(CO)_3L_3]^{0/+}$ (M = Tc, Re) complexes[23-25] that are completely stable with regard to CO release *in vitro* and *in vivo* and can be even excreted intact from animals where they were injected as imaging agents.[26]

This difference in the behavior of the CO release profile of *fac*-$Mo^{0}(CO)_3$ and *fac*-$Mn^{I}(CO)_3$ carbonyl complexes opens the possibility of using $Mo(CO)_3L_3$ complexes as CO releasers. As already mentioned, most of the examples of these complexes collected in Table 3 are quite fast releasers with rather impressive amounts of CO liberated after 6h under the standardized conditions of Fig. 1. However, CO release experiments carried out in the apparatus of Fig. 1, also in the dark but under N_2 showed that the highly water soluble anionic complexes $Na[Mo(CO)_3(hist)]$, $Na_3[Mo(CO)_3(cit)]$ and $Na_3[Mo(CO)_3(nita)]$, are completely stable towards CO loss (see table 4).

Table 4: Equivalents of CO released in H_2O under N_2 in the dark at room temperature.

Time	$Na[Mo(CO)_3(hist)]$	$Na_3[Mo(CO)_3(cit)]$	$Na_3[Mo(CO)_3(nita)]$
6h	0.00	0.00	0.00

The same assays as in Table 4 were repeated under N_2 and ordinary laboratory light. All the compounds released less than 0.1 equiv. CO after 6h, except $Na_3[Mo(CO)_3(nita)]$. However, even in this case the amount of CO released was still marginal: 0.18, 0.29 and 0.29 equiv. CO after 2h, 4h and 6h, respectively. When a water solution of $Na[Mo(CO)_3(hist)]$ is treated with excess sodium histidinate, CO release is noticeably retarded. Taken altogether these results show that the trigger to the extensive CO release observed in the above mentioned Mo^0 complexes is their reaction with O_2. The simple reaction sequence shown in scheme 1 explains these observations. When excess ligand (e.g. histidinate) is present the first equilibrium is pushed to the left and access of O_2 to the Mo atom in the unsaturated 16-electron intermediate is more difficult and the CO release started by the oxidation of Mo^0 by O_2 is retarded.

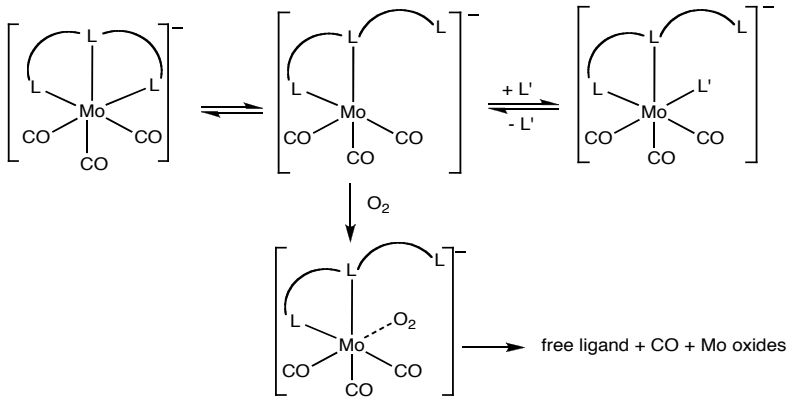

Scheme 1: O_2 attack on the *fac*-$Mo(CO)_3$ compounds leading to CO release and Mo oxides formation

All three binding atoms of the histidinate ligand are different but we have not identified which is the one that is more prone to dissociate as in the first step of

scheme 1. When other tridentate ligands are considered to bind the $Mo^0(CO)_3$ fragment, the situation should be similar to that of the histidinate complex.

Therefore, the difference in total release of CO between the $[Mo(CO)_3(hist)]^-$ or $[Mo(CO)_3(nita)]^-$ and $[Mo(CO)_3(cit)]^-$ is quite surprising and remains unexplained. The decomposition of the histidinate complex is almost complete whereas the citrate complex only releases about one half of its total CO content in the same time span. It is possible that the citrate complex originates dimeric species that are slow to decompose and release CO.

In principle, scheme 1 should be applicable to the description of the CO release process of the macrocyclic derivatives $(TTCN)Mo(CO)_3$ and $(TACN)Mo(CO)_3$. The main difference should arise from the higher rigidity of these macrocyclic rings and their more favorable coordination to the *fac*-$Mo(CO)_3$ fragment which disfavors the opening of a vacant coordination position for attack by O_2. Indeed, $[(TACN)Mo(CO)_3]$, liberates ½ of its CO content after 6h under standardized conditions. The importance of the macrocyclic effect on the stabilization of the $Mo(CO)_3$ fragment becomes evident when this result is compared to the 82% CO release in 6h obtained with the tripodal κ^3-N ligand bpa in $(bpa)Mo(CO)_3$. It is also possible that the reactivity of $(TACN)Mo(CO)_3$ is influenced by other factors, namely pH, because the compound can be oxidized with H^+ or with Br_2 to give characterized Mo(II) complexes $[Mo(CO)_3(TACN)X]^+$ (X = H, Br).[27] Furthermore, the stability of the oxidized complexes is dependent on the nature of the counter-ion since hexafluorophosphate or perchlorate salts give air stable complexes while Br_3^- gives an unstable and explosive complex.

Two other compounds contrast with $(TACN)Mo(CO)_3$: the tripodal κ^3-S macrocycle $(TTCN)Mo(CO)_3$ and the soluble, cationic Mn^I analogue, $[Mn(CO)_3(TACN)][BF_4]$ both of which are completely stable towards CO release under the standardized conditions. On the one hand, it is quite likely that the extremely low solubility of $(TTCN)Mo(CO)_3$ provides a strong protection against oxidation and decomposition. On the other hand, the already discussed stability of *fac*-$Mn(CO)_3$ complexes explains the total inertness of $[Mn(CO)_3(TACN)][BF_4]$.

However, the formal oxidation state of the metal *per se* is not a unique label that codes for oxidative stability because the soluble tris-phosphine complex $[Mo(CO)_3(PTA)_3]$ is totally stable like all the other tested soluble or insoluble PR_3 derivatives of Mo^0, like $[Mo(CO)_5(PR_3)]$ and $[Mo(CO)_4(PR_3)_2]$.

A variety of mono and bidentate ligands has been tested in the family of $[Mo(CO)_4L_2]^{0/n-}$ derivatives. The first surprising result was provided by the bipyridyl derivatives in which case solubility in water causes a strong destabilization of the compounds with a high impact on CO release. In fact, the completely water insoluble $Mo(CO)_4$(bipy) doesn't release any CO under the standardized conditions. However, the introduction of water solubilizing substituents in the bipyridyl rings, such sulfonates and carboxilate substituents at the 4 and 4' positions of the 2,2'-bipyridyl ligand, leads to ready decomposition of the complex and strong CO release. HPLC analysis of aqueous solutions of these soluble complexes reveals that this rapid decomposition takes place in water even under N_2 atmosphere but is clearly faster under air. Therefore, it seems that the high stability of the $Mo(CO)_4$(bipy) was simply due to its total hydrophobicity. Once brought into solution this type of complexes become rather labile and CO is rapidly lost. However, as pointed out by Angelici and Graham when comparing the rates of CO substitution of $Cr(CO)_4$(bipy) and $Cr(CO)_4$(4,4'-Me_2bipy) the higher basicity of the disubstituted bipiridyl might be enough to also explain the higher lability of CO in the case of $Mo(CO)_4${4,4'-$(NaO_3SCH_2CH_2)_2$bipy} *vs.* $Mo(CO)_4$(bipy).[19] In fact, a harder ligand results in higher CO lability.

The vast majority of the diazabutadiene and diimine analogues were also very stable under our standardized conditions but, again, this might be due to the poor solubility of the examples tested so far. Indeed, the only compounds able to release CO in measurable amounts are the 4,4'-substituted bipyridils that could be partially or totally solubilized. Nevertheless, imparting solubility to these complexes still remains a real challenge.

The instability of the complexes with diamine type ligands is even higher and clearly accelerated by O_2. For instance, the fairly air stable $Mo(CO)_4$(methyl-piperazine)$_2$ decomposes very rapidly when dissolved in water or under the standardized conditions. The traces of HPLC solutions in water under normal atmosphere show a mixture of several decomposition products among which $Mo(CO)_6$ seems to be always present. However, if the same experiment is performed under N_2 its stability highly increases and no decomposition is observed within 6h.

Complexes with β-diketone ligands, e.g. acetylacetonate,[28] have a decomposition profile rather similar to that of the amines and $Mo(CO)_6$ is also identified as a decomposition product in HPLC analysis of aqueous solutions.

Only one Mn complex of the type $Mn^I(CO)_4L_2$ was tested under our standardized conditions: $Mn^I(CO)_4(S_2CPh)$. No CO release was observed within 6h but since only one example of Mn-dithiolate ligand was tested no conclusions can be drawn from this result, whether this observed stability is due to the insolubility of the complex or it's overall stability.

Another example showing that hydrophobicity alone does not prevent CO release is provided by $Fe(CO)_4I_2$ which is insoluble in RPMI and yet releases CO both under N_2 and O_2. Comparatively to other iodide substituted MCCs this is a rather unexpected behavior, since all the iodide derivatives showed low CO release rates. The fast rate of CO exchange for $Fe(CO)_4I_2$ with ^{14}CO was reported by Wojcicki and Basolo[17] and described as an associative mechanism. This was attributed to a greater positive charge on Fe, tending to promote nucleophilic attack, which in the present case, in a rich nucleophilic environment like RPMI should lead to a high CO release rate (as observed).

Rather unexpectedly, we observed that the derivatives of the $Ru^{II}(CO)_3$ fragment do not release CO to the headspace of their aqueous solutions irrespectively of the variety of ancillary ligands that has been used. At least, they do not do so to a concentration level that can be monitored by GC-TCD. In this sense they form a different class of CO releasers which has been reported to mediate a variety of

biological activities allegedly via CO delivery.[29, 30] The chemistry of these metal carbonyls is rather different from that of the octahedral Mo^0 and Mn^I analogues and will be dealt in Chapter V.

One further comment should be made on the influence of the counter-ions in the CO release from ionic complexes because the development of ionic compounds for pharmaceutical applications encompasses some important, particular issues. The nature of the counter-ion influences the solubility as well as the stability of the complex and its choice is also dependent on toxicological effects. Therefore, the choice of the counter-ion is not a secondary aspect and has to be taken into account when considering an ionic compound to become a drug candidate.

For anionic complexes sodium and potassium are logical first choices as counter-cations since they are ubiquitous ions in the body performing a variety of known functions. The ratio sodium/potassium concentrations in intercellular and extracellular fluids is responsible for the transport ions through the cellular membranes (ionic channels), the regulation of the osmotic pressure inside the cell, the transmission of nervous pulses and other electrophysiological functions[31] therefore our system is already prepared to handle these ions.

However, from the point of view of drug development it is not always possible to use sodium or potassium as cations due to the constraints that charge or size introduce in the lattice energy of the ionic compounds. In fact, organometallic chemistry rarely uses alkali metal ions as counter-ions to organometallic anions because the resulting solid state structures are not stable due to the very large difference in the ionic radii of both cation and anion. In practical terms, tetraalkylammonium, crown-ether complexes of alkali ions and a few other large organic cations or anions are used to produce stable, ionic solid state lattices. Pharmaceutically acceptable cations are very few, choline and lysine being the most often used.[32] Organometallic complexes with large anion/cation combinations are usually soluble in organic solvents where their purification and spectroscopic characterization is much easier than in water. Although facilitating compound purification, this low water solubility is not a desirable property for

biological and pharmaceutical useful compounds and poses severe problems to our screening studies. As an example, Fig. 4 shows the variations observed in the amount of CO released by the sparingly water soluble $[Et_4N][Mo(CO)_5Br]$ along seven independent tests all under the same nominal standardized conditions.

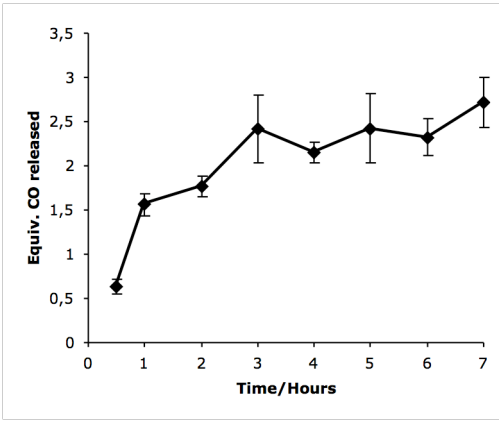

Figure 4: Average of seven CO release experiments of $[Et_4N][Mo(CO)_5Br]$ performed in the apparatus of Fig. 1 in RPMI(10%FBS) under CO_2 free air, at room temperature and 37ºC.

A series of pentacarbonyl $[Mo(CO)_5I]^-$ complexes was prepared in diglyme solvent as the sodium, potassium, ammonium and tetraalkylammonium salts. Attempts to prepare divalent calcium and magnesium cations led to a rather unstable 1:2 complex with two $[Mo(CO)_5I]^-$ anions *per* Ca or Mg cation. They could be characterized but decomposed very rapidly, showing that salts of $[Mo(CO)_5I]^-$ with small dications are not stable enough for practical use.

The complexes prepared with small cations, such as sodium, potassium and ammonium held coordinated diglyme molecules. In this way the small cations are spontaneously turned into large cationic species with the diglyme coordinating the small cation. This is very similar to the effect obtained by coordinating the cation to a crown-ether and also results in enhanced lattice stability. The same effect is observed with sodium salts of hydride carbonyls.[33] Nevertheless, the sodium and potassium salts both released similar amounts of CO with differences of only 4%. The ammonium salt released slightly less CO but the variations expected for tests with poorly soluble compounds absorb well this difference. In abstract, the same rate was expected due to similar stability in solution that would be provided by K^+ and NH_4^+since they have similar hydrated radii (1.45Å). Both the Na^+/crown-

ether and tetrabutylammonium salts present a less extensive CO release which we believe is mainly due to their lower solubility.

Looking further at the data in table 3, it is immediately apparent that the nature of the counter-ion does not influence the CO release profile of a given ionic MCC provided the complexes are soluble. Taking the fully soluble anionic $[Mo(CO)_3(hist)]^-$ complexes as an example, it is clear that the values obtained for the sodium and potassium salts only differ by 10%. The results obtained for the $[Mo(CO)_3(nita)]^-$ and $[Mo(CO)_3(cit)]^-$ families of complexes essentially corroborate the above conclusions in spite of the wider variations in size of the counter-ions. The choline derivative of the $[Mo(CO)_3(cit)]^-$ releases a slightly higher amount of CO after 6h but the difference is not drastic. It is clear and somehow expectable that the release of CO is being triggered by the reactivity of the MCC anion independently of the cation since they are both separated in the strongly polar aqueous solutions.

Besides the influence of the counter-ion it was also studied the influence of pH variation on CO release. The interest of studying the effect of pH on the rate of CO release of metal carbonyl based CO-RMs results from several practical reasons. The first one relates to the need of improving solubility of the compounds in aqueous media. In general, and excepting the ionic compounds with Na^+, K^+ or halide counter-ions, most organometallic complexes are rather lipophilic and have very limited solubility in aqueous solutions. This lipophilicity, which increases with the number of CO ligands, imposes a very strong limitation on the selection of MCCs to act as CO-RMs because it hampers the possibility of testing them both in cell culture tests *in vitro* and in injectable administrations *in vivo*. One of the ways to circumvent this difficulty takes advantage of the possible protonation of some uncoordinated functions present in the ligands thereby forming water-soluble cationic species. Once solubilized in the appropriate buffers such species may remain soluble for testing and/or administration. However, this approach also relies on the stability of the MCCs at the low pH values needed for protonation.

The other interest of testing the CO release profile of CO-RMs with pH variation has to do with the fact that pH variations may be used as passive targeting for CO delivery to specific tissues/cells and also because oral administration subjects the drugs to extensive pH variations in their transit through the gastrointestinal track. The values of the pH in the different tissues of an animal are not all exactly the same, as can be seen in Table 5.

Table 5: pH Values of Human Body fluids and secretions[34]

Body Fluid or Secretion	pH
Blood	7.4
Milk	6.6-6.9
Hepatic Bile	7.4-8.5
Gall bladder bile	5.4-6.9
Urine (normal)	6.0
Urine (in various disease states)	4.8-7.5
Gastric juice (parietal secretion)	0.87
Pancreatic juice	8.0
Intestinal juice	7.7
Cerebrospinal fluid	7.4
Saliva	7.2
Aqueous humor of eye	7.2
Tears	7.4
Feces	7.0-7.5
Muscle cells, resting (at 37ºC; extracellular pH=7.4)	6.94-7.06 (intracellular)

These variations, albeit small, may provide the basis for passive drug targeting. Using pH sensitive compounds the local release of CO can be enhanced or decreased, according with the desired effect. In diseases like duodenal ulcer, gastric ulcer and gastroesophageal reflux where a strong inflammatory component is present, a local CO delivery promoted by acidic pH would be ideal for oral applications. It is, therefore very important to determine the behavior of CO-RMs in water at an acid pH that mimics stomach conditions and also at basic pH, which mimics the intestine where most of the drugs are absorbed.

In the initial stages of the biological research on CO-RMs the family of $[Mo(CO)_3L_3]^{0,/z-}$ derivatives stood up as a very useful one. More importantly, many of them were capable of releasing well defined amounts of CO *in vivo* guiding the initial studies of CO-RM activity which were interpreted under the light of existing CO inhalation data. The most versatile compound was the aminoacid derivative $[Mo(CO)_3(hist)]^-$, which proved therapeutically effective in many animal models of inflammatory diseases including the prevention of

stomach ulcers induced by non-steroidal anti-inflammatory drugs (NSAIDs). Since this involves delivery to the stomach it seemed reasonable to select this family of compounds to study of the effect of pH variations on the CO release profile of a CO-RM. All studies were done under normal aerobic conditions and the results are summarized in table 6.

Table 6: Equivalents of CO released in H_2O (pH=2.5), distilled water (pH~5.5), PBS 7.4 and H_2O (pH=8.5) in the dark, in air (2h; 4h; 6hours).

Compound	H_2O (pH 2.5)	H_2O (pH~5.5)	PBS (pH 7.4)	H_2O (pH 8.5)	Time
$Na[Mo(CO)_3(hist)]$	1.3 1.5 1.4	2.3 2.5 2.5	2.7 2.8 2.8	2.7 2.9 2.7	2h 4h 6h
$Na_3[Mo(CO)_3(cit)]$	--- 0.8 0.8	1.2 1.2 1.2	1.3 1.4 1.4	1.4 1.2 ---	2h 4h 6h
$[choline]_3[Mo(CO)_3(cit)]$	---	1.3 1.4 1.3	1.1 1.1 1.1	---	2h 4h 6h
$Na_3[Mo(CO)_3(nita)]$	1.0 0.9 1.0	1.6 1.5 1.6	2.1 2.1 2.3	1.4 1.4 1.4	2h 4h 6h
$Na_5[Mo(CO)_3(detpa)]$	1.4 1.4 1.3	2.6 2.8 2.9	3.0 3.1 3.2	3.6 3.6 2.6	2h 4h 6h

After 2h the CO released by these compounds to the headspace is already very close to the maximum amount obtained after 6h, showing that the reaction is very fast in all the media tested. $Na_5[Mo(CO)_3(detpa)]$ is quantitatively decarbonylated after 2h in distilled water or PBS solutions and in basic pH surpasses the total amount of carbonyls present in the molecule (3), suggesting a base-catalyzed decomposition of the organic ligand detpa. Some reproducibility problems were found and the values in table 6 are arithmetic means of several independent tests. The major trigger for CO release is O_2, and since the amount of O_2 present in each experiment is not controlled the CO release may vary accordingly. This issue will be addressed later in Chapter III. However, these differences were more common during the first 2 to 4 hours of the assay but after the 6h the final values were very

similar. Even when the initial CO release was much higher the reaction tended to the same end-point and the final amount of CO liberated was the same.

In order to check these observations, the reactions were analyzed at earlier time points to see CO evolution in the first 2h in PBS7.4 and distilled water.

The results obtained in these short-term assays are summarized in table 7 and complete those of table 6.

Table 7: Equivalents of CO released in distilled water and PBS7.4, in air, in the dark at room temperature at 30min, 1h, 1h30min and 2h.

Compound	**H_2O (pH~5.5)**	**PBS (pH 7.4)**	**Time (Hours)**
$Na[Mo(CO)_3(hist)]$	0.9	0.8	0.5
	1.9	1.3	1
	2.1	1.9	1.5
	2.2	2.2	2
$Na_3[Mo(CO)_3(cit)]$	0.5	0.5	0.5
	0.8	0.6	1
	1.1	1.0	1.5
	1.1	1.2	2
$Na_3[Mo(CO)_3(nita)]$	0.8	1.1	0.5
	1.4	1.6	1
	1.7	1.7	1.5
	1.7	1.7	2
$Na_5[Mo(CO)_3(detpa)]$	1.5	1.2	0.5
	2.1	2.0	1
	2.5	2.3	1.5
	3.0	2.5	2

The compounds $Na_3[Mo(CO)_3(hist)]$ and $Na_5[Mo(CO)_3(detpa)]$ are the fastest and most extensive releasers that is, both in percentage of CO released and also in speed. After 2 hours, in water, the 3 COs are released by $Na_5[Mo(CO)_3(detpa)]$ and almost all by $Na[Mo(CO)_3(hist)]$ (88%). It is interesting to note that $Na_5[Mo(CO)_3(detpa)]$ loses 2 COs in the first 30 min, probably with O_2 playing a very important role in this initial burst. The other 2 compounds are more stable, $Na_3[Mo(CO)_3(nita)]$ releases roughly half of the available COs and reaches a plateau of 1.7 equivalents after 1h30m. $Na_3[Mo(CO)_3(cit)]$ is the compound that releases less CO in water, only 1 equiv., also after 1h30m.

$Na_3[Mo(CO)_3(cit)]$ and $Na_3[Mo(CO)_3(nita)]$ have very similar profiles both in PBS and in water suggesting that they are not dependent on the interference of the electrolytes present in PBS. $Na_5[Mo(CO)_3(detpa)]$ and $Na_3[Mo(CO)_3(hist)]$ show a higher variability in the results particularly at the initial times which may be related to their higher sensitivity to variations in the concentration of O_2.

Overall, $Na_3[Mo(CO)_3(cit)]$ has a different profile from its ionic $[Mo(CO)_3L_3]^{0,/z-}$ analogues. It releases less than 50% of the total amount of CO and shows similar kinetics in RPMI, PBS and water. The oxidation of this complex could in principle lead to an analogue of the known compound $K_4[MoO_3(cit)]\cdot H_2O$[35] however as we can see from the GC results this isn't the case. To some extent $Na_3[Mo(CO)_3(nita)]$ is similar but the amounts of CO released are slightly higher. No consistent explanation for these facts has yet been reached.

The HPLC trace of a $Na_3[Mo(CO)_3(cit)]$ and $[choline]_3[Mo(CO)_3(cit)]$ in water solution under normal atmosphere conditions shows a decomposition profile in which $Mo(CO)_6$ raises concentration, similarly to what as been observed with the diamine and β-diketonate complexes (Fig. 5).

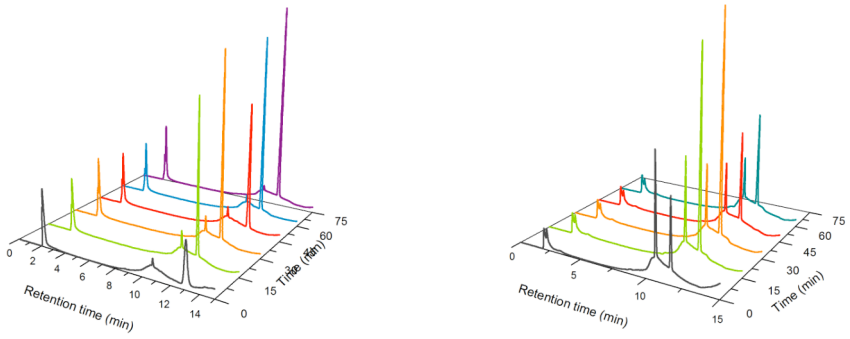

Figure 5: **Left:** HPLC trace of a water solution of $Na_3[Mo(CO)_3(cit)]$ under air at room temperature over 75 min. At the time of dissolution (t=0), the product is observed at RT= 10.78 min, $Mo(CO)_6$ formation is observed at RT=13.7 min and Na_2MoO_4 at RT=2.29 min. After 15 min, $Mo(CO)_6$ RT is 12.12 min. **Right:** HPLC trace of a water solution of $[choline]_3[Mo(CO)_3(cit)]$ under air at room temperature over 75 min. At the time of dissolution (t=0), the product is observed at RT=11.03 min, $Mo(CO)_6$ formation is observed at RT=12.04 min and $[choline]_2MoO_4$ at RT=2.22 min. After 15 min the product is observed at RT=10.68 min and $Mo(CO)_6$ formation is observed at RT=11.72 min.

An early peak is also eluted at RT~2.32 min and the UV absorbance spectrum is similar to that of sodium molybdate. $Mo(CO)_6$ typically raises concentration in solution until saturation and then precipitates decreasing its concentration in solution.

In spite of the structural similarities of the complexes, and their high activity as CO releasers, some interesting trends are still observable. First, the general tendency demonstrated in these results is that the stability of the compounds decreases as the pH increases, that is, compounds tend to be more stable under acidic conditions. This trend is most likely due to the nucleophilic displacement of the ligands by excess HO^- at higher pH. Given its high CO labilizing power, the hydroxide ligand will accelerate the overall rate of CO substitution. In the case of the $[Mo(CO)_3(hist)]^-$ complex deprotonation of a coordinated NH_2 ligand at higher pH will also result in strong CO labilization by the amido $-NH^-$ ligand. This kind of effect is known in the chemistry of ammine and amino complexes of classical Werner type coordination complexes (no organometallic ligands).[36] In practical terms this also means that these chemically sensitive and highly active CO-RMs can be administered orally and are likely to survive the acidic conditions in the stomach.

Another interesting observation is that in spite of its basic pH, RPMI seems to slightly slow down CO release in all cases except that of $[choline]_3[Mo(CO)_3(cit)]$ (see tables 4 and 6). This retarding effect is more pronounced in the earlier period of the reaction, that is, up to 2h reaction time. Given the complexity of the composition of RPMI we cannot assign a clear reason to this stabilizing effect. Nevertheless, the hypothesis that this initial retardation is due to the protective, anti-oxidant effects of species present in the RPMI/FBS mixture is quite strong. Likewise, the hypothesis of the stabilization by interaction of the CO-RMs with the RPMI/FBS proteins cannot be discarded. In any case, the suggestion that a biological environment may protect the MCC against fast decomposition seems plausible and improves the confidence on the use of metal carbonyl complexes as therapeutic CO-RMs.

4.2 CO release profiles of the polyene and polyenyl carbonyl complexes

Contrary to the classical N and O ligands, and similarly to CO, the bonding of alkenes, dienes, arenes and their anionic counterparts (like cyclopentadienyls) to metal atoms or ions, also contains a strong and decisive component of π-backdonation. However, this contribution relative to σ-donation varies widely across this series of ligands and it shows a strong dependency on the substituents attached to the sp^2 carbons of these ligands.

In general, alkene ligands in carbonyl complexes are quite labile because CO removes most of the electronic π-density and weakens the (alkene)-M backbonding. Of course, a decrease in the number of CO ligands around a given metal improves the stability of eventual neutral polyalkene or arene ligands. In this work we only dealt with one such polyene-carbonyl complex, namely the cycloheptatriene (CHT) derivative $[(\eta^6\text{-}C_7H_8)Mo(CO)_3]$. The substitution kinetics of this complex has been reported in the literature long ago in many solvents and with many nucleophiles under anaerobic conditions, but the result was always substitution of the CHT ligand by three incoming nucleophiles, leaving the three CO ligands as unchanged spectators.[18] These reactions are usually dependent on the concentration of the incoming ligands and have a fascinating kinetic and mechanistic subtlety, which is highly relevant for the understanding of the chemistry of coordinated olefins in catalytic transformations. However, in the present case, the fact that the reactions are being studied under O_2 results in very fast molecular substitution and decomposition with strong release of the CO ligands. In fact, $[Mo(\eta^6\text{-}C_7H_8)(CO)_3]$ is completely water insoluble and totally stable under N_2 in water suspension. However, under O_2 its suspensions rapidly decompose with quite fast and extensive liberation of CO (76% of total CO; see table 6). One could imagine that if such complex was water soluble, its CO release kinetics would probably be among the fastest examined. This is also understandable if one notes that water as well as most other ligands present in

RPMI/FBS are not π-acceptors and the majority are even π-donors. Such π-donors which were mentioned above to aptly labilize M-CO bonds are even more efficient in labilizing M-alkene bonds since these have a weaker π-accepting component and are, therefore, more fragile.

This kind of reactivity is expected to be followed by arene complexes but we haven't studied any of those (see reference [18] and references cited therein). However, their isoelectronic 6-electron donor counterparts, the cyclopentadienyls were intensively studied and represent a different reactivity paradigm.

The cyclopentadienyl, $[\eta^5\text{-}C_5H_5]^-$ ligand (usually abbreviated to Cp) and its substituted analogues, $[\eta^5\text{-}C_5H_{5-n}R_n]^-$ (generally abbreviated as Cp'), are aromatic, planar, carbanionic ligands that possess a set of orbitals with a geometry and electronic energy which is almost ideal to coordinate transition metals. In this coordination the metal sits on the middle of the Cp ring with all carbon atoms equidistant. Formally this ligand provides three electron pair (6 electrons) and occupies three coordination positions. In this way, a complex like $[CpM(CO)_3]^{z\pm}$ can be regarded as a distorted octahedron where the Cp ligand occupies one face and the three carbonyls occupy the opposite one, as sketched in figure 6.

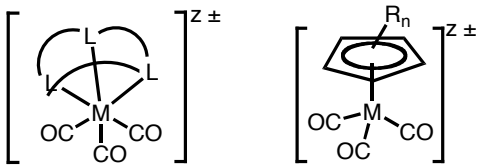

Figure 6: Comparison between the $CpM(CO)_3$ and $(\kappa^3\text{-}L)M(CO)_3$ octahedral structures.

This privileged bonding mode generates a very strong stability on the Cp-M fragment which retains its coordination almost unchanged across a very wide set of chemical transformations of their complexes. In other words, the Cp ligand usually behaves as spectator to the chemistry that takes place with the other ligands of the complex. It is this fact that explains the ubiquitous presence of Cp-M complexes in organometallic chemistry since this kind of ligand accommodates a wide variation of metals, oxidation states and ancillary ligands. The exhaustive

oxidative decarbonylation shown in scheme 2 which spans six (!) oxidation states exemplifies the extension of this capacity of electronic accommodation and metal binding of the Cp type ligand.[37]

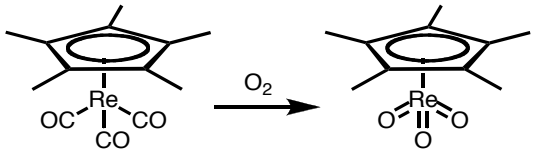

Scheme 2: Six electron oxidative decarbonylation of $Cp^*Re^{I}(CO)_3$ to $Cp^*Re^{VII}O_3$.

Within this framework one may expect that complexes $[Cp'M(CO)_xL_y]^{z\pm}$ containing both Cp type ligands, CO and group 6-8 metals, will display useful CO releasing profiles. CO substitution kinetics will follow the same D, A or Id/Ia paradigms (see Chapter I, section 4) found for octahedral CO complexes as summarized by Howell and Burkinshaw on the basis of reactions carried out in organic solvents under anaerobic conditions.[18]

Table 8 collects some appropriate data on selected complexes with the unsubstituted Cp ligand.

A first inspection of this table immediately reveals that the cyclopentadienyl complexes examined are rather inert with regard to CO loss, and therefore poor CO releasers.

In the case of the derivatives of the $CpFe^{II}(CO)_2$ fragment only the Cl, Br and carboxylate derivatives liberate CO after 6 h in RPMI, at 37°C, under air and in the dark. All the alkyl and acyl derivatives, as well as the iodide $CpFe(CO)_2I$, are completely inert under these conditions. These variations closely follow those observed for instance in the $Mn(CO)_5X$ family and the underlying factors pertaining to CO labilization are certainly the same. Reverse migratory insertion of the CO in the acyl complexes is obviously playing no role under these mild biological conditions since both acyl complexes are completely stable. This reaction would need the initial dissociation of one CO ligand in agreement with

the fact that it is either photochemically activated or thermally activated above 130°C for 2h.[38, 39]

Table 8: Solubility in the medium and equivalents of CO released by $CpM(CO)_xX$ complexes of Mo, Fe and Ru in RPMI (10% FBS), at 37ºC after 6h in the dark.

Family of compounds	**X group**	**Solubility**	**Equivalents of CO released in RPMI after 6h**
$(\eta^6\text{-}C_7H_8)Mo(CO)_3$	---	insoluble	2.3
$CpFe(CO)_2X$	Cl	sp soluble	0.5
	Br	sp soluble	0.3
	I	insoluble	0.0
	$OCOC_6H_4OBF_2$	sp soluble	0.2
	CH_3	sp soluble	0.0
	CH_2Ph	insoluble	0.0
	$COCH_3$	insoluble	0.0
	COC_6H_5	insoluble	0.0
	$CH_2CH_2CH_2Cl$	immiscible oil	0.1
	CH_2CONH_2	soluble	0.0
	CH_2COOH	soluble	0.0
$CpRu(CO)_2X$	Cl	insoluble	0.0
	I	insoluble	0.0
$CpMo(CO)_3X$	Cl	sp soluble	0.4
	I	insoluble	0.0
	$OCOC_8H_6OBF_2$	insoluble	0.2
	CH_3	insoluble	0.0
	CH_2CONH_2	soluble	0.7
	CH_2COOH	insoluble	0.8
	$CH_2CONHCH_2OH$	soluble	0.2
	$CH_2COOC(CH_3)_2C_6H_5$	insoluble	0.0
	$CH_2CONHCH_2COOMe$	insoluble	0.0

The increase in the strength of Ru-X bonds compared to the Fe-X bonds in analogue compounds justifies the high stability of both halide derivatives $CpRu(CO)_2X$ (X = Cl, I).

The $CpMo(CO)_3X$ complexes show some similarities and differences when compared to their Fe analogues. Again, the chloride complex $CpMo(CO)_3Cl$ is a better CO releaser than its iodide and methyl analogues. The carboxylate ($OCOC_6H_4OBF_2$) derivatives of both families have a similar behavior. In contrast to the $CpFe(CO)_2X$ family, both $CpMo(CO)_3(CH_2CONH_2)$ and $CpMo(CO)_3(CH_2COOH)$ are better releasers than $CpMo(CO)_3Cl$. One might argue that the solubility of $CpMo(CO)_3(CH_2CONH_2)$ may facilitate its decomposition. However, $CpMo(CO)_3(CH_2COOH)$ is completely insoluble and still presents a slightly higher amount of CO released. Indeed, there seems to be no clear predictability regarding CO release since, for example, $CpMo(CO)_3(\eta^1$-N-maleimidato) was already used as labeling tool and showed high kinetic stability.[40]

The relatively good thermal and oxidative stability of the alkyl derivatives of this family has been noted.[41, 42] In this family of compounds, CO release is often attained by photochemical substitution reactions[43] or nucleophilic substitution with e.g. phosphines[44], arsenites[45], NO or under harsh thermal conditions[46] not found in biological environments.

In a thorough study of $CpM(CO)_3(CH_2CONH_2)$, $CpM(CO)_3(CH_2COOH)$ and close analogues (M = Mo, W), Bergman and coworkers identified a facile photo induced or chemical loss of CO form these compounds which is stabilized by the formation of an oxa-allyl complex. The same authors also report that the Mo complexes are less stable than those of tungsten which provided the basis for most of their work.[47]

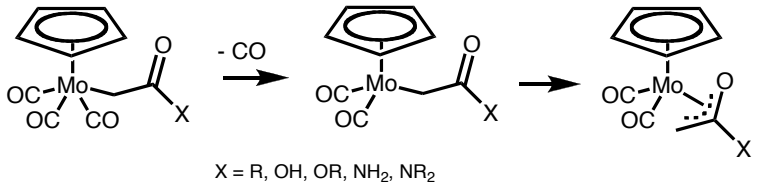

Scheme 3: Conversion of η^1-enolates into η^3-oxa-allyl complexes induced by CO loss

We believe that the stabilization caused by this η^3-ligand may assist the unexpectedly faster CO loss from these compounds when compared to their simple alkyl counterparts which are inert. Dissociation of CO would be immediately assisted intramolecularly by the haptotropic change from η^1-$CH_2C(O)X$ to η^3-$CH_2C(O)X$, facilitating CO loss from the molecule (scheme 3).

In fact, aqueous solutions of $CpMo(CO)_3(CH_2CONH_2)$ under N_2 atmosphere slowly acquire a green tinge and liberate CO slowly over 24h in the dark. The same color change is rapidly seen and goes to deep blue within a few hours when the aqueous solution is exposed to ordinary laboratory light. In both cases this color change is accompanied by CO release.

The similar conversion of the allyl complex $CpMo(CO)_3(\eta^1$-$CH_2CHCH_2)$ to $CpMo(CO)_2(\eta^3$-$CH_2CHCH_2)$ and of $CpMo(CO)_3(\eta^1$-$CH_2C_6H_5)$ to $CpMo(CO)_2(\eta^3$-$CH_2C_6H_5)$ are classic textbook examples of this type of reactivity.[48-52]

Although it is only superficially understood, it is clear that the nature of the ligands is able to tune CO release rates, either by modifying the complex stability or by simply changing solubility and/or redox potential. The presence of different substituents in the Cp type rings provides another handle to attempt fine tuning CO release profiles. A number of complexes containing modified Cp rings were prepared and tested and the results are summarized in table 9.

Table 9: Solubility in the medium and equivalents of CO released by Cp'$Mo(CO)_3L$ complexes (where L is Cl, I or Me) in RPMI (10% FBS), at 37ºC after 6h in the dark.

Family of compounds	RR' group	Solubility	Equivalents of CO released in RPMI after 6h
$(\eta^5\text{-}C_5R_4R')Mo(CO)_3Cl$	R=R'=H	sp soluble	0.4
	R=H; $R=CO_2CH_3$	sp soluble	0.2
	$R=R'=CH_3$	insoluble	0.0
	R=Ph; R'=OH	insoluble	0.0
$(\eta^5\text{-}C_5H_4R)Mo(CO)_3I$	H	insoluble	0.0
	COOH	sp. soluble	0.1
$(\eta^5\text{-}C_5H_4R)Mo(CO)_3CH_3$	H	insoluble	0.0
	CH_2CH_3	imisc. liquid	0.0
	$CH_2CH_2CH_3$	imisc. liquid	0.0
	$CH_2CH_2CH_2CH_3$	imisc. liquid	0.0
	$CH_2C_6H_5$	insoluble	0.0

Changing substituents on the Cp ring may induce some changes in solubility as well as in the strength of the M-Ligand bonds in the complex. Alkyl substituents will increase the electron donor power of the cyclopentadienyl ring and will reinforce its bond as well as the M-CO backbonding. This seems to be the case if we compare $CpMo(CO)_3Cl$ with $(C_5Me_5)Mo(CO)_3Cl$. On the other hand, COOH or COOR substituents will decrease M-CO backdonation, and eventually facilitate CO release, as suggested by the difference between $(C_5H_4COOMe)Mo(CO)_3Cl$ and $CpMo(CO)_3Cl$ or $(C_5H_4COOH)Mo(CO)_3I$ and $CpMo(CO)_3Cl$. However, these effects are not very strong and only cause minor changes in the total amount of CO released. This attests to the high chemical stability of the cyclopentadienyl carbonyl complexes.

The same Mo-CO bond weakening is promoted by the introduction of a COOH group in the cyclopentadienyl of the $CpMo(CO)_3I$ complex, forming a slightly more water soluble complex but no differences were attained in the CO release rate.

The $(\eta^5\text{-}C_5H_4R)Mo(CO)_3CH_3$ family with several alkyl chains bound to the Cp ring didn't reveal any differences in terms of either CO release or water solubility. On the contrary, the structural changes prompted different and important toxicological responses that will be discussed in the next section. As the result of this unexpected hurdle in the biological activity of Cp containing complexes, these studies were discontinued and no further correlations/observations were established. In the literature there is one study around a family of $Cp'Fe(CO)_2X$ complexes as CO donors but CO release is not measured chromatographically in the headspace of the solutions of the compounds making it impossible to draw comparisons with these results.[53]

4.3 Toxicity of cyclopentadienyl metal carbonyl complexes

The main goal of most studies reported in this dissertation is to provide as much information as possible about the compounds behavior in diverse situations so that this information may be used as a useful tool to develop or improve existing biologically active molecules. Although toxicity lies aside the central topic of this discussion, the importance of the issue justifies the following excursion.

The structural modifications introduced are often the most chemically logical ones but like it was demonstrated before, they may carry major biological consequences. Toxicity is a broad field to which many factors contribute and simple changes may accomplish major differences in the toxicological profile of the molecule.

The toxicity of aromatic rings, namely benzene and cyclopentadienyl ring in metal carbonyl complexes was first reported by Strohmeier in 1963 and became documented through studies on methylcyclopentadienyl manganese tricarbonyl (MMT) and cyclopentadienyl manganese tricarbonyl (CMT).[54, 55]

Animal studies have shown that exposure to MMT can result in damage due to accumulation in the liver, kidney, lungs and brain[56-59] and neurotoxicity studies showed that seizure activity and death was related and could be due to GABA-A

activity.[60, 61] The analogous compound CMT, which doesn't have a methyl substituent in the Cp ring, presents a similar toxicological profile. [62-65]

In our studies we observed that compounds of the form $CpM(CO)_xCl$ (where M is Mo and x=3 or M=Fe, Ru and x=2) or $CpMo(CO)_3CH_3$ showed highly toxic profiles with very low MTDs (typically < 10 mg/Kg). By introducing long or bulky alkyl substituents in the Cp ring we were able to decrease the toxicity profile, both by preventing seizures and increasing MTD by more than 50-fold.

It was already demonstrated that the intrinsic CO releasing potential doesn't change with the alkyl chain length (see table 9) but the *in vivo* toxicity study showed that the structural modifications allowed an increase of the MTD. The longer and bulky chains reduced the seizures and lethality in a direct fashion. The reasons for this behavior are still unknown, but it is clear that the changes in the toxicological profile are due to steric effects.

4.4 CO release profile from cyclodextrin-encapsulated complexes

Another potentially interesting approach to the modification of CO delivering systems based on metal carbonyl complexes involves the use of cyclodextrins (CDs) as protective agents.[66-70] CDs are cyclic oligosaccharides that form inclusion complexes with a wide range of molecules, including organic molecules, inorganic ions and organometallic species.[71-75]

The use of CDs as carrier devices to promote controlled release, to improve solubility, half-lives or bio-availability is nowadays a widespread technique with success with many drugs.[76-79]

Organometallic complexes immobilized in CDs often exhibit markedly different physical and chemical characteristics compared to the bulk material, for example in their nonlinear optical properties, ligand substitution/insertion reactions and catalysis.

CDs are known to host a broad variety of half-sandwich metal carbonyl compounds containing Cp and η^6-arene rings like ferrocene derivatives,

metallocene dihalides and aromatic ruthenium (and chromium) compounds. In these compounds the CDs act as second-sphere ligands non-covalently attached to the first-sphere ligands of the metal centre.

Given the limited solubility of many MCCs in aqueous physiological media, the "true" potential of many complexes has not been realized or even evaluated. Therefore, the inclusion of MCCs in modified CDs such as 2,3,6-tri-*O*-methyl-β-cyclodextrin (TRIMEB) may circumvent this problem. Hydrophobic molecules encapsulated in cyclodextrins would then be easily distributed in the circulation releasing biologically active compounds under specific conditions in the diseased tissues.[80] Usually, the controlled degradation of such complexes is pH dependent, leading to the cleavage of hydrogen or ionic bonds between the host and the guest molecules. Alternative means for disruption of the host-guest complexes take advantage of the action of enzymes able to cleave α-1,4 linkages between glucose monomers. Besides this classical way of using the cyclodextrin host-guest complexes we also hypothesized that inclusion of MCCs in CDs might keep reactive MCCs longer in circulation thereby improving their chance of reaching the diseased tissues.

In this study 1:1 inclusion complexes of $Mn(CO)_5Br$, $CpFe(CO)_2Cl$, $[Et_4N][Mo(CO)_5Br]$, $CpMo(CO)_3Cl$ and $(Ac\text{-}Cp)Mo(CO)_3Cl$ were prepared and characterized by the group of Isabel S. Gonçalves at the Universidade de Aveiro, Portugal, using unmodified β-cyclodextrin (β-CD) and 2,3,6-tri-*O*-methyl-β-cyclodextrin (TRIMEB).[69, 81] Their performance as CO releasers is summarized in Table 10.

Table 10: Equivalents of CO released by the complexes $Mn(CO)_5Br$, $CpFe(CO)_2Cl$, $[Et_4N][Mo(CO)_5Br]$, $CpMo(CO)_3Cl$ and $(Ac\text{-}Cp)Mo(CO)_3Cl$ and their encapsulated forms in TRIMEB and also $CpFe(CO)_2Cl$ encapsulated in β-CD, in RPMI after 2h, 4h and 6h, at room temperature, in the dark, under reconstituted CO_2 free air.

"Free" Compound	Equiv. CO released	Encapsulated compound	Equiv. CO released	Time of reaction
$Mn(CO)_5Br$	0.7 1.2 1.6	$Mn(CO)_5Br$@TRIMEB	0.7 1.0 1.1	2h 4h 6h
$CpFe(CO)_2Cl$	0.2 0.4 0.5	$CpFe(CO)_2Cl$@β-CD	0.0 0.0 0.0	2h 4h 6h
$CpFe(CO)_2Cl$	0.2 0.4 0.5	$CpFe(CO)_2Cl$@TRIMEB	0.0 0.1 0.1	2h 4h 6h
$[Et_4N][Mo(CO)_5Br]$	1.7 2.1 2.4	$[Et_4N][Mo(CO)_5Br]$@TRIMEB	1.2 1.6 1.6	2h 4h 6h
$CpMo(CO)_3Cl$	0.1 0.2 0.4	$CpMo(CO)_3Cl$@TRIMEB	0.1 0.3 0.5	2h 4h 6h
$(Ac\text{-}Cp)Mo(CO)_3Cl$	0.1 0.2 0.2	$(Ac\text{-}Cp)Mo(CO)_3Cl$@TRIMEB	0.1 0.3 0.4	2h 4h 6h

As expected, all the compounds become more water-soluble after encapsulation. However, the differences observed between the CO release profile of the "free" and the corresponding encapsulated compounds, are not drastic. Considering that within these small variations it is dangerous to extract general rules, one can still accommodate some of the trends into a plausible set of explanations. Both $Mn(CO)_5Br$ and $CpFe(CO)_2Cl$ are air stable complexes where CO release is expected to follow simple ligand substitution mechanisms. Regardless of being associative of dissociative, such mechanisms imply modifications in the coordination sphere of the metal atom, which are clearly affected by the encapsulation of the MCC inside the CD. Inside the host cavity the exchange of ligands is hampered and therefore retarded by physical reasons. Accordingly, $Mn(CO)_5Br$ and $CpFe(CO)_2Cl$ should be protected upon encapsulation as is indeed observed.

In contrast, $CpMo(CO)_3Cl$ and $(Ac\text{-}Cp)Mo(CO)_3Cl$ are not air stable and CO release at physiological temperature in the dark, even minor as it is, requires

oxygen. Given its small size, O_2 will have ready access to the guests inside the cavity and trigger CO release. Under these circumstances the rate of CO release will remain essentially unaffected by encapsulation, as is observed. The case of $[Et_4N][Mo(CO)_5Br]$ is more complex because the compound, besides being very little soluble is both substitutionally very labile and oxidatively sensitive. Therefore, the information available is not readily interpreted. Nevertheless, the encapsulated compound is protected inside the CDs corresponding to a 14% decrease when compared with the values obtained after 6h with the free complex.

4.5 The influence of O_2 in the CO release from metal carbonyl complexes

As extensively observed and mentioned in the above results, oxygen is the main trigger promoting CO release from metal carbonyl complexes in biological compatible media. Experiments performed under N_2 showed that the molecules were stable, in some cases up to 24h in water. Light was also evaluated as a possible trigger but only marginal differences were observed among the assays performed with light and in the dark.

There is not much data reported in the literature concerning the interaction of metal carbonyl complexes with O_2. The photochemical experiments of the groups of Poliakoff and Downs are almost the only source of information on these reactions.[82, 83] As hypothesized also in the introduction, the oxidation of the metal carbonyl can happen through an inner or an outer sphere mechanism. In the latter case, the formation of superoxide as the result of an electron transfer between the electron rich metal carbonyl complex and molecular oxygen would be a likely outcome. In order to shed some light onto this process a series of Electron Spin Resonance (ESR) spin trap studies using the spin trap BMPO was performed with four model compounds (Figure 7).

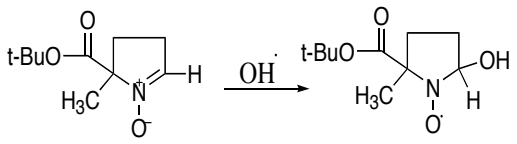

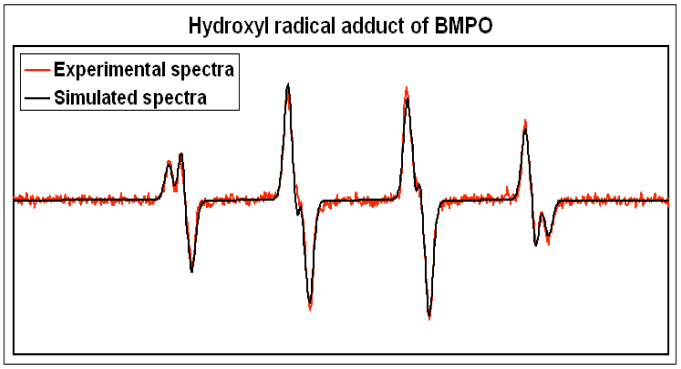

Figure 7: **Top-**Hydroxyl radical attack to 5-*tert*-butoxycarbonyl 5-methyl-1-pyrroline N-oxide (BMPO); **Bottom**-ESR spectrum of the adduct obtained.

Compounds $[Et_4N][Mo(CO)_5Br]$, $Na[Mo(CO)_3(hist)]$, $Na_3[Mo(CO)_3(cit)]$ and $[Mo(CO)_3(bpa)]$ were selected based on the results of the GC assays. $Na[Mo(CO)_3(hist)]$ and $Na_3[Mo(CO)_3(cit)]$ are ionic compounds and while the first one is a very fast CO releaser that very rapidly loses the 3 COs, the second one is more stable, only releasing roughly 1 CO in water and decomposes leading to the formation of $Mo(CO)_6$ and other unknown species. $[Et_4N][Mo(CO)_5Br]$ is also an ionic compound that readily loses 2 to 3 COs in water depending on the conditions. On the other hand, $[Mo(CO)_3(bpa)]$ is a neutral compound also with a high rate of CO liberation. The spin trap used, BMPO, is a water soluble cyclic nitrone able to detect superoxide and hydroxyl radicals with a half-life of 23 min.[84] Upon hydroxyl attack the adduct obtained gives the characteristic ESR spectrum depicted in Fig.7.

To assess the effect of O_2 in the oxidation of the selected model metal carbonyls an ESR study was performed as follows: a solution of the compound in water was prepared under N_2 and an aliquot transferred to the ESR tube together with the spin trap BMPO. A control spectrum was taken and no signal was detected in

every case. Oxygen was then bubbled in the solution for 3-4 min and another sample was taken and analyzed. The spectra obtained are given in Figure 8.

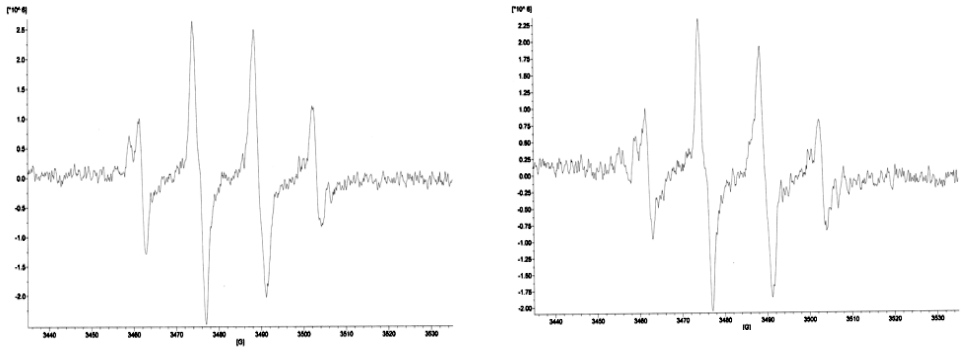

Figure 8: ESR spectrum obtained after O_2 bubbling in a water solution containing: **Left** - Na[Mo(CO)$_3$(hist)] (203 μM) and BMPO (12.5 mM); **Right** - Na_3[Mo(CO)$_3$(cit)] (200 μM) and BMPO (25 mM).

The same procedure was performed with compounds [Et_4N][$Mo(CO)_5Br$] and [Mo(CO)$_3$(bpa)] but bubbling air instead of pure O_2. The spectra obtained are given in Figure 9.

The results obtained for Na[Mo(CO)$_3$(his)], and Na_3[Mo(CO)$_3$(cit)] showed the unequivocal formation of hydroxyl radical. No superoxide was detected even the decay of superoxide to hydroxyl should be discarded since this conversion is not plausible in non-enzymatic conditions.[84]

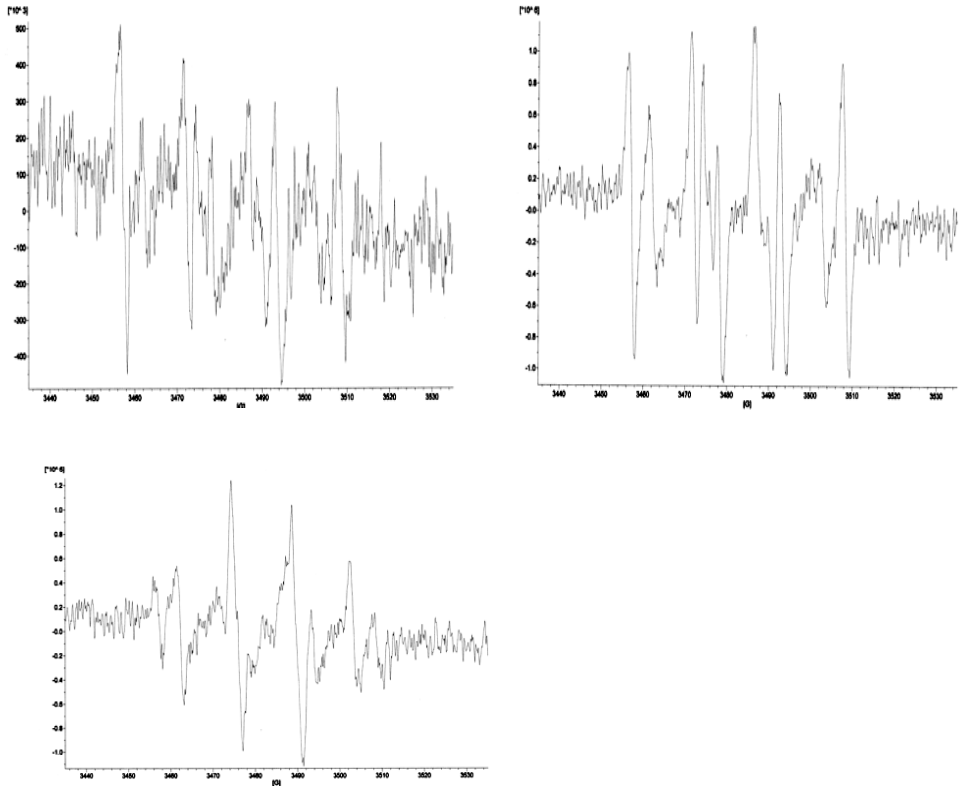

Figure 9: ESR spectrum obtained after air was bubbled in a water solution containing: **Top Left** - $[Et_4N][Mo(CO)_5Br]$ (199 μM; 0.7% MeOH) and BMPO (25mM); **Top Right** - $[Mo(CO)_3(bpa)]$ (200 μM; 0.6% MeOH) and BMPO (25 mM); **Bottom -** ESR spectrum obtained after O_2 was bubbled in the $[Et_4N][Mo(CO)_5Br]$ solution.

Although with less clear spectra, both $[Et_4N][Mo(CO)_5Br]$ and $[Mo(CO)_3(bpa)]$ also produced the hydroxyl radical in their reactions with O_2 from air (Figure 9). No signal typical of the superoxide-BMPO adduct was detected. Therefore, the formation of the hydroxyl radical in all these oxidations of Mo^0 carbonyls by molecular oxygen (O_2) is an unequivocal event under these reaction conditions. With the exception of the interactions of O_2 with Fe ions in heme proteins, relatively little is known about the mechanisms of the reduction of O_2 by transition metal complexes. As a matter of fact, the understanding of these mechanisms is emerging as a major research area given the need to understand the complex mechanism(s) of the reduction of O_2, a decisive process in the areas of

fuel cells and other sustainable energy processes.[85, 86] In the case of zerovalent transition metal complexes in water, we are not aware of any study of this kind. Therefore, we can only attempt to propose a mechanism for this hydroxyl radical formation based upon information gathered in related systems. Our proposal in depicted in scheme 4 and is briefly discussed.

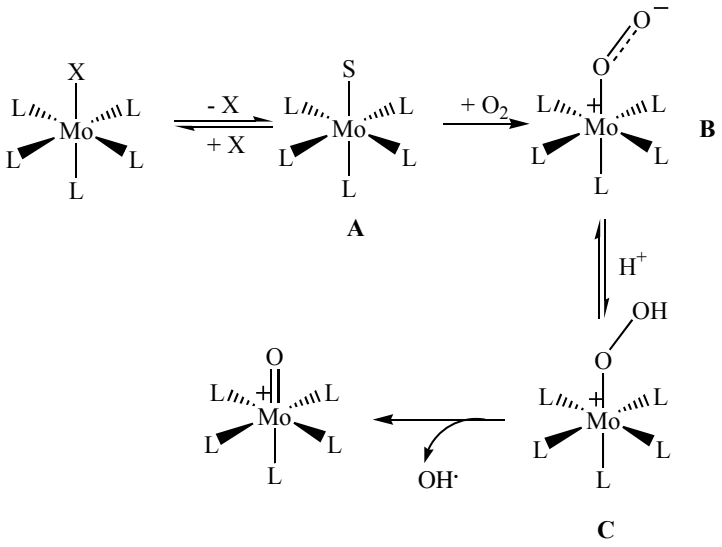

Scheme 4:: Proposed mechanism for the formation of HO· radicals in the oxidation of Mo^0 complexes by molecular oxygen (O_2). S represents the solvent.

The reaction starts by dissociation of one labile ligand X forming an unsaturated 16-electron complex (A), where the solvent occupies the ligand site. O_2 coordinates to this vacant position. In the new bond some charge transfer from the very electron rich Mo^0 to the highly electronegative O_2 takes place, forming what can also be described as a superoxo complex L_5Mo^I-(O_2^-) (B). In aqueous medium this species is protonated at the distal O atom to form (C). The strong tendency of Mo to stabilize terminal Mo=O bonds and its strong reducing power certainly assists the breaking of the remaining O-OH bond, thereby facilitating the formation of the HO radical which is irreversibly trapped by BMPO. This mechanism is reminiscent of the formation of the ferryl (heme)-Fe^{IV}=O species in the cytochrome P450. In the later, the breaking of the O=O bond from the initially

formed (heme)-Fe^{II}(O=O) involves addition of two H^+ ions to the distal O atom, leading to (heme)-Fe^{IV}=O and H_2O. In the case of the L_5Mo(O-OH) complex (C) the O=O bond breaking takes place without the need to add another proton and we propose that an oxo-Mo complex is formed. Reduction of O_2 at the surface of Pt electrodes in aqueous solution, where HO radicals are formed, seems to follow a similar path through the fission of the O-O bond of the Pt-O-OH species formed at the surface of the negatively charged, electron rich Pt electrode.[87]

5. Final Remarks and Conclusions

The study of CO release from metal carbonyl complexes that is described in this chapter must not be regarded as a quantitative, accurate mechanistic description of the chemistry that presides to this particular decomposition process. Instead, this screening intends to

- reveal the viability of using MCCs to deliver CO in biological media
- reveal which structures and metal ligand combinations are better suited for such CO delivery
- understand the main molecular properties that contribute to the profile of CO release of MCCs
- identify the main parameters that have to be controlled in order to eventually optimize CO release profiles from given MCCs.

The results reported lead to the following main conclusions:

- MCCs are largely compatible with biological media and the vast majority is actually rather stable towards decomposition with CO release.
- the fastest and more extensive CO releasers were identified among the Mo^0 octahedral derivatives $[Mo^0(CO)_3L_3]^{0/z-}$ bearing hard donor ligands mainly those of biological relevance, e.g. amines, carboxylates, aminoacids.

- CO release from these complexes is mainly triggered by O_2 and this process seems to favor production of $OH^{\cdot}$ radicals over $O_2^{\cdot -}$
- CO release from $[Mo^0(CO)_3L_3]^{0/z-}$ complexes can be regulated *via* appropriate π-acceptor ligands.
- Encapsulation of the MCCs in cyclodextrins retards CO release only in those cases where this is not strongly O_2 dependent.
- $Mn^I(CO)_5L$ and $Mn^I(CO)_4L_2$ lose CO dissociatively to form stable, inert $[Mn(CO)_3X_3]^+$ products.
- Cyclopentadienyl complexes of Mo^{II}, Fe^{II}, Ru^{II} and Mn^I are very weak CO releasers.
- The toxicity of $CpM(CO)_xL$ (M=Fe, Ru and x=2; M=Mo and x=3) complexes can be decreased by introducing long and/or bulky substituents in the Cp ring.
- $[Ru^{II}(CO)_3L_3]$ complexes do not release CO to the headspace of their aqueous solutions.
- Solubility and air stability are the most important properties that need to be manipulated in order to obtain chemically reliable Metal Carbonyl CO-RMs.

These data do not intend to elaborate a group of rigorous rules of CO release in biological conditions, let alone a "manual" for drug development of organometallic carbonyl complexes.

However, it is fascinating to see how some organometallic chemistry basic principles may be applied to the development of potential pharmaceuticals. The electronic tuning of the metal center, the modification introduced in the first sphere of coordination e.g. changing the halide, introducing an alkyl or aryl substituent as well as changing the π acidity of ancillary ligands are some special features that determine directly stability to O_2 and the CO release rate of the molecules and ultimately, how the "active principle" is delivered.

From this point onwards achieve good stability in aqueous medium stands out as the next important topic to tackle as the way to transform MCCs in pharmacologically acceptable CO-RMs.

6. References

1. Feldstein, M., *Prog. Chem. Toxicol.* **1967**, 3, 99.
2. Peng, C., *Chromatographia* **1990**, 29, 347.
3. Ohlin, C.A., Dyson, P.J., Laurenczy, G., *Chem. Commun.* **2004**, 1070.
4. Obirai, J.C., Hamadi, S., Ithurbide, A., Wartelle, C., Nyokong, T., Zagal, J., Top, S., Bedioui, F., *Electroanalysis* **2006**, 18, 1689.
5. Motterlini, R. WO 2005/114161 A1, 2005.
6. Vreman, H.J., Kwong, L.K., Stevenson, D.K., *Clin. Chem.* **1984**, 30, 1382.
7. Collison, H.A., Rodkey, F.L., Oneal, J.D., *Clin. Chem.* **1968**, 14, 162.
8. Vreman, H.J., Stevenson, D.K., Zwart, A., *Clin. Chem.* **1987**, 33, 694.
9. Sundin, A.M., Larsson, J.E., *J. Chromatogr., B: Anal. Technol. Biomed. Life Sci.* **2002**, 766, 115.
10. Costantino, A.G., Park, J., Caplan, Y.H., *J. Anal. Toxicol.* **1986**, 10, 190.
11. Moore, G.E., Gerner, R.E., Franklin, H.A., *JAMA* **1967**, 199, 519.
12. Abel, E.W., Bennett, M.A., Burton, R., Wilkinson, G., *J. Chem. Soc.* **1958**, 4559.
13. Darensbourg, D.J., Kump, R.L., *Inorg. Chem.* **1978**, 17, 2680.
14. Darensbourg, D.J., Ortiz, C.G., Kamplain, J.W., *Organometallics* **2004**, 23, 1747.
15. Takuma, M., Ohki, Y., Tatsumi, K., *Organometallics* **2005**, 24, 1344.
16. Angelici, R.J., Basolo, F., *J. Am. Chem. Soc.* **1962**, 84, 2495.
17. Wojcicki, A., Basolo, F., *J. Am. Chem. Soc.* **1961**, 83, 525.
18. Howell, J.A.S., Burkinshaw, P.M., *Chem. Rev.* **1983**, 83, 557.
19. Angelici, R.J., Graham, J.R., *J. Am. Chem. Soc.* **1965**, 87, 5586.
20. Pearson, R.G., *J. Am. Chem. Soc.* **1963**, 85, 3533.
21. Burgess, J., Duffield, A.J., *J. Organomet. Chem.* **1979**, 177, 435.
22. Macgregor, S.A., MacQueen, D., *Inorg. Chem.* **1999**, 38, 4868.
23. Alberto, R., Schibli, R., Waibel, R., Abram, U., Schubiger, A.P., *Coord. Chem. Rev.* **1999**, 192, 901.
24. Schibli, R., La Bella, R., Alberto, R., Garcia-Garayoa, E., Ortner, K., Abram, U., Schubiger, P.A., *Bioconjugate Chem.* **2000**, 11, 345.
25. Alberto, R., *J. Organomet. Chem.* **2007**, 692, 1179.
26. Satpati, D., Bapat, K., Mukherjee, A., Banerjee, S., Kothari, K., Venkatesh, M., *Appl. Radiat. Isot.* **2006**, 64, 888.
27. Chaudhuri, P., Wieghardt, K., Tsai, Y.H., Kruger, C., *Inorg. Chem.* **1984**, 23, 427.
28. Bacac, M., Hotze, A.C.G., van der Schilden, K., Haasnoot, J.G., Pacor, S., Alessio, E., Sava, G., Reedijk, J., *J. Inorg. Biochem.* **2004**, 98, 402.
29. Motterlini, R., Mann, B.E., Foresti, R., *Expert Opin. Investig. Drugs* **2005**, 14, 1305.
30. Motterlini, R., *Biochemical Society Transactions* **2007**, 35, 1142.

31. Fraústo da Silva, J.J.R., Williams, R.J.P., *The biological chemistry of the elements: The inorganic chemistry of life,* 2nd ed., Oxford University Press, Oxford, **2001**.
32. *Handbook of Pharmaceutical Salts, Properties Selection and Use,* (Eds.:P. H. Stahl; C. G. Wermuth) Wiley-VCH, Zurich, **2002**.
33. Abel, E.W., Bennett, M.A., Wilkinson, G., *Chem. Ind.* **1960**, 442.
34. Kerns, E.H., Di, L., *Drug-like Properties: Concepts, Structure Design and Methods: from ADME to Toxicity Optimization,* 1st edition ed., Academic Press Burlington, **2008**.
35. Zhou, Z.H., Wan, H.L., Tsai, K.R., *Inorg. Chem.* **2000**, 39, 59.
36. Tobe, M.L., *Inorganic Reaction Mechanisms,* T. Nelson and Sons, London, **1972**.
37. Herrmann, W.A., Serrano, R., Bock, H., *Angew. Chem. Int. Edit. Engl.* **1984**, 23, 383.
38. King, R.B., *J. Am. Chem. Soc.* **1963**, 85, 1918.
39. Coffield, T.H., Kozikowski, J., Closson, R.D., *Abstracts of Papers submitted at the International Conference on Coordination Chemistry, London* **1959**, Chemical Society Special Publication 13, 126.
40. Rudolf, B., Palusiak, M., Zakrzewski, J., Salmain, M., Jaouen, G., *Bioconjugate Chem.* **2005**, 16, 1218.
41. Piper, T.S., Wilkinson, G., *J. Inorg. Nucl. Chem.* **1956**, 3, 104.
42. Davison, A., Mccleverty, J.A., Wilkinson, G., *J. Chem. Soc.* **1963**, 1133.
43. Alway, D.G., Barnett, K.W., *Inorg. Chem.* **1980**, 19, 1533.
44. Semion, V.A., Chapovskii, Y.A., Struchkov, Y.T., Nesmeyanov, A.N., *Chem. Commun.* **1968**, 666.
45. Haines, R.J., Nyholm, R.S., Stiddard, M.H., *J. Chem. Soc. A* **1967**, 94.
46. Barnett, K.W., Slocum, D.W., *J. Organomet. Chem.* **1972**, 44, 1.
47. Burkhardt, E.R., Doney, J.J., Bergman, R.G., Heathcock, C.H., *J. Am. Chem. Soc.* **1987**, 109, 2022.
48. Cousins, M., Green, M.L.H., *J. Chem. Soc.* **1963**, 889.
49. Faller, J.W., Incorvia, M.J., *Inorg. Chem.* **1968**, 7, 840.
50. Limberg, C., Downs, A.J., Greene, T.M., Wistuba, T., *Eur. J. Inorg. Chem.* **2001**, 2613.
51. Bitterwolf, T.E., Bays, J.T., Scallorn, B., Weiss, C.A., George, M.W., Virrels, I.G., Linehan, J.C., Yonker, C.R., *Eur. J. Inorg. Chem.* **2001**, 2619.
52. King, R.B., Fronzagl.A, *J. Am. Chem. Soc.* **1966**, 88, 709.
53. Scapens, D., Adams, H., Johnson, T.R., Mann, B.E., Sawle, P., Aqil, R., Perrior, T., Motterlini, R., *Dalton Trans.* **2007**, 4962.
54. Strohmeier, W., *Angew. Chem.* **1963**, 75, 1024.
55. Strohmeier, W., *Z. Naturforsch., B.* **1964**, B 19, 540.
56. Komura, J., Sakamoto, M., *Toxicol. Lett.* **1994**, 73, 65.
57. Hysell, D.K., Moore, W., Stara, J.F., Miller, R., Campbell, K.I., *Environ. Res.* **1974**, 7, 158.
58. McGinley, P.A., Morris, J.B., Clay, R.J., Gianutsos, G., *Toxicol. Lett.* **1987**, 36, 137.
59. Gianutsos, G., Seltzer, M.D., Saymeh, R., Wu, M.L., Michel, R.G., *Arch. Toxicol.* **1985**, 57, 272.
60. Fishman, B.E., McGinley, P.A., Gianutsos, G., *Toxicology* **1987**, 45, 193.
61. Gianutsos, G., Murray, M.T., *Neurotoxicology* **1982**, 3, 75.
62. Blanchard, K.T., Morris, J.B., *Toxicol. Lett.* **1994**, 70, 253.

63. Blanchard, K.T., Clay, R.J., Morris, J.B., *Toxicol. Appl. Pharmacol.* **1996**, 136, 280.
64. Clay, R.J., Morris, J.B., *Toxicol. Appl. Pharmacol.* **1989**, 98, 434.
65. Penney, D.A., Hogberg, K., Traiger, G.J., Hanzlik, R.P., *Toxicology* **1985**, 34, 341.
66. Petrovski, Z., Braga, S.S., Santos, A.M., Rodrigues, S.S., Goncalves, I.S., Pillinger, M., Kuhn, F.E., Romao, C.C., *Inorg. Chim. Acta* **2005**, 358, 981.
67. Rossi, L.I., de Rossi, R.H., *Appl. Catal., A* **2004**, 267, 267.
68. Caron, L., Bricout, H., Tilloy, S., Ponchel, A., Landy, D., Fourmentin, S., Monflier, E., *Adv. Synth. Catal.* **2004**, 346, 1449.
69. Braga, S.S., Gago, S., Seixas, J.D., Valente, A.A., Pillinger, M., Santos, T.M., Goncalves, I.S., Romao, C.C., *Inorg. Chim. Acta* **2006**, 359, 4757.
70. Fukushima, M., Tatsumi, K., *J. Mol. Catal. A: Chem.* **2006**, 245, 178.
71. Johnson, M.D., Reinsborough, V.C., *J. Solution Chem.* **1994**, 23, 185.
72. Lewis, L.N., Sumpter, C.A., Stein, J., *J. Inorg. Organomet. Polym.* **1996**, 6, 123.
73. Hapiot, F., Tilloy, S., Monflier, E., *Chem. Rev.* **2006**, 106, 767.
74. Sliwa, W., Girek, T., *Heterocycles* **2003**, 60, 2147.
75. Hongbing, Z., Minquan, W., Wenzhe, C., Guanghui, L., *Optical Materials* **2003**, 22, 377.
76. Hirayama, F., Uekama, K., *Adv. Drug Deliv. Rev.* **1999**, 36, 125.
77. Duchene, D., Wouessidjewe, D., Ponchel, G., *J. Control Release* **1999**, 62, 263.
78. Woldum, H.S., Larsen, K.L., Madsen, F., *Drug Deliv.* **2008**, 15, 69.
79. Fernandes, C.M., Vieira, M.T., Veiga, F.J.B., *Eur. J. Pharm. Sci.* **2002**, 15, 79.
80. Loftsson, T., Masson, M., *Int. J. Pharm.* **2001**, 225, 15.
81. Braga, S.S., Paz, F.A.A., Pillinger, M., Seixas, J.D., Romao, C.C., Goncalves, I.S., *Eur. J. Inorg. Chem.* **2006**, 1662.
82. Almond, M.J., Crayston, J.A., Downs, A.J., Poliakoff, M., Turner, J.J., *Inorg. Chem.* **1986**, 25, 19.
83. Crayston, J.A., Almond, M.J., Downs, A.J., Poliakoff, M., Turner, J.J., *Inorg. Chem.* **1984**, 23, 3051.
84. Zhao, H.T., Joseph, J., Zhang, H., Karoui, H., Kalyanaraman, B., *Free Radic. Biol. Med.* **2001**, 31, 599.
85. Bakac, A., *Inorg. Chem.* **2010**, 49, 3584.
86. Tolman, W.B., Solomon, E.I., *Inorg. Chem.* **2010**, 49, 3555 and references cited therein.
87. Wang, Y.X., Balbuena, P.B., *J. Phys. Chem. B* **2005**, 109, 14896.

7. Acknowledgments

Prof. Isabel Gonçalves, from Universidade de Aveiro is acknowledged for the synthesis and characterization of cyclodextrin encapasulated complexes.

Prof. Miguel Teixeira, from ITQB is acknowledged for recording the ESR spectra and helpful discussion.

Alfama's chemists Sandra Rodrigues and Marta Norton de Matos are acknowledged for the preparation of some compounds as indicated in Table A1, Annex 1.

Bruno Guerreiro and Lukas Kromer are acknowledged for the preparation of some compounds and help with the HPLC measurements.

José Fernandes is acknowledged for the preparation of $[choline]_3[Mo(CO)_3(citrate)]$.

Ana Margarida Gonçalves is acknowledged for measurements of CO release through GC.

Chapter III: Evaluating ROS induced CO release from Metal Carbonyls by Gas Chromatography

1. Summary

As mentioned in Chapter II, many of the MCCs presented are stable entities that don't release any CO or only marginal amounts when exposed to aerobic aqueous environment. Therefore, to become CO-RMs they need some kind of activation. In diseased tissues, reactive oxygen species (ROS) are highly expressed and the use of stable MCCs that may be specifically activated by ROS inside cells seems a reasonable and promising strategy for targeting CO-RMs, especially if they have reasonable half-lives in the organism.

Presently, very little is known about the reactivity of organometallic carbonyls under any of these conditions and in this Chapter the studies on this type of CO release profile is described.

Most of the complexes studied do not resist ROS as triggers for CO release and the oxidation can be tuned by the nature of the ancillary ligand in the case of $Mn^{I}(CO)_5X$, $Mo^{0}(CO)_5X$ and $CpMo^{II}(CO)_3X$ complexes. $Mn^{I}(CO)_3$ and $Ru^{II}(CO)_3$ complexes do not respond to the ROS used.

2. Introduction

2.1 Reactive oxygen species and biologic oxidative processes

It is well established that ROS and reactive nitrogen species (RNS) are involved in a wide variety of human diseases, ranging from atherosclerosis to myocardial infarction, cystic fybrosis, fulminant hepatic failure, neurodegenerative diseases and diabetes[1-5]. Sometimes they play a pivotal role as injury promoters, while in other settings they have a less important contribution as intermediary or signaling

agents. A common feature in inflammatory scenarios is the presence of high amounts of ROS and RNS due to a disregulation of the oxidative imbalance between oxidative agents and anti-oxidant defenses, a process known as *oxidative stress*. These noxious process can be fought *in vivo* by decreasing the oxidative agents or enhancing the endogenous or exogenous reducing agents. Most of these oxidative agents are free radicals like superoxide ($O_2^{\bullet-}$), hydroxyl ($OH^{\bullet}$), peroxyl ($RO_2^{\bullet}$), alkoxyl ($RO^{\bullet}$), hydroperoxyl ($HO_2^{\bullet}$) but also some non-radicals like hydrogen peroxide (H_2O_2), hypochlorous acid (HOCl), peroxynitrite (ONO_2) and alkylperoxides (ROOH).

In case of injury or any kind of exogenous aggression where an immune response is triggered, ROS/RNS are generated through mediators like phagocytes, neutrophiles or macrophages that are activated to fight the injury.[6]

All these radicals are very different in terms of reactivity or stability, and so the damages caused by each of the species produced are different. The difference in reactivity arises not only from intrinsic properties but also from the circumstances of the event. When a radical meets a non-radical, a new radical results and a chain reaction may be started, until two radicals meet to produce a non-radical and terminate the chain reaction.

The most common radical reactions are summarized in Scheme 1:

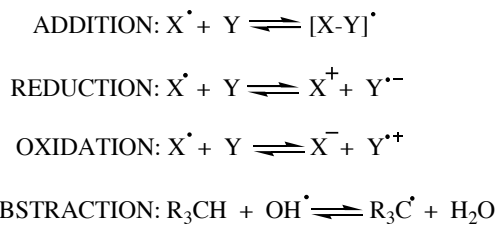

Scheme 1: Main radical reactions

From all the radicals produced during inflammatory processes, the hydroxyl radical is by far the most reactive. It has a life-span of virtually zero because as soon as it is formed it reacts with molecules in the vicinity making it the predominant species contributing to cellular damage [7-10]. It can be generated by

several reactions but the most common *in vivo* sources are the Fenton reaction (Eq. 1) and the reaction between hypochlorous acid and superoxide[11] (Eq. 2).

$$H_2O_2 + Fe^{2+} \rightleftharpoons Fe(III) + OH^{\bullet} + OH^- \qquad \textbf{Equation 1}$$

$$HOCl + O_2^{\bullet -} \rightleftharpoons O_2 + Cl^- + OH^{\bullet} \qquad \textbf{Equation 2}$$

Peroxyl and alkoxyl radicals[12-16] usually undergo molecular rearrangement to other radical species, often abstracting hydrogen and contributing to lipid peroxidation.[17, 18] However, the hydroxyl radical essentially reacts with everything! The type of reaction depends on the neighboring targets. It may react by hydrogen abstraction (e.g. initiating lipid peroxidation), addition reactions[19] and electron transfer[16, 20] but independently of the target, the rates of reaction are essentially equal. Because no discrimination is made the reactions proceed with all the entities at a very fast rate turning all biomolecules into scavengers.

On the contrary, according to Sawyer[21] superoxide is "not so super" since it is much less reactive with non-radicals in aqueous solutions. It is produced *in vivo* (e.g. by activated phagocytic cells) and reacts quickly with $NO^{\bullet}$, Fe-S clusters and phenoxyl radicals (from tyrosine hydrogen abstraction) contributing directly to oxidative damage by several mechanisms like lowering the activity of some anti-oxidant defences (e.g. glutathione peroxidase and catalase[22]) which facilitate H_2O_2 toxicity, generating more damaging reactive species like peroxynitrite (Eq. 3 at scheme 2) or hydroxyl radical *via* Haber-Weiss reaction catalyzed by transition metal ions, the so-called superoxide-assisted Fenton reaction (Eq. 4 in scheme 2)

However, *in vivo*, it's unlikely that a large contribution to hydroxyl radical formation is given by Equation 4 since cells contain many reducing agents at millimolar concentrations (GSH, NAD(P)H, cysteine, ascorbic acid) which can reduce Fe(III) and Cu^{2+} while superoxide concentration is only at picomolar to nanomolar levels.[23]

$$O_2^{\bullet -} + NO^{\bullet} \rightleftharpoons ONOO \qquad \textbf{Equation 3}$$

oxidized metal complex + $O_2^{\bullet -}$ $\rightleftharpoons$ reduced metal complex + O_2
reduced metal complex + H_2O_2 $\rightleftharpoons$ oxidized metal complex + $OH^{\bullet}$ + OH^-

Net reaction: $$H_2O_2 + O_2^{\bullet -} \xrightleftharpoons{\text{M catalyst}} OH^{\bullet} + OH^- + O_2 \qquad \textbf{Equation 4}$$

M=Fe(III/II) or Cu(II/I) catalyzed Haber-Weiss reaction[24]

Scheme 2: Superoxide radical reactions to give peroxinitrite (Equation 3) and hydroxyl radical (Equation 4).

Nevertheless the importance of superoxide can't be neglected, mainly because when protonated $HO_2^{\bullet}$ has a higher reactivity than $O_2^{\bullet -}$ and is a more powerful reducing agent. Since it is uncharged it can enter the membrane and is also able to abstract $H^{\bullet}$ from some isolated fatty acids such as linoleic, linolenic and arachidonic acid initiating lipid peroxidation. [25-28]

Hydrogen peroxide is a weak oxidizing and reducing agent with very low reactivity. It is, however, toxic to most cells in the 10-100 μM range and is able to directly induce some cellular damage e.g. inactivating glyceraldehydes-3-phosphate dehydrogenase, but it doesn't react with most lipids, DNA and proteins. Since it is very diffusible it can cross cell membranes and react with cell constituents like iron and copper ions rendering much more damaging species. This oxidative damage is not mediated by H_2O_2 alone although it may degrade certain heme proteins[29] (including Mb, Hb, Cyt C) to release iron ions and generate the hydroxyl radical.

The reactivity of these species is not necessarily harmful, although they may initiate many adverse events. It is widely known that ROS and RNS play an important role in several pathophysiological conditions.[2, 30, 31] Given their oxidative potential, ROS may offer a possible targeting mechanism for site-specific CO generation. In fact, stable metal carbonyls (like many presented in Chapter II) that don't release any CO or release only marginal amounts in solution

in physiological medium, are electron-rich complexes, thus quite likely to be oxidized by ROS, thereby triggering CO release under specific conditions in inflamed tissues or sites.

2.2 Oxidative decarbonylation of metal carbonyl complexes

Although very well recognized, the oxidation of metal carbonyls with O_2, peroxides and related species has not been systematically studied and literature is often contradictory and inexact regarding the nature of the gas(es) evolved during the oxidative process.[32, 33] *A priori* such a process may result in loss of unchanged CO or oxidation of the same to CO_2. Even the low temperature matrix studies already mentioned in Chapter II may lead to some CO_2 formation which accompanies CO liberation.[34]

The oxidative decarbonylation of $Cp^*Re(CO)_3$ with O_2 and light[35] and also with H_2O_2[32] was studied by Herrmann and co-workers. In the first case the ratio of $CO:CO_2$ was reported to be 3:1 and in the second case 1:2. Wolowiec and Kochi[36] oxidized the same compound with dimethyldioxirane (DMDO) and determined the relative ratio of $CO:CO_2$ as 2:1. However, this ratio showed to be highly dependent on the substrate concentration, the rate of DMDO addition and the temperature.

The broad field of heterogeneous and homogeneous catalysis has indirectly become a fruitful source of information regarding metal carbonyl oxidation due to the industrial importance of several metal oxides. A famous example is methyltrioxorhenium, $MeReO_3$, known as MTO, that is used as a catalyst in several significant reactions in industry, like olefin epoxidation (using H_2O_2 as the oxidant), Bayer-Villiger oxidation and aromatic oxidation.[37-39]

Olefin epoxidation reactions are also catalyzed by Cp^*MoO_2Cl[40] and in the recent years it was found that complexes of the type $CpMoO_2X$ could be easily prepared by reaction of $CpMo(CO)_3X$ with *tert*-butylhydroperoxide (TBHP) in *n*-decane at room temperature[41] with evolution of 3 equivalents of CO.[42]

The $CpMo(CO)_3R$ (R = alkyl, halide…) family was widely studied for catalytic purposes, but rarely were these studies performed in aqueous environment.[43] Often due to the lack of solubility in water the oxidative decarbonylation studies are performed in organic solvents with oxidants like TBHP.

Apart from the catalytic studies TBHP is used to stimulate microsomal peroxidation *in vivo*. It decomposes to alkoxyl or peroxyl radicals and accelerates the chain reaction of lipid peroxidation attacking membrane lipids as well as fatty acids and lipoproteins.[44, 45]

This set of properties designated H_2O_2 and TBHP as front models to simulate an oxidative stress environment and evaluate the potential ability of the compounds to release CO under oxidative conditions. It was already demonstrated that some compounds may release CO at higher rates depending on pH or O_2 and another key aspect is to understand if compounds that are stable in solution can be oxidized and release CO as a result of an oxidative process. The main advantage of this approach is the possibility of preventing Hemoglobin loading with CO, liberated from spontaneous CO releasers. This process would allow the molecules to keep their full "potential" until they reach the target, promoting an *in situ* release of CO directly to the inflamed tissues.

3. *Experimental Section*

3.1 Methodology

The CO liberated from the reaction of the MCCs with ROS species was quantified in the headspace with the same GC/TCD method described in Chapter II. The decomposition reactions were done under inert atmosphere (N_2), at room temperature in the same apparatus of Fig.1 (Chapter II) or in calibrated vials. Two biological relevant oxidants were used: hydrogen peroxide (H_2O_2 30% in water)

and *tert*-butylhydroperoxide ($(CH_3)_3COOH$ 70% aqueous solution). The concentration of $O_2^{\bullet-}$, H_2O_2 and $OH^{\bullet}$ in normal cells is in the order of 10^{-11}, 10^{-9} and 10^{-15} M, respectively, but in inflamed tissues may rise up to 10^{-3} M. Based on these values it was decided to test the compounds with a large excess of oxidant over the substrate. The standard conditions of 100:1 (oxidant:MCC) molar ratio were set up with typical H_2O_2 and TBHP concentrations of 0.9M. Under these conditions any reaction between the MCC and the peroxide will be easily identified and quantified in terms of the amount of CO liberated. Other gases, like CO_2 or O_2 which can be formed in these reactions by oxidation of CO or by decomposition of H_2O_2 are also identified and quantified in the same GC/TCD set-up.

Gas Chromatography:

Method description:

The reactions were performed using *tert*-butyl hydroperoxide (70% aqueous solution from *Aldrich*) and H_2O_2 (30% aqueous solution from *Aldrich*) as solvents. The reactions were carried out at room temperature, under N_2, without light and samples were taken with a Gastight syringe from Hamilton® after 1, 3, 5 and 24 h and analyzed. CO and CO_2 were quantified using a calibration curve recorded prior to the reaction course. Blank reactions were performed with water and *t*-BuOOH or H_2O_2 (without compound) and showed that no CO or CO_2 was liberated. The H_2O_2 used was titrated prior to use.

Reactions of $CpMo(CO)_3CH_2CONH_2$ with $[Cp_2Fe]BF_4$, $AgNO_3$ and $AgBF_4$ (IR and GC):

The reaction between equimolar amounts of $[Cp_2Fe]BF_4$ and $CpMo(CO)_3(CH_2CONH_2)$ was performed in a closed vial, with 2 mL of solvent (H_2O, dichloromethane, acetone, THF and acetonitrile) at room temperature, under N_2 and in the dark. Gas samples were taken after 1h and quantified in the GC. The reaction with acetonitrile was extended to 24h.

In addition, IR solution spectra were acquired after finishing the reactions and the background acquired in the proper solvent.

The analogous reaction of $CpMo(CO)_3(CH_2CONH_2)$ with $AgBF_4$ (in dichloromethane) was performed both in 1:1 and 1:10 molar ratios at room temperature, under N_2 and in the dark. Samples were analyzed by Gas Chromatography after 24h and the final product analyzed by ^1H NMR after 48h. In a parallel setup the same reaction was performed and samples were taken periodically and a solution IR spectrum acquired after 30min, 3h, 5h and 24h.

The same reaction was performed with $AgNO_3$ (in H_2O) also in 1:1 and 1:10 ratios. Samples were taken to GC analysis after 24h and the final product was also characterized by IR and ^1H NMR.

3.2 Technical Details

Synthetic Work:

All the compounds were prepared as indicated in Table A1 in Annex I.

4. Results and Discussion

A series of experiments was performed to determine the possibility of using ROS, modeled by H_2O_2 and TBHP to trigger CO release from MCCs. The compounds were selected from Table A1, Annex I, and the presentation of the results is done according to the metal selected for possible biological applications, namely, Mn, Mo, and Fe. The studies performed with Ru CO-RMs will be addressed in Chapter V.

The objectives of the present screening are

i. identify the compounds that are reactive towards H_2O_2 or TBHP;
ii. identify the nature of the gaseous products of these oxidation reactions;
iii. identify any different reactivity (selectivity) between both these ROS models.

At the outset is seems quite obvious that most, if not all, MCCs will react with these oxidants, because, as it has been already pointed out, MCCs usually contain metals in low oxidation states and are expected to be rather electron rich, therefore, prone to being oxidized. However, the kinetic stability to such oxidations may be high and prevent reaction between certain MCCs and peroxides at useful rates. Once again, two kinds of extreme pathways are available for reaction: outer sphere and inner sphere electron transfer between the MCC and the peroxide. Like in the case of the reaction between O_2 and a MCC, outer sphere electron transfer from the electron rich MCC to the oxidizing, electron accepting peroxide will result in the formation of a 17-electron MCC complex which will be highly activated towards CO substitution (see scheme 5 in Chapter I).

In the case of an inner sphere mechanism the peroxide molecule will act as any other nucleophile and bind to the metal center of the MCC following a normal ligand substitution process. Once coordinated to the metal, electronic rearrangement leads to formal oxidation of the metal which triggers further modifications in the coordination sphere. In the case of MCCs, the main possibilities are: release of CO, release of CO_2 by oxidation of CO, release of O_2 by metal catalyzed decomposition of the peroxide. Of course, this bonding interaction between the peroxide and the metal will be different for H_2O_2 and TBHP or other alkylhydroperoxides. The fate of the metal will be much more difficult to predict but formation of oxo, peroxo, hydroxo and aqua complexes is most likely, depending on the nature of the metal, pH and the nature of the biological ligands present in the medium. Most likely a number of species will be

formed in the final equilibrium which will be defined by the reaction conditions, namely the nature and concentration of the biological ligands, pH and the concentration of the complex as well as the nature and concentration of the ROS. Also important to note is the different aqueous chemistry of each of the metals under study. To give an example, the final oxidation products of Mo in aqueous solution are likely to be molybdate or polyoxomolybdates, depending on the pH, which are the most stable water soluble forms of MoO_3, the final product of combustion of Mo metal.[46] In the cases of Mn and Fe complexes the nature of the final oxidation state of the metal ion is not so obvious. Therefore, it is more useful to organize the discussion of the screening on a metal by metal basis.

Given all this complexity, it is expectable that almost each kind of MCC to be tested will represent a different case where the nature of the products, reaction intermediates and mechanisms will be different. The expected wide variation of mechanistic details is not a problem since they are not necessary to achieve the operational objectives i)-iii) above. Later detailed studies may be required on specific complexes that have been shown to possess relevant biological/therapeutic activity and are selected for further development as therapeutic CO-RMs.

4.1 The Manganese compounds

The results obtained on the CO release profiles induced by H_2O_2 and TBHP on a small number of selected Mn carbonyls are summarized in Table 1. This small collection of compounds exemplifies different profiles that cover the main possible situations of CO release stimulation by ROS in Mn carbonyls.

Table 1: Equivalents of CO and CO_2 released by the manganese compounds with 100 equiv. molar excess of TBHP and H_2O_2 in water. Gas samples were taken after 1h, 3h, 5h and 24h and quantified by GC/TCD.

Compound	Equiv. CO released after 6h in RPMI	TBHP		H_2O_2		Time of reaction
		CO	CO_2	CO	CO_2	
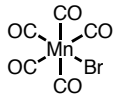 **1**	1.6	1.2 3.0 3.6 3.7	0.2 0.6 0.8 0.9	1.0 3.1 3.7 3.5	0.2 0.6 0.8 1.1	1h 3h 5h 24h
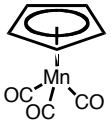 **2**	0.0	0.0 0.1 0.0 0.1	0.0 0.0 0.0 0.2	0.0 0.0 0.0 0.2	0.1 0.1 0.2 0.5	1h 3h 5h 24h
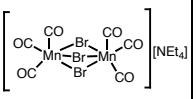 **3**	0.0	0.1 0.8 1.6 4.3	0.0 0.0 0.0 0.1	0.8 1.4 1.8 4.1	0.0 0.0 0.0 0.0	1h 3h 5h 24h
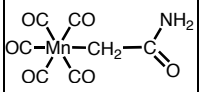 **4**	0.3	2.0 2.8 3.0 2.9	0.4 0.8 1.0 1.2	1.2 1.2 1.3 1.4	0.1 0.3 0.3 0.4	1h 3h 5h 24h
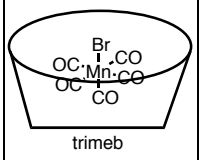 **5**	1.1	0.5 2.6 2.8 2.8	0.1 0.5 0.7 0.8	1.3 1.7 1.4 1.4	0.4 0.2 0.2 0.4	1h 3h 5h 24h

Among the compounds selected, **2**, **3** and **4** do not spontaneously release CO in RPMI after 6h under the standardized conditions of Fig. 1 in Chapter II. The other two, **1** and **5** release relatively small amounts, 33% and 22%, respectively. Compound **2** (CMT discussed in chapter II) is completely inert towards oxidation

by both peroxides. This is a very rare case but fits in with the tremendous oxidative stability of $CpM(CO)_3$ complexes (M = Mn, Tc, Re). In fact, $CpMn(CO)_3$ has been commercialized as an antiknock gasoline additive. Its oxidative electrochemistry has only been addressed recently.[47]

This stability allows the use of $CpTc(CO)_3$ derivatives in radioimaging applications.[48, 49] The cold counterpart of the useful ^{99m}Tc complex, $CpRe(CO)_3$, has been found to be stable in circulation and recovered after excretion with the Cp ring hydroxilated. This metabolic pathway resembles that of benzene and other aromatic rings.[50] Of course, one might blame this inertness on the total insolubility of the compound in the aqueous reaction media. However, as will be seen in other examples insolubility alone does not prevent oxidation under these conditions.

In contrast, both water soluble complexes **3** and **4** are strongly activated by TBHP and H_2O_2. The former does not show a preference for any of the peroxides but the later is clearly more reactive towards TBHP. **3** represents a situation where the *fac*-$Mn^I(CO)_3$ fragment was no longer able to deliver CO because it had reached high substitutional stability, even under O_2. Table 1 shows that ROS can induce CO release from this kind of fragment. In a way, **3** exemplifies some of the properties of one kind of desirable profile for a CO-RM: some solubility and good stability in aqueous solution which is reversed in the presence of ROS to liberate CO in inflamed tissues.

Complex **3** does not catalyze the oxidation of CO to CO_2. Interestingly, **4** which is also water soluble and stable in aqueous biological solutions would be expected to have a similar oxidative chemistry. Instead, it reacts differently with TBHP and H_2O_2 and liberates CO and CO_2 in ca. 3:1 ratio. Moreover, this oxidation is very fast and essentially terminated after 3h of reaction in TBHP or 1h in H_2O_2. Some CO in the initial compound is wasted by oxidation to CO_2 a process most likely catalyzed by some Mn species.

Compound **1** is a spontaneous CO releaser in aqueous biological aerobic solutions. Nevertheless, both TBHP and H_2O_2 strongly activate this release and

the compound liberates its CO load as a $CO:CO_2$ mixture (ca. 4:1), in an essentially quantitative way after 5h reaction.

Complex **5** is formed by encapsulation of **1** in TRIMEB, a functionalized form of β-cyclodextrin. The result of this encapsulation is the reduction of its spontaneous CO release output by 33%. In the case of the reaction with TBHP, after 5h, this inhibition is only 21%. This is surprising because it could be expected that the size of TBHP would make its interaction with the encapsulated MCC more difficult. This simple expectation is not obviously met. However, when H_2O_2 is used as oxidant, the inhibition of CO release is 62% and, interestingly, the ratio $CO:CO_2$ increases to 7:1 which reveals a strong interference of the encapsulation on the mechanism of oxidation of **1** by H_2O_2.

4.2 The Molybdenum compounds

The number of Molybdenum carbonyls tested is much larger and covers a wider spectrum of behaviors. To simplify the discussion and allow a more systematic analysis of results, the compounds are arranged in several tables according to their structural type and reactivity profiles.

The influence of solubility on CO release is a recurrent problem in all the screenings and will be discussed right at the beginning of this study.

The compounds assembled in Table 2 were chosen to evaluate the importance of solubility in the ROS induced profile of CO release. They are all totally insoluble in the aqueous reaction medium, yet they all react slowly with TBHP and H_2O_2 to liberate CO.

Table 2: Equivalents of CO and CO_2 released by some insoluble molybdenum compounds with 100 equiv. molar excess of TBHP and H_2O_2 in water. Gas samples were taken after 1h, 3h, 5h and 24h and quantified by GC/TCD.

Compound	Equiv. CO released after 6h in RPMI	TBHP		H_2O_2		Time of reaction
		CO	CO_2	CO	CO_2	
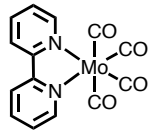 **6**	0.0	0.1 0.3 0.6 2.4	0.0 0.1 0.2 0.7	0.0 0.3 0.5 1.8	0.0 0.1 0.2 0.5	1h 3h 5h 24h
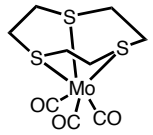 **7**	0.0	0.0 0.4 0.8 1.9	0.0 0.2 0.5 1.4	0.2 1.2 1.5 1.4	0.1 0.9 1.2 1.2	1h 3h 5h 24h
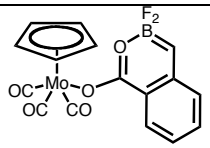 **8**	0.2	0.0 0.1 0.2 0.9	0.0 0.0 0.0 0.1	0.1 0.1 0.2 0.7	0.0 0.0 0.0 0.1	1h 3h 5h 24h

With **6,** after 24h reaction time the amount of CO liberated is significantly larger than the one obtained after 5h. The reaction is also more extensive with TBHP than with H_2O_2. The other two compounds show the same reactivity trends but are still slower releasers in aqueous solution. It is nevertheless important to realize that complex **7** loses all its CO as a mixture of CO and CO_2 after 24h reaction with TBHP. On the other hand, with H_2O_2 the reaction is completed after 5h reaction time. This behavior is totally opposite to complex **8** which is highly inert during the first 5h of reaction and only after 24h reaction high amounts of CO are liberated.

When complex **6** is reacted with TBHP in *n*-decane using dichloromethane as solvent instead of water, a much faster reaction is observed with evolution of roughly 2.5 equiv. CO and 1 equiv. CO_2 (Table 3). A white powder which showed

the characteristic Mo=O stretching vibrations at 901, 931cm^{-1} was obtained at the end of the reaction but wasn't fully characterized.

The interesting observation though, is that the results obtained in dichloromethane after ca. 8h are very similar to the results obtained in water after 24h. This similarity suggests that insolubility is mainly delaying the aqueous reaction, since the outcome of the experiment is essentially the same in the long term. However, no reliable analysis of the results can be made at shorter reaction times.

In any case, it seems reasonable to conclude that lack of reaction of a given MCC with TBHP or H_2O_2 in water after 24h really corresponds to an oxidatively stable compound, as shown before for $CpMn(CO)_3$.

Table 3: Equivalents of CO and CO_2 released by **6** dissolved in CH_2Cl_2 with 10 equiv. molar excess of TBHP in *n*-decane. Gas samples were taken after 1h, 3h, 5h, 8h and 24h and quantified by GC/TCD.

Time/Hours	Equiv. CO	Equiv. CO_2
1	1.0±0.1	0.2±0.1
3	1.9±0.1	0.6±0.1
5	2.2±0.0	0.8±0.1
8	2.5±0.0	0.9±0.1
24	2.6±0.0	0.9±0.1

After these initial tests, a series of eight derivatives of the $(\eta^5\text{-}C_5R_5)Mo(CO)_3R$ family was studied and the results are shown in Table 4.

Table 4: Equivalents of CO and CO_2 released by $(\eta^5\text{-}C_5R_5)Mo(CO)_3R$ compounds with 100 equiv. molar excess of TBHP and H_2O_2 in water. Samples were taken after 1h, 3h, 5h and 24h. Gas samples were taken after 1h, 3h, 5h and 24h and quantified by GC/TCD.

Compound	Equiv. CO released after 6h in RPMI	TBHP		H_2O_2		Time of reaction
		CO	CO_2	CO	CO_2	
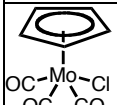 **9**	0.4	0.4 1.7 2.6 2.9	0.0 0.2 0.3 0.3	0.1 0.5 1.1 2.9	0.0 0.0 0.1 0.4	1h 3h 5h 24h

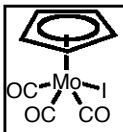 **10**	0.0	0.0 0.1 0.3 2.0	0.0 0.0 0.2 1.2	0.7 1.4 1.6 1.1	0.3 1.1 1.2 0.9	1h 3h 5h 24h
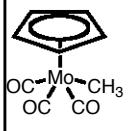 **11**	0.0	0.4 1.4 1.9 2.1	0.0 0.1 0.2 0.3	0.2 0.7 1.1 1.7	0.0 0.0 0.0 0.1	1h 3h 5h 24h
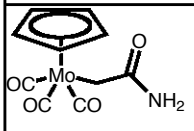 **12**	0.7	0.5 1.4 1.7 1.9	0.1 0.3 0.4 0.5	1.4 2.3 2.3 2.3	0.1 0.2 0.3 0.3	1h 3h 5h 24h
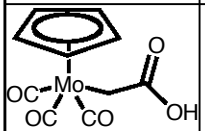 **13**	0.8	0.0 0.0 0.0 0.2	0.0 0.0 0.0 1.2	0.0 0.1 0.2 1.4	0.0 0.0 0.0 0.2	1h 3h 5h 24h
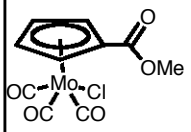 **14**	0.2	0.2 1.2 1.9 1.9	0.0 0.5 0.8 0.9	0.4 1.1 1.3 1.1	0.2 0.6 0.7 0.6	1h 3h 5h 24h
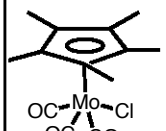 **15**	0.0	0.2 1.0 1.6 2.3	0.1 0.3 0.4 0.7	0.0 0.1 0.2 1.8	0.0 0.0 0.0 0.3	1h 3h 5h 24h
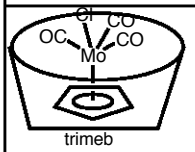 **16**	0.5	0.2 1.0 1.6 2.0	0.0 0.1 0.2 0.3	0.4 1.6 1.9 1.6	0.0 0.1 0.2 2.1	1h 3h 5h 24h

The first observation regards the selectivity of the complexes towards both oxidants. Looking at the late stages of the reaction, that is 24h reaction time, only

two compounds show a stronger release with H_2O_2: **12** and **13**. More extensive reactions with TBHP are found for all other compounds except **9** that gives almost identical results with both oxidants. In fact, this compound loses quantitatively the three carbonyls to CO and CO_2 in a ca. 8:1 ratio with both TBHP and H_2O_2, respectively, at 24h. However, the reaction is faster with TBHP up to 5h. The later results agree with those reported previously for the oxidative decarbonylation of **9** in non-aqueous medium.[42] The reaction was performed in CH_2Cl_2 with 10 equivalents of TBHP in decane and was completed in 3 to 4h with 3 equivalents of CO released and a CO/CO_2 ratio of ≈ 80 . The *in situ* decarbonylation led to metal-oxo complexes like $CpMoO_2Cl$ which are active olefin epoxidation and thioether oxidation catalysts with TBHP as oxidant.[41]

Somewhat surprisingly, the replacement of chloride by iodide has a strong effect on the reactivity with both oxidants. Indeed, $CpMo(CO)_3I$ (**10**) reacts initially in a very slow rate with TBHP but the reaction goes almost to completion at 24h although with a higher amount of CO_2 being formed ($CO:CO_2$ = 2:1.2). On the other hand, the same $CpMo(CO)_3I$ reacts initially with H_2O_2 at a rate similar to that observed for the chloride analogue, but the reaction comes to an halt after ca. 3h, again with $CO:CO_2 < 2:1$. Such behavior suggests the formation of intermediate species along the reactions, most likely oligomeric species, which change the course of the reaction and/or slow down CO release.

The alkyl analogue of these two compounds, $CpMo(CO)_3CH_3$ (**11**), shows a very smooth oxidation profile with both oxidants but is clearly faster with TBHP. Like in the case of **9**, the oxidative decarbonylation of $CpMo(CO)_3CH_3$ was already studied for catalytic epoxidation[51] in non-protic media, but the CO/CO_2 release was not quantified. To allow a comparison between organic and aqueous medium the study of the CO release profile under the catalytic conditions (in CH_2Cl_2 with 10 equiv. molar excess of TBHP in *n*-decane) was performed and the results are given in Table 5.

Table 5: Equivalents of CO and CO_2 released by **11** dissolved in CH_2Cl_2 with 10 equiv. molar excess of TBHP in *n*-decane. Gas samples were taken after 1h, 2h, 5h and 24h and quantified by GC/TCD.

Time/Hours	Equiv. CO	Equiv. CO_2
1	0.2±0.0	0.0±0.0
2	0.6±0.0	0.0±0.0
5	1.7±0.0	0.0±0.2
24	2.2±0.1	0.7±0.2

Despite a slightly slower initial rate of CO release in dichloromethane, the results of both assays become very close after 5h with 1.7 equiv. of CO liberated in organic medium against 1.9 equiv. in aqueous solution. The final amount of CO released (2.2 equiv.) is nearly the same in both conditions although a higher amount of CO_2 is formed in CH_2Cl_2 solution. These data show that all the carbonyls were released but 23% are lost as CO_2 while in aqueous solution only 9% CO_2 was produced. Importantly, no CH_4 was formed in any of the reactions either in water or in CH_2Cl_2. Therefore, it is quite likely that oxo species as the well known $CpMo(O)_2CH_3$[52] are formed under these conditions in a controlled way.

Introducing a functionalization at the alkyl substituent, as in the cases of $CpMo(CO)_3\{CH_2C(O)NH_2)\}$ (**12**) and $CpMo(CO)_3\{CH_2C(O)OH\}$ (**13**) produces a drastic change in the reactivity of the complexes.

As already noted above these two compounds are the only in the list that show a stronger release with H_2O_2. In fact, **13** doesn't even react with TBHP at 24h and stimulation with H_2O_2 only produced appreciable amounts (1.4 equiv. CO; 47% of the total CO contents) after 24h. In contrast, **12** reacts smoothly with TBHP (similar to the alkyl analogue) but shows a very strong activation in the presence of H_2O_2 which is completed before 3h reaction time. This reaction is discussed below in a closer detail.

The three last compounds in table 4 introduce different types of perturbations relative to $CpMo(CO)_3Cl$.

The introduction of an electron withdrawing group on the cyclopentadienyl ring as in (η^5-$C_5H_4C(O)OMe$)$Mo(CO)_3Cl$ (**14**), does not alter the relative reactivity towards TBHP and H_2O_2 in a very significant way but reduces the reactivity in both instances relative to $CpMo(CO)_3Cl$. It seems that the electron-withdrawing effect of the substituent on the ring makes the compound a little more difficult to oxidize and, therefore, a slower releaser compared to its parent, unsubstituted congener. This is a logical and expected variation. Some increase in steric hindrance may also contribute to slow down the reaction.

The presence of five methyl substituents on the ring in $Cp^*Mo(CO)_3Cl$ (**15**) should have the opposite effect: the metal becomes more electron rich and is easier to oxidize than the parent unsubstituted $CpMo(CO)_3Cl$. However, the increased steric bulk introduced by the five methyl substituents together with the increase in the Mo-CO bond strength resulting from a better π-backdonation from the richer Mo to the CO ligands should make the approach of the oxidants to the inner sphere of the complex much more difficult and, therefore, retard the reactivity of the complex with both TBHP and H_2O_2. In other words, this kind of substitution might favor an outer sphere electron transfer reaction between the complex and the oxidant but disfavor an inner sphere oxidation mechanism that requires coordination of the peroxides to the metal.

The experimental results in Table 4 reveal not only a general decrease in oxidation rates but also a widening of the reactivity gap between **15** and **9** from 0 to 5h reaction time. While the reaction with H_2O_2 was clearly disfavored (7% CO released for **15** vs 35% for **9** at 5h), that with TBHP occurred smoothly (52% at 5h for **15**) albeit slower than that of **9** (88% at 5h). This fact strongly suggests that there is an important mechanistic difference between the oxidation induced by TBHP and by H_2O_2 in these complexes. This difference is also apparent in the studies of catalytic oxidation performed with both types of systems, that is $Cp'Mo(CO)_3X$/TBHP vs $Cp'Mo(CO)_3X/H_2O_2$ and will be further infirmed below in the context of the detailed study of the oxidation of $CpMo(CO)_3\{CH_2C(O)NH_2)\}$.

In any case, the overall effect of introducing substituent groups on the Cp ring showed a reactivity decrease relative to the parent unsubstituted compounds. From the molecules studied, **9** is the only that loses 3 carbonyls with both oxidants, effectively as CO, similarly to what was demonstrated in organic medium.

As expected,[53] encapsulation of **9** in TRIMEB ($CpMo(CO)_3Cl$@TRIMEB) (**16**) clearly decreased the rate of decarbonylation. With TBHP only 2.0 equiv. CO are released after 24h against 3 equiv. of the free compound **9**. The difference in the amount of CO released for **9** and **16** after 5 h was 1 equivalent and this difference was maintained up to 24 h with a final $CO:CO_2$ ratio close to 8:1. With H_2O_2, decarbonylation of **16** starts faster but at 24h when completion is attained, the $CO:CO_2$ ratio is close to 0.8. This means that somehow encapsulation has changed the pathway of the oxidative reaction with H_2O_2 and produced an oxidant species capable of oxidizing CO to CO_2 in good yields. Furthermore the total amount of CO + CO_2 at 24h (3.7 equivalents) exceeds that of the initial CO (3 equivalents) so that the oxidant which is formed is capable of oxidizing either the cyclodextrin or the Cp ring.

Again, the difference between activation by H_2O_2 and TBHP is notorious and may lead to different chemical outcomes.

Besides, it seems clear that the host:guest interaction is relatively strong in aqueous solution and that association of the complex with the cyclodextrin strongly reduces its reactivity towards the oxidants (including O_2 as seen in chapter II, table 8).

Information on the oxidation reactions of a last group of Mo carbonyls complexes all containing the fragment $Mo(CO)_5$ is collected in Table 6. In terms of spontaneous CO release, these compounds vary from high stability in aerobic aqueous RPMI solution, as the cyano (**19**) and the phosphine derivatives (**21**-**24**) to a rather high instability that gives rise to an extensive and fast CO release, as found for the sparingly water soluble $[NEt_4][Mo(CO)_5Br]$ (**17**). Another subdivision of these complexes can be made according to their charge since five

of them are anionic and the other three are neutral. However, there is a large chemical difference between the effects expected from a metal based negative charge as in (X = Br, I, CN) (**17-19**) and those expected from a highly ionizable charge located at the distal, non-coordinating end of the structure of the phosphonated triphenylphosphine derivative (**24**). Indeed, the chemistry of $P(C_6H_5SO_3Na)_3$ is recognized as essentially similar to that of PPh_3 with the exception that it allows its complexes to be water soluble.[54, 55] For this reason the next discussion considers the complex $[Mo(CO_5)P(C_6H_5SO_3Na)_3]$ as a "neutral" species like the other PR_3 derivatives considered.

Table 6: Equivalents of CO and CO_2 released by molybdenum pentacarbonyl compounds with 100 equiv. molar excess of TBHP and H_2O_2 in water. Gas samples were taken after 1h, 3h, 5h and 24h and quantified by GC/TCD.

Compound	Equiv. CO released in RPMI after 6h	TBHP		H_2O_2		Time of reaction
		CO	CO_2	CO	CO_2	
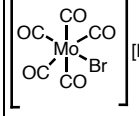 **17**	2.4	2.5 3.8 3.9 3.9	0.5 1.0 1.1 1.1	1.1 1.5 1.5 1.4	0.4 0.8 0.9 0.9	1h 3h 5h 24h
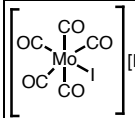 **18**	1.0	0.5 1.8 3.5 4.3	0.0 0.2 0.6 1.0	1.3 3.0 3.2 ---	0.1 0.4 0.5 ---	1h 3h 5h 24h
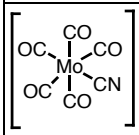 **19**	0.5	1.6 2.9 3.1 3.1	0.4 0.7 0.7 0.8	1.8 2.8 2.6 ---	0.7 1.3 1.2 ---	1h 3h 5h 24h
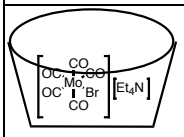 trimeb **20**	1.6	1.9 2.9 3.2 3.2	0.4 0.9 1.0 1.1	1.7 2.4 2.6 2.2	1.0 1.6 1.8 1.6	1h 3h 5h 24h
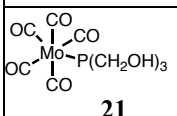 **21**	0.0	0.0 0.0 0.1 0.4	0.0 0.0 0.0 0.2	0.2 2.7 4.6 4.5	0.0 0.1 0.2 0.3	1h 3h 5h 24h

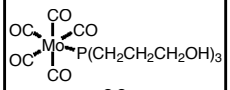 **22**	0.0	0.0 0.0 0.0 0.3	0.0 0.0 0.0 0.1	0.1 2.4 3.9 2.6	0.0 0.4 0.2 0.2	1h 3h 5h 24h
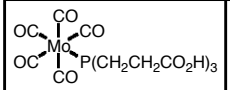 **23**	0.2	0.0 0.0 0.0 0.1	0.0 0.0 0.0 0.1	0.1 0.5 1.7 1.7	0.0 0.0 0.1 0.1	1h 3h 5h 24h
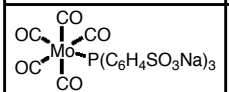 **24**	0.0	0.0 0.1 0.2 1.1	0.0 0.0 0.1 0.4	0.2 0.4 0.6 1.3	0.0 0.1 0.1 0.3	1h 3h 5h 24h

In terms of the relative reactivity with TBHP and H_2O_2, the anionic complexes are more reactive towards TBHP than towards H_2O_2 whereas the neutral ones are essentially unreactive with TBHP but reactive towards H_2O_2. Insolubility of the PR_3 derivatives is not the cause of such low reactivity because the water soluble **24** is also rather unreactive towards aqueous TBHP.

Although **17** and **18** are recognizedly substitutionally labile, the cyanide complex **19** is not. Yet their rates of reaction with TBHP are relatively close to each other. Certainly, TBHP is able to trigger its oxidation reactions in a different mode than H_2O_2. *A priori,* the substitutional inertness of the PR_3 complexes suggested a very low reactivity towards both TBHP and H_2O_2. This is the case for TBHP but not for H_2O_2 which oxidizes the complexes. It is possible that oxidation of the PR_3 ligand to the labile phosphine oxide OPR_3 is the actual trigger to the oxidation of the neutral PR_3 complexes by H_2O_2. This interpretation is entirely consistent with the observation that the amount of CO released is inversely correlated to the bulk of the PR_3 substituents. Even without quantifying cone angles for these phosphines the increase in this bulk rises obviously in the order:

$R= CH_2OH < CH_2CH_2CH_2OH < CH_2CH_2CO_2H < C_6H_5SO_3^-$.

The higher bulk of TBHP might be enough to block any reaction within this family of complexes. Yet, the smaller size of some phosphines might still allow H_2O_2 to interact with the coordinated P atom and oxidize it. Once OPR_3 is formed

it will be rapidly lost leaving a vacancy that will allow for faster oxidation of the Mo center by coordinated H_2O_2. This peroxide attack at the empty orbitals of the P atom of coordinated PR_3 is essentially of the same kind proposed to explain the 2nd order, associative term in the substitution reactions of $M(CO)_5PR_3$ complexes (M = Mo, W).[56]

Encapsulation of **17** in TRIMEB produced a modest decrease of the rate of CO release induced by TBHP from **20** relative to the free metal carbonyl compound. Interestingly, the reverse happened with regard to the reaction with H_2O_2 which is actually faster for **20** than for the free metal carbonyl compound **17**.

In any case, all examples shown reveal that interaction of $[Mo(CO)_5L]^{0/-}$ complexes with peroxides leads to a faster and more extensive liberation of CO which can reach 4 equivalents: **18** could triplicate the amount of CO spontaneously released while **19**, previously a non-releaser, is able to release nearly 3 COs in a short period of time (3h). With TBHP the $CO:CO_2$ ratio is usually close to 4:1 and there are no signs of the formation of a strong oxidation catalyst during the reaction which might lead to higher values for CO_2. Nevertheless, reactions of the anionic complexes in water essentially sacrifice one equivalent of CO via oxidation to CO_2. As an example, the reaction of **17** with TBHP in water gives a $CO:CO_2$ ratio of 4:1 but in CH_2Cl_2 solvent with TBHP/*n*-decane leads to the essentially quantitative liberation of 5 equivalents of CO and only a small amount of CO_2 as can be seen in table 7.

Reactivity with H_2O_2 is not so consistent. The reaction is always incomplete and none of the compounds released the 5 carbonyls. The maximum amount liberated is roughly 4 equiv. ($3CO + 1CO_2$) and in general lower amounts of CO are obtained.

Table 7: Equivalents of CO and CO_2 released by **17** dissolved in CH_2Cl_2 with 10 equiv. molar excess of TBHP in *n*-decane. Gas samples were taken after 5min, 30min, 1h, 1h30m, 2h and 3h and quantified by GC/TCD.

Time	Equiv. CO	Equiv. CO_2
5min	0.9±0.2	0.0±0.0
30min	2.9±0.1	0.0±0.2
1h	4.1±0.1	0.1±0.2
1h30min	4.4±0.1	0.1±0.2
2h	4.7±0.1	0.2±0.2
3h	4.9±0.1	0.2±0.2

Comparing the several instances tested, it is fair to say that the parallelism observed between the oxidation assays in organic and aqueous medium shows that the reaction course is the same in both situations. The main differences are kinetic aspects since the reaction in aqueous solution is slower and sometimes is incomplete. These results show that the "oxidative yield" is comparable after 24h and the different rates observed within the first hours of the assay may indeed be partially influenced by solubility factors.

4.3 The Iron compounds

The group of iron carbonyl complexes examined with regard to ROS induced CO release is presented in Table 8. It is a modest sample in terms of the vast amount of Fe-carbonyl complexes available in the literature but features two types of structurally important species in terms of putatively useful CO release profiles for therapeutic applications. The cyclopentadienyl containing complexes of the type $Cp'Fe(CO)_2X$ are readily available, usually fairly air stable complexes which can be modified at the Cp and X ligands to provide for adequate tuning of their solubility and biocompatibility as well as CO release properties. Under the conditions of these tests, they will release CO to the headspace irreversibly like all compounds studied and examined up to this point. On the contrary, the example of the second type of Fe carbonyl complexes chosen for this study, $Fe(cyst)_2(CO)_2$, is a reversible CO carrier where the moiety $Fe(cyst)_2$ loses CO

which after being lost may be recaptured at atmospheric pressure.[57, 58] This compound has even been claimed to play a role in the homeostasis of CO and Fe^{2+} liberated by Heme-Oxygenase and part of catalytic oxidation of Cysteine in cells.[59] At the outset of these experiments we were also aware of the difficulties that might arise due to the well established chemistry involving Fe ions and peroxides. However, no predictions could be made on a safe basis.

Table 8: Equivalents of CO and CO_2 released by some iron compounds with 100 equiv. molar excess of TBHP and H_2O_2 in water. Gas samples were taken after 1h, 3h, 5h and 24h and quantified by GC/TCD.

Compound	Equiv. CO released in RPMI after 6h	TBHP		H_2O_2		Time of reaction
		CO	CO_2	CO	CO_2	
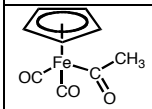 **28**	0.0	0.0 0.0 0.0 0.2	0.0 0.0 0.0 0.2	0.6 0.6 0.3 0.1	0.5 2.5 2.8 2.1	1h 3h 5h 24h
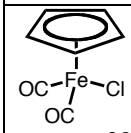 **29**	0.5	0.0 0.0 0.2 0.8	0.0 0.0 0.1 1.0	0.8 0.7 0.5 0.4	1.4 2.6 2.3 2.1	1h 3h 5h 24h
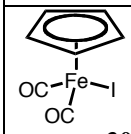 **30**	0.0	0.0 0.0 0.0 0.0	0.0 0.0 0.0 0.1	0.0 0.2 0.3 1.0	0.0 0.2 0.2 1.6	1h 3h 5h 24h
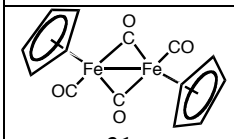 **31**	0.0	0.0 0.1 0.1 0.6	0.0 0.1 0.1 0.6	0.0 0.2 0.4 0.9	0.0 0.3 0.7 4.1	1h 3h 5h 24h
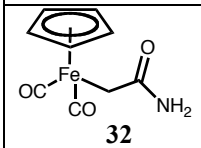 **32**	0.0	0.0 0.0 0.0 0.0	0.0 0.0 0.1 0.4	0.3 0.5 0.5 0.5	0.4 0.8 0.9 1.0	1h 3h 5h 24h
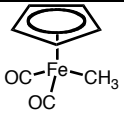 **33**	0.0	0.1 0.2 0.2 0.2	0.2 0.4 0.6 0.7	0.2 0.2 0.3 0.3	0.3 1.2 2.1 3.3	1h 3h 5h 24h

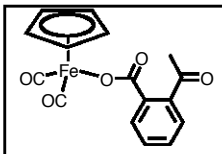 **34**	0.0	0.0 0.0 0.0 0.5	0.0 0.1 0.1 0.3	0.0 0.4 0.6 0.7	0.0 0.4 0.8 1.0	1h 3h 5h 24h
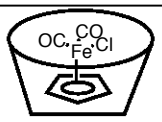 **35**	0.1	0.0 0.1 0.1 0.5	0.0 0.0 0.1 0.7	0.4 0.6 0.8 0.8	0.4 1.5 2.7 8.9	1h 3h 5h 24h
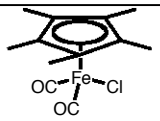 **36**	0.0	0.2 0.8 1.1 1.0	0.1 0.4 0.6 1.0	0.7 0.5 0.5 0.4	1.6 2.9 3.4 4.3	1h 3h 5h 24h
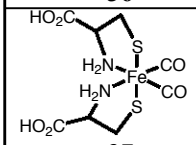 **37**	0.9	0.5 0.9 1.0 1.0	0.2 0.6 0.7 1.0	0.2 0.2 0.2 0.2	1.2 1.2 1.3 1.4	1h 3h 5h 24h

Inspection of table 8 reveals that most of the iron carbonyl complexes tested do not react readily with TBHP. Weak signs of decomposition can only be measured at 24h reaction time. The exceptions are $Fe(cys)_2(CO)_2$ (**37**) and $Cp^*Fe(CO)_2Cl$ (**36**) the only compounds that are able to release 1 equiv CO at 5h. In each of them, both CO ligands are liberated but one of them is oxidized to CO_2 since the final $CO:CO_2$ ratio becomes 1 at long reaction times (24h). In the case of **36** the ratio $CO:CO_2$ is ca. 2:1 in the beginning of the reaction up to 5h . However, this ratio becomes 1 at 24h. The results show that one of the CO ligands initially liberated was later oxidized to CO_2 by some species present in solution.

The reaction of **37** has a similar profile although the excess CO over CO_2 is always small. Nevertheless, the final $CO:CO_2$ ratio also becomes 1 at long reaction times (24h). Most interestingly, this profile is almost identical to that observed under O_2 in RPMI. It seems that TBHP does not really interfere with the dissociative kinetics typical of this reversible CO carrier.

The reactions with H_2O_2 are quite different and in some cases very surprising because:

- the amount of CO_2 always exceeds that of CO in the cases studied;
- in several cases the final amount of liberated CO + CO_2 exceeds the 2 equivalents of CO present in the initial complexes;
- some of these reactions are very fast compared to those of the other metals, like Mn and Mo.

The two first observations are consistent with the formation of oxidation catalysts that are able to oxidize CO and some of the ancillary ligands. The example of the encapsulated complex $CpFe(CO)_2Cl$@TRIMEB (**35**) is remarkably clear with regard to this catalytic mechanism because it is able to produce ca. 9(!) equivalents of CO_2 at 24h reaction time. This amount actually surpasses the amount expected from the total oxidation of the metal guest which should yield 7 equiv. of CO_2 at the limit. Therefore, it is necessary to conclude that part of the host cyclodextrin is also being oxidized. There is literature precedent for this behavior because cyclodextrins were reported to favor Fenton Chemistry "inside" the cavity, by coupling iron ions and H_2O_2 in processes aiming at the destruction of organic matter in environmental disposals.[60, 61]

Some complexes show an initial fast reaction that liberates a considerable amount of CO at 1h which, however, is oxidized during the rest of the experiment due to the high excess of oxidant.

To better understand this process the reaction of **29** with sub-stoichiometric amounts H_2O_2 was carried out and the results are shown in table 9. The reaction proceeds, with small amounts of CO released even under an 8-fold excess complex over H_2O_2. This process is slightly accelerated when the ratio **29**:H_2O_2 is raised to 4:1. When the reagents reach a 1:1 stoichiometry, the initial reaction is clearly a fast CO burst, corresponding to the release of ca. 25% of the total CO available in the initial complex, after only 5 minutes. However, this amount increases very slowly only to reach 1 equivalent of CO released after 24h. In any case, the amount of CO does not decrease as in the standard assays of table 8 where the excess of H_2O_2 is much larger and consumes free CO.

These findings substantiate the idea that a high excess of oxidant is deleterious for the CO releasing process from iron carbonyls, leading to undesired oxidation to CO_2.

Table 9: Equivalents of CO released from oxidation of **29** with H_2O_2 using different substrate:oxidant ratios. Gas samples were taken after 5min, 30min, 1h, 3h, 5h and 24h and quantified by GC/TCD.

		substrate:oxidant ratio		
Time	**Control complex 29 in H_2O**	**8:1**	**4:1**	**1:1**
5min	0.0	0.1	-	0.5
30min	0.0	0.1	-	0.6
1h	0.0	0.1	0.2	0.6
3h	0.0	-	0.2	0.6
5h	0.1	0.2	0.2	0.6
24h	0.1	0.3	0.3	0.9

It is quite likely that this chemistry is the result of the so-called "Fenton Chemistry", a broad collection of free radical reactions catalyzed by transition metals, namely Fe^{2+}. It was first described by the British chemist Henry John H. Fenton who reported in 1876 the oxidation of tartaric acid by Fe^{2+}/H_2O_2 system.[62-64] The mechanism of oxidation was object of debate for decades, however the commonly accepted general reaction is shown in Equation 5:

"Fenton Reaction"

$$H_2O_2 + Fe^{2+} \rightleftharpoons Fe(III) + OH^{\bullet} + OH^- \qquad \textbf{Equation 5}$$

The basis for the mechanistic studies were seeded by Haber and Weiss[65] showing the relevance of radical intermediates like $OH^{\bullet}$ and $HO_2^{\bullet}$. New mechanistic details and contributions from different authors led to modifications[66, 67] of the original theory and some highlighted the importance of intermediate species like ferryl ion $(Fe^{IV}O)^{2+}$ [68] instead of the highly reactive hydroxyl radical.[69, 70]

Since most of the mechanisms studied were developed for classical $Fe^{2+/3+}$

complex ions, the situation in our organometallic complexes could not be immediately applicable. Nevertheless, it is possible to imagine that small amounts of $Fe^{2+/3+}$ ions are generated in solution from decomposition of the organometallic species, and that these ions carry on their powerful oxidizing chemistry with the excess H_2O_2 present.

The number of possible reactions already identified in many chemical and biological studies is large (see scheme 1) and depends on the nature of the Fe complex, pH and H_2O_2/complex ratio.

Independently of mechanistic details it is now generally accepted that when excess Fe^{2+} over H_2O_2 is employed a quantitative oxidation of Fe^{2+} to Fe(III) occurs.

$$2\ Fe^{2+} + H_2O_2 \rightleftharpoons 2Fe(III) + 2OH^- \qquad \textbf{Equation 6}$$

In the presence of excess H_2O_2, in addition to iron oxidation, a catalytic decomposition of H_2O_2 is observed.

$$2H_2O_2 \rightleftharpoons 2H_2O + O_2 \qquad \textbf{Equation 7}$$

It is also accepted that further reactions of Fe(III) with excess peroxide lead to superoxide formation, although this is a slower reaction at physiological pH and dependent on the ligand coordinated to Fe(III). This class of reactions, involving products of Fenton reaction or catalysts like Cu(I) or Mn (II) are called *Fenton-like chemistry* and are generally believed to proceed via similar mechanisms[71-73] as oxidation reactions.

$$H_2O_2 + Fe(III) \rightleftharpoons Fe^{2+} + O_2^{\bullet -} + 2H^{\bullet +} \qquad \textbf{Equation 8}$$

Other parallel reactions can also occur (Scheme 3):

$$OH^{\bullet} + H_2O_2 \rightleftharpoons H_2O + H^+ + O_2^{\bullet -}$$

$$O_2^{\bullet -} + Fe(III) \rightleftharpoons Fe^{2+} + O_2$$

$$HO_2^{\bullet} + Fe^{2+} + H^+ \rightleftharpoons Fe(III) + H_2O_2$$

$$OH^{\bullet} + Fe^{2+} \rightleftharpoons Fe(III) + OH^-$$

$$HO_2^{\bullet} + Fe(III) \rightleftharpoons Fe^{2+} + H^+ + O_2$$

Scheme 3: Parallel radical reactions occurring *in vivo* involving iron and H_2O_2 derived species.[74]

Assuming that $OH^{\bullet}$ is formed, it is expected to attack aromatic rings, namely Cp.[75, 76]

This attack leads to the disruption of the aromatic ring and its oxidation with the release of CO_2. In all the compounds tested the amount of CO_2 released was higher than the amount of carbonyls in the molecule so CO_2 must come from the oxidation of the organic material.

Interestingly, the CO releasing rate of $CpFe(CO)_2$(acetylsalicylate) (**34**) is continuous and the amount of CO_2 obtained is not exaggerated. Since the only structural difference to the other $CpFe(CO)_2$ complexes studied is the presence of the acetylsalicylate ligand we propose that its anti-oxidant power[77, 78] is actually slowing down the decomposition of the organometallic compound.

4.4 Complementary observations relevant for the understanding of ROS induced CO release processes

4.4.1 Methane formation in TBHP assays

It was noted above that TBHP is used as a model for alkylhydroperoxides, ROOH, which are formed *in vivo* in the process of lipid peroxidation. It was also noted that TBHP has a different activation mode than H_2O_2 since most MCCs used can discriminate between both reagents. Moreover, the presence of a *tert*-

butyl substituent in TBHP opens a number of competing pathways for its decomposition that must be kept in mind when interpreting its redox chemistry. In particular, the *tert*-butyl radical is a rather stable alkyl radical with several decomposition pathways available.

In fact, an important result that was observed in some TBHP assays and isn't reported in the previous tables is the high amount of methane detected in some experiments.

Although the quantification of methane was not possible under our experimental conditions, it is still possible to compare chromatographic peak areas to rank the compounds according to their "methane producing" capacity.

The order observed was the following (area under peak):

Complex **15** >> **35** > **9** > **11** > **12** > **29** > **33**

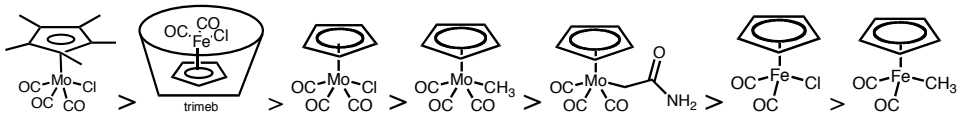

Interestingly, all these compounds have the same structure, $CpM(CO)_nR$, where Cp is either Cp or Cp*, M = Mo or Fe, n is 3 for Mo and 2 for Fe and R is either Cl, CH_3 or CH_2CONH_2.

Due to the very similar geometry of the complexes it seems logical to conclude that the reactivity observed is structurally related. Even more interesting is the fact that the 3 most active complexes all have a chloride as a co-ligand suggesting an active role of the halide in the reaction mechanism. Moreover, the first two compounds in the list have a modified Cp (**15**) and an encapsulated compound (**35**), while the remaining compounds all have "naked" molecules. This also suggests that a bulky steric hindrance or active metallic center protection is also relevant.

TBHP radical decomposition is dependent on many factors[79, 80] and some pathways lead to methyl radical formation. The usually accepted mechanism

involves peroxide one electron reduction originating the *tert*-butoxyl radical and hydroxide anion. A β scission then occurs giving a methyl radical (see Scheme 4).

$$(CH_3)_3COOH + e^- \rightleftharpoons (CH_3)_3CO^{\bullet} + OH^-$$

$$(CH_3)_3CO^{\bullet} \rightleftharpoons {}^{\bullet}CH_3 + (CH_3)_2CO$$

Scheme 4: Methyl radical formation from *t*-BuOOH

This methyl radical in aqueous solution can easily capture an hydrogen giving methane. This mechanism was already documented in literature and demonstrated by *spin trapping* techniques with Fe(II)/Fe(III) working as an electron donating system.[81]

Interestingly, this mechanism fits well the observed steric influence. Indeed, when electron transfer from the metal to TBHP takes place within the activated complex $[L_nM(CO)_x.(HOO^tBu)]^{\neq}$, steric repulsion favors the expulsion of bulky $(CH_3)_3CO^{\cdot}$ and it's subsequent breakdown, when the L_n ligands are also bulky.

If the steric room around the metal is larger, other pathways may be more favorable for the evolution of the $[L_nM(CO)_x.(HOO^tBu)]^{\neq}$ species.

4.4.2 Oxygen formation in TBHP and H_2O_2 assays

Also in some TBHP assays an unusual O_2 burst was observed. These results were obtained with ruthenium compounds $CpRu(CO)_2Cl$ (**38**) and $Ru(CO)_3Cl$(glycinate) (**39**) and also the iron complex **29**. In these cases a different decomposition pathway is observed, with formation of other radicals (Equation 9). A *tert*-butylperoxyl radical is formed from the homolytic decomposition of M^{II}-O-O-Bu^t adduct and two of these radicals couple together to generate *tert*-butoxyl radical and oxygen.[82, 83]

$$2(CH_3)_3COO^{\bullet} \rightleftharpoons 2(CH_3)_3CO^{\bullet} + O_2$$ **Equation 9**

A large amount of oxygen formation was a peculiar feature also observed in the course of the assays with H_2O_2. Once more it was not quantified but from the peak areas it was possible to rank the compounds according to the amount of O_2 detected. When compared with the TBHP assays the levels of O_2 measured were substantially higher. The speed of the reaction was also very high, sometimes was almost immediate, since after the first hour the maximum levels of O_2 were already achieved. This reactivity was observed with a wide variety of complexes and is also dependent on the H_2O_2 concentration. Nevertheless the compounds that produced more O_2 were the following:

Complex **28** > **38** > **29** > **18** > **$Co_2(CO)_6$(PhCCPh)** > **5** > **31** > **39**

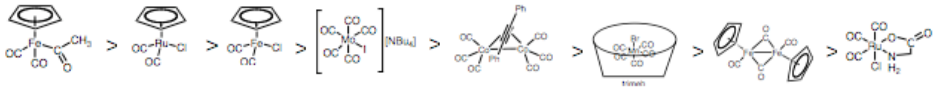

Hydrogen peroxide decomposition with O_2 evolution is a well-known biological relevant reaction since it is one of the anti-oxidant defensive mechanisms performed by catalases (Eq. 10).

$$2H_2O_2 \rightleftharpoons 2H_2O + O_2$$ **Equation 10**

In the present case no correlation among the complexes could be found. Within the first 6 complexes, 2 are iron compounds (**28** and **29**), 1 is a ruthenium compound (**38**), 1 is a molybdenum compound (**18**) and 1 is a cobalt compound (**$Co_2(CO)_6$(PhCCPh)**). Except for the first three compounds in the series that share the same structural feature $CpM(CO)_2L$ (and **31**:$[CpFe(CO)_2]_2$), none of the other complexes are structurally related. As demonstrated above the iron complexes also have Fenton chemistry reactivity, therefore, the two effects are competing. In an *in vivo* situation the outcome of the reaction would be dependant

on various factors, and factors like the local concentration of ROS and iron complex will be vital to determine which of the opposing reactions will prevail.

4.5 Oxidative Decarbonylation of $CpMo(CO)_3(CH_2CONH_2)$: a case study

It is now clear that oxidation is a main inducer or accelerator of CO release from a MCC. In scheme 5, chapter I, this situation was sketched in terms of the dramatic acceleration that substitution of CO can exhibit in 17-electron complexes *vs* their 18-electron counterparts. The first kinetic evidence for this acceleration was obtained from *de bona fide* 17-electron complexes. For instance, $V(CO)_6$ reacts with phosphines ca. 10^{10} times faster than its 18-electron isostructural analogue $[Cr(CO)_6]$, and $[V(CO)_6]^-$ is practically unreactive in the dark.[84] Likewise nucleophilic substitution of $[Fe(CO)_3(PPh_3)_2]^+$ by pyridine nucleophiles occurs 10^9 times faster than for the 18-electron analogue $Fe(CO)_3(PPh_3)_2$.[85] Later on Kochi and coworkers led this observation to practical applications in electrocatalysis where the 17-electron catalysts were obtained by electrochemical oxidation of comparatively inert 18-electron precursors.[86-88]

Due to its favorable stability and solubility properties $CpMo(CO)_3(CH_2CONH_2)$ (**12**) was selected as a model to study the effect of oxidation on CO labilization.

It is an 18-electron complex soluble in most organic polar solvents like dichloromethane, chloroform, diethyl ether, THF, acetone, acetonitrile and methanol. It is also soluble in water at low concentrations and very stable when kept under N_2 and in the dark. The presence of O_2, oxidants and light initiates a decomposition process that leads to CO release. In aerobic RPMI solution this release is small reaching 0.7 equiv CO in 6h. However, as shown in Table 4 this compound is activated both by TBHP and by H_2O_2 to release 1.4 and 2.3 equiv CO after 3h in TBHP and H_2O_2, respectively. We performed our studies in the dark since light also triggers CO release from this complex.

4.5.1 Reaction with 1-electron oxidants

A set of experiments was performed to establish whether a 1 electron oxidation was enough to trigger off CO release from $CpMo(CO)_3(CH_2CONH_2)$. $[Cp_2Fe]BF_4$, $AgBF_4$ and $AgNO_3$ were employed as 1-electron oxidants in different solvents and the reaction was followed by GC and IR.

The reaction between equimolar amounts of $[Cp_2Fe]BF_4$ and $CpMo(CO)_3(CH_2CONH_2)$ was followed over 24 h at room temperature, under N_2 and in the dark. The very intense characteristic purple color of $[Cp_2Fe]^+$ disappears rapidly upon mixing both reagents and CO liberation stops after 1h. The amount of CO liberated in several solvents during the first hour remained essentially unchanged up to 24h with the exception of NCMe which double that value as seen in Table 10.

Table 10: Equivalents of CO liberated after 1h or 24h upon reaction of $[Cp_2Fe]BF_4$ and $CpMo(CO)_3(CH_2CONH_2)$ in 1:1 molar ratio, at room temperature, under N_2 and in the dark in several solvents.

Equiv. CO released from $CpMo(CO)_3(CH_2CONH_2)$ with $[Cp_2Fe]^+$ (time; h)*					
H_2O(1h)	CH_2Cl_2(1h)	$(CH_3)_2CO$(1h)	THF(1h)	CH_3CN(1h)	CH_3CN(24h)
0.3	0.1	0.3	0.3	0.3	0.6

*CO_2 was present but not quantified

Although the redox reaction was fast, as judged by the rapid disappearance of the characteristic color of $[Cp_2Fe]^+$, it is obvious that CO release stopped at ca. 10% after 1h for all solvents, except for NCMe where it reached 20% CO release after 24h. This is also visible in the IR spectra of the solutions because the stretching CO vibrations of $CpMo(CO)_3(CH_2CONH_2)$ remained unchanged in all solvents except NCMe. $CpMo(CO)_3(CH_2CONH_2)$ has 2 bands at 2025 and 1932cm^{-1}. After reaction with ferrocenium in NCMe they shifted to 2032 and 1942 cm^{-1} with a new band appearing at 2082 cm^{-1} (see Fig. 1). To exclude the possibility that

these changes were caused by reaction of $CpMo(CO)_3(CH_2CONH_2)$ with the solvent a control spectrum of the compound alone was recorded in NCMe and no differences were observed showing clearly that it is not solvent interference. The spectra of free chloroacetamide, pure ferrocenium and ferrocenium with chloroacetamide were also recorded as controls and no reaction is observed between both species.

The slight change of νCO values to higher energy in NCMe, where the reaction was a bit more extensive, agrees with the expected formation of cationic species that should present increased values for νCO.

The analogous reaction of $CpMo(CO)_3(CH_2CONH_2)$ with $AgBF_4$ was performed in dichloromethane both in 1:1 (from now on designated R1) and 1:10 (from now on designated R10) molar ratios and followed by solution IR, CO release and ^1H NMR. In the R1 reaction the IR spectrum shows that after 24h some of the original $CpMo(CO)_3(CH_2CONH_2)$ is still unreacted in solution after a steady concentration decrease (see Fig. 3). The total amount of CO released was 0.46 equiv. CO. After 48h the reaction mixture was evaporated to dryness and the residue taken up in CD_2Cl_2, filtered and examined by ^1H NMR. The spectrum (Fig. 5) shows two small signals of the initial $CpMo(CO)_3(CH_2CONH_2)$ (δ 5.42 ppm (C_5H_5) and δ 1.80 ppm CH_2). There is a slighlty more intense signal in the region typical of the η^5-Cp protons (δ 5.42 ppm) but the largest signal appears as a sharp singlet at δ 1.26 ppm and a multiplet at δ 0.88 ppm. These signals and other smaller ones remained unassigned. In contrast, all the CO ligands were removed from $CpMo(CO)_3(CH_2CONH_2)$ after 3h in the presence of a 10-fold excess Ag^+, as can be concluded from the disappearance of the CO stretching vibrations in the IR spectrum of Figure 4. ^1H NMR analysis of the residue of the reaction after 48h (Fig. 6) shows the same resonances at δ 1.26 ppm and a multiplet at δ 0.88 ppm. However no resonance is present in the region assigned to the η^5-Cp protons and a new multiplet appears at δ 1.37 ppm.

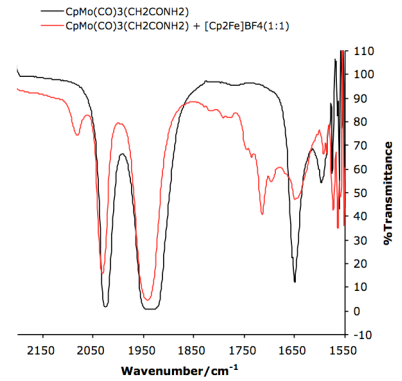

Figure 1: IR spectra of $CpMo(CO)_3(CH_2CONH_2)$ and of $CpMo(CO)_3(CH_2CONH_2)$ + $[Cp_2Fe]BF_4$ (1:1) in NCMe solution (carbonyl region)

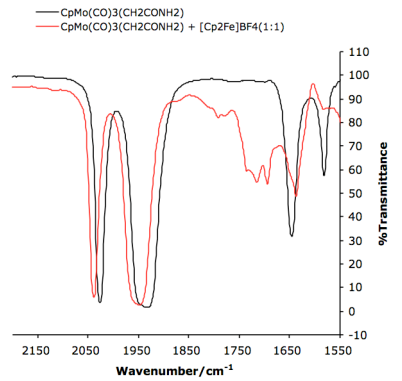

Figure 2: IR spectra of $CpMo(CO)_3(CH_2CONH_2)$ and of $CpMo(CO)_3(CH_2CONH_2)$ + $[Cp_2Fe]BF_4$ (1:1) in CH_2Cl_2 solution (carbonyl region)

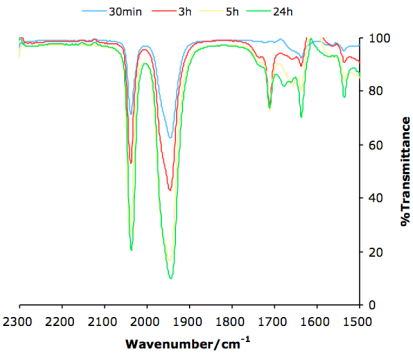

Figure 3: IR transmittance spectra of $CpMo(CO)_3(CH_2CONH_2)$ and $AgBF_4$ (R1) in CH_2Cl_2 over time (carbonyl region).

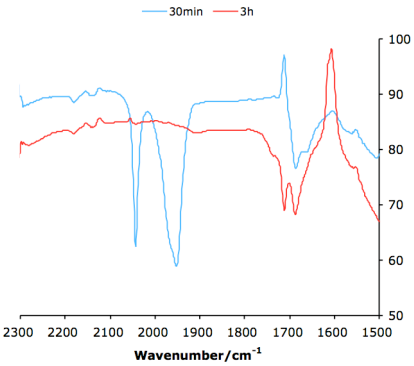

Figure 4: IR transmittance spectra of $CpMo(CO)_3(CH_2CONH_2)$ and $AgBF_4$ (R10) in CH_2Cl_2 over time (carbonyl region).

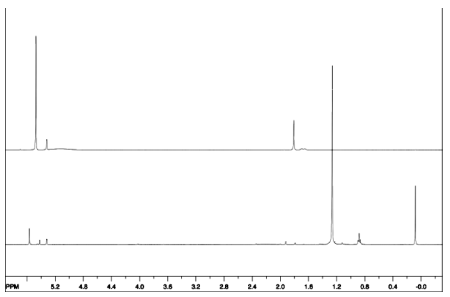

Figure 5: ^{1}H NMR spectra of $CpMo(CO)_3(CH_2CONH_2)$ (top) and $CpMo(CO)_3(CH_2CONH_2)$ with $AgBF_4$ (R1) in CD_2Cl_2 after 48h reaction

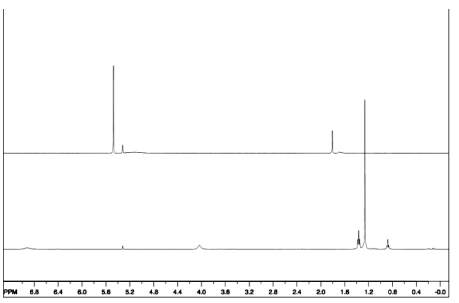

Figure 6: ^{1}H NMR spectra of $CpMo(CO)_3(CH_2CONH_2)$ (top) and $CpMo(CO)_3(CH_2CONH_2)$ with $AgBF_4$ (R10) in CD_2Cl_2 after 48h reaction

In summary, 1 equivalent of Ag^+ is not enough to induce quantitative CO release from $CpMo(CO)_3(CH_2CONH_2)$, even after 48h in CH_2Cl_2. However, use of a 10-fold excess of Ag^+ in the same solvent leads to quantitative decarbonylation of $CpMo(CO)_3(CH_2CONH_2)$ in less than 3h (Fig. 4).

A similar experiment carried out in water, using $AgNO_3$ instead of $AgBF_4$, corroborated these results. FT-IR and ^{1}H NMR spectra of the product obtained after 24h reaction of $CpMo(CO)_3(CH_2CONH_2)$ with 10-fold excess Ag^+ showed no CO bands and no Cp ring proton resonances, respectively. When the reaction was done in a 1:1 stoichiometry part of the initial $CpMo(CO)_3(CH_2CONH_2)$ is still unchanged in the reaction mixture after 24h as shown by IR and ^{1}H NMR spectroscopies.

These data agree with the CO release reported in table 10 but the mass balance of the initial CO cannot be done because CO_2 was detected but not quantified.

Table 11: Equivalents of CO released in the reactions of $CpMo(CO)_3(CH_2CONH_2)$ and $AgNO_3$ and $Ag[BF_4]$ in the molar ratios 1.1 and 1.10 measured with the vial method at 24h. Reagents were mixed together in degassed water, under N_2, in the dark and at room temperature.

Equiv. CO released from $CpMo(CO)_3(CH_2CONH_2)$ with Ag^+ (24h)*		
Reagent / Solvent	Reagent ratio 1:1	Reagent ratio 1:10
$Ag[BF_4]$ /CH_2Cl_2	0.46±0.04	1.67±0.03
$AgNO_3$ / Water	0.60±0.04	1.91±0.03

* CO_2 was present but not quantified.

Nevertheless, the amounts of CO released with excess oxidant far exceed those measured in aerobic RPMI.

This behavior is also in agreement with the results obtained by Tyler and co-workers, who generated water-soluble radicals by photolysis of $(CpCOO^-)_2W_2(CO)_6$,[89] $(CpCH_2CH_2NH_3^+)_2Mo_2(CO)_6$[90] and $(CpCH_2CH_2NMe_3^+)_2Mo_2(CO)_6$ dimers and showed that their behavior in aqueous solution is analogous to the chemistry in organic solvents.

4.5.2 Reaction with peroxides

The complex $CpMo(CO)_3(CH_2CONH_2)$ (**12**) is strongly activated by a 100-fold excess H_2O_2, as shown in table 4. In order to better understand this process, we first tried to determine the course of this reaction at lower H_2O_2:**12** ratios. As shown Table 12, after 3h the amount of CO released from **12** is the same with a 10-fold or a 100-fold excess H_2O_2. In practice, the reaction is complete in both cases with a total amount of 3 equivalents of CO being liberated. If the stoichiometry is 1:1 then only ca. 2 equivalents of CO are released after 3h but the liberation of CO continues slowly as seen at 24h.

Table 12: Equivalents of CO released by $CpMo(CO)_3(CH_2CONH_2)$ with aqueous H_2O_2 at room temperature, in the dark, under air. Gas samples were taken after 3h, 5h and 24h and quantified by GC/TCD.

Time	1eq. H_2O_2	10eq. H_2O_2	100eq. H_2O_2
3h	(1.74±0.03)	(2.65±0.04)	(2.64±0.04)
5h	(1.77±0.03)	(2.57±0.04)	(2.64±0.04)
24h	(2.11±0.03)	(2.47±0.04)	-----

These results show that the 100-fold excess is actually not necessary to drive all CO out of the initial complex. In another experiment, summarized in Table 13, it again becomes clear that the reaction is indeed completed in less than 30 min when a 10-fold excess H_2O_2 is used.

Table 13: Equivalents of CO released by $CpMo(CO)_3(CH_2CONH_2)$ in H_2O_2 at room temperature, in the dark, under air. Gas samples were taken after 30min, 1h and 2h and quantified by GC/TCD.

Time	1eq. H_2O_2	10eq. H_2O_2
30min	(1.37±0.03)	(2.56±0.04)
1h	(1.62±0.03)	(2.64±0.04)
2h	(1.69±0.03)	(2.63±0.04)

Since **12** is light sensitive, the experiments need to be carried out in the dark. If they are carried out under ordinary laboratory light the amount of CO liberated is slightly more elevated (5-8%) in some measurements. In the presence of light the solutions of **12** in any solvent slowly change color to green while releasing some CO. The 1:1 stoichiometry reaction between **12** and H_2O_2 also goes green in the light or turquoise blue in the dark. However, when the 10-fold excess H_2O_2 is added to **12**, these color variations are no longer observed and the initial dark yellow/orange solution of **12** rapidly becomes light yellow.

The presence of such a rapid**,** reproducible and quantitative reaction prompted the identification of its product. So, the reaction was performed on a preparative scale between $CpMo(CO)_3(CH_2CONH_2)$ (1.14 mmol) and H_2O_2 (11.6 mmol) in H_2O for 1h. In a first attempt, excess H_2O_2 was quenched with MnO_2 and a sensitive

yellow product was isolated. However, this product was paramagnetic as shown by ESR spectroscopy and result from the reaction of the initial reaction product with added MnO_2. This result was later confirmed as described below.

In order to avoid these problems, the synthesis was then repeated under similar conditions but a different method was used to isolate the reaction product. Ethanol was added to the reaction mixture at the end of the reaction and the resulting solution placed at 4ºC overnight. The yellow precipitate that separated was filtered and dried in vacuum. Unfortunately, we were unable to characterize this product because it readily explodes when dry and touched with a spatula. Such explosive properties are known for peroxo complexes[91].

Since the oxidation reaction seemed rather fast and clean, we attempted to study it by means of HPLC/MS, thereby avoiding the need to isolate the reaction product as a dry solid. This work was performed in collaboration with Bruno Guerreiro, a chemist from Alfama Inc., working in the laboratories of IKARIA Inc., Seattle, WA, USA, within a protocol of collaboration between both companies.

The compound dissolved in saline (NaCl 0.9%) was oxidized with 14 equiv. of H_2O_2 at room temperature under air and in the dark. The HPLC chromatogram of this mixture was analyzed at several time points and compared to the HPLC trace of the starting compound.

As can be seen in Fig. 7, the starting material was completely absent after 1h and only one new peak was detected with a retention time, RT=6.01 min. This result confirms that the removal of CO by H_2O_2 oxidation is very fast and is essentially complete in less than 1h in agreement with the results reported in Table 13. This was confirmed after 3h when the IR spectrum showed that all CO ligands present in the original complex had been removed (see Fig. 8).

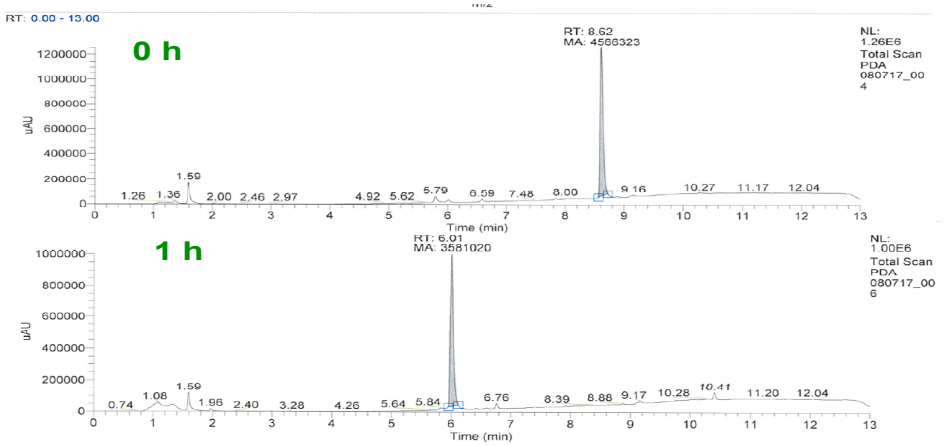

Figure 7: **(top)** HPLC trace of $CpMo(CO)_3(CH_2CONH_2)$ in saline solution before addition of H_2O_2 (14 molar equivalents); (**bottom**) HPLC trace of the reaction mixture after 1h reaction time.

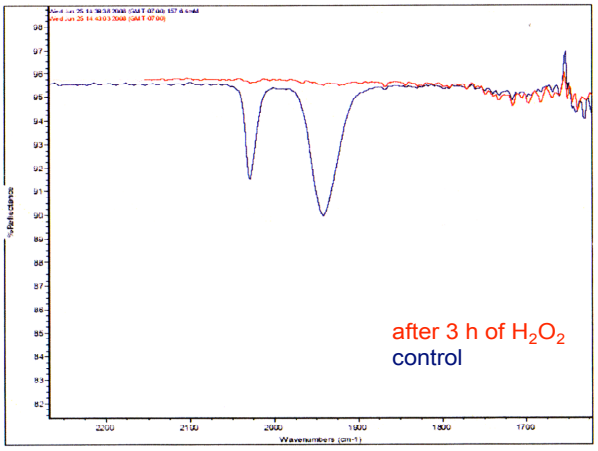

Figure 8:: IR spectra of $CpMo(CO)_3(CH_2CONH_2)$ in saline solution before and 3h after adding H_2O_2 (14 molar equivalents). Experiment performed at room temperature, in the dark and under air.

The ESI-MS of the single product at RT=6.01 min has its main peak at a *m/z* = 269.98 and a possible structure is (MW $(Cp^{98}MoO(\eta^2\text{-}O_2)(CH_2CONH_2) + H^+$ = 270.06). In order to carry out a better characterization of the compound, it was then isolated by preparative HPLC using a C18 reverse phase column and a MeOH/water gradient.

A new HPLC-MS analysis of the fraction corresponding to the product was carried out and the corresponding MS is given in Fig. 9.

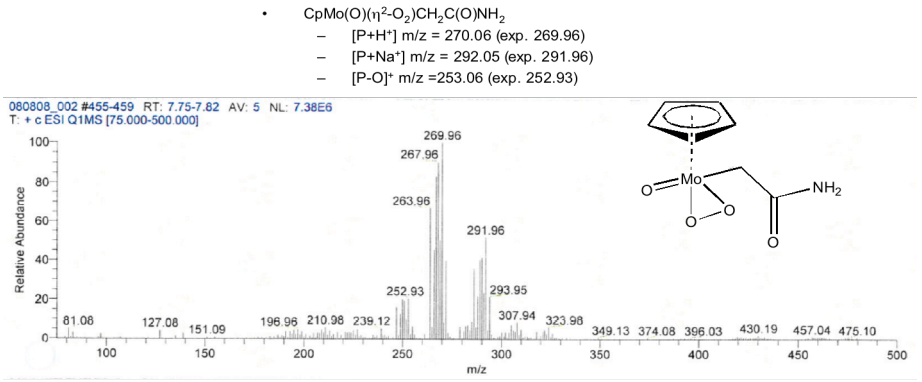

Figure 9: HPLC-MS analysis of the fraction corresponding to the product with RT=6.01 min.

The mass pattern is coherent with the oxo-peroxo structure proposed for the compound. This type of compound was first identified by Trost and Bergman who isolated Cp*MoO(η^2-O_2)Cl from the reaction of Cp*Mo$(CO)_3$Cl and O_2 with light.[40] Also, the ^{1}H NMR spectrum of the compound isolated by preparative HPLC supports the structure of the oxo-peroxo species (Fig. 10).

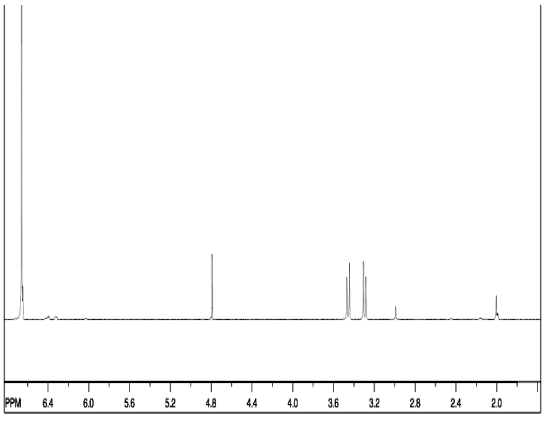

Figure 10: ^{1}H NMR spectrum in D_2O (δ 4.79 ppm) of the species isolated in the HPLC at RT=6.01 min which is assigned as CpMoO(η^2-O_2)CH_2CONH_2. The Cp signal is observed at δ 6.66 ppm (s,5H) and the protons from the amide observed at δ 3.31 (d,1H) and 3.47 (d,1H) ppm.

The signal corresponding to the Cp protons appears at δ 6.66 ppm in D_2O and the diastereotopic protons of the acetamide ligand appear as a pair of doublets at δ 3.47 and δ 3.31 ppm.

According to our HPLC analysis of the reaction of $CpMo(CO)_3(CH_2CONH_2)$ with 14 equivalents of H_2O_2 (a reasonable excess), the oxo-peroxo complex $CpMoO(\eta^2\text{-}O_2)(CH_2CONH_2)$ is initially formed (RT=7.70 min) but after 1.5 h it starts to decompose as shown in Fig. 11.

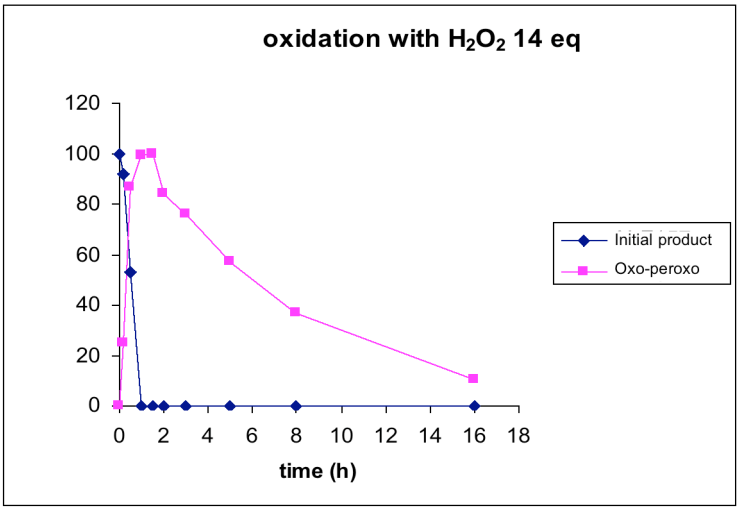

Figure 11: Formation and decay of $CpMoO(\eta^2\text{-}O_2)CH_2CONH_2$ in aqueous saline solution, evaluated by HPLC.

Following this decay by HPLC/MS, a very small peak with RT=7.58 min appeared. It was identified as the protonated form of the dioxo complex $CpMoO_2(CH_2CONH_2)$ with *m/z* $(Cp^{98}MoO_2(CH_2CONH_2) + H^+) = 254.06$. This dioxo complex is similar to $CpMoO_2Cl$, one of the first ever reported molecular organometallic oxides that was formed, isolated and characterized in organic, water free solvents.[92] More recent work has proposed $CpMoO_2X$ (X = Cl, CH_3) as the active species in the epoxidation and sulfoxidation reactions catalyzed by the system $CpMo(CO)_3X$ + TBHP in $CHCl_3$.[41, 51, 93] The relationship between the oxo-peroxo and the dioxo complexes was first identified in the reaction of Equation 11.[40]

$$Cp^*MoO_2Cl + TBHP \rightleftharpoons Cp^*MoO(\eta^2 - O_2)Cl + H_2O \qquad \textbf{Equation 11}$$

However, $CpMoO_2X$ complexes have never been identified in aqueous solution with H_2O_2 as oxidant and their stability in such media has been a matter of some controversy. The fact that the system $CpMo(CO)_3X + H_2O_2$ is completely inefficient for the epoxidation of olefins in the presence of water has been taken as a hint that $CpMoO_2Cl$ is not stable in aqueous media. As a matter of fact, our HPLC/MS experiments show that the concentration of $CpMoO_2(CH_2CONH_2)$ does not build-up in the reaction medium. On the contrary, highly ring substituted analogues $Cp^{Rn}MoO_2X$ are perfectly stable in water and active oxidation catalysts with H_2O_2 as oxidant.[51, 94, 95]

A similar decay study of $CpMoO(\eta^2\text{-}O_2)(CH_2CONH_2)$ was done in the presence of MnO_2, showing that the disappearance of the oxo-peroxo complex is faster. This observation helps explaining our failure in isolating this complex when we attempted to destroy excess H_2O_2 with MnO_2 (vide supra).

Interestingly, attempts to follow the reaction of $CpMo(CO_3)(CH_2CONH_2)$ with TBHP in aqueous solution (water or saline) only gave very complicated HPLC chromatograms with a large number of peaks in low concentrations. A similar procedure was adopted, dissolving the compound in saline and oxidation was carried out with 14 equiv. of $TBHP_{aq}$ at room temperature, under air and in the dark. The HPLC chromatogram of this mixture was analyzed at several time points and compared to the HPLC trace of the starting compound. After 7h a major peak at retention time RT=8.64 min was observed, corresponding to the parent complex. Although its intensity and AUC decreased over time this was still the major species in solution together with some minor peaks at RT=7.56 min and 9.32 min but with lower AUC values. The reaction proceeded up to 24h at which time several minor peaks (parent compound included) were observed, all with similar low intensities. Due to the complicated distribution of small peaks in the HPLC the identification of the reaction products was not possible. One could assign the peak at RT=7.56 min to the dioxo compound, $CpMo(O)_2(CH_2CONH_2)$.

This would be the expectable result bearing in mind the high yield formation of $CpMo(O)_2Cl$ from $CpMo(CO)_3Cl$ and TBHP in CH_2Cl_2.[41] However, we were unable to obtain a clean, positive ESI-MS spectrum that could confirm this expectation.

In summary, the experiments described in this case study clearly show that oxidation is an effective way of triggering CO release from an otherwise rather water and air stable metal carbonyl complex such as $CpMo(CO)_3(CH_2CONH_2)$. The rapid disappearance of the violet color of Fc^+ and the immediate appearance of metallic Ag when Fc^+ and Ag^+, respectively, are mixed with 1 equivalent of $CpMo(CO)_3(CH_2CONH_2)$ show that one electron oxidation of the Mo complex is very rapid. Although this oxidation is not followed by extensive CO release, some CO is still set free in solution. In other words, the process is not catalytic in the presence of the solvent. More equivalents of oxidant are necessary to result in extensive liberation of CO.

This is also seen in the reactions of $CpMo(CO)_3(CH_2CONH_2)$ with H_2O_2: a quantitative liberation of CO only takes place when a certain threshold excess of H_2O_2 is present. In this case, a molar ratio of H_2O_2:$CpMo(CO)_3(CH_2CONH_2)$ of 14:1 leads to total CO release in less than 1h, as ascertained by HPLC. The reaction product accumulates in high quantities exemplifying what may happen to a molecular MCC scaffold when activated by H_2O_2. The activation with TBHP is also effective to induce CO release but produces a much more complicated range of reaction products which we did not consider important to identify.

5. Final Remarks and Conclusions

The study that is described in this Chapter of CO release MCCs induced by *t*-BuOOH and/or H_2O_2, as representative examples of ROS present and active in biological media, and namely in inflamed tissues, is a screening that intends to:

- reveal the possibility of stimulating MCCs to release CO by reaction with ROS type oxidants;
- reveal the possibility that MCCs may discriminate between different ROS oxidants;
- draw a first draft of Structure Activity Relationships (SAR) for this type of chemistry.

The results reported lead to the following main conclusions:

- The concept of using oxidation as a trigger to start/enhance CO release from a MCC has been shown to be valid even in the case of some stoichiometric 1-electron oxidations;
- The number of complexes tested that resisted oxidation by ROS oxidants is very small;
- In most of the families of MCCs studied the release of CO is effectively enhanced relative to the spontaneous value at least by one of the two ROS oxidants tested, TBHP and H_2O_2;
- High lipophilicity and encapsulation slows down but does not prevent oxidation by ROS;
- Oxidation by ROS can be tuned by the nature of the ancillary ligands; the broadest spectrum of reactivities was found for $Mn^{I}(CO)_5X$, $Mo^{0}(CO)_5X$ and $CpMo^{II}(CO)_3X$ complexes;
- Most MCCs tested react preferentially with one of the two ROS used depending on their ancillary ligands and oxidation state;
- Derivatives of $Mn^{I}(CO)_3$ and $Ru^{II}(CO)_3$ do not respond to the ROS used; the former do not react, whereas the later rapidly decompose the ROS reagent to release O_2 and/or induce strong catalytic oxidation with formation of CO_2;
- $CpFe(CO)_2X$ complexes do not react with TBHP but react with H_2O_2 to produce more CO_2 than CO ($CO:CO_2 < 1$); a weak catalytic oxidation

activity is observed in these systems contrary to those of Mn and Mo where $CO:CO_2$ is usually > 2.

The ultimate purpose of this study was to test the possibility of using the naturally occurring oxidizing ROS as a means of inducing or triggering release of CO from MCCs at the places of inflammation or oxidative stress where they are particularly abundant and damaging. The results just summarized confirm that this strategy of passive, anti-ROS targeting mode is indeed a possibility. The oxidants used are only a minor fraction of the possible *in vivo* oxidizing triggers, and these crude tests were performed in conditions of large excess of ROS which surpass, by far, those concentrations found in vivo. Nevertheless ***it is possible to see that the oxidation of some MCCs turns them into CO-RMs because they release mostly CO*** and do not act just as simple peroxide scavengers or do not catalyze CO oxidation to CO_2. The last situations are also possible and seen to be the real ones for the $Ru(CO)_3$ complexes.

Some specificity was achieved since in some cases the complexes could discriminate between oxidizing agents. This can be an advantageous property that may allow even more specificity since the nature of the ROS produced endogenously is also dependent on the site of inflammation. Not all the tissues or organs have the same anti-inflammatory response and different tissues "request" different intermediates that produce different responses depending on the aggression and localization. Therefore, a distinct response towards oxidative stimuli may be a very effective method to ensure that CO is delivered to the exact target.

Of course, this does not exclude the utility of the indiscriminate CO releasers that may be useful for different indications where the need of CO delivery in multiple sites of inflammation is requested.

An important final note contemplates the fact that it is possible to tune the sensitivity towards ROS which is a most useful handle to improve the therapeutic effectiveness of the Metal Carbonyl based CO-RMs.

6. References

1. Beckman, K.B., Ames, B.N., *Phys. Rev.* **1998**, 78, 547.
2. Halliwell, B., Gutteridge, J.M., *Free Radicals In Biology and Medicine,* 3rd ed., Oxford University Press, New York, **1999**.
3. Finkel, T., Holbrook, N.J., *Nature* **2000**, 408, 239.
4. Xia, Y., Khatchikian, G., Zweier, J.L., *J. Biol. Chem.* **1996**, 271, 10096.
5. Wiseman, H., Halliwell, B., *Biochem. J.* **1996**, 313, 17.
6. Gilbert, D.L., Colton, C.A., *Reactive Oxygen Species in Biological Systems: An Interdisciplinary Approach,* Kluwer Academic/Plenum Publishers, New York, **1999**.
7. Halliwell, B., Gutteridge, J.M.C., *Biochem. J.* **1984**, 219, 1.
8. Halliwell, B., *Am. J. Med.* **1991**, 91, 14S.
9. Halliwell, B., Chirico, S., *Am. J. Clin. Nutr.* **1993**, 57, 715S.
10. Stadtman, E.R., *Free Radic. Biol. Med.* **1990**, 9, 315.
11. Folkes, L.K., Candeias, L.P., Wardman, P., *Arch. Biochem. Biophys.* **1995**, 323, 120.
12. Forni, L.G., Willson, R.L., *Biochem. J.* **1986**, 240, 897.
13. Paya, M., Halliwell, B., Hoult, J.R.S., *Free Radic. Res. Commun.* **1992**, 17, 293.
14. Richeson, C.E., Mulder, P., Bowry, V.W., Ingold, K.U., *J. Am. Chem. Soc.* **1998**, 120, 7211.
15. Alfassi, Z.B., *The Chemistry of Free Radicals: Peroxyl Radicals,* Wiley, New York, **1997**.
16. Sonntag, C.v., *The Chemical Basis of Radiation Biology,* Taylor & Francis, London, **1987**.
17. Farmer, E.H., Sutton, D.A., *J. Chem. Soc.* **1943**, 119.
18. Farmer, E.H., Sutton, D.A., *J. Chem. Soc.* **1943**, 122.
19. Alfassi, Z.B., Huie, R.E., Neta, P., *J. Phys. Chem.* **1993**, 97, 6835.
20. Marcus, R.A., Sutin, N., *Biochim. Biophys. Acta* **1985**, 811, 265.
21. Sawyer, D.T., Valentine, J.S., *Acc. Chem. Res.* **1981**, 14, 393.
22. Lardinois, O.M., *Free Rad. Res.* **1995**, 22, 251.
23. Qian, S.Y., Buettner, G.R., *Free Radic. Biol. Med.* **1999**, 26, 1447.
24. Halliwell, B., Gutteridge, J.M., *Methods in enzymology* **1990**, 186, 1.
25. Bolland, J.L., *Quarterly Reviews* **1949**, 3, 1.
26. Porter, N.A., Weber, B.A., Weenen, H., Khan, J.A., *J. Am. Chem. Soc.* **1980**, 102, 5597.
27. Porter, N.A., Wolf, R.A., Yarbro, E.M., Weenen, H., *Biochem. Biophys. Res. Commun.* **1979**, 89, 1058.
28. Porter, N.A., Wolf, R.A., Weenen, H., *Lipids* **1980**, 15, 163.
29. Gutteridge, J.M., *FEBS Lett* **1986**, 201, 291.

30. Halliwell, B., Gutteridge, J.M.C., Cross, C.E., *Journal of Laboratory and Clinical Medicine* **1992**, 119, 598.
31. Southorn, P.A., Powis, G., *Mayo Clinic Proceedings* **1988**, 63, 390.
32. Herrmann, W.A., Okuda, J., *J. Mol. Catal.* **1987**, 41, 109.
33. Wallis, J.M., Kochi, J.K., *Inorg. Chim. Acta* **1989**, 160, 217.
34. Crayston, J.A., Almond, M.J., Downs, A.J., Poliakoff, M., Turner, J.J., *Inorg. Chem.* **1984**, 23, 3051.
35. Herrmann, W.A., Serrano, R., Bock, H., *Angew. Chem. Int. Edit. Engl.* **1984**, 23, 383.
36. Wolowiec, S., Kochi, J.K., *Inorg. Chem.* **1991**, 30, 1215.
37. Herrmann, W.A., *J. Organomet. Chem.* **1995**, 500, 149.
38. Romao, C.C., Kuhn, F.E., Herrmann, W.A., *Chem. Rev.* **1997**, 97, 3197.
39. Romão, C., Royo, B., *Comprehensive Organometallic Chemistry III,* (Eds.:R. H. Crabtree; M. P. Mingos) Elsevier, Oxford, **2006**; Vol. 5, p 855.
40. Trost, M.K., Bergman, R.G., *Organometallics* **1991**, 10, 1172.
41. Abrantes, M., Santos, A.M., Mink, J., Kuhn, F.E., Romao, C.C., *Organometallics* **2003**, 22, 2112.
42. Valente, A.A., Seixas, J.D., Goncalves, I.S., Abrantes, M., Pillinger, M., Romao, C.C., *Catal. Lett.* **2005**, 101, 127.
43. Sinou, D., *Metal Catalysis in Water,* Springer Verlag, Berlin Heidelberg, **1999**; Vol. 206, p 41.
44. Bedard, L., Young, M.J., Hall, D., Paul, T., Ingold, K.U., *J. Am. Chem. Soc.* **2001**, 123, 12439.
45. Schnellmann, R.G., *Am J Physiol* **1988**, 255, C28.
46. Greenwood, N.N., Earnshaw, A., *Chemistry of The Elements,* 2nd ed., Butterworth-Heinemann, Oxford, **1997**; p 1005.
47. Laws, D.R., Chong, D.S., Nash, K., Rheingold, A.L., Geiger, W.E., *J. Am. Chem. Soc.* **2008**, 130, 9859.
48. Liu, Y., Spingler, B., Schmutz, P., Alberto, R., *J. Am. Chem. Soc.* **2008**, 130, 1554.
49. Alberto, R., *J. Organomet. Chem.* **2007**, 692, 1179.
50. Uehara, T., Koike, M., Nakata, H., Miyamoto, S., Motoishi, S., Hashimoto, K., Oku, N., Nakayama, M., Arano, Y., *Nucl. Med. Biol.* **2003**, 30, 327.
51. Zhao, J., Santos, A.M., Herdtweck, E., Kuhn, F.E., *J. Mol. Catal. A: Chem.* **2004**, 222, 265.
52. Legzdins, P., Phillips, E.C., Rettig, S.J., Sanchez, L., Trotter, J., Yee, V.C., *Organometallics* **1988**, 7, 1877.
53. Balula, S.S., Coelho, A.C., Braga, S.S., Hazell, A., Valente, A.A., Pillinger, M., Seixas, J.D., Romao, C.C., Goncalves, I.S., *Organometallics* **2007**, 26, 6857.
54. Herrmann, W.A., Kohlpaintner, C.W., *Angew. Chem. Int. Edit. Engl.* **1993**, 32, 1524.
55. Pinault, N., Bruce, D.W., *Coord. Chem. Rev.* **2003**, 241, 1.
56. Dobson, G.R., *Acc. Chem. Res.* **1976**, 9, 300.
57. Schubert, M.P., *J. Am. Chem. Soc.* **1933**, 55, 3336.
58. Schubert, M.P., *J. Am. Chem. Soc.* **1933**, 55, 4563.
59. Tomita, A., Hirai, H., Makishima, S., *Inorg. Chem.* **1968**, 7, 760.
60. Veignie, E., Rafin, C., Landy, D., Fourmentin, S., Surpateanu, G., *J. Hazard. Mater.* **2009**, 168, 1296.
61. Lindsey, M.E., Xu, G., Lu, J., Tarr, M.A., *Sci. Total Environ.* **2003**, 307, 215.
62. Fenton, H.J.H., *Chemical News* **1876**, 33, 190.

63. Fenton, H.J.H., *J. Chem. Soc., Trans.* **1894**, 65, 899.
64. Walling, C., *Acc. Chem. Res.* **1975**, 8, 125.
65. Haber, F., Weiss, J., *Proc. Roy. Soc. London A* **1934**, 147, 332.
66. Barb, W.G., Baxendale, J.H., George, P., Hargrave, K.R., *Trans. Faraday Soc.* **1951**, 47, 462.
67. Kremer, M.L., *Phys. Chem. Chem. Phys.* **1999**, 1, 3595.
68. Bray, W.C., Gorin, M.H., *J. Am. Chem. Soc.* **1932**, 54, 2124.
69. URI, N., *Chem. Rev.* **1952**, 50, 375.
70. Luzzatto, E., Cohen, H., Stockheim, C., Wieghardt, K., Meyerstein, D., *Free Rad. Res.* **1995**, 23, 453.
71. Rodriguez, M.L., Timokhin, V.I., Contreras, S., Chamarro, E., Esplugas, S., *Adv. Environ. Res.* **2003**, 7, 583.
72. Anastasi, A.E., Lienke, A., Comba, P., Rohwer, H., McGrady, J.E., *Eur. J. Inorg. Chem.* **2007**, 65.
73. Goldstein, S., Meyerstein, D., *Acc. Chem. Res.* **1999**, 32, 547.
74. Symons, M.C.R., Gutteridge, J.M.C., *Free Radicals and Iron: Chemistry, Biology, and Medicine,* Oxford University Press, Oxford, **1998**.
75. Grootveld, M., Halliwell, B., *Free Radic. Res. Commun.* **1986**, 1, 243.
76. Moorhouse, C.P., Halliwell, B., Grootveld, M., Gutteridge, J.M., *Biochim. Biophys. Acta* **1985**, 843, 261.
77. Mouithys-Mickalad, A.M., Zheng, S.X., Deby-Dupont, G.P., Deby, C.M., Lamy, M.M., Reginster, J.Y., Henrotin, Y.E., *Free Radic Res* **2000**, 33, 607.
78. Koncic, M.Z., Rajic, Z., Petric, N., Zorc, B., *Acta Pharmaceutica* **2009**, 59, 235.
79. Barton, D.H.R., Le Gloahec, V.N., Patin, H., *New J. Chem.* **1998**, 22, 565.
80. Barton, D.H.R., Le Gloahec, V.N., Patin, H., Launay, F., *New J. Chem.* **1998**, 22, 559.
81. Jones, C.M., Burkitt, M.J., *J. Am. Chem. Soc.* **2003**, 125, 6946.
82. Russell, G.A., *J. Am. Chem. Soc.* **2002**, 79, 3871.
83. Blanchard, H.S., *J. Am. Chem. Soc.* **1959**, 81, 4548.
84. SHI, Q.Z., Richmond, T.G., Trogler, W.C., Basolo, F., *J. Am. Chem. Soc.* **1982**, 104, 4032.
85. Therien, M.J., Ni, C.L., Anson, F.C., Osteryoung, J.G., Trogler, W.C., *J. Am. Chem. Soc.* **1986**, 108, 4037.
86. Hershberger, J.W., Klingler, R.J., Kochi, J.K., *J. Am. Chem. Soc.* **1982**, 104, 3034.
87. Hershberger, J.W., Klingler, R.J., Kochi, J.K., *J. Am. Chem. Soc.* **1983**, 105, 61.
88. Zizelman, P.M., Amatore, C., Kochi, J.K., *J. Am. Chem. Soc.* **1984**, 106, 3771.
89. Avey, A., Tenhaeff, S.C., Weakley, T.J.R., Tyler, D.R., *Organometallics* **1991**, 10, 3607.
90. Avey, A., Tyler, D.R., *Organometallics* **1992**, 11, 3856.
91. Bhengu, T.T., Sanyal, D.K., *Thermochim. Acta* **2003**, 397, 181.
92. Cousins, M., Green, M.L.H., *J. Chem. Soc.* **1964**, 1567.
93. Herrmann, W.A., Correia, J.D.G., Kuhn, F.E., Artus, G.R.J., Romao, C.C., *Chem-Eur J* **1996**, 2, 168.
94. Poli, R., *Chem-Eur J* **2004**, 10, 332.
95. Martins, A.M., Romao, C.C., Abrantes, M., Azevedo, M.C., Cui, J.L., Dias, A.R., Duarte, M.T., Lemos, M.A., Lourenco, T., Poli, R., *Organometallics* **2005**, 24, 2582.

7. Acknowledgments

Bruno Guerreiro is acknowledged for the HPLC/MS oxidation study performed with $CpMo(CO)_3CH_2CONH_2$ and H_2O_2.

Ana Margarida Gonçalves is acknowledged for measurements of CO/CO_2 release through GC.

Chapter IV: Study of reactivity between Metal Carbonyl Complexes and Heme Proteins

1. Summary

Myoglobin (Mb) and Hemoglobin (Hb) are strong scavengers for CO. Upon CO binding to deoxy-Mb this is converted into carboxy-myoglobin, CO-Mb (also called carbonmonoxy-myoglobin). This can be quantified using the characteristic optical absorption spectrum of CO-Mb. In this Chapter, Section 4.1, the rate of CO release from several MCCs is evaluated by incubating them with deoxy-Mb and following the rise of CO-Mb. Since MCCs are electron-rich species, they may engage in electron transfer processes with redox active proteins, namely Mb or Cytochrome C. A selected group of MCCs was also used to survey this problem as described in Section 4.2. Finally, Section 4.3 deals with the transfer of CO from MCCs to whole blood *in vitro*.

2. Introduction

Myoglobin can exist in three different redox forms: deoxy-Mb, oxy-Mb (O_2-Mb) and met-myoglobin (met-Mb).[1] The latter contains Fe(III) while the other ones contain Fe(II) bound to the heme. In the presence of CO, another ferrous form can be formed, namely carbonmonoxy-myoglobin (CO-Mb) since CO strongly binds to the reduced heme center. The optical absorption spectrum of Mb varies among all these species. A strong Soret band is observed in the 400 nm region and a weaker absorption due to the α and β bands is observed in the 500 to 600 nm region, where the number and location of maxima strongly depends on the ligand bound to the heme Fe^{II} ion (see Table 1).[2]

Table 1: Maxima of the UV-VIS absorbance spectrum of several Mb forms

Mb-Form	Soret band/nm	500-600 nm region
deoxy-Mb	433	555
CO-Mb	422	541; 578
O_2-Mb	416	543; 581
met-Mb	409	504; 531

The spectra depicted in Fig.1 show that met-Mb has two broad and low intensity absorbance bands with maxima at 531 nm and 504 nm (orange line) and when the protein is reduced (deoxy-Mb) they are replaced by one single band with the maximum at 555 nm (green line). The Soret band, at 409 nm in the oxidized protein (met-Mb; orange line) moves to 433 nm after reduction (green line).

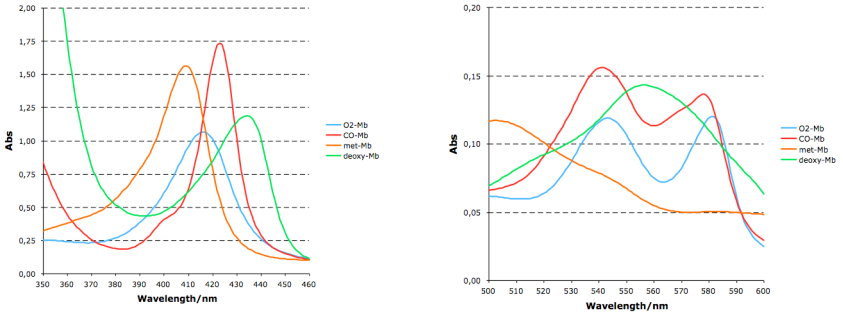

Figure 1: UV-VIS absorbance spectrum of deoxy-Mb (Fe^{2+}), O_2-Mb (Fe^{2+}), CO-Mb (Fe^{2+}) and met-Mb (Fe^{3+}) in PBS.74 at a concentration of 11μM. **Left**: Soret band; **Right**: α and β bands

When CO is bubbled into the met-Mb (Fe^{3+}) solution no changes are observed (data not shown), however, when CO is bubbled in the reduced protein solution, two major changes occur (red line). The peak at 555 nm disappears and two new peaks with maxima at 541 nm and 578 nm appear, and the Soret band shifts to 422 nm. On the other hand, when O_2 is bubbled into the deoxy-Mb preparation oxy-Mb is formed (blue line). This has a spectrum very similar to that of CO-Mb with the maxima at 543 and 581 nm and the Soret band at 416 nm.

These very characteristic spectral changes are also observed with hemoglobin and have proven useful as an indirect method to quantify the amount of CO in blood through the spectrophotometric determination of carboxy-hemoglobin.[3-6]

Based on these observations Motterlini and coworkers developed a new methodology that measures the amount of CO in solution by following the conversion of added deoxy-myoglobin into carbonmonoxy-myoglobin.[7] This spectrophotometric method was then applied to the quantification of CO release from CO-RMs through the quantification of CO-Mb measured by the absorbance at 540 nm (ε_{540} = 15.4 $mM^{-1}.cm^{-1}$).

3. Experimental Section

3.1 Methodology

CO release determination with the Mb assay:

Method**:**

The following experiments were performed using the method developed by Motterlini,[7] however, the quantification of the amount of CO liberated was calculated in a different way.

Typically, a stock solution of Myoglobin (Mb) from equine skeletal muscle was prepared by dissolving the protein in PBS7.4. From this solution aliquots were taken to a cuvette (final concentration between 50 μM to 70 μM) and $Na_2S_2O_4$ in PBS7.4 (10 mg/ml solution; 0.1% final concentration) was added to convert met-Mb into deoxy-Mb. The yellow brown-red met-Mb solution turns yellow-red after being reduced.

Since Mb was purchased and used without purification for each new batch of protein the molar extinction coefficient (ε) was determined. A series of standards were prepared, at different concentrations and the absorbance read at 555 nm. The experimental plot of Abs vs Concentration allowed the experimental ε value to be determined as (9.6±0.3) $mM^{-1}.cm^{-1}$ for batch#1, (11.5±0.5) $mM^{-1}.cm^{-1}$ for batch#2 and (9.2±0.3) $mM^{-1}.cm^{-1}$ for batch#3. This discrepancy among the values obtained is not surprising since among the published literature independent determinations of the molar extinction coefficient by different authors do not agree.[8] The

reactions were done by mixing in the same cuvette and by this order, the Mb stock solution, the $Na_2S_2O_4$ solution, a calculated amount of a solution of the CO-RM and adding PBS to obtain the desired final volume. The cuvettes were sealed with parafilm.

Before adding the CO-RM solution a control spectrum was always acquired to see if the protein had been properly reduced with sodium dithionite.

Two controls were done in duplicate, the negative control (0% CO-Mb), a deoxy-Mb solution and the positive control (100% CO-Mb), obtained by bubbling pure CO gas into the deoxy-Mb solution for 10-15 min.

The experimental spectrum was fitted as a weighted sum of the deoxy-Mb and the CO-Mb spectra. The Solver function in MS Excel was used to calculate the percentage of CO-Mb by deconvolution of the spectra using as controls both positive and negative standards.[9]

The absorbance spectrum was converted into a percentage of CO-Mb and presented as a function of time. Based on the initial amount of CO-RM in solution the amount of CO liberated was calculated as equivalents of CO.

Material**:**

Myoglobin, from equine skeletal muscle, 95-100%, essentially salt free, lyophilized powder from *Sigma*; Disposable Polystyrene Cuvettes (b=10mm); Sodium dithionite pa. from *Panreac*.

UV-VIS absorbance spectrophotometric measurement of the reaction between MCCs and Cytochrome C:

Method**:**

Native oxidized Cytochrome C (5 μM) was mixed with the metal complex (50 μM) in PBS7.4. The UV-VIS absorbance spectrum was recorded immediately after mixing the species and depending on the result, in some cases 1h and 2h later. In a different experiment Cytochrome C was reduced with $Na_2S_2O_4$ (0.1%) and then the compound added in a suitable solvent. The spectrum was recorded immediately after mixing the species and depending on the result, in some cases

also 1h and 2h later. As a control CO gas was bubbled into both the oxidized and reduced Cytochrome C solutions for 20 min. No changes were observed in both spectra.

Material**:**

Cytochrome C provided by Dra. Célia Romão at ITQB; Disposable Polystyrene Cuvettes (b=10mm); Sodium dithionite pa. from *Panreac*.

UV-VIS absorbance spectrophotometric measurement of the reaction between MCCs and Myoglobin:

Method**:**

A stock solution of Myoglobin (11 μM) was prepared by dissolving the protein in PBS7.4 and the compound (50 μM) added in a suitable solvent. The UV-VIS absorbance spectrum was recorded immediately after mixing the species and in some cases 1h later.

Material**:**

Myoglobin, from equine skeletal muscle, 95-100%, essentially salt free, lyophilized powder from *Sigma*; Disposable Polystyrene Cuvettes (b=10mm); Sodium dithionite pa. from *Panreac*.

***In vitro* measurement of CO-Hb levels in blood:**

Method:

A CO-RM solution was prepared in a suitable medium (PBS (pH7.4), DMSO or MeOH), and 50 μL are added to 1 mL of blood and incubated at 37ºC. Samples were kept inside closed plastic culture tubes with closures (5 mL; 12x75 mm) and analyzed over time in the oximeter following the raise in CO-Hb levels. The amount of CO liberated was calculated based on the amount of compound initially added, total amount of Hemoglobin and %CO-Hb (both given by the oximeter). Each compound was tested in a concentration previously calculated in order to mimic relevant *in vivo* doses (typically 25 mg/kg and 50 mg/kg). Assuming a 20 g mouse with 8% blood volume (1.6 mL), 25 mg/kg correspond to

0.5 mg of compound/animal, therefore 0.5 mg/1.6 mL blood, there is 0.313 mg/mL. Conversely, the final CO-RM concentration in blood mimicking 50 mg/kg is 0.626 mg/mL.
Control spectra were always recorded with the medium alone without compound.

Material:
Avoximeter 4000 from A-vox Instruments Inc.; Disposable Cuvettes for Avoximeter 4000 from A-vox Instruments Inc.; Sheep whole blood in alsevers solution, from Innovative Research.

3.2 Technical Details

Synthetic Work:
All the compounds were prepared as described in Chapter II or table A1 in Annex I.

4. Results and Discussion

4.1 Evaluating CO release through CO transfer from Metal Carbonyls to Myoglobin

In the following study we adopted the method developed by Motterlini but modified the way in which the amount of CO liberated was calculated as explained in the Experimental Section. With this methodology it is possible to follow the rise in CO-Mb concentration along the time in a mixture of deoxy-Mb and CO-RM and calculate the equivalents of CO released. The experiments were performed with the compounds fully dissolved. In some cases this required a water miscible co-solvent to increase solubility. The experiments were carried out under normal atmosphere. Control experiments showed that under the conditions used, deoxy-Mb is not oxidized by O_2 for a period up to 2 hours. For this reason

all experiments were stopped after 2h. The experiments performed under N_2 were done with degassed solvents and the solutions prepared in a schlenk tube, under N_2.

Since Mb is a very strong scavenger for CO one may assume that no gas is lost from the solution and all the CO liberated from the molecule is captured by the protein. The CO-Mb formation can be interpreted as a 2 step reaction, first through dissociation of the CO group which then is captured by deoxy-Mb (Equation 1).

$$LM(CO)_n + \text{deoxy-Mb} \underset{}{\overset{k_1}{\rightleftharpoons}} LM(CO)_{n-1} + CO + \text{deoxy-Mb}$$

$$LM(CO)_{n-1} + CO + \text{deoxy-Mb} \overset{k_2}{\rightleftharpoons} LM(CO)_{n-1} + \text{Mb-CO} \qquad \textbf{Equation 1}$$

It is plausible to consider that CO binding to deoxy-Mb is much faster than the decarbonylation process ($k_2 >> k_1$), therefore, no free gaseous CO exists in solution and the reaction can be properly written as follows:

$$LM(CO)_n + \text{deoxy-Mb} \rightleftharpoons LM(CO)_{n-1} + \text{Mb-CO} \qquad \textbf{Equation 2}$$

Taking reaction 2 into consideration it's possible to determine the CO-RM *half-life* ($t_{1/2}$) as the time needed for the formation of [CO-Mb] corresponding to half of the initial CO-RM concentration.

Typically, when 50 μM of a given compound is incubated with deoxy-Mb (60 μM), the *half-life* ($t_{1/2}$) is achieved when 25 μM of CO-Mb are obtained. This value corresponds to half of the initial CO-RM concentration and also to the liberation of 0.5 equivalents of CO.

Since the Mb stock solutions don't always have the same concentration the *half-life* measurement allows a comparison between all the experiments without the need for highly reproducible conditions. One can also determine the influence of

different effects like the medium, pH or different CO-RM concentrations on the rate of release by comparing the different half-lives in the respective conditions.

Table 2 lists the experimentally determined half-lives for a wide range of complexes (Figure 2), the total amount of CO released after 2h reaction and the reaction conditions. Indeed, comparing half-lives provides information about the rate of CO release but doesn't reveal the extent of the reaction. Measuring these 2 parameters allows the distinction between fast and slow releasers and to account for the total capacity of CO release from a given compound.

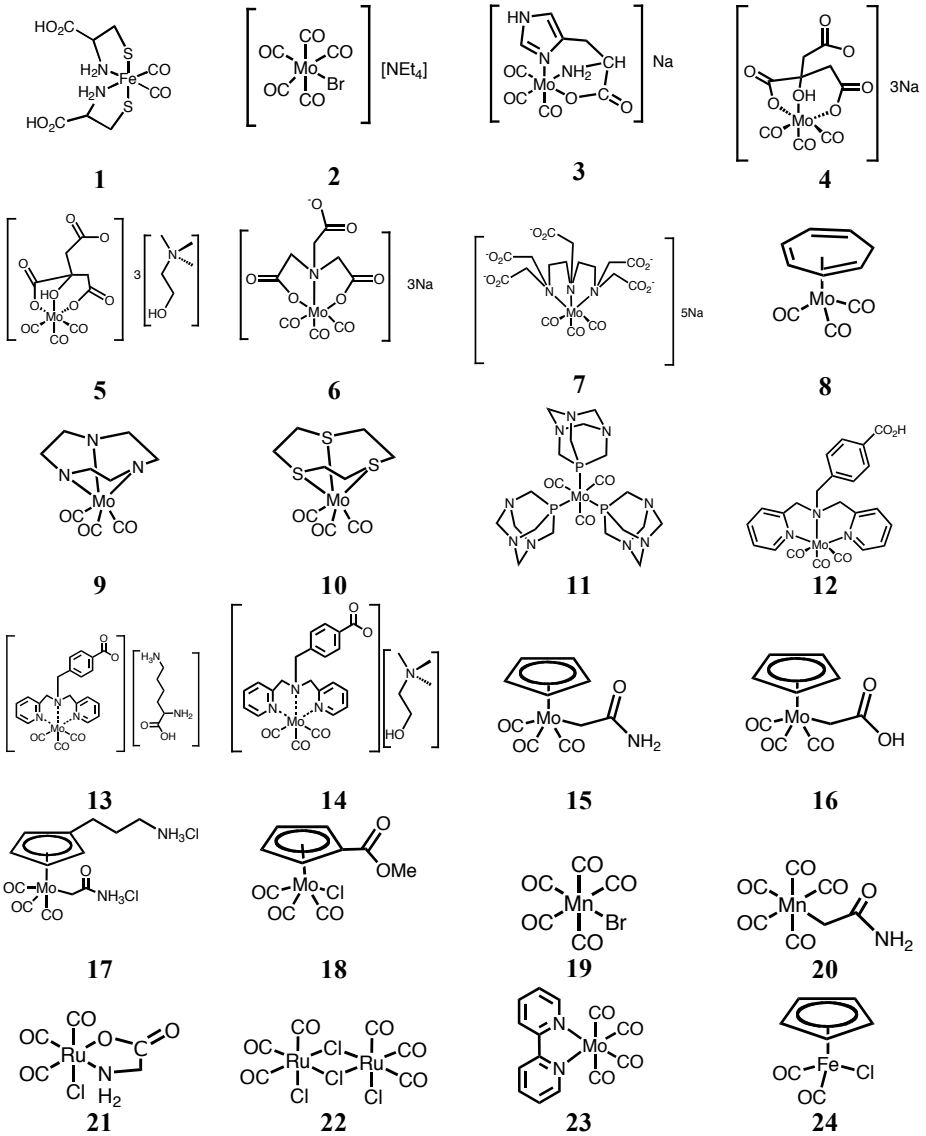

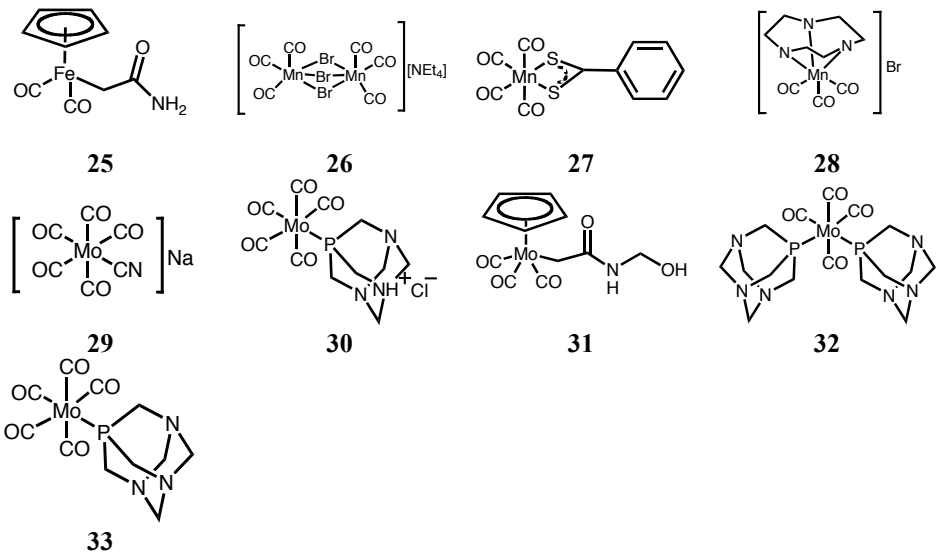

Figure 2: Structure of the MCCs tested in this Chapter.

Table 2: Half-life and amount of CO transferred to deoxy-Mb after 2h incubation. The amount of CO transferred is expressed in equivalents of CO and percentage of the maximum amount of CO possible to liberate. Half-lives were calculated adjusting the experimental data to fitted curves. Experiments were performed under normal atmospheric air at room temperature. Solvent is PBS7.4 unless stated otherwise.

Entry	Half-life/ min	Equiv. CO transferred after 2h (% of maximum CO)	Reaction conditions
1	115	0.50 (25%)	[1] = 50 μM [deoxy-Mb] = 62 μM
2	64	0.61 (12%)	a) [2] = 50 μM (0.9% MeOH) [deoxy-Mb] =56 μM
	14	0.73 (15%)	b) [2] = 51 μM (1.7% DMSO) [deoxy-Mb] =55 μM
	27939	0.25 (5%)	c) [2] = 50 μM [deoxy-Mb] = 57 μM
3	25	0.94 (31%)	[3] = 50 μM [deoxy-Mb] = 62 μM
4	11	1.41 (47%)	[4] = 30 μM [deoxy-Mb] = 62 μM
5	9	1.02 (33%)	[5] = 30 μM [deoxy-Mb] = 62 μM
6	42	0.86 (29%)	[6] = 30 μM [deoxy-Mb] = 62 μM
7	60	0.87 (29%)	[7] = 30 μM [deoxy-Mb] = 62 μM

8	11	1.10 (37%)	[8] = 50 μM (2.5% MeOH) [deoxy-Mb] = 62 μM
9	120	0.50 (17%)	[9] = 100 μM (5.2% DMSO) [deoxy-Mb] = 62 μM
10	∞	0 (0%)	[10] = 100 μM (1.1% DMSO) [deoxy-Mb] = 56 μM
11	449	0.24 (8%)	[11] = 50 μM [deoxy-Mb] = 62 μM
12	195	0.36 (12%)	[12] = 100 μM (4.7% MeOH) [deoxy-Mb] = 56 μM
13	101	0.51 (17%)	[13] = 30 μM [deoxy-Mb] = 62 μM
14	105	0.53 (18%)	[14] = 30 μM [deoxy-Mb] = 62 μM
15	832	0.13 (4%)	[15] = 80 μM [deoxy-Mb] = 62 μM
16	308	0.20 (7%)	[16] = 100 μM (1% MeOH) [deoxy-Mb] = 62 μM
17	822	0.14 (5%)	[17] = 100 μM [deoxy-Mb] = 62 μM
18	27	1.00 (33%)	[18] = 50 μM (2.4% MeOH) [deoxy-Mb] = 62 μM
19	134	0.47 (9%)	[19] = 100 μM (6.1% MeOH) [deoxy-Mb] = 63 μM
20	∞	0 (0%)	[20] = 47 μM [deoxy-Mb] = 55 μM
21	<2	1.00 (33%)	[21] = 50 μM [deoxy-Mb] = 57 μM
22	<1	1.5-2 (25%-33%)	[22] = 20 μM (0.5-1.6% DMSO) [deoxy-Mb] = 61 μM

To set up the basis for this discussion it is useful to start our analysis with compound **1**, which is a reversible CO carrier[10, 11] that is believed to form *in vivo* as an intermediate of the catalytic oxidation reaction of cysteine which may occur in living cells[12] (Equation 3)

$$Fe(cysteine)_2(CO)_2 \rightleftharpoons Fe(cysteine)_2 + 2CO$$ **Equation 3**

In terms of the CO release rate **1** can be classified as a slow releaser that presents a continuous, slow increase in CO-Mb, liberating 0.5 to 0.6 equiv. CO after 2h. This result matches exactly the one obtained in the standard, macroscopic

chemical CO release tests in RPMI in the absence of Mb: 26% CO liberated to the gas phase, during the same period of time in the apparatus of Fig.1 (Chapter II).
As can be seen in Fig.3 this amount of CO is not strongly affected by the presence of O_2 meaning that oxygen is not triggering the CO release.

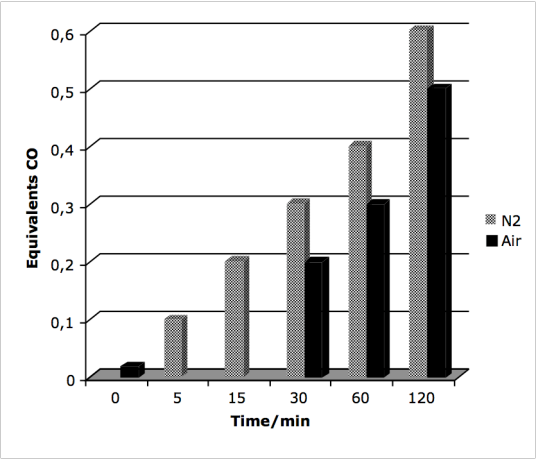

Figure 3: Equiv. CO released to deoxy-Mb by **1** in air and under N_2. Assays performed in PBS7.4 at room temperature with [deoxy-Mb] = 56 μM and [**1**] = 100 μM (air assay); [deoxy-Mb] = 56 μM and [**1**] = 50 μM (N_2 assay).

Although the compound has a limited solubility at the concentrations used in the GC experiments, some of these compounds have shown that the rate of CO release wasn't affected by pH changes or addition of ROS species and remained similar to the one measured in the presence of the strong CO scavenger, Mb. The rate of release is therefore dependant on the dissociation of the compound, slowly liberating CO at a constant rate over a large period of time.

Compound **2** exhibits a rather different profile. Incubation of **2** with deoxy-Mb was performed under different conditions, with **2** being pre-dissolved in distilled water, MeOH and DMSO and tested with deoxy-Mb at different concentrations.
The results obtained showed that the solvent interferes with the amount of CO released.
As can be observed from the Fig. 4 the amount of CO released varies with the solvent in the order H_2O < MeOH < DMSO.
Although the absolute amounts of CO released are different, similar kinetic profiles are observed, suggesting that the differences observed are mainly due to the initial solubilization. In the macroscopic GC assays **2** is able to release 5 equivalents of CO in 2h when dissolved in DMSO but only 2.1 equiv. within the

same period, when dissolved in MeOH and 1.4 equiv. in H_2O, however, these results also reflect the different solubility (or insolubility) in the media. On the contrary, at 50 μM concentration the compound is fully solubilized in the three solvents but still the same variability is observed supporting that most probably the initial solubilization and reactivity towards the solubilizing solvent is the rate determinant step.

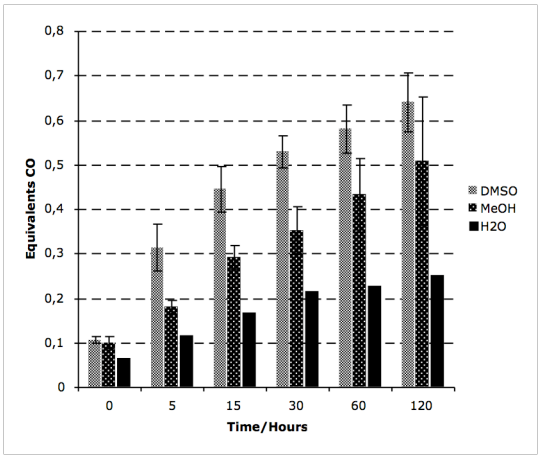

Figure 4: Equiv. CO released to deoxy-Mb by **2** at 50 μM, pre-dissolved in different solvents. The values in MeOH are the average of 2 assays with final MeOH content of 1.9% and 0.9%. The values in DMSO are the average of 2 assays with final DMSO content of 1.7% and 3%. Assays performed in PBS7.4 under air at room temperature with [deoxy-Mb]= 56μM. Experiments performed with different [**2**] presented similar CO release rates.

Compounds **3** to **7** are a group of water-soluble compounds that were presented in Chapter II as fast and spontaneous CO releasers. It was also demonstrated that O_2 was triggering the CO release (see Chapter II) since no CO was detected in the headspace of their solutions under N_2.

As seen in table 2, when incubated with Mb these compounds form CO-Mb at a rate that corresponds to some of the shorter values of $t_{1/2}$ among all the compounds presented. Compounds **3**, **4**, and **5** are among the fastest CO releasers to Mb. Besides the rate, the extension of the transfer of CO is also high. Indeed, the total amount of CO released reaches ca. 1 equiv. CO after 2h. Compound **4**, whose reactivity is still poorly understood liberates 1.4 equiv. CO after 2h, which is the maximum amount obtained in this assay.

Although compounds **6** and **7** are slower and less extensive CO releasers to Mb, the complexes **3** to **7** show an overall similar behavior. This is not surprising in

view of the fact that they all have the same kind of structure where a $Mo(CO)_3$ core is coordinated to anionic hard N and O donors.

As mentioned before, in the absence of Mb, O_2 is necessary to trigger off the release of CO from these complexes to the headspace. One would hypothesize that the interactions between the complexes and the protein might change this situation. This was probed by performing the incubation of Mb with compounds **3** and **4** under N_2, using degassed PBS7.4 solution. As can be seen in Table 3, CO is still being transferred to Mb although there is a marked increase in $t_{1/2}$ and a decrease of the total amount of CO liberated when compared to the similar aerobic experiments.

Table 3: Half-life and amount of CO transferred from **3** and **4** to deoxy-Mb after 2h incubation. Half-lives were calculated adjusting the experimental data to fitted curves. Experiments were performed under N_2, at room temperature.

Entry	Half-life/ min	Equiv. CO transferred after 2h (% of maximum CO)	Reaction conditions
3	97	0.61 (20%)	[**3**] = 60 μM [deoxy-Mb] = 62 μM
4	45	1.32 (44%)	[**4**] = 30 μM [deoxy-Mb] = 62 μM

This slower decarbonylation process is also depicted in Figure 5, where one can observe a clear difference between aerobic and anaerobic CO release.

Under N_2, roughly half of the CO is transferred and it takes 1h to achieve the same amount that is liberated in air within 5 min!

The GC experiments had shown that **3** doesn't release CO in aqueous solution, namely in PBS7.4 under N_2, at least during 6h. The results obtained with Mb under N_2 (which were replicated at different concentrations but not shown) demonstrate that CO-Mb formation is still occurring in 2h. One may, therefore, conclude that Mb is able to abstract CO from the complex following some interaction between both and not simply scavenging free, dissolved CO. To this process we herein call *CO donation*.

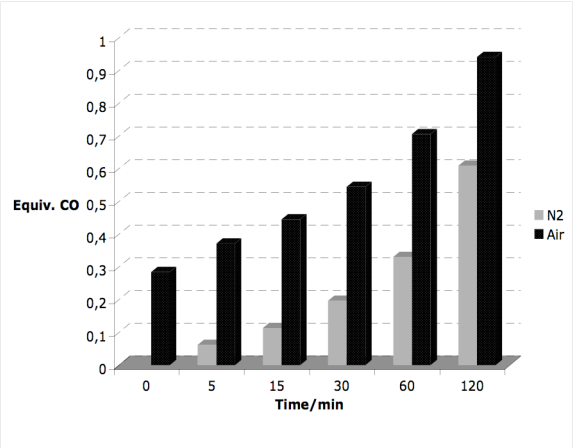

Figure 5: Equiv. CO released to deoxy-Mb (62μM) by **3** at 60μM (under N_2) and 50μM (under air). The assay under N_2 was performed in degassed PBS7.4 and prepared inside a schlenk apparatus under anaerobic conditions and the assay under air performed in normal aerated PBS7.4. Both assays performed at room temperature.

The class of compounds that don't release CO to the headspace but rather deliver it directly to the CO-Mb target we termed *CO donors*. The donation process consists on the specific delivery of CO to a target instead of dissociation from the CO-RM followed by capture of the free gaseous CO.

With the present data nothing can be said on the mechanism leading to this CO donation but interactions between both CO-RM and Mb are certainly present and relevant. Evidences of Mb-CO-RM adducts for compounds **3**, **4**, **6** and **7** were observed through UV-VIS and ICP-AES and the data is currently being rationalized by other collaborators.

Nevertheless, even in the presence of the transfer mechanism the rate of CO-Mb formation in aerobic conditions is faster than in anaerobic medium. This suggests that in aerobic conditions compound **3** is liberating CO through 2 different mechanisms, the donation and a spontaneous release triggered by O_2.

The ability to *donate* CO to Mb in opposition to *release* from the molecule will be further addressed in Chapter V.

Compound **4** is relatively similar to **3** in terms of CO transfer to Mb but has a smaller rate difference between aerobic and anaerobic conditions, as can be seen in Figure 6.

The half-life of **4**, didn't change as much as that of **3** and the same amount of CO is donated in aerobic and anaerobic conditions after 2h. Since **4** is also stable under N_2 for several hours this results suggest that in the case of **4** CO-Mb formation is occurring mainly through a CO donation process.

In principle, the same behavior could be expected for the complexes **9** and **10** which also have a *fac*-$Mo^0(CO)_3$ fragment. However, both compounds have very long half-lives and only a marginal amount of CO is transferred to Mb. In Chapter II we hypothesized that complex **10** wasn't liberating any CO to the headspace due to the lack of solubility. However, at the 100 μM concentration used in the experiments with Mb it is fully solubilized and yet it is highly inert towards CO loss. This fact is best ascribed to the extraordinary stabilization provided by the macrocyclic trithianonane ligand. The tris-phosphine complex **11**, $Mo(CO)_3(PTA)_3$ is not totally inert towards CO loss to Mb but the amount released is also very small.

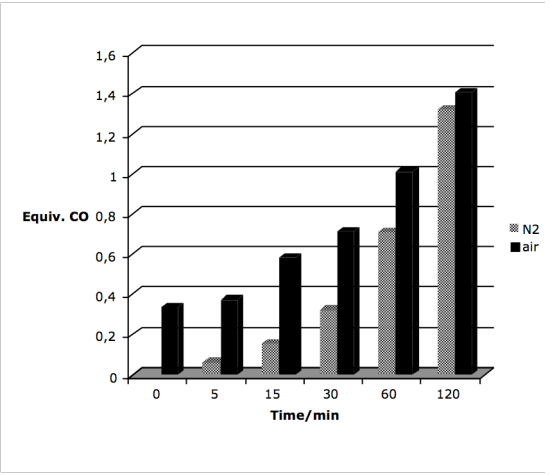

Figure 6: Equivalents of CO released after incubation of deoxy-Mb (58 μM) and **4** (30 μM) under air (black) and deoxy-Mb (62 μM) and **4** (30 μM) under N_2 (grey). Assay under N_2 was performed in degassed PBS7.4 and prepared inside a schlenk apparatus under anaerobic conditions and assay under air performed in normal aerated PBS7.4. Both assays performed at room temperature.

Also for **12** and its ionized analogues with lysine (**13)** and choline (**14)** salts long $t_{1/2}$ values are obtained, reflecting the stability of the complex anion which is not affected by the negative charge present at the distal ligand free arm.

At the μM range all these three compounds are fully solubilized in the PBS medium and the total amount of CO delivered to Mb after 2h, is similar for the 3 compounds (12%, 17% and 18%, for **12**, **13** and **14** respectively).

As discussed in Chapter II, generally, the bond between alkenes and metal carbonyls is often weak and labile since CO removes most of the electronic π density thereby weakening the alkene-metal backbonding. This lability is even more pronounced in solvents with pi-donor atoms such as ethers, alcohols or water. Therefore, in such solvents, the lability of ligands like the cycloheptatriene of complex **8** is well established. Once the double bonds are successively pushed away from the metal center, open coordination positions are available for O_2 attack according with Scheme 1 (Chapter II) which then promotes fast decomposition kinetics with a rapid liberation of CO. The profile exhibited by **8** is in accordance with these observations, since it presents a very short half-life ($t_{1/2}$= 11 min) with a large amount of CO being released after 1h (1.1 equiv. CO). The same experiment performed under N_2, leads to the increase of half-life to 91min and decrease of the total amount of CO liberated to 0.63 equiv. after 1h. This supports the role of O_2 in the decomposition profile of the compound with concomitant CO release.

In contrast to the simple alkenes, the delocalized, aromatic, cyclopentadienyl anion Cp forms very stable Cp-M bonds and $CpM(CO)_x$ complexes. The stability of this motif is reflected in the group of Cp'-Mo^{II} complexes **15**, **16** and **17** which are poor CO releasers with very long half–lives (> 300 min) and low amounts of CO released within 2h (< 0.3 equiv. CO).

As in Chapter II, the $CpMo(CO)_3$-alkyl family shows a relatively good thermal and oxidative stability and CO substitution at mild temperatures is only afforded *via* photoactivated reactions, nucleophilic substitutions with phosphines or oxidation with NO.[13, 14] Monoalkyl-substitutions on the Cp ring, like the one introduced in **17** vs. **15**, often lead to differences in the solubility properties but no relevant differences were expected or obtained regarding the CO release kinetics. If any, CO release should be slower due to a stronger Mo-CO bond.

On the contrary, ring substitutions like that of **18** should favor CO release due to the weakening of the Mo-CO bonds which results from the increased electron-withdrawing power of the Cp ring substituted with an electron-withdrawing group. Although **18** presents a much shorter half-life than the other Cp analogues ($t_{1/2}$=27 min), liberating a higher amount of CO after 2h (1.0 equiv.) it is not possible to assign this higher activity to the ring-substitution since the ancillary chloride ligand may play a more relevant role in electron depletion from the metal than the ring substitution. Indeed, the chloride lowers the electron density at the metal relative to the -CH_2CONH_2 substituent in **15**, by virtue of its higher electronegativity. Moreover, the stabilized alkyl substituent, -CH_2CONH_2 does not undergo hydrolysis at physiological pH (see Chapter III, section 4.2) whereas the Mo-Cl bond is likely to undergo such a reaction which favors the decomposition of the complex in comparison with the alkyl derivatives. Incubation of **18** with Mb under N_2 did not change much the profile of the carbonylation of Mb relative to the aerobic reaction. In fact, both processes have a similar rate of CO release with minor changes in half-life and total CO release values ($t_{1/2}$=59 min and 0.93 eq. CO released in 2h). This supports the idea that O_2 is not the main promoter of CO release for the Cp'$Mo(CO)_3X$ complexes. The known chemistry of $CpMo(CO)_3X$ complexes strongly suggests that Mo-Cl hydrolysis is most probably initiating decomposition and CO release.

The different profile between an alkyl and halide substituent is also noted in the pair of Mn pentacarbonyl complexes **19** and **20**. Although complex **19** with a bromide substituent presents a fairly stable profile, only losing ca. 10% of the total CO amount after 2h, it is nevertheless a much better CO releaser than the totally inert analogue **20**, which has the -CH_2CONH_2 ancillary ligand.

The ruthenium complexes **21** and **22** showed the unique property of producing an immediate donation of CO to deoxy-Mb. These compounds do not release CO to the headspace in any conditions tested in aqueous media. However, when incubated with deoxy-Mb the Mb-CO formation is almost immediate. The donation process was previously observed with other compounds but never at

such a fast rate and so evident. The CO donation is completed within the first 5 to 10 min and exactly one equivalent of CO is donated to deoxy-Mb. This very fast CO transfer is an exclusive property of the ruthenium compounds and it occurs either under air or under N_2.

Due to this very fast profile of CO-Mb formation the reaction of **21** with deoxy-Mb was followed minute-by-minute during the first 10 min and then every 2 min until 20 min to determine when the maximum CO-Mb values were reached. The CO donation profile of **22** is also presented for comparative purposes (Fig. 7).

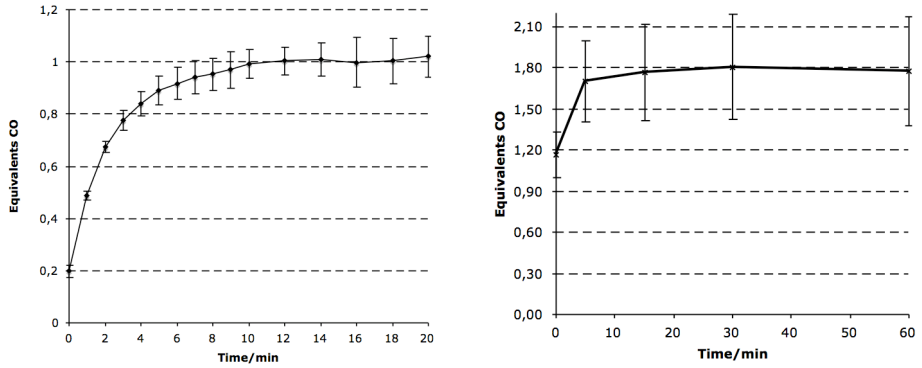

Figure 7: Equiv. CO transferred to deoxy-Mb by **21** and **22**. **Left**: Assays performed in PBS7.4 under air at room temperature with [deoxy-Mb]= 57 μM and [**21**] = 50 μM (average of 2 assays). **Right**: Assays performed in PBS7.4 under air at room temperature with [deoxy-Mb]= 61 μM and [**22**] = 20 μM (average of 3 assays; final DMSO content 0.5-1.6%).

The CO donation capacity of **21** and **22** was already reported in the literature, although with a mechanistically loose denomination – CO release.[7, 15]

The amount of CO released from **21** (1 equiv. CO) is in agreement with the results reported in the aforementioned study[7] but the results obtained with **22** are different. Motterlini and co-workers reported that 0.7 moles of CO were released *per* molecule of $[Ru(CO)_3Cl_2]_2$, a value obtained by titrating deoxy-Mb with a DMSO solution of **22**. A more recent study[15] followed the same methodology and reported 0.46 mol *per* molecule of **22**.

The discrepancies found are associated with the different methodology adopted in our system and in the reported studies. The $[Ru(CO)_3Cl_2]_2$ dimer is unstable in DMSO leading to the formation of different species with different donation capacity. These different *equilibria* originate the variety of results obtained and will be addressed in detail in Chapter V.

4.1.1 Discussion

The results just described suggest two topics for discussion: methodological questions and chemical questions.
The former consider the two methodologies used to evaluate and quantify CO release: measuring CO in the headspace of a solution or measuring CO-Mb formed upon incubation of a CO-RM with deoxy-myoglobin solutions.
The chemical questions compare the CO release profile of the compounds tested as measured by the Myoglobin method.

Quantification of CO release: GC or Myoglobin?

In Chapters II and III we studied the ability of metal carbonyls to release CO under different chemical conditions by measuring the amount of CO liberated to the headspace of solutions of CO-RMs exposed to several media and chemical conditions. These very versatile and practical measurements were, however, subject to an important drawback. Due to the range of concentrations of CO gas that could be measured with accuracy with TCD detection, the concentrations of the CO-RMs used were typically in the order of the 10^{-3} M. These relatively high concentrations posed severe problems in the measurement of the CO release properties of sparingly soluble compounds and precluded the proper evaluation of water insoluble compounds. However, this concentration range posed yet another important problem: the minor biological relevance of this concentration range.

Since the vast majority of biological *in vitro* tests are performed in the 1-100 μM range the compounds should also be studied in this concentration range.

When the working range changes 1000-fold, from mM to μM, obvious differences are observed. In the μM range solubility becomes a less problematic issue and the CO releasing rate is strongly modulated by the very low concentrations of the CO-RM in the medium. At these low concentrations all compounds are fully dissolved and, therefore, CO release data becomes more precise. Moreover, the low concentrations also minimize the influence of the nature of the vehicle that may have to be used to facilitate the solubilization of the compound in the aqueous media, because reactions are much slower. Therefore, the measurement of CO release with the Myoglobin method developed by Motterlini has many advantages over the GC/TCD method due to elimination of mass transfer limitations. Of course, this would no longer be true if the GC method would allow a higher sensitivity for CO quantification. In principle this could be achieved with a FID detection system operating downstream of a methanizer. However, in spite of hard and prolonged efforts, supported by the technical assistance of the supplier of the appropriate chromatograph, we were unable to use CO detection in the range required by CO-RM concentrations of ca. 10-50 μM due to the formation of impurities in the methanizer that distorted the base line beyond acceptable values. The recent acquisition of a GC/RCP (Reducing Compound Photometer), specific only for CO and H_2 overcomes this problem and allows measurements of CO in the low ppb range without any interferences. However, this range is unfortunately too low for the routine evaluation of CO-RMs because the amount of CO needed for the measurement is too low and successive gas dilutions are necessary.

In spite of its mentioned advantages, the Mb method has some disadvantages because it requires a critical interpretation.

In fact, the incubation of a CO-RM with Mb is not a straightforward process because several situations may occur that lead to CO-Mb formation:

1. The CO-RM independently liberates CO which is simply scavenged by Myoglobin;
2. Myoglobin reacts with the CO-RM abstracting its CO directly;
3. Both previous situations compete.

Under the conditions of item 1 the amount of CO-Mb measured in an experiment should match the amount of CO measured by the appropriate GC method. The CO-RM may simply dissociate CO or may be activated by some chemical trigger independent of Mb (e.g. O_2). Free CO is then scavenged, and as pointed out in the beginning of this section, no CO should escape due to the high affinity and reactivity of deoxy-Mb towards CO.

The prototypical example of this situation was provided by compound **1** which gives the same CO release profile in both methods. The dissociation of **1** is not influenced by Mb or O_2 and both methods give the same result (see below).

On the contrary, large deviations between both methods are observed in some aerobic Mb assays when compared with the GC experiments: the amount of CO liberated to deoxy-Mb (either by donation or spontaneous release) is always less than the amount obtained by GC. Complexes **3**, **6** and **7** are the most elucidative examples since the Mb method only accounts for 1/3 of the amount of CO liberated in PBS7.4 in the GC experiments. The same is observed with other sparingly soluble complexes like **2** and **12**. These results are due to an experimental artifact, needed to create the proper conditions to the Mb assay; the addition of sodium dithionite removes O_2 from O_2-Mb and reduces met-Mb (unable to bind CO) to deoxy-Mb

$$S_2O_4^{2-} + O_2 + 2\ OH^- \rightleftharpoons SO_3^{2-} + SO_4^{2-} + H_2O \qquad \textbf{Equation 4}$$

$$S_2O_4^{2-} \rightleftharpoons 2\ SO_2^{\cdot-} \overset{Fe(III)}{\rightleftharpoons} S_xO_y + Fe(II) \qquad \textbf{Equation 5}$$

Sodium dithionite is widely used in biochemical assays to generate or maintain reduced states of enzymes. However, it also creates artificial anoxic conditions since it removes dissolved O_2 from the aqueous medium.[16-21] This decrease in normal [O_2] prevents or slows down CO dissociation from the most O_2 sensitive complexes. Molybdenum (0) compounds like **2**, **3**, **6** and **7** to which O_2 is the main CO release trigger are the most affected by this factor. As a consequence of the deoxygenated conditions created by dithionite the compounds become more stable and don't release as much CO as they would in aerated PBS. This is a general behavior observed with all the O_2 induced releasers (all the Mo(0) compounds) that showed levels of CO-Mb formation much lower than those expected from CO release experiments by Gas Chromatography.

However, the amount of dithionite is not enough to totally prevent O_2 assisted decomposition due to several factors: the dithionite has limited life-time in PBS solution, the solvents are not deoxygenated (in experiments performed under air) and the system is not closed so oxygen from air does induce some decomposition in aerobic assays. Since these factors are not easily controllable or accounted for, the results obtained by the CO-Mb method are highly biased by dithionite when the compound is activated by O_2 unless they are strictly performed under N_2 atmosphere which, in turn, has no biological relevance. This is clearly the major limitation of this assay and one that affects the vast majority of CO-RMs which react under the conditions of item 3 above, that is, are sensitive to oxygen or triggers other than Mb (e.g. pH, light).

Of course, the greatest advantage of the Mb method is that it is the only way to identify compounds that, like the Ru(II) derivatives **21** and **22** cannot release CO to the headspace but do transfer CO to Mb. This advantage is non-obvious and applies only to a handful of compounds as will be discussed more extensively in Chapter V.

4.1.2 Comparing CO release profiles by the Mb method

By eliminating the mass transfer limitations interesting details of the kinetics of CO release are revealed. Compound **1** is a rare case of a compound with a purely dissociative decomposition rate. It is totally unaffected by the [O_2], shows a identical rate of decomposition at 14 mM and 50 μM despite not being totally solubilized at higher concentrations and is not affected by the presence of deoxy-Mb. This is the clearest case of CO release controlled by the self-dissociation rate of the Fe-CO bond. This should be the typical CO release profile of reversible CO carriers of which this is the only example in the present dissertation.

Compound **2**, on the other hand, shows different results from the GC assay which are no longer plagued by the uncontrollable effects of low solubility. The GC assays were helpful to determine the influence of the several media in the CO release rate, however, since the compound was not completely soluble in all the media an effective comparison couldn't be performed. The results of the Mb assay showed slightly different rates, but not so distinctive as in the GC experiments. Nevertheless, the influence of the co-solvent is obvious but we do not have data that allows its interpretation.

At this point it is important to remember that higher solubility does not imply a higher rate of CO release. In fact **10** that was shown in Chapter II to be strictly ROS activated and totally insoluble in water was solubilized in DMSO but still unable to deliver any CO to Mb after 2h. The same lack of reactivity towards Mb is observed with several complexes, e.g. **9**, **10**, **11**, **15-17**, **20**. These compounds are all very stable, both thermodynamically and kinetically, and the GC experiments showed that they only release CO when activated by ROS. Obviously, Mb is not capable of interacting with these highly substitutionally inert MCCs to scavenge CO. In agreement with this view, the Cp' derivative **18** which has a substitutionally labile Mo-Cl bond (more so in aqueous media) that may allow for O_2 entry or Mb attack has a much higher rate of release than that of the other Cp derivatives **15-17**. Some interaction with Mb due to the acetyl group

can't be discarded however it is more likely that a different hydrolytic process is taking place, namely Mo-Cl bond rupture.

The notion that ligand lability goes hand-in-hand with easy reaction with Mb and concomitant CO-Mb formation is exemplified by the chemically labile, ionic, water-soluble compounds **3-7**. These are stable in aqueous solution under N_2 but in the presence of Mb they also form CO-Mb very rapidly and extensively. This can only mean that they reacted with deoxy-Mb in a way that allowed the transfer of CO from Mo(0) to Fe(II). These complexes, together with the $Ru^{II}(CO)_3$ analogues are the best examples of the CO donation process to Mb.

Two major processes originate the formation of CO-Mb from a MCC: CO dissociation from the MCC as a free molecule and capture by deoxy-Mb, and a direct donation between the compound and Mb. In some cases e.g. **1**, **15** and **17** only the first mechanism seems to be present; in others only the second mechanism is present e.g. **21** and **22;** The cases in which the mixed situation predicted in item 3 above where both mechanisms are simultaneous, is exemplified by **3** and **4**. Only the combination of the results from the two techniques allowed the discovery of the ability to *donate* CO to Mb and this new feature wouldn't be detected if only a single assay was used to quantify CO release.

The interactions between the CO-RMs and Mb have to be taken into account since it is sometimes determinant for the fate of reaction (this issue will be further developed in Chapter VI). In spite of all limitations, the Mb assay is extremely useful to understand some properties of the compounds and without it wouldn't be possible to detect some special features like the CO donation of the ruthenium complexes.

4.2 Redox interaction between Metal Carbonyl Complexes, Cytochrome C and Myoglobin

Since these metal carbonyls possess a metal center in low oxidation state, they may behave as reductants in biological conditions thereby assuming other roles beyond CO release. An exploratory study was performed, in which the redox behavior of some metal carbonyl complexes was studied with two different heme-proteins, Cytochrome C and Myoglobin.

Cyt C mediates single electron transfer between the protein complex ubiquinol-Cytochrome C oxidorreductase to the complex Cytochrome C oxidase thereby playing a pivotal role in the respiratory chain reactions.[22] This protein undergoes reversible oxidation-reduction steps, and when isolated pure does not bind O_2 or CO under physiological conditions.[23, 24] However, it was recently found that CO can associate to the complex Cyt C-cardiolipin with extraordinary positive consequences on anti-apoptotic mechanisms.[25]

Although they are involved in different functions both proteins are part of the complex process where CO may be involved and so this study may contribute for further understanding of interactions between metal carbonyls and heme proteins.

4.2.1. Results

Cytochrome C

Native oxidized Cytochrome C (5 μM) was incubated with the metal complex in 10-fold excess in PBS7.4. The UV-VIS absorbance spectrum was recorded immediately after incubation and if no reaction was taking place the spectrum was recorded again 1h and 2h later. The same procedure was performed with reduced Cyt C. As a control CO gas was bubbled into both the oxidized and reduced Cyt C solutions for 20 min, however no changes were observed in both spectra.

The reaction between the compounds and the reduced Cyt C didn't show any modification in the absorption spectrum of Cyt C.

On the other hand, three distinct behaviors were observed among the compounds that were incubated with oxidized Cyt C (Figure 8).

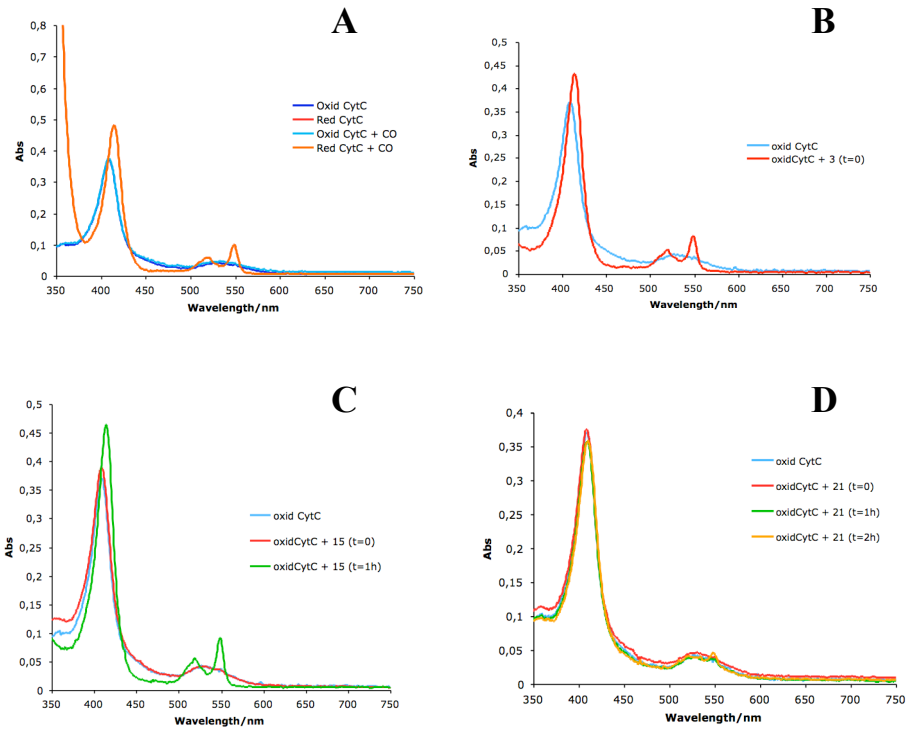

Figure 8: **A** - UV-VIS absorbance spectrum of reduced and oxidized Cyt C (5 μM) before and after CO bubbling for 20min. Spectrum recorded in PBS7.4 at RT; **B** - Typical UV-VIS absorbance spectrum of class I compounds (data from **3**) with oxidized Cyt C (10:1). Spectrum recorded in PBS7.4 at RT immediately after incubation with Cyt C; **C** - Typical UV-VIS absorbance spectrum of class II compounds (data from **15**) with oxidized Cyt C (10:1). Spectrum recorded in PBS7.4 at RT immediately after incubation with Cyt C and after 1h; **D** - UV-VIS absorbance spectrum of **21** with oxidized Cyt C (10:1). Spectrum recorded in PBS7.4 at RT immediately after incubation with Cyt C, after 1h and 2h.

Class I compounds (**2**, **3**, **4**, **6** and **7**) were able to immediately reduce oxidized Cyt C at the time of addition. Class II compounds (**15** and **17**) were only able to

complete reduction after 1h. Class III (**21**) didn't reduce the cytochrome. However, after 2h incubation it was observed a very slight shift of the Soret band and also the formation of a peak characteristic of the Cyt reduced form (at 548 nm).

The small group of compounds tested clearly showed distinct activities, depending on the oxidation state of the metal or its reducing capability. Class I compounds are the air sensitive, ionic Mo(0) complexes, while class II are rather air stable neutral Mo(II) complexes. It was observed that the Mo(0) complexes were able to immediately reduce Cyt C while Mo(II) compounds were slower in achieving this reduction, since it was only observed after 1h. There is an interesting correlation between this redox activity and the CO releasing capacity of these two classes of compounds. While Class I integrates fast spontaneous releasers, the Class II contains more stable complexes, and only ROS induced releasers. However, the controls performed with CO gas showed that this Cyt C reduction is totally independent of the CO release rate and only dependent on the reducing potential of the complexes.

Another important issue that shouldn't be neglected is the electrostatic interaction between the MCC-Cyt C couple. The binding surface of Cyt C includes several lysine residues[26-30] which at physiological pH have a net charge of +8. This charged state may repel positively charged complexes like **17** and delay the reduction reaction. However, this interpretation is entirely speculative at the time.

The only compound that didn't reduce Cyt C was the Ru(II) complex **21**. Interestingly, after 2h some minor deviations are observed in the Soret and β sheet region. This may indicate that a partial reduction is occurring although with a slower kinetics. In fact, **21** can be reduced as a consequence of OH^- attack at the coordinated CO. Hydride species are identified by NMR in its aqueous solutions (see Chapter V).

In view of the classical observation that reduced Cyt C is unable to bind CO these results might not look particularly important. However, the very recent finding that reduced Cyt C is able to bind CO when associated with the phospholipid

cardiolipin[31, 32] completely changes this view.[25] In fact, recent data suggest that the carbonylation of the Cyt C-cardiolipin complex stabilizes the Cyt C against its detrimental peroxidative activity[33] and may prevent its leaking out the mitochondial membrane.

The release of Cyt C from mitochondria to cytoplasm is believed to trigger the apoptotic cascade through two different mechanisms: one involving Apaf-1, pro-caspase-9 and dATP/ATP interactions[34] and another based on the interaction of Cyt C with cardiolipin prior to its release from the mitochondria.[33, 35, 36]

Having this in mind it is hard to imagine a better explanation for the well-established anti-apoptotic activity of CO[37-39] than its stabilization of the Cyt C inside the mitochondrion. In this case, the coupling of reduction with CO transfer should play a powerful role in the anti-apoptotic activity of CO-RMs.

Myoglobin

Due to its biological function Mb is necessarily a different protein than Cyt C. One relevant aspect is the fact that Mb, when in its reduced form is able to bind O_2 and CO, but with much higher affinity for the later.

This behavior is reflected in the present study, since it is observed that when the protein is reduced it is immediately carbonylated with the CO liberated from the complexes. The Mb reduction is achieved through oxidation of the metal carbonyl which, when oxidized, liberates CO that carbonylates the reduced Mb. This is observed by the changes in the Soret band that moved accordingly with figure 9 CO gas doesn't react with native, oxidized Mb.

The results obtained allowed the division of the compounds tested into two classes; Class I are compounds that reduce and carbonylate Mb and Class II are compounds that do not reduce the protein.

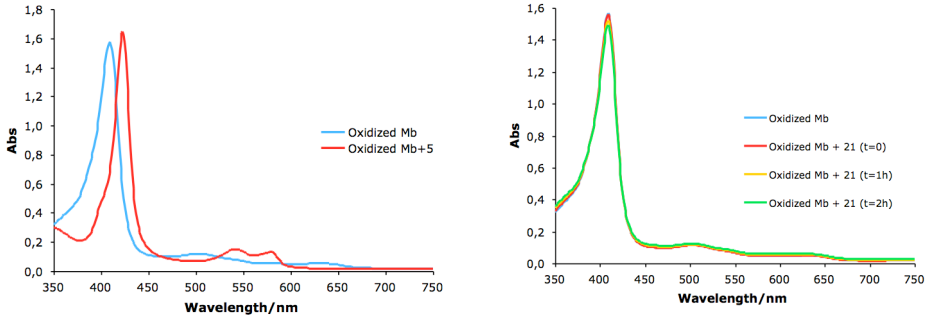

Figure 9: **Left**: Typical UV-VIS absorbance spectrum of class I compounds (50 µM) with Oxidized Mb (11 µM). Spectrum recorded in PBS7.4 at RT immediately after incubation with Fe^{3+}-Mb (data from **5**). **Right:** Typical UV-VIS absorbance spectrum of class II compounds (50 µM) with Oxidized Mb (11 µM). Spectrum recorded in PBS7.4 at RT immediately after incubation with Fe^{3+}-Mb (data from **21**).

Table 4: Results of the incubation of Fe^{3+}-Mb (11 µM) with different MCCs (50 µM). Class I compounds immediately reduce and carbonylate Mb while class II compounds do not have any redox action on Mb.

Class I	**Class II**				
Mo(0)	Mo(0)	Mo(II)	Ru(II)	Fe(II)	Mn(I)
3	***2***	***15***	***21***	***1***	***19***
4	***10***	***17***	***22***	***24***	***20***
5	***23***	***18***		***25***	***26***
6					***27***
7					
8					
9					
12					
13					
14					

Similarly to what was observed with Cyt C, most of the Mo(0) compounds rapidly reduced Myoglobin and transferred CO immediately to give CO-Mb, with only three exceptions, **2**, **23** and **10**. Whereas the later two compounds are very

stable even in the presence of ROS (see Chapter III) and therefore not prone to react with Mb, **2** is an unexpected case since it was unable to reduce Mb even on a 5 to 10-fold excess. However Mb was effectively reduced and carbonylated in a 1 mM solution of **2** and 10 μM of Mb. Most likely, the true reducing compound is some decomposition product of **2.**

The largest fraction of complexes are class II compounds that don't reduce Mb. None of the Mo(II), Ru(II), Fe(II) or Mn(I) complexes were able to reduce Mb despite the different ligands, CO release rate or structure of the complexes. The assays with Ru complexes were followed up to 2h and still no reduction was observed, contrary to the observed with **21** and Cyt C. These data suggests that the results obtained are primarily dependent on the redox potential of the complexes which, of course, is lower in the Mo(0) complexes than in all other class II complexes. Nevertheless, ligand lability seems to be an important property to ensure rapid reduction of Mb by Mo(0) metal carbonyls.

4.2.2 Discussion

The results obtained are *per se* revealing. Most of the compounds tested do not interfere with the redox state of heme-proteins but almost all the Mo(0) complexes are strongly reducing agents and this reduction is accompanied by CO transfer to the reduced Myoglobin to give CO-Mb. This effect *in vivo* doesn't seem to block any vital process of the respiratory pathway since none of the compounds shown here presented high toxicity levels *in vivo* or led to fatal episodes following administration.

The reducing activity of Mo(0) compounds towards Mb may unveil a different type of activity. The impact on the metabolic process is for now unknown but the same behavior is observed with hemoglobin (data not shown), reducing met-hemoglobin to deoxy-hemoglobin and carbonylating it to give carboxy-hemoglobin.

Met-hemoglobin has been ascribed as playing a major role in several iron-related diseases, like methemoglobinemia which is characterized by inadequate tissue oxygenation caused by excessive levels of met-hemoglobin in blood.[40, 41] Recently, it was also related with cerebral malaria[42] as a key factor during the disease development. The reported results may represent a window of opportunity for the development of this family of compounds due a set of specific redox properties.

4.3 Behavior of CO-RMs in blood

Once administered to an animal, a CO-RM will enter the blood circulation which carries and distributes it around the whole body. During this process the CO-RM will interact with all the blood components, namely proteins and red blood cells (RBC). If a CO-RM is meant to be delivered intact to a certain tissue it must be able to survive these interactions in the blood stream until it finally reaches the target cells where CO will be released. The interaction of drugs in circulation with blood proteins such as albumin and transferrin (addressed in Chapter VI) is a matter of great importance since it strongly influences the stability and the half-life of the drugs in circulation. In the case of CO-RMs these interactions may affect the stability of the coordination sphere and thereby alter the kinetics of CO release which may be a positive or a negative event depending on whether interaction results in CO-RM stabilization or destabilization, respectively. This is particularly important in the blood stream because the hemoglobin in red blood cells is actually capable of removing and scavenging any CO that is set free. Therefore, viable CO-RMs must be designed to resist decomposition by the blood components and to be unable to enter RBC where hemoglobin will most likely scavenge their CO load. Altogether, this can be readily evaluated by measuring the values of CO-Hb that are reached when a given CO-RM is incubated with blood. If the CO-RM is stable and doesn't enter RBC the values of CO-Hb should remain low. If the compound is unstable in the blood stream or enters RBC, the values of CO-Hb will be clearly raised with a certain kinetic profile.

This problem was studied experimentally by incubating the compounds with sheep blood and following the evolution in CO-Hb levels over time by means of a standard oximeter. The concentration of the CO-RMs was adjusted to mimic the administration of doses of 25 or 50 mg/kg in *in vivo* animal experiments (see experimental part for details). From the experimental values of CO-Hb measured for a given amount of blood and CO-RM concentration the number of equivalents of CO transferred to Hb was calculated. The results presented were selected from a large amount of collected data and are judged adequate to illustrate the typical profile of several CO-RM families studied.

4.3.1 Results and Discussion

The experimental values are collected in Table 5. Some CO-RMs required pre-dissolution in small amounts of DMSO or MeOH to improve their solubility to the desired concentration range. Since these solvents, especially DMSO, have a slight interference in the exact measurement of CO-Hb in the oximeter, the amount of CO liberated (in equivalents) was rounded to the closest integer value and the CO-Hb levels below 0.5 equiv. CO were labeled as < 0.5 equiv. CO, meaning that the compounds are stable in the assay.

Although the values of CO-Hb were measured at several time points, only the one at which the highest value of CO-Hb was reached is reported. This option stems from the simple observation of the values reported in the table 5. Indeed, the first immediate conclusion drawn from that table is that very few compounds present a slow, regularly increasing CO-Hb formation profile.

Table 5: Amount of CO transferred from CO-RMs to Hb in blood at 37ºC. Time at which the maximum levels of CO-Hb are attained (T_{max}).

Entry	Equivalents of CO transferred to Hb	T_{max}/min
2*	5	75
3	3	0
4	1	2
5	3	2
6	3	4
7	3	8
8*	2	2
9**	2	2
11	<0,5	30
12*	3	10
13	2	10
14	3	30
15	<0,5	120
19**	2	4
20	<0,5	30
21	<0,5	120
22**	<0,5	30
28	<0,5	30
29*	<0,5	30
30	<0,5	30
31**	<0,5	120
32**	<0,5	30
33**	<0,5	40

* compounds pre-dissolved in MeOH
** compounds pre-dissolved in DMSO

On the contrary, the vast majority of the complexes tested either release CO to the blood in a very fast manner or are fairly stable over time liberating only small amounts of CO to Hb. This is a very surprising result which casts a dark shadow on most of the previously expended arguments concerning the fine-tuning of CO release with different ligands.

Most of the previously discussed electronic considerations regarding CO-RM stability, although still valid do not reflect the behavior of CO-RMs in blood. Indeed, all the compounds previously classified as spontaneous CO releasers and described as the fastest and more extensive CO-RMs present an enhanced capability to release CO in blood.

Their kinetics of CO dissociation in blood is much faster than in the several media tested. For the vast majority of compounds in this class all the 3 CO ligands are released to blood within minutes. Compound **3** liberates exactly 3 CO equivalents to hemoglobin within the time of mixing with blood and measuring in the oximeter. In this way its administration can be described as a bolus injection of "solid CO". If applied intravenously these compounds do not afford an effective delivery of CO to tissues but may effectively mimic a fast administration of

gaseous, inhaled CO. In this case Hb will be the main CO carrier, similarly to what happens with CO gas therapy.

A similar profile is observed with **5, 6** and **7** that lose 3 carbonyls within 2, 4 and 8 min, respectively. Compound **4** is once more an exception within this family releasing less CO than the remaining compounds (only 1 CO). However, it must be noted that it releases only 1 equivalent of CO also very fast and then CO release stops. It is tempting to interpret these CO release profiles as the result of very strong interactions with blood proteins. In the case of **4** these interactions may be stabilizing whereas in the other four examples, they are obviously quite destabilizing in terms of facilitating liberation of CO. Further evidence for these strong interactions will be presented in Chapter VI.

The action of aerated blood upon other neutral Mo(0) compounds results in the unexpectedly fast and extensive decomposition profile observed with **8**, **9** and **12**. Within a few minutes of incubation with blood these CO-RMs release 2 to 3 equivalents of CO to Hb, which corresponds to more than 65% of the CO available in the molecule. Another relevant aspect is that this takes place with three compounds that have quite different ancillary ligands and donor atoms. In previous experiments compound **9** proved to be rather stable due to its macrocyclic triazacyclononane ligand. Nevertheless, in blood it behaves like the much more labile and flexible **12** with its tripodal pyridine ligand and **8** with its labile triene ligand. The rate of Hb carbonylation is quite similar and even the extent of CO release is very close.

On the other end of the stability spectrum, we find compounds with several different characteristics. The two Mo(II) complexes $CpMo(CO)_3\{CH_2C(O)NHR\}$ **15** and **31** or the tris-phosphine $Mo^0(CO)_3$ (**11**) do not liberate CO up to 30 min in blood. In fact, the phosphine derivatives $Mo^0(CO)_n(PR_3)_{6-n}$ (n = 3,4,5) are highly stable molecules, independently of the number of carbonyls, as can be observed with the series of **11**, **30**, **32** and **33.** Stability in blood is also observed for the air stable, water soluble ionic species $Na[Mo(CO)_5(CN)]$ (**29**).

Table 5 also presents three examples of Mn based CO-RMs which provide some very important insights for the interpretation of the data described for the Mo compounds. Of these three complexes, the only one that has a very fast release to blood is **19**. This compound is air stable but its reactivity, which has been extensively studied in carbonyl substitution reactions[43-46] is dominated by the sequential replacement of two CO ligands cis to Br^- according to equation 6.

$$Mn(CO)_5Br + L \rightleftharpoons \textit{cis}\text{-}Mn(CO)_4LBr$$
$$Mn(CO)_4LBr + L' \rightleftharpoons \textit{fac}\text{-}Mn(CO)_3LL'Br \qquad \textbf{Equation 6}$$

This process is dissociatively activated and induced by the pi-donation ability of the bromide ligand. Therefore one expects that suitable nucleophiles will rapidly replace the two CO ligands of **19** (cis to Br^-) forming a derivative of the *fac*-$Mn^I(CO)_3$ fragment which is well know to be highly kinetically and thermodynamically stable towards oxidation and further CO loss. Blood proteins are the most likely sources of the nucleophiles responsible for these substitution reactions. Complex **28** exemplifies the stability of a derivative of the *fac*-$Mn^I(CO)_3$ fragment and stays in strong contrast to the blood labile analogue **9**. Complex **20,** isostructural and isoelectronic with **19** is also oxidatively stable to O_2. However, it is substitutionally inert and hydrolytically stable because its -$CH_2C(O)NH_2$ ligand lacks the ability to activate CO dissociation. Therefore its stability to blood is understandable.

Complex **2** represents the best instance of a compound that slowly but steadily delivers all its CO ligands to blood Hb. Unfortunately, the complexity of the decomposition chemistry of this complex prevents any safe explanation for this behavior. In Chapter II we have seen that **2** releases CO in different rates and amounts depending on a series of variables and experimental conditions, e.g. concentration of compound, solvent, medium, [O_2]. However, loss of 5 equivalents of CO was only observed in pure DMSO. The decomposition pathway of the chromium analogue $[Et_4N][Cr(CO)_5Br]$ was established in water

by real time IR spectroscopy.[47] It was shown that hydrolysis is more important than oxidation for the initiation of decomposition. Therefore, it is quite likely that the initial steps of decomposition of **2** also result from hydrolysis or protein attack on the complex and the final stages involve oxidation by O_2 with CO release from Mo species in higher oxidation states. Like this the release of CO increased steadily with time until all CO was scavenged by blood Hb.

A set of interesting results was obtained with the Ruthenium compounds **21** and **22**. None of these complexes elevated baseline CO-Hb levels higher than 2% corresponding to CO amounts of 0.1 to 0.2 equiv. The ruthenium compounds have a very special chemical behavior and this was again observed in this experiment. Although they're able to donate 1 CO to Mb and free-Hb (data not shown) no CO-Hb elevation is observed when the compounds are incubated in blood. This is a curious observation but these results reinforce the donation concept, that a direct interaction between the Ru CO-RMs and the heme protein target is needed for CO transfer to occur. As it has been demonstrated in Chapter II the Ru compounds do not liberate CO to the headspace. As shown in the previous section they only transfer it to the target heme protein (Mb) in its direct presence. In blood the compounds do not cross the RBC membrane and therefore no CO is transferred to Hb. Indeed, treatment of a sample of lyzed RBC with $Ru^{II}(CO)_3$ compounds like **21** or **22** leads to instantaneous and complete transfer of CO to free Hb (data not shown).

From all these observations we can conclude that kinetic stability towards CO substitution is the main factor necessary to achieve stability of transition metal based CO-RMs in blood. Although oxidation obviously plays a role, which can even synergize with substitutional lability, it is not the key factor to determine stability of transition metal CO-RMs in blood.

A second factor which is less obvious would be CO-RM permeation into RBC membranes which would take the CO-RM close to the Hb and facilitate CO-Hb formation. With the present data it is not possible to judge on this effect.

5. Final remarks and conclusions

In this chapter, the results of the interactions of several MCCs with heme centers were presented. They include Mb, Hb and Cyt C heme carbonylation as well as Mb and Cyt C reduction by the low valent MCCs.

The reaction of Mb with MCCs introduced by Motterlini, is a very convenient test to evaluate the CO donation capability of CO-RMs because it can easily accommodate experiments with water insoluble or sparingly soluble molecules by means of their previous dissolution in biologically compatible co-solvents like DMSO or MeOH.

In fact, at the concentration needed for this test (ca. 50 μM) completely water insoluble compounds can be previously dissolved in DMSO or MeOH solutions and then added to aqueous solutions of Mb (ca. 50 μM) to determine the accurate rate of CO-Mb formation. Following Motterlini, such rate was taken as the rate of CO release of a given CO-RM in aqueous medium. The results obtained supported those determined by the GC assays for all complexes except those of Mo(0) and Ru(II). The former are highly sensitive to O_2 and give imprecise results due to the variable, uncontrolled anoxic conditions created by sodium dithionite in the Mb test. The latter transfer CO to deoxy-Mb but do not liberate CO to the headspace in this process. We named this direct mechanism of CO transfer from a CO-RM to Mb as ***CO donation***. This type of mechanism is observed with other compounds like the tricarbonyl $Mo^0(CO)_3$ anionic complexes but the donation effect is not as fast or extensive as with the $Ru^{II}(CO)_3$ compounds.

This study shows that both the term and the underlying concept of "CO release" are ambiguous and can be applied to two different situations. In one situation the CO-RM is expected to liberate free CO gas which may escape the solution and can be quantified by GC or even MS methods. In the other situation, the CO-RM reacts with Mb and CO is donated (transferred) from the CO-RM to the Mb heme without accumulation in the solution and/or headspace. Therefore, the combined

use of both techniques is necessary to identify the behavior of each given family of compounds in a safe way. For example, a complex like $Ru(CO)_3Cl$(glycinate) wouldn't have been considered a CO-RM if it was studied exclusively by GC or MS methods.

Therefore, it is important to mention which method is being used to evaluate "CO release rates" before any comparative conclusions between different types of complexes are attempted.

Regardless of merits and flaws which of these methods is the most useful guide to establish the profile of a CO-RM with useful therapeutical properties?

To be therapeutically useful a CO-RM will have to be administered to an animal or human and enter the blood stream in order to reach the diseased tissue. In fact, one of the advantages of using CO-RMs over CO gas is exactly the possibility of delivering CO directly to tissues instead of loading blood Hb with CO and expect that Hb carries it to the right place.

According to the results obtained with the tests carried out with whole blood, none of the above "CO release" tests has a clear predictive value, that is, none of them simulates the *in vivo* situation when the compound enters the blood stream. Indeed, it seems that blood separates the MCCs into two rather distant groups: one where all the compounds expel all its CO within a very short period of time after incubation, and other where they fully resist decomposition in the sense that they do not release free CO that can be scavenged by Hb within intact red blood cells.

Therefore, we must conclude that the interaction of a MCC with whole blood is the decisive test that allows the identification and subsequent dismissal of the complexes that are too fragile to resist decomposition and release CO shortly after entering circulation, thereby leading to therapeutically unacceptable, toxic, high levels of CO-Hb (>10-12%).

The blood assay has a crucial role in understanding the CO release profile of the molecules *in vivo* and is completely reliable for the determination of the maximum amount of CO-Hb levels obtained with different doses of compounds.

It is a clean, cheap, fast and solid *in vitro* assay that also avoids the use of mice to determine CO-Hb levels.

Although pivotal for the identification of the non-candidate CO-RMs, the blood test is unable to provide other types of positive markers that enable a selection among the MCCs which resist decomposition in blood. Other types of tests have to be taken into consideration in order to make such a selection.

What is the cause for this "differentiating" effect of blood? This was indeed a totally unexpected observation and at present no specific tests have yet been designed to characterize its origin. However, a superficial analysis of the data in Table 5 strongly suggests that the high lability of the ancillary ligands leads to blood unstable species. If this is so, it is quite likely that the plasma proteins are playing a decisive role in substituting these ligands and promoting CO release. Since studies of the reactivity of MCCs and plasma proteins are virtually inexistent, we cannot firmly corroborate this hypothesis but studies in this direction are clearly necessary.

The results obtained with the Ruthenium complexes are another example where the reaction of the complexes with proteins may be controlling the chemistry of CO transfer. Indeed these $Ru^{II}(CO)_3$ complexes are very fragile molecules in aqueous solution and are excellent CO donors to deoxy-Mb most likely because they react with it and facilitate the transfer of CO from the Ru ion to the heme.

The redox experiments with Cyt C and Mb showed a new kind of reactivity of a specific family of compounds. The impact of this discovery in the mitochondrial system (if any) remains to be determined but opens a new window of possibilities and questions about the mode of action of this specific class of compounds and the possibility of a concerted mechanism coupling redox activity with CO release.

Last, but not least, the data collected with all these assays revealed that organometallic carbonyl complexes can be engineered to provide a favorable stability profile in blood and still be able to release CO under biological conditions.

6. References

1. Jr, G.N.P. in *Myoglobin*.in *Handbook of metalloproteins*,Vol. 1, (Ed.:A. Messerschmidt; R. Huber; K. Wieghardt; T. Poulos) Wiley VCH, Chichester, **2001**; pp 5.
2. Smith, D.W., Williams, R.J.P., *Structure and Bonding* **1970**, 7, 8.
3. Katsumata, Y., Aoki, M., Sato, K., Suzuki, O., Oya, M., Yada, S., *J. Forensic Sci.* **1982**, 27, 928.
4. Stonek, F., Dietrich, W., Schneeberger, C., Vycudilik, W., Tschugguel, W., *J. Biochem. Biophys. Methods* **2004**, 58, 49.
5. Rodkey, F.L., Hill, T.A., Pitts, L.L., Robertson, R.F., *Clin. Chem.* **1979**, 25, 1388.
6. Lopez-Rivadulla, M., Bermejo, A.M., Fernandez, P., Cruz, A., Concheiro, L., *Forensic Sci. Int.* **1989**, 40, 261.
7. Motterlini, R., Clark, J.E., Foresti, R., Sarathchandra, P., Mann, B.E., Green, C.J., *Circ. Res.* **2002**, 90, E17.
8. Bowen, W.J., *J. Biol. Chem.* **1949**, 179, 235.
9. Harris, D.C., *J. Chem. Educ.* **1998**, 75, 119.
10. Szakacsschmidt, A., Kreisz, J., Marko, L., Nagymagos, Z., Takacs, J., *Inorg. Chim. Acta* **1992**, 200, 401.
11. Takacs, J., Soos, E., Nagymagos, Z., Marko, L., Gervasio, G., Hoffmann, T., *Inorg. Chim. Acta* **1989**, 166, 39.
12. Tomita, A., Hirai, H., Makishim.S, *Inorg. Chem.* **1968**, 7, 760.
13. Alway, D.G., Barnett, K.W., *Inorg. Chem.* **1980**, 19, 1533.
14. Semion, V.A., Chapovskii, Y.A., Struchkov, Y.T., Nesmeyanov, A.N., *Chem. Commun.* **1968**, 666.
15. Obirai, J.C., Hamadi, S., Ithurbide, A., Wartelle, C., Nyokong, T., Zagal, J., Top, S., Bedioui, F., *Electroanalysis* **2006**, 18, 1689.
16. Dixon, M., *Biochim. Biophys. Acta* **1971**, 226, 241.
17. Lambeth, D.O., Palmer, G., *J. Biol. Chem.* **1973**, 248, 6095.
18. Mayhew, S.G., Massey, V., *Biochim. Biophys. Acta* **1973**, 315, 181.
19. Olivas, E., De Waal, D.J., Wilkins, R.G., *J. Biol. Chem.* **1977**, 252, 4038.
20. Cox, R.P., Hollaway, M.R., *Eur. J. Biochem.* **1977**, 74, 575.
21. Ohlsson, P.I., Blanck, J., Ruckpaul, K., *Eur. J. Biochem.* **1986**, 158, 451.
22. Banci, L., Assfalg, M. in *Mytochondrial Cytochrome C*.in *Handbook of metalloproteins*,Vol. 1, (Ed.:A. Messerschmidt; R. Huber; K. Wieghardt; T. Poulos) Wiley VCH, Chichester, **2001**; pp 33.
23. Silkstone, G., Jasaitis, A., Wilson, M.T., Vos, M.H., *J. Biol. Chem.* **2007**, 282, 1638.
24. Moore, T.A., Greenwood, C., Wilson, M.T., *Biochem. J.* **1975**, 147, 335.
25. Kapetanaki, S.M., Silkstone, G., Husu, I., Liebl, U., Wilson, M.T., Vos, M.H., *Biochemistry* **2009**, 48, 1613.
26. Huang, Y.Y., Kimura, T., *Biochemistry* **1984**, 23, 2231.
27. Gorbenko, G.P., Domanov, Y.A., *Biophys. Chem.* **2003**, 103, 239.
28. Gorbenko, G.P., Molotkovsky, J.G., Kinnunen, P.K., *Biophys. J.* **2006**, 90, 4093.
29. Kawai, C., Prado, F.M., Nunes, G.L., Di Mascio, P., Carmona-Ribeiro, A.M., Nantes, I.L., *J. Biol. Chem.* **2005**, 280, 34709.
30. Kostrzewa, A., Pali, T., Froncisz, W., Marsh, D., *Biochemistry* **2000**, 39, 6066.
31. Krebs, J.J., Hauser, H., Carafoli, E., *J. Biol. Chem.* **1979**, 254, 5308.

32. Daum, G., *Biochim. Biophys. Acta* **1985**, 822, 1.
33. Basova, L.V., Kurnikov, I.V., Wang, L., Ritov, V.B., Belikova, N.A., Vlasova, II, Pacheco, A.A., Winnica, D.E., Peterson, J., Bayir, H., Waldeck, D.H., Kagan, V.E., *Biochemistry* **2007**, 46, 3423.
34. Ow, Y.P., Green, D.R., Hao, Z., Mak, T.W., *Nat. Rev. Mol. Cell Biol.* **2008**, 9, 532.
35. Belikova, N.A., Vladimirov, Y.A., Osipov, A.N., Kapralov, A.A., Tyurin, V.A., Potapovich, M.V., Basova, L.V., Peterson, J., Kurnikov, I.V., Kagan, V.E., *Biochemistry* **2006**, 45, 4998.
36. Vlasova, II, Tyurin, V.A., Kapralov, A.A., Kurnikov, I.V., Osipov, A.N., Potapovich, M.V., Stoyanovsky, D.A., Kagan, V.E., *J. Biol. Chem.* **2006**, 281, 14554.
37. Bilban, M., Haschemi, A., Wegiel, B., Chin, B.Y., Wagner, O., Otterbein, L.E., *J. Mol. Med.* **2008**, 86, 267.
38. Brouard, S., Berberat, P.O., Tobiasch, E., Seldon, M.P., Bach, F.H., Soares, M.P., *J. Biol. Chem.* **2002**, 277, 17950.
39. Zhang, X., Shan, P., Alam, J., Fu, X.Y., Lee, P.J., *J. Biol. Chem.* **2005**, 280, 8714.
40. Ashurst, J.V., Wasson, M.N., Hauger, W., Fritz, W.T., *J. Am. Osteopath. Assoc.* **2010**, 110, 16.
41. Ward, K.E., McCarthy, M.W., *Ann. Pharmacother.* **1998**, 32, 549.
42. Pamplona, A., Hanscheid, T., Epiphanio, S., Mota, M.M., Vigario, A.M., *Int. J. Biochem. Cell Biol.* **2009**, 41, 711.
43. Howell, J.A.S., Burkinshaw, P.M., *Chem. Rev.* **1983**, 83, 557.
44. Angelici, R.J., Basolo, F., *J. Am. Chem. Soc.* **1962**, 84, 2495.
45. Blandamer, M.J., Burgess, J., Duffield, A.J., *J. Organomet. Chem.* **1979**, 175, 293.
46. Burgess, J., Duffield, A.J., *J. Organomet. Chem.* **1979**, 177, 435.
47. Zhang, W.Q., Atkin, A.J., Thatcher, R.J., Whitwood, A.C., Fairlamb, I.J.S., Lynam, J.M., *Dalton Trans.* **2009**, 4351.

Chapter V: Chemical and biological studies with Ruthenium-based CO-RMs

1. Summary

CORM-2 and CORM-3 are the most studied CO-releasing molecules in the literature. Their CO release profile is quite similar and carbonylation of deoxy-Mb solutions upon incubation with these compounds occurs in minutes. Given the widespread use of these molecules in several *in vivo* and *in vitro* models of disease, a thorough study of the CORM-2 decomposition profile is presented as well as the identification of the active species formed.

The ability of these species to decompose hydrogen peroxide, in a similar way to catalytic peroxide scavengers was evaluated and found to be much less extensive than other known compounds. These results are presented at the end of this Chapter.

A new series of Ru-tricarbonyl compounds of the general formula $Ru(CO)_3Cl_2L$ have been prepared, where L is a ligand with a N-, O-, P- or S- donor atom. These complexes were characterized and their CO releasing profile evaluated by Gas Chromatography and in the presence of Myoglobin. None of the compounds releases CO to the headspace of their solutions, measured by GC, but all are able to transfer CO to deoxy-Mb. The amount of CO transferred varies from 0.2 equiv. (when L is a strong donating ligand) to 1 equiv. CO (when L is a weak donating ligand).

2. Introduction

The use of Ruthenium complexes as metallopharmaceuticals[1] has been developed mainly as anticancer compounds. NAMI, Na{*trans*-$[RuCl_4(DMSO)(Im)]$} was the first ruthenium complex entering clinical trials and

is one of the most studied anticancer organometallic complexes after *cis*-platin.[2-7] NAMI was later transformed into NAMI-A (ImH){*trans*-[$RuCl_4$(DMSO)(Im)]} and KP1019 (IndH){*trans*-[$RuCl_4(Ind)_2$]}, two more stable and reproducible derivatives with similar pharmacological properties[8-11] which displayed a high degree of anti-cancer activity and represent some of the most promising Ru-based drug candidates.

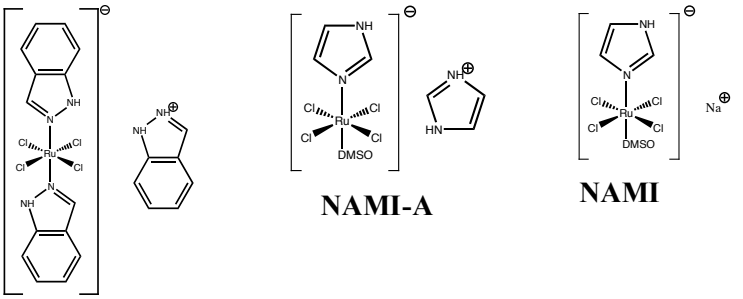

Figure 1: The chemical structure of KP1019, NAMI-A and NAMI.

Since the development of the early Keppler's compounds of general formula *trans*-$HL^+[Ru^{III}L_2Cl_4]^-$ where L is a heterocycle like indazole or imidazole,[12, 13] the quest for new ruthenium-based complexes didn't explore many possibilities for ligands, remaining "restricted" mainly to ammine, amine and imines. Complexes with different ligands were also developed but abandoned due to different reasons. Thiolate ligands are often kinetically unstable[14] and pterins and flavins tend to be photochemically unstable[15, 16] Ammine and amine Ru(II) complexes are usually octahedral, fairly inert to ligand substitution and tend to selectively bind to imine sites in biomolecules, serving as target device for specific tissues. More recently, the ligand field was diversified and some Ru(II) arene complexes are being developed for different applications with very promising *in vitro* and *in vivo* results.[17-19]

Apart from their applications in antitumoral therapy and diagnosis, Ru complexes present a wide variety of biological effects that makes their use as drugs not

confined to this field. Cyclosporin A is the most widely used immunosuppressant agent and interferes with the calcium-dependent step in the immune response[20] and also prevents Ca^{2+}-dependent opening of a megachannel permeability transition pore in the inner mithochondrial membrane. Ruthenium red and Ru360 interfere with Ca^{2+} uptake[21-23] leading to the assumption that ruthenium red related complexes may interfere with the immune response. Indeed, several studies showed that Ru(II/III) complexes with nitrogen ligands[24] (NH_3, imidazole, py) can be potent immunosupressants.[25, 26]

Another interesting application is found in the radiopharmaceutical field. The radiophysical properties of ^{97}Ru are very good for some radiodiagnostic imaging. It decays by electron capture with $t_{½}$ of 2.88 days and emits a 216 KeV γ-ray that can be used in common radioscintigraphic instruments.

NO releasers are another field of application. The similarities between Fe and Ru suggest Ru complexes as alternatives to nitroprusside ($Na_2[NO(CN)_5Fe].2H_2O$) where the rate of NO release can be modulated by the introduction of different ligands.

A similar approach can be applied to the development of CO-RMs, and indeed Ruthenium complexes are among the leading CO releasing molecules. The lipophilic CORM-2 ($[Ru(CO)_3Cl_2]_2$) and water-soluble CORM-3 ($Ru(CO)_3Cl$(glycinate)) are the most studied compounds in the literature with good *in vitro* and *in vivo* results in many cell tests and animal models of disease which have been subject of several publications and also some reviews.[27, 28]

CORM-3 has a variety of reported biological effects; induces vasorelaxation,[29] prevents hypoxia-reoxygenation damage in rat cardiomiocytes and protects against ischemia/reperfusion injury in isolated hearts.[30, 31] In mice CORM-3 reduces infarct size and prolongs the viability of cardiac allografts following transplantation.[30, 32] It also showed renoprotective effects in mice following ischemia-reperfusion induced renal failure[33] and in a model of *cis*-platin induced nephrotoxicity in rats.[34] CORM-3 also improved renal function following cold ischemia in isolated rabbit kidneys and this effect was associated with increased

vascular perfusion, glomerular filtration rate and mitocondrial respiration.[35] It is also an effective anti-inflammatory agent inhibiting NO and TNFα production in macrophages and microglia stimulated with pro-inflammatory mediators,[36-38] attenuates the adhesion of polymorphonuclear neutrophils to endothelial cells *in vitro* and *in vivo*,[39] down-regulates the responsiveness of human neutrophils to inflammatory stimuli by decreasing superoxide production and CD-11 expression[40] and protects against ischemia-reperfusion injury in an experimental model of controlled nonheartbeating donor kidney.[41] Recently, CORM-3 also exhibited some anti-bactericidal effect since it was effective against *Escherechia Coli*[42] and *Pseudomonas aeruginosa*.[43]

Similarly, CORM-2 is also vasoactive[44, 45] (showing vasodilatory effects both in isolated vessels and hearts as well as in rats *in vivo*).[46] CORM-2 mimicked the antiproliferative effect of HO-1-derived CO in both arterial and airways smooth-muscle cells as well as in human Jurkat T-cells. CO-mediated guanylate cyclase and potassium channel activation by CORM-2 have also been implicated in inhibition of afferent arteriole constriction in kidney,[47] anal sphincter relaxation, [48] non-adrenergic non-cholinergic inhibitory neurotransmission in porcine jejunum,[49] immunophotoprotection against UV radiation in rat skin,[50] modulation of ion transport in human intestinal epithelial cells[51] and vasorelaxation in hypertensive animals following exercise training.[44] CORM-2 also protects against cell death and increase in ROS induced by 3-NP,[52] protects against lung injury by limb ischemia-reperfusion,[53] modulates the inflammatory process[54] and protects against ischemia induced acute renal failure.[33]

It showed good anti-inflammatory properties on leukocyte sequestration in lung thermally injured mice.[55] Furthermore it showed good bactericidal properties activity in models developed by Alfama and others.[43, 56, 57]

The vast panoply of positive results obtained both *in vitro* and *in vivo* with these 2 molecules, justifies a more detailed study of this class of compounds. Moreover, the ruthenium complexes were the only compounds that showed the ability to

transfer CO to deoxy-Mb without previous liberation of the gas to the headspace, which suggests a rather distinctive mode of action in their CO release chemistry.

3. *Experimental Section*

3.1 Methodology

Gas Chromatography:

Gas Chromatography assays were performed as described in Chapter II.

Quantification of CO release through the Mb assay:

CO release/donation to deoxy-Mb was performed as described in Chapter IV.

The CO donation capacity of aged solutions was determined as follows:

The compound was dissolved in the suitable medium and the solution kept on the bench for the desired period of time, under normal atmospheric air, at room temperature. After this "ageing" period, the sample was added to the deoxy-Mb preparation and incubated for a period no less than 15 min and no more than 30 min. This is the period of time needed to complete the deoxy-Mb carbonylation process and reach the maximum levels of CO-Mb. The deconvolution procedure explained in Chapter IV is applied to calculate the percentage of CO-Mb and correspondent amount of CO transferred from the molecule to the protein.

High-Pressure Liquid Chromatography:

HPLC trace of the compounds was acquired using the method described in Chapter II.

Horseradish Peroxidase Assay:

These assays were performed by Dr. Ana Rita Marques, a colleague biologist in ALFAMA.

Method:

The ability of the compounds to decompose H_2O_2 was investigated using a horseradish peroxidase (HRP)-based assay. The assay is based on the HRP oxidation of phenol red by H_2O_2 which results in the formation of a compound demonstrating increased absorbance at 655 nm. A linear relationship between absorbance at 655 nm and concentration of H_2O_2 was found in the 1–250 μM range.

Serial ½ dilutions of H_2O_2 were prepared in water and were incubated with the compounds in the ratio 1:1, 1:10, 1:50 or 1:100 (compound: H_2O_2) for up to 240 minutes. At specific time points, 10 μl of H_2O_2 solutions were removed and were allowed to react in the wells of a 96-well plate in the presence of 3 units of HRP, 0.5 mM phenol red in sodium phosphate buffer 0.1M (pH 7). The control of the experiment was performed in the same way but using the different H_2O_2 solutions prepared that have not been incubated with compounds. The reaction was stopped after 10 minutes by the addition of 10 μl of 1N NaOH and the plate was read at 655 nm in a microplate reader (Bio-RAD). The amount of H_2O_2 present in solution at the different time points was calculated based on the linear range of the calibration curve of the control performed with the different H_2O_2 solutions prepared. The results were plotted in a graph as percentage of H_2O_2 present in solution at the different time points considering the control as 100%.

Material:

HRP was acquired from *Sigma* (ref. P6782); Phenol red was acquired from *Sigma* (ref. P3535); H_2O_2 was acquired from *Sigma Aldrich* and titrated prior to use.

3.2 Technical Details

General Considerations:

Elemental Analysis were performed at ITQB, Oeiras, in the Elemental Analysis Laboratory by Engª Conceição Almeida and at the Elemental Analysis Service of the London Metropolitan University by Stephen Boyer. Infrared spectra were

recorded on a Unicam Mattson 7000 FTIR spectrophotometer using KBr pellets. ^{1}H NMR and ^{13}C NMR spectra were recorded on a Bruker Avance III 400mHz. Chemical shifts are quoted in parts per million from $SiMe_4$ (TMS). UV-VIS spectra were acquired in Perkin Elmer Lamda35 spectrophotometer.

Synthetic Work:

All the reactions were carried out under a nitrogen atmosphere, using common schlenk techniques. Solvents were dried by standard procedures, distilled under N_2 and kept over 4Å molecular sieves, except DMSO that was used as received (*p.a.* from *Panreac*). $[Ru(CO)_3Cl_2]_2$ was bought from *Strem Chemicals*; DL-Methionine sulfoxide, L-Methionine sulfoxide and 2-Hydroxy-4-(methylthio)butyric acid calcium salt were bought from *Fluka*; the pyridine ligands were bought from *Asis Chem. Inc.*; 1,3,5–Triaza–7–phosphaadamantane (PTA), methyl β-D-thiogalactoside (Gal-S-Me) and N-acetyl-cysteine (NAC) were bought from *Aldrich*; $Ru(DMSO)_4Cl_2$ was bought from *Strem Chemicals.* 3,7-diacetyl-1,3,7–triaza–5–phosphabicyclo[3.3.1]nonane (DAPTA) was prepared from PTA according to published literature as referred in Chapter II. The compound $Ru(CO)_3(DMSO)Cl_2$ (**1**) was prepared according to the method described in the literature.[58]

$Ru(CO)_2(DMSO)_2Cl_2$ (**2**)

$[Ru(CO)_3Cl_2]_2$ (0.398g; 0.778E-03mol; 512.02g/mol) was dissolved in 3 ml of DMSO. An orange solution was obtained and small bubbles were released from solution. After 30min, Et_2O was added and the solution placed at 4ºC overnight. A biphasic solution was obtained and separated. The orange DMSO solution was extracted several times with Et_2O until the extracts were colorless. The ether filtrates were collected together and concentrated. The solution was placed at 4ºC overnight. An off-white powder was obtained and dried in vacuum. **Yield**: 90%.

IR (KBr/cm^{-1}; C≡O): 2077(s) 2020(s);

E.A.: Calc. for $RuC_6H_{12}O_4S_2Cl_2$: %C:18.75, %H:3.15, %S:16.69; Found: %C:19.31, %H:2.73, %S:16.10;

^{1}H NMR ($CDCl_3$, 400MHz, rt, δ in ppm): δ = 3.44 (s, 2H) assigned to *cis, trans, cis*- isomer; 3.43 (s,1H), 3.17 (s,1H), 2.88 (s,1H), 2.85 (s,1H) assigned to *cis, cis, cis*- isomer;

^{13}C NMR ($CDCl_3$, 100MHz, rt, δ in ppm): δ = 185.7 (CO), 45.1 assigned to *cis, trans, cis*- isomer; 186.1 (CO), 47.5, 42.2, 39.3, 38.9 assigned to *cis, cis, cis*- isomer.

$Ru(CO)(DMSO)_3Cl_2$ **(3)**

$[Ru(CO)_3Cl_2]_2$ (0.53 g; 1.035 mmol; 512.02 g/mol) was dissolved in 15 ml of DMSO giving an orange solution to which toluene (15 ml) was added. The solution was heated to reflux for 2h becoming light yellow. It was cooled to room temperature, giving a turbid suspension that was filtered. To the filtrate, Et_2O was added and the solution placed at -30ºC overnight.

An oily yellow residue mixed with a white crystalline product was precipitated. From the cold filtrate, another fraction of white crystalline product with yellow contamination was obtained. This was extracted with ether, leaving a yellow powder behind and a white powder started to precipitate from the ethereal solution. After concentration and cooling the precipitate was filtered, washed with hexane and dried in vacuum affording a white powder (Fraction 1). The yellow solid left behind was recrystallized from CH_2Cl_2/hexane at -30ºC affording yellow crystals (Fraction 2). **Yield**: 31%.

IR (KBr/cm^{-1}; C≡O): Fraction 1: 2001(vs); Fraction 2: 2003(vs);

E.A.: Calc. for $RuC_7H_{18}O_4S_3Cl_2$: %C:19.36, %H:4.18, %S:22.15; Found (Fraction 1): %C:19.40, %H:3.84, %S:22.40; Fraction 2: %C:19.83, %H:3.81, %S:22.32;

^{1}H NMR ($CDCl_3$, 400MHz, rt, δ in ppm): Both fractions present the same isomers but in different ratios: δ = 2.75 (s,1H), 2.78 (s,1H), 3.17 (s,1H), 3.45 (s,2H), 3.52 (s,1H) assigned to the *cis, cis, cis*- isomer; 2.85 (s,2H), 3.25 (s,2H), 3.43 (s,2H) assigned to the *cis, cis, trans*- isomer; 3.41 (s,2H), 3.43 (s,2H), 3.51 (s,2H) assigned to the *cis, mer*- isomer;

^{13}C NMR ($CDCl_3$, 100MHz, rt, δ in ppm): δ = 38.5, 39.0, 43.5, 45.3, 46.8, 50.2 assigned to the *cis, cis, cis*- isomer; 39.1, 43.7, 47.6 assigned to the *cis, cis, trans*- isomer; 42.9, 46.4, 47.4 assigned to the *cis, mer*- isomer.
Fraction 1 has CO resonances at δ = 192.3 and 191.0 ppm; In Fraction 2, the CO resonances were not observed.

The same procedure was used to prepare complexes **5**, **6, 7** and **12**. The synthesis of **6** is presented.

L-$Ru(CO)_3Cl_2(H_3CSO(CH_2)_2CH(NH_2)CO_2H)$ **(6)**

$[Ru(CO)_3Cl_2]_2$ (0.918 g; 1.793 mmol; 512.02 g/mol) and L-methionine sulfoxide (0.592 g; 3.586 mmol; 165.21 g/mol) were mixed together in 100 ml of acetone. A slightly yellow suspension with some insoluble product was obtained and stirred overnight at room temperature. After 20h the reaction was stopped and a small amount of a white powder remained insoluble in the bottom. The pale yellow solution was filtered and concentrated. The concentrated solution was slowly added *via* cannula to another schlenk, already partially filled with a large portion of Et_2O. An abundant white precipitate was formed. The solution was filtered and the precipitate washed with 2x20 ml of Et_2O. It was dried in vacuum giving an off white powder. **Yield**: 83%.
IR (KBr/cm^{-1}): 2131(s), 2055(s) (C≡O); 1651(s) (C=O);
E.A.: Calc. for $RuC_8H_{11}NO_6SCl_2$: %C:23.07, %H:2.64, %N:2.73, %S:7.57; Found: %C:22.73, %H:2.99, %N:2.95, %S:7.48;
^{1}H NMR (MeOD, 400MHz, rt, δ in ppm): δ = 4.1-3.8 (m,1H), 3.1-2.9 (m,2H), 2.70 (s,3H), 2.5-2.1 (m,2H).

D,L-$Ru(CO)_3Cl_2(H_3CSO(CH_2)_2CH(NH_2)CO_2H)$ **(5)**

Precipitation of the complex was induced at -30ºC overnight.
Yield: 36%; **IR** (KBr/cm^{-1}): 2133(s), 2056(s) (C≡O); 1651(s) (C=O);

E.A.: Calc. for $RuC_8H_{11}NO_6SCl_2$: %C:23.07, %H:2.64, %N:2.73, %S:7.57; Found: %C:23.17, %H:2.79, %N:3.11, %S:7.21;

^{1}H NMR (D_2O, 400MHz, rt, δ in ppm**):** δ = 4.06 (m,1H), 3.09 (m,2H), 2.76 (s,3H), 2.39 (m,2H)

$Ru(CO)_3Cl_2(3\text{-}NC_5H_4(CH_2)_2SO_3Na)$ **(7)**

Precipitation of the complex was induced at -30ºC overnight.

Yield: 63%; **IR** (KBr/cm^{-1}; C≡O): 2137(s), 2053(s);

E.A.: Calc. for $RuC_{10}H_8NO_6SNaCl_2$: %C:25.82, %H:1.73, %N:3.01, %S:6.89; Found: %C:25.40, %H:1.98, %N:2.77, %S:7.12;

^{1}H NMR (D_2O, 400MHz, rt, δ in ppm): δ = 8.75 (s,1H), 8.67 (d,1H), 8.58 (d,1H), 8.03 (t,1H), 3.34 (s,4H).

$Ru(CO)_3Cl_2(H_3CS(CH_2)_2CH(OH)CO_2H)$ **(12)**

The ligand was first synthesized through the following procedure:

$[H_3CS(CH_2)_2CH(OH)COO]_2Ca$ (0.880 g; 2.600 mmol; 338.45 g/mol) was dissolved in 30 ml of water and the solution stirred for a couple of minutes, after which all the product was dissolved. Sulfuric Acid (1M) was slowly added (2.6 ml; 1 equiv.) and the clear solution became turbid after some minutes. It was further stirred for 90 min after which the reaction was stopped. A white precipitate ($CaSO_4$) was filtered off and washed with a small amount of MeOH. The solution was taken to dryness affording a pale yellow oily residue. It was extracted with MeOH, leaving a small amount of a white powder behind ($CaSO_4$). The pale yellow filtrate was taken to dryness affording a yellow oil that was kept at - 30ºC. **Yield:** 85%.

IR (KBr/cm^{-1}): 1733 (s) (C=O); 1437(m), 1276(w), 1224(m), 1173(m), 1096(s), 970(w), 799(w), 752(w), 656(w), 647(w);

^{1}H NMR (CD_3OD, 400MHz, rt, δ in ppm): δ = 4.26 (m,1H), 2.62 (t,2H), 2.09 (s,3H), 2.03 (m,1H), 1.88 (m,1H);

^{13}C NMR (CD_3OD, 100MHz, rt, δ in ppm): δ = 177.6 (CO), 70.0, 34.8, 30.6, 15.1.

The complex **12** was obtained following the procedure described above for **6** but precipitating the product at -90ºC. **Yield:** 83%.

IR(KBr/cm^{-1}): 2141(s), 2077(s), 2063(s) (C≡O); 1793(s) (C=O);

E.A.: Calc. for $RuC_8H_{10}O_6SCl_2$: %C:23.66, %H:2.48, %S:7.89; Found: %C:23.56, %H:3.40, %S:7.94;

^{1}H NMR (MeOD, 400MHz, rt, δ in ppm): δ = 2.65 (m,1H), 2.09 (s,3H), 1.55-1.63 (m,4H).

The following complexes (**8**, **9**, **10**, **11**, **13** and **14**) were synthesized with slight modifications of the previous method, using MeOH instead of acetone. The use of MeOH as solvent implies some limitations in the crystallization procedure since the compounds should not be precipitated at low temperature due to the risk of esterification in one of the carbonyl groups, affording compounds of the type $RuCl_2(CO)_2(COOMe)L$ as described by Moreno *at al*.[59]

A standard preparation is described for **8**, and deviations from this procedure are mentioned for each case.

$Ru(CO)_3Cl_2(4\text{-}NC_5H_4(CH_2)_2SO_3Na)$ **(8)**

The ligand (0.320 g; 1.530 mmol; 209.2012 g/mol) was dissolved in 50 ml of MeOH and added to $[Ru(CO)_3Cl_2]_2$ (0.392 g; 0.765 mmol; 512.02 g/mol) dissolved in 20 ml of MeOH. The clear colorless solution was stirred at room temperature overnight.

The slightly turbid solution was filtered giving a colorless solution that was concentrated. Et_2O was slowly added and a precipitate started to form. The solution was filtered and a white aggregate was obtained. It was washed with 2x10 ml of Et_2O and dried in vacuum giving a white powder. **Yield:** 53%.

IR (KBr/cm^{-1}; C≡O): 2137(s), 2053(s);

E.A.: Calc. for $RuC_{10}H_8NO_6SNaCl_2$: %C:25.82, %H:1.73, %N:3.01, %S:6.89; Found: %C:26.10, %H:2.20, %N:3.21, %S:6.96;

^{1}H NMR (D_2O, 400MHz, rt, δ in ppm): δ = 8.69 (d,2H), 8.02 (d,2H), 3.40 (s,4H).

$Ru(CO)_3Cl_2$(3-$NC_5H_4(CH_2)_2NMe_3I$) **(9)**

Yield: 12%; **E.A.:** Calc. for $RuC_{13}H_{17}N_2O_3Cl_2I$: %C:28.48, %H:3.13, %N:5.11; Found : %C:29.00; %H:3.30; %N:5.53;

IR (KBr/cm^{-1}; C≡O): 2129(s); 2051(s); 1981(s);

^{1}H NMR (D_2O, 400MHz, rt, δ in ppm): δ = 8.78-8.73 (d,2H); 8.52 (d,1H); 8.02 (t,1H); 3.74-3.43 (m,4H); 3.27 (s,9H).

$Ru(CO)_3Cl_2$(PTA) **(10)**

The reaction was performed in 15min after which a large amount of white product precipitated. It was washed with MeOH and dried in vacuum.

Yield: 56%; **E.A.**: Calc. for $N_3O_3PCl_2RuC_9H_{12}$: %C:26.16, %H:2.93, %N:10.17; Found: %C:25.90, %H:3.30, %N:10.18;

IR (KBr/cm^{-1}; C≡O): 2134(w), 2060(s), 1994(s);

The compound is insoluble in all the deuterated solvents tested. It could only be solubilized in d^6-DMSO but with decomposition.

$Ru(CO)_3Cl_2$(DAPTA) **(11)**

The reaction time was 2h and the product was washed with CH_2Cl_2 instead of Et_2O.

Yield: 75%; **E.A.**: Calc. for $C_{12}H_{16}Cl_2N_3O_5PRu$: %C:29.70, %H:3.32, %N:8.66; Found: %C:29.34, %H:3.65, %N:8.47;

IR (KBr/cm^{-1}): 2135(w), 2067(s), 2001(s) (C≡O); 1635(s) (C=O);

^{1}H NMR (D_2O, 400MHz, rt, δ in ppm): δ = 5.7-3.8 (m,8H), 3.28 (s,2H), 2.12 (s, 6H);

^{31}P NMR (D_2O, 162MHz, rt, δ in ppm): δ = 5.87.

$Ru(CO)_3Cl_2$(Gal-S-Me) **(13)**

Yield: 79%; **E.A.**: Calc. for $O_8SCl_2RuC_{10}H_{14}$: %C:25.76, %H:3.03, %S:6.88; Found: %C:25.68, %H:3.74, %S:6.73;

IR (KBr/cm^{-1}; C≡O): 2138(s), 2057(s);

^{1}H NMR (D_2O, 400MHz, rt, δ in ppm): δ = 4.38 (d,1H), 3.98 (m,1H), 3.75-3.58 (m,5H), 2.23 (s,3H).

$Ru(CO)_3Cl_2$(NAC) **(14)**

The reaction time was 4h and the precipitation was induced at -30ºC overnight.

Yield: 61%; **E.A.:** Calc. for $C_8H_8Cl_2NO_6RuS$: %C:22.98, %H:1.93, %N:3.35, %S:7.67; Found: %C:23.20, %H:2.03, %N:3.11, %S:7.32;

IR (KBr/cm^{-1}): 2126(s), 2062(s) (C≡O); 1749(s) (C=O);

^{1}H NMR (D_2O, 400MHz, rt, δ in ppm): δ = 4.46 (m,1H), 3.78 (m,2H), 3.0-3.34 (m,1H), 2.05 (s,3H).

4. Results and Discussion

4.1 Identification of the species present in DMSO solutions of $[Ru(CO)_3Cl_2]_2$ (CORM-2)

4.1.1 Chemical and spectroscopical studies

Di-μ-halobis(halotricarbonylruthenium) complexes of formula $[Ru(CO)_3X_2]_2$ (X=Cl, Br) are known since the 1960s and can be obtained through different methodologies.[60-66] Their chemical reactivity with oxygenated solvents and N-, O-, P- and S-donor ligands was object of interest for many decades,[67-71] but it was just recently that their potential as CO-releasing drugs was evaluated.

In 2002, Motterlini and co-workers published the first paper introducing the concept of CO-releasing molecules, as well as their biochemical and vascular activity.[46]

In this same paper $[Ru(CO)_3Cl_2]_2$ is named as CORM-2 and its biochemical and vascular properties are described. Its CO release capacity was also determined by adding aliquots of the complex in DMSO directly into a deoxy-Mb preparation in a similar setup to what has been described in Chapter IV. As recognized by the authors, $[Ru(CO)_3Cl_2]_2$ reacts with DMSO upon dissolution and the reaction products between the compound and DMSO were identified by NMR analysis.[46] $[Ru(CO)_3Cl_2]_2$ was dissolved in DMSO and diluted in $CDCl_3$. The spectra were taken during the first 23 min following dissolution and show that DMSO breaks the dimer into two monomers of **1**, and further replacement of one carbonyl occurs with species **1** and **2** co-existing in solution.

The observed ^{13}C NMR chemical shifts coincide with those published and assigned by Alessio *et al.*[58] to *fac*-$RuCl_2(DMSO)(CO)_3$ (**1**, δ 183.0 (2 CO), 187.0 (1 CO)) and *cis,trans,cis*-$RuCl_2(DMSO)_2(CO)_2$ (**2a**, δ 185.0 (2 CO)).

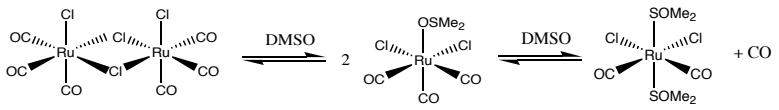

CORM-2 **1** **2a**

Scheme 1: CORM-2 decomposition in DMSO to give tri-(**1**) and di-carbonyl (**2a**) species through displacement of CO.

The sample was then heated to 50ºC for 5 min and a new spectrum accumulated overnight. Two new peaks appear from a new species *cis,cis,cis*-$RuCl_2(DMSO)_2(CO)_2$ (**2b**, δ 186.1 and 191.9 ppm) as well as two different carbonyl signals at δ 187.9 and 190.5 ppm from an unidentified species.

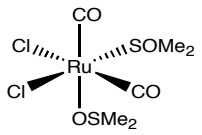

Figure 2: Structure of **2b** *cis,cis,cis* - $RuCl_2(DMSO)_2(CO)_2$

It is important to note that the isomers formed have been described in the literature using different nomenclatures, depending on the way the coordination formula was written. For clarity reasons and to allow an unambiguous identification of the compounds in this text we will adopt the nomenclature $RuCl_2(DMSO)_n(CO)_{4-n}$ (n=1-3) where the *cis, trans*, *mer* or *fac* italicized prefixes will refer to the pairs and/or triplets of ligands, respectively, as they appear in the formula, from the left to right. Moreover, since the sulfoxide ligand(s) can coordinate *via* the sulfur or the oxygen atom, the coordinating atom will be indicated in italics when relevant.

Since Motterlini's initial comunication[46] CORM-2 has been extensively used in biological studies because of its convenient commercial availability. In all these studies the compound is first dissolved in DMSO and the solution diluted in aqueous buffers to biological compatible DMSO concentrations. Due to the above mentioned equilibria it is not clear which species are actually present in the solutions when they are applied in the biological tests, and it is not determined which one (or ones) of these isomers is the therapeutically active CO releaser.

In order to attempt answering this question, monomeric compounds with different CO/Ru stoichiometries ranging from 3 to 1 were prepared separately in order to test and compare their properties, namely biological activity. The corresponding CO free analogue, $RuCl_2(DMSO)_4$ was used as a form of negative control for CORM-2. In principle, all these species might be present in a solution of CORM-2 in DMSO. To initiate this study, the several possible species were first synthesized and individually characterized both by NMR and FT-IR.

The tricarbonyl compound *fac*-$RuCl_2(DMSO)(CO)_3$ (**1**) was prepared by bubbling CO in a solution of $Ru(DMSO)_4Cl_2$ according to literature procedures (see Experimental Section). The IR spectrum of (**1**) in KBr has a band at 903 cm^{-1} showing that the Me_2SO group is coordinated through the oxygen atom. In the carbonyl region there's a sharp peak at 2131 cm^{-1} and another broader peak at

2060 cm^{-1}. The ^1H NMR in $CDCl_3$ has a singlet at δ 2.82 ppm from the 6 protons of the coordinated Me_2SO group. ^{13}C NMR spectrum in d^6-DMSO showed 2 peaks at δ 188.3 and 184.3 ppm in a 1:2 ratio that correspond to the CO ligands of a *fac*-$M(CO)_3$ compound.

The dicarbonyl analogue $RuCl_2(DMSO)_2(CO)_2$ was prepared by a different method and was directly separated from the reaction mixture of $[Ru(CO)_3Cl_2]_2$ in DMSO (see Experimental Section). The IR spectrum of $RuCl_2(DMSO)_2(CO)_2$ in KBr has two very sharp peaks with similar intensities in the carbonyl region at 2077 and 2020 cm^{-1}. In the Me_2SO region there are three major peaks, two at 927 and 1132 cm^{-1} characteristic of oxygen and sulfur coordinated Me_2SO, respectively, and other peak at 1029 cm^{-1} from another sulfur coordinated Me_2SO.

Table 1: ^1H and ^{13}C chemical shifts of $RuCl_2(DMSO)_2(CO)_2$ (**2**) in $CDCl_3$.

	a *-cis,trans,cis-* $RuCl_2(DMSO)_2(CO)_2$	***b*** *- cis,cis,cis-* $RuCl_2(DMSO)(DMSO)(CO)_2$
^1H chemical shift/ppm	3.44(12)	2.85(3); 2.88(3); 3.17(3); 3.43(3)
^{13}C chemical shift/ppm	45.1 185.7	38.9; 39.3; 42.2; 47.5 186.1; 191.9*

* from the literature, not observed

The Me_2SO bands showed the presence of different isomers **2a** and **2b** that were identified by ^1H NMR in $CDCl_3$, by comparison with the published literature.[58]

The mono-carbonyl complex $RuCl_2(DMSO)_3(CO)$ (**3**) was obtained from the reaction of $[Ru(CO)_3Cl_2]_2$ in DMSO (see Experimental Section). As stated above, DMSO has 2 different coordinating atoms therefore a high number of isomers could possibly be obtained, some being linkage isomers.

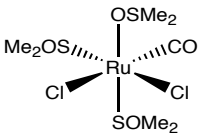

3a - cis,cis,cis

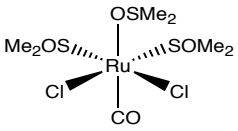

3b -cis,cis,trans

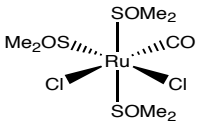

3c - cis,mer

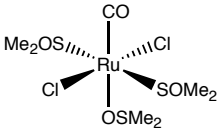

3d - trans,trans,trans

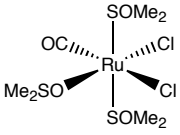

3e - cis,trans,cis

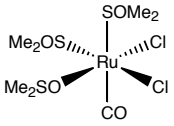

3f -cis,cis,trans

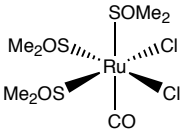

3g - cis,fac

Figure 3: Isomeric structures of $RuCl_2(DMSO)_3(CO)$. A-D were isolated and characterized and are the most electronic favored isomers (D not included in the DFT study). E is electronically favored but was never observed in solution while F and G are electronically disfavored. S-bonded DMSO *trans* to CO has never been observed in Ru-DMSO carbonyls.[58, 72] A is a linkage isomer of C and E; B is a linkage isomer of F and G.

However, DFT calculations[73] showed that the most energetically favored are the *cis,cis,cis*- (**3a**), *cis,cis,trans*- (**3b**), and *cis,mer*-$RuCl_2(DMSO)_3(CO)$ (**3c**) isomers. These have been isolated and characterized separately.[74] Another isomer, *cis,trans,cis*- (**3e**) although energetically favored, was never detected in solution maybe due to kinetic factors.

From our reaction of $[Ru(CO)_3Cl_2]_2$ in DMSO two different fractions (**F1** and **F2**) were obtained, both containing a mixture of the three most common isomers **3a**, **3b** and **3c,** which were assigned based on published data.[74]

Table 2: ^{1}H and ^{13}C NMR chemical shifts of $RuCl_2(DMSO)_3(CO)$ (**3**) (fraction **F2**) in $CDCl_3$.

	A - *cis, cis, cis*	**B** - *cis,cis,trans*	**C** - *cis,mer*
^{1}H chemical shift/ppm	2.75(3); 2.78(3); 3.17(3); 3.45(6); 3.52(3)	2.85(6); 3.25(6); 3.43(6)	3.41(6); 3.43(6); 3.51(6)
^{13}C* chemical shift/ppm	38.5; 39.0; 43.5; 45.3; 46.8; 50.2	39.1; 43.7; 47.6	42.9; 46.4; 47.4

* carbonyl resonances were observed at δ 191.0 and 192.4 ppm

The ^{1}H NMR spectra of both fractions showed different ratios between the isomers but more importantly, it was observed that independently of the ratio between the isomers in the solid state, the abundance of the isomers formed in solution is strongly influenced by the medium where they are dissolved. In $CDCl_3$, formation of **3a** and **3c** is favored over **3b**, but in CD_2Cl_2 the equilibrium is inverted and formation of **3b** is favored over the other 2 species.

In d^6-DMSO, the ^{13}C NMR spectrum of fraction **F1** presents two peaks at δ 191.3 and 193.3 ppm. Although it is not clear to which isomer they correspond, after 28h a new peak is observed at δ 197.7 ppm, arising from a new isomer formed. In $CDCl_3$, the same fraction shows two major carbonyl peaks at δ 191.0 and δ 192.4 ppm, however, after 29h no changes are detected. These differences reinforce the importance of the solvent in the equilibrium between the isomers formed.

The ratio between the isomers also influences the product's color in the solid state. Fraction **F1** is white and the most abundant isomer is **3a** which is colorless while fraction **F2** gets the yellow color of its main component **3b**. In spite of the differences in the solid state the IR spectrum of both fractions is similar and shows one single carbonyl peak of high intensity at 2003 cm^{-1}. Regarding the coordinated Me_2SO there are two peaks corresponding to oxygen coordination at 924 and 985 cm^{-1} and two other peaks at 1023 and 1115 cm^{-1} corresponding to sulfur coordination.

The isostructural and isoelectronic carbonyl free compound, $RuCl_2(DMSO)_4$ (**4**), provides fundamental information that may be useful for understanding similar processes with the carbonyl analogues in aqueous solution.

Analysis of commercial $RuCl_2(DMSO)_4$ shows that it is a mixture of *trans* and *cis* isomers. The *cis* isomer has both S- and O- bonded Me_2SO while the *trans* isomer only has S- bonded Me_2SO.

In the solid state the IR spectrum has the most intense peaks at 1108 cm^{-1} and 1087 cm^{-1} (both from S- bonded Me_2SO) and 926 cm^{-1} (from O- bonded) characteristic of the *cis* isomer. The ^1H NMR spectrum in $CDCl_3$ presents two singlets at δ 3.50 and 3.33 ppm that correspond to the two S- bonded Me_2SO, and another singlet at δ 2.73 ppm that corresponds to the O- bonded Me_2SO. These peaks integrate in a 3:1 ratio against a singlet at δ 2.61 ppm that corresponds to the free Me_2SO. A major peak at δ 3.43 ppm that is due to the S-bonded Me_2SO of the *trans* isomer is also observed. This lability of Me_2SO is due to a constant exchange with H_2O; the exchange with $(CD_3)_2SO$ is fairly rapid and after 24h complete exchange has taken place.[75] The resulting equilibria, characterized by the groups of Wilkinson and Alessio, are quite complex with different products obtained for each isomer as shown in Schemes 2 and 3. [75, 76]

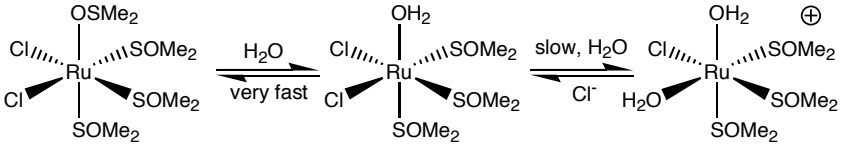

Scheme 2: Behavior of *cis*- $RuCl_2(DMSO)_4$ in aqueous solution

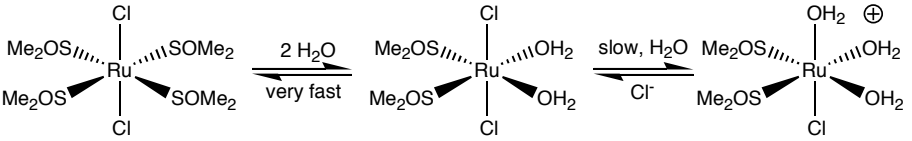

Scheme 3: Behavior of *trans*- $RuCl_2(DMSO)_4$ in aqueous solution

This type of substitution process may also occur with the other carbonyl molecules leading to complicated and unforeseen equilibria *in vivo*.

After having characterized the three different carbonyl derivatives, **1**-**3**, they were studied in DMSO to follow their possible modifications, and to make a parallelism to the behavior of CORM-2. Changes in the carbonyl pattern were monitored by IR and ^{13}C NMR in d^6-DMSO.

a. Reactivity in DMSO

The ^{13}C NMR spectrum of the monocarbonyl complex (**3**) immediately after dissolution in d^6-DMSO presents carbonyl peaks at δ 191.3 and 193.3 ppm corresponding to different isomers, most probably **3a** and **3b** although it is not known which corresponds to which. The same sample recorded after 28h presents a new peak at δ 197.7 ppm probably from **3c**. The new isomer formed was not detectable in the initial period, most probably because it was present in low concentration.

The changes were also followed by IR. A concentrated solution of (**3**) in DMSO (1.4 mg in 100 μL; 32 mM) was prepared and sample drops from this solution were taken and added to a KBr pellet along the time. A single broad band was observed at 2000 cm^{-1} which remained unchanged after 2h, 5h and 24 hours. Therefore, the possible substitution of the carbonyl **3** by DMSO to give $RuCl_2(DMSO)_4$ (**4**) does not take place at room temperature in pure DMSO solvent. The same kind of study done with the dicarbonyl species **2** (9.1 mg in 300 μL DMSO; 79 mM) demonstrated that it doesn't undergo CO substitution to give either the monocarbonyl compound **3** or the carbonyl free **4**. The bands at 2012 and 2076 cm^{-1} in the IR spectrum of **2** dissolved in DMSO remain unchanged up to 51h (Figure 4).

The ^{13}C NMR spectrum of **2** dissolved in d^6-DMSO presented carbonyl peaks at δ 193.0 and 187.9 ppm corresponding to the *cis,cis,cis*- (**2b**) isomer and another one

at δ 186.8 ppm from the *cis,trans,cis*- (**2a**) isomer. A similar spectrum is obtained after 51h reaction (Figure 5).

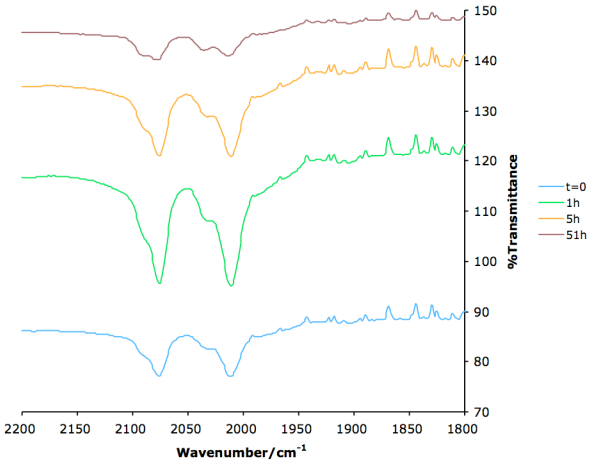

Figure 4: Time evolution of the IR spectrum of **2** in DMSO at room temperature. Drop of solution over a KBr pellet.

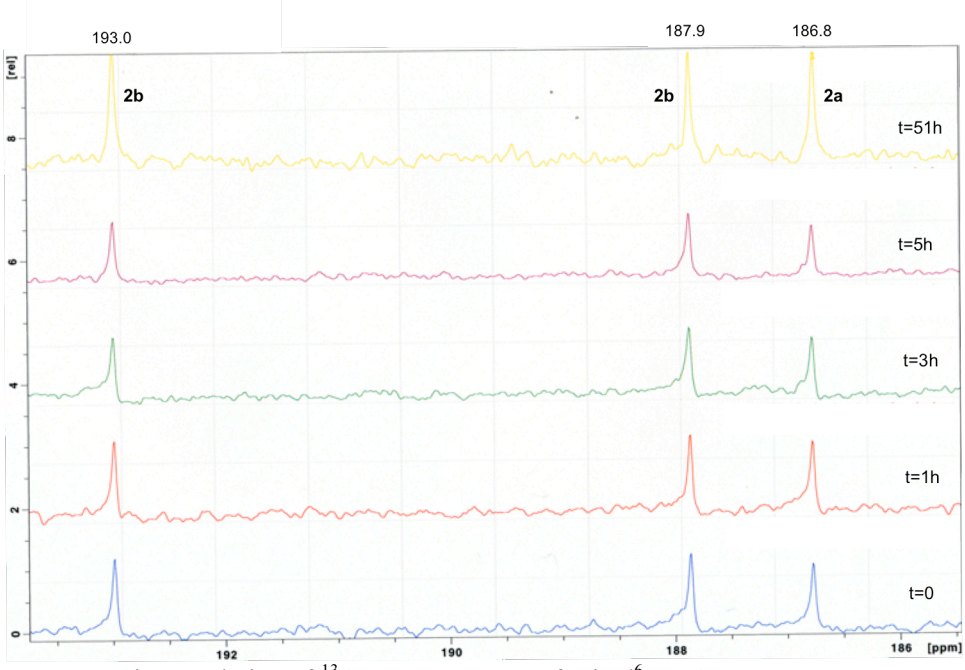

Figure 5: Time evolution of ^{13}C NMR spectrum of **2** in d^6-DMSO, at room temperature, in the carbonyl region at t=0; t=1h; t=3h; t=5h; t=51h. Each spectrum was acquired over 29 min.

The same procedure was followed for complex **1.** A solution of **1** in DMSO was prepared (6.1 mg in 200 μL DMSO; 91 mM) and the changes followed by IR taking sample drops that were added to a KBr pellet. The spectra were recorded periodically and the changes in the CO pattern monitored (Figure 6).

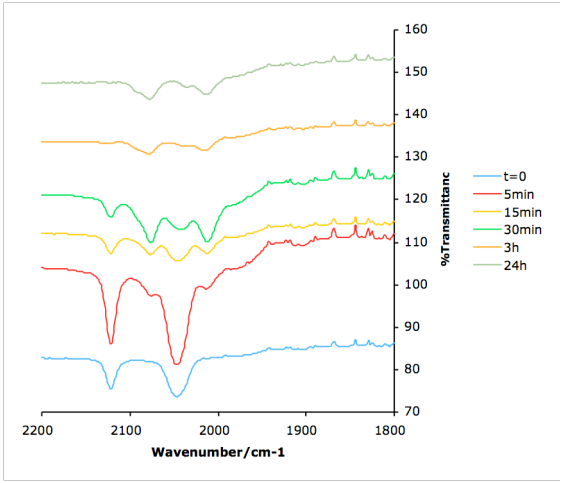

Figure 6: Time evolution of the IR spectrum of **1** in DMSO. Drop of solution over a KBr pellet.

At the time of dissolution two strong bands at 2121 and 2076 cm^{-1} are obtained, the later being broader as expected for a $M(CO)_3$ fragment. After 5 min some shoulders are already noted and 15 min later these bands decrease intensity and 2 new bands start to appear at 2077 and 2012 cm^{-1}. After 30 min the new bands are already higher in intensity than the initial ones. After 3h the spectrum shows a similar profile to the one presented after 24 hours with two major bands of equal intensity at 2079 and 2014 cm^{-1} which are characteristic of complex **2**.

It was also noted that when the compound is dissolved in DMSO a colorless solution is obtained that turns yellow within some seconds. The yellow solution deepens color with time during the first 5 to 15 min and some bubbles are observed. Then, after some minutes it slowly starts to lose color and after 24h is almost colorless.

A similar study was performed by ^{13}C NMR periodically recording spectra of a sample of **1** dissolved in d^6-DMSO (Figure 7).

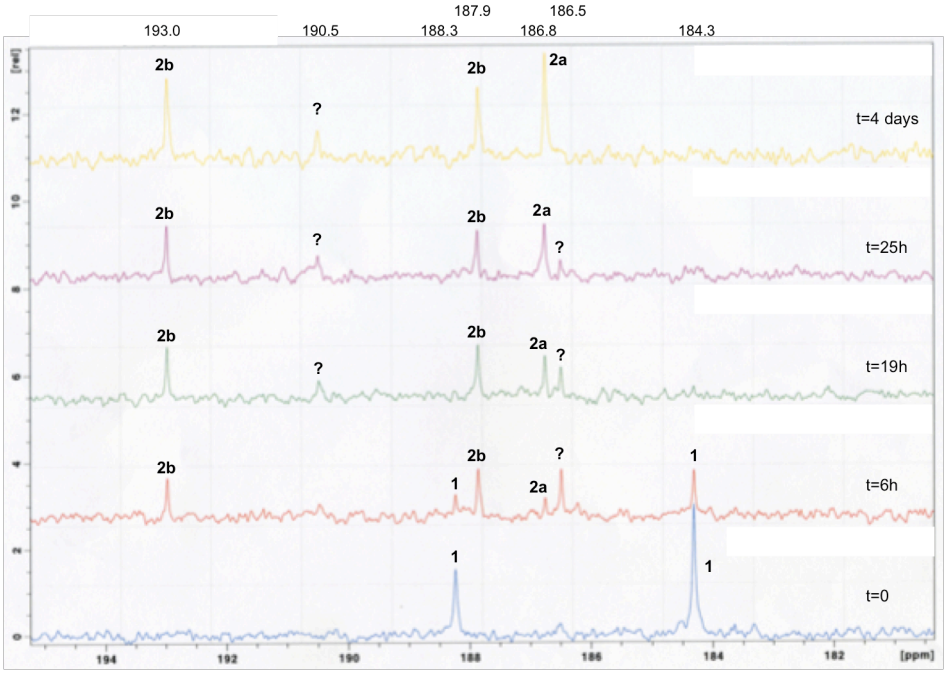

Figure 7: Time evolution of the ^{13}C NMR spectrum of **1** in d^6-DMSO in the carbonyl region at t=0; t=6h; t=19h; t=25h; t=4 days. Each spectrum was acquired over 29 min.

As can be seen from Figure 7, at the time of dissolution **1** has 2 peaks at δ 188.3 and δ 184.3 ppm in a 1:2 ratio, corresponding to the tricarbonyl compound. These values are slightly different from the ones obtained by Alessio *et al* for the same compound (δ 186.7 and 183.4 ppm in $CDCl_3$) however the differences in the solvent account for this discrepancy.

In this spectrum the peak at δ 188.3 ppm has almost disappeared, while 4 new peaks from the dicarbonyl species **2** appeared meanwhile at δ 193.0, 187.9, 186.8 and 186.5 ppm. The first two peaks were assigned to the **2b** isomer, the one at δ 186.8 ppm to the **2a** isomer and the one at δ 186.5 ppm cannot be clearly assigned to any species, based on the data collected.

After 19h the tricarbonyl compound **1** was already totally converted into dicarbonyl species **2** and the **2a** isomer is increasing in solution, while the species corresponding to the peak at δ 186.5 ppm is decreasing. This tendency is

reinforced after 25h with only minor amounts of the unknown species present. After 4 days in solution only the **2a** and **2b** isomers are present in solution and a new peak at δ 190.5 ppm is observed. The origin of this peak is unknown and we didn't attempt to assign it because its slow formation makes it irrelevant for the biological studies.

The same experiment was performed with CORM-2. In the solid state, the CORM-2 dimer has a IR spectrum with 3 equivalent CO stretching bands at 2145, 2092 and 2066 cm^{-1}. When it is dissolved in DMSO (9.7 mg in 300 µL; 63 mM) the IR spectra start evolving similarly to those of **1** (Figure 8).

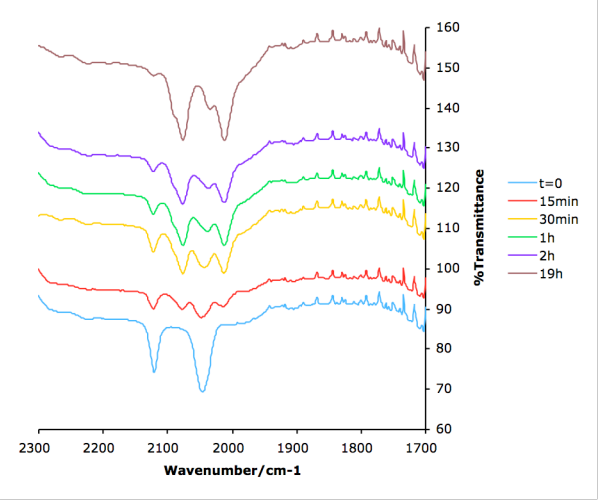

Figure 8: IR spectrum of **CORM-2** in DMSO solution at RT; Drop of solution over a KBr pellet.

At the time of dissolution there are two strong bands at 2121 and 2046 cm^{-1}, the later being broader. After 15 min these bands decrease in intensity and 2 new bands start to appear at 2077 and 2013 cm^{-1}. This evolution continues up to 24h when two major bands appear at 2077 and 2012 cm^{-1} with only small shoulders at 2037 and 2122 cm^{-1}.

These latter bands arise from the new species into which CORM-2 has converted and are characteristic of the dicarbonyl species.

When CORM-2 is dissolved in DMSO the initial colorless solution turns yellow within minutes. The yellow solution deepens color during the first 5 to 15 min and some gas bubbles are formed. After a while the color starts to become lighter. This sequence is identical to that observed in the dissolution of **1** in DMSO. The ^{13}C NMR spectrum in d^6-DMSO was recorded along time and the changes in the

carbonyl peaks were followed (Figure 9). The observed peaks were assigned on the basis of the previously characterized individual species.

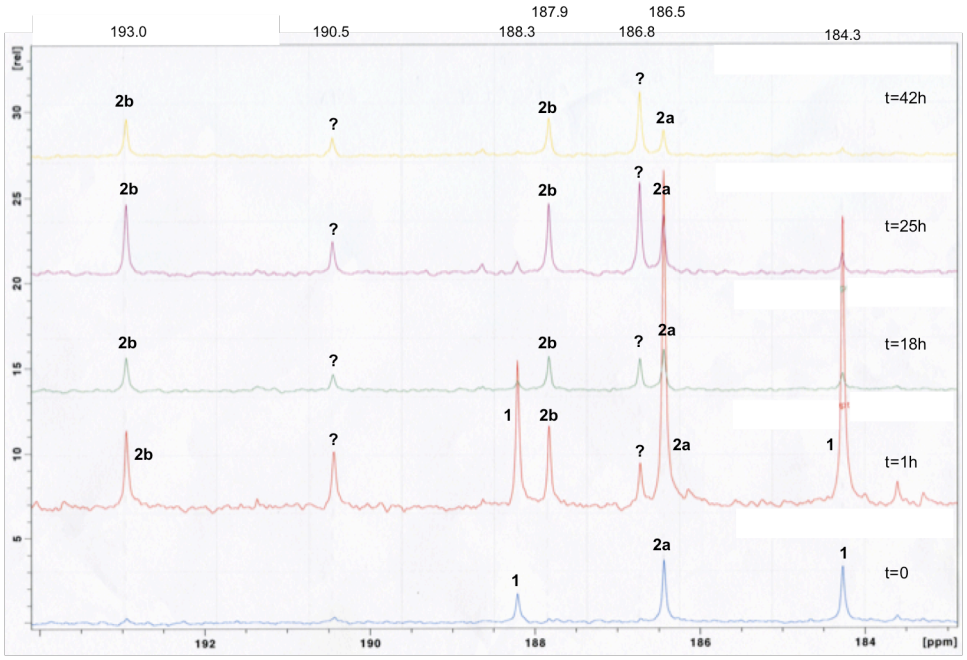

Figure 9: Time evolution of ^{13}C NMR spectrum of **CORM-2** in d^6-DMSO, at room temperature, in the carbonyl region at t=0; t=1h; t=18h; t=25h; t=42h. Each spectrum was acquired over 29min, except t=1h that was acquired over 3h.

At the time of dissolution 3 peaks are observed, two at δ 184.3 and 188.3 ppm from **1** and one peak at δ 186.5 ppm from **2a**. After 1h three isomers of dicarbonyl species are observed and an unknown peak is observed at δ 190.5 ppm. Later in time, after 18h **1** and **2a** concentrations' decreased and **2b** isomer increased in solution. This tendency results in the formation of dicarbonyl isomers with the *cis,trans,cis*- as the main species after 42h.

Table 3: Identification of the carbonyl peaks observed in the ^{13}C NMR spectrum of CORM-2 dissolved in d^6-DMSO.

TIME	SPECIES	^{13}C chemical shift (CO)
0	**1** *fac*- $RuCl_2(DMSO)(CO)_3$	184.3; 188.3
	2a *cis,trans,cis* -$RuCl_2(DMSO)_2(CO)_2$	186.5
1h	**1** *fac*-$RuCl_2(DMSO)(CO)_3$	184.3; 188.3
	2a *cis,trans,cis* -$RuCl_2(DMSO)_2(CO)_2$	186.5
	2b *cis,cis,cis*-$RuCl_2(DMSO)_2(CO)_2$	187.9; 193.0
	Unidentified	186.8
	Unidentified	190.3
18h	**1** *fac*-$RuCl_2(DMSO)(CO)_3$	184.3; 188.3
	2a *cis,trans,cis* -$RuCl_2(DMSO)_2(CO)_2$	186.5
	2b *cis,cis,cis*-$RuCl_2(DMSO)_2(CO)_2$	187.9; 193.0
	Unidentified	186.8
	Unidentified	190.3
25h	**2a** *cis,trans,cis* -$RuCl_2(DMSO)_2(CO)_2$	186.5
	2b *cis,cis,cis*-$RuCl_2(DMSO)_2(CO)_2$	187.9; 193.0
	Unidentified	186.8
	Unidentified	190.3
42h	**2a** *cis,trans,cis* -$RuCl_2(DMSO)_2(CO)_2$	186.5
	2b *cis,cis,cis*-$RuCl_2(DMSO)_2(CO)_2$	187.9; 193.0
	Unidentified	186.8
	Unidentified	190.3

b. Summary

The results presented showed that when CORM-2 is dissolved in DMSO a tricarbonyl complex *fac*-$Ru(CO)_3(DMSO)Cl_2$ (**1**) is immediately formed, as well as a dicarbonyl complex *cis,trans,cis*-$RuCl_2(DMSO)_2(CO)_2$ (**2a**). Over time the tricarbonyl complex is fully converted into dicarbonyl species and several isomers are present in solution. ^{13}C NMR shows the presence of an unidentified peak at δ 190.5 ppm after 1h in solution.

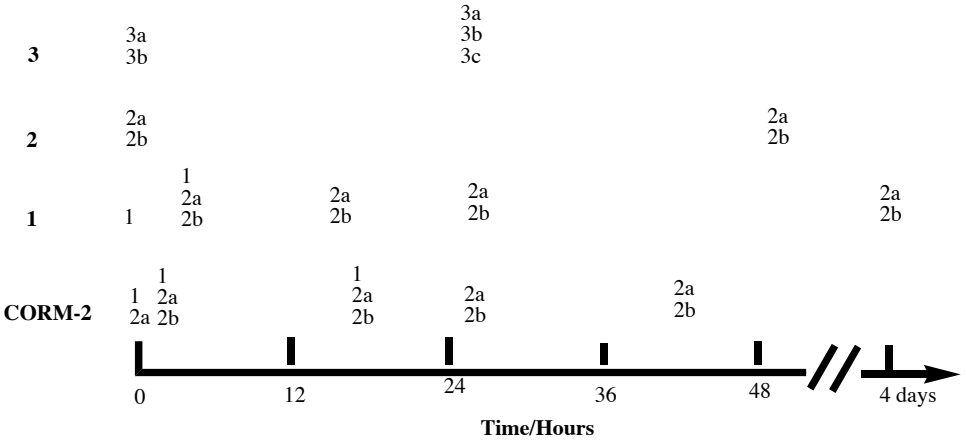

Figure 10: Time evolution of the species formed after dissolving **CORM-2**, **1**, **2** and **3** in DMSO, at room temperature.

The reaction profile is similar to the one observed with **1** in DMSO with two major differences. Upon dissolution of CORM-2 in DMSO the *cis,trans,cis*-$RuCl_2(DMSO)_2(CO)_2$ isomer is immediately formed, together with the tricarbonyl **1**. However, when pure **1** is dissolved in DMSO the formation of a dicarbonyl species doesn't occur immediately. The other major difference is the unknown peak with a ^{13}C resonance at δ 190.5 ppm that is observed after 1h with CORM-2 but only starts to appear after 25h in the case of the dissolution of **1** in DMSO.

The origin of this peak is unknown and although it could arise from a monocarbonyl compound it is highly improbable based on the other spectroscopic evidences. The ^{13}C NMR (and also IR) spectrum evolution of **2** in DMSO didn't reflect any changes in the CO pattern (Figures 6 and 7), therefore, the formation of a monocarbonyl complex through substitution of one CO is not expected under these experimental conditions. Moreover, the new peak formation occurs readily after 1h therefore a monocarbonyl compound is less likely to form so fast.

An alternative explanation is the formation of different dicarbonyl isomer not previously characterized and is more viable based on the spectroscopic arguments stated above.

In addition, exchanges between coordinated and free DMSO, as well as H_2O, occur at fast rates and are dependent on the amount of water present in the system and the concentration of the complex in DMSO solution. Since d^6-DMSO is not 100% dry, some water is present in solution. This water effect was observed in the ^1H NMR spectra of the samples through the changes in the water chemical shift. These changes suggest that water coordinates to the metal and a dynamic equilibrium is obtained between free and coordinated water which strongly influences the nature of the species formed. Therefore, this "hydration" leads to the formation of new carbonyl species with H_2O ligands through replacement of the DMSO and chloride ligands.

This is a similar process to what is observed with **4** (Schemes 2 and 3) and the unidentified carbonyl peaks at δ 190.5 and 186.5 ppm are likely to be due to these new species.

Although conclusions regarding the number of carbonyl groups in the molecule are valid based on the ^{13}C NMR and FT-IR studies, caution has to be taken when making considerations regarding the remaining ligands in the molecule.

In summary, incubation of CORM-2 in DMSO may afford tri- and dicarbonyl ruthenium dichloride dimethylsulfoxide complexes in a manner dependent on factors such as compound concentration, compound:DMSO ratio and $\%H_2O$ in the DMSO vehicle.

The full characterization of the CO release profile of this set of compounds was studied by the two different methods already explained in Chapters II and IV – gas chromatography and the Mb assay.

4.1.2 CO release profiles of CORM-3, CORM-2 and its derivatives in DMSO

a. CO release to the headspace in aqueous media

The GC assays were performed with the complexes **1**, **2**, **3**, CORM-3 and CORM-2. The CO release rate of the compounds was evaluated under the standard conditions described in Chapter II, Figure 1, in RPMI (10% FBS), PBS7.4 and H_2O. The same result was obtained with the 5 complexes in the different media – no CO was detected during 24 hours in the headspace of their solutions (ca. 14 mM) using TCD detection. CORM-2 and CORM-3 were tested with a variety of solvents and buffers at different pH values (pH2 to pH9) and from the media tested only DMSO could promote some CO displacement, although in very low amounts (less than 5% after 24h).

b. CO transfer to deoxy-Myoglobin

On the contrary, the Mb assay showed very interesting results with different amounts of CO donated to deoxy-Mb, depending on the number of carbonyls in the molecule, as can be seen in Figure 11. The monocarbonyl **3** does not transfer any CO to deoxy-Mb, the dicarbonyl **2** donates around 0.5 equiv. CO and the tricarbonyl **1** donates 1.0 equiv CO. The same donation profile is observed with CORM-2 and CORM-3 (see Chapter IV, Fig. 7), with CO-Mb formation completed after 5 min. After this rapid transfer has taken place a plateau is maintained over time without further carbonylation or decarbonylation of Mb.
The amount of CO donated by **1** is the same as that of CORM-3, showing that the amount of CO donated is clearly related to the number of carbonyls and not the co-ligands: the $Ru(CO)_3$ complexes are able to transfer 1 CO to deoxy-Mb and not more. **2** only transfers half equivalent, meaning that decreasing the number of carbonyls from 3 to 2 decreases the amount of CO donated to deoxy-Mb. This trend continues to the mono-carbonyl complex that is not able to transfer its CO to deoxy-Mb.

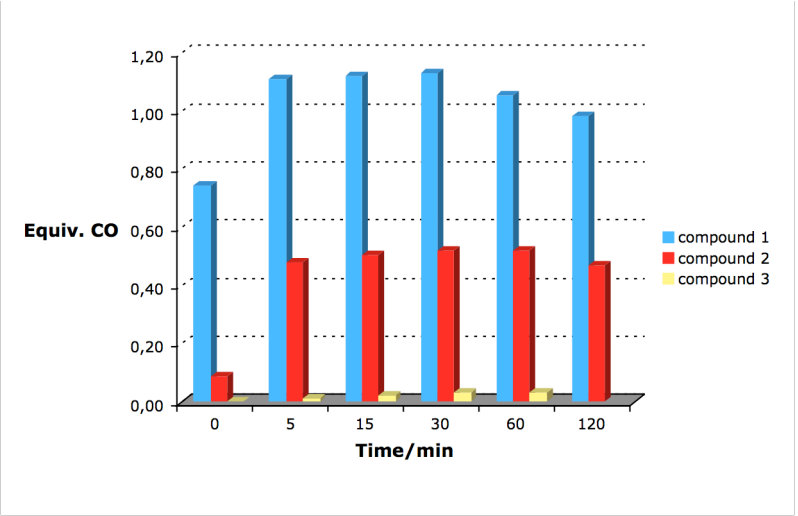

Figure 11: Equivalents of CO transferred from compounds **1**, **2** and **3** to deoxy-Mb in PBS7.4 at room temperature. Compound **1** was pre-dissolved in MeOH and added to a deoxy-Mb solution (58µM) giving a final concentration of 50µM (2.8% MeOH). Compound **2** was pre-dissolved in MeOH and added to a deoxy-Mb solution (58µM) giving a final concentration of 50µM (2.4% MeOH). Compound **3** was pre-dissolved in DMSO and added to a deoxy-Mb solution (58µM) giving a final concentration of 50µM (2.4% DMSO).

These data help to understand the results obtained with CORM-2 that donates around 1.7 equiv. CO to deoxy-Mb. Pre-mixing the compound in DMSO gives a mixture of **1** and **2** and if this ratio is 1:1 then 1.5 equiv. CO would be obtained (1 equiv. from **1** and 0.5 equiv. from **2**). Depending on factors such as the concentration of the stock solution or the amount of time evolved before adding the solution to Mb the ratio between **1** and **2** varies giving no more than 2 equiv. CO (if only **1** is present in solution) and no less than 1 equiv. CO (if only **2** is present in solution).

4.1.3 Final Remarks

The study performed allowed the identification of the species formed when CORM-2 is dissolved in DMSO, a tricarbonyl and dicarbonyl complexes. The results obtained must be interpreted with a degree of tolerance, since it shouldn't be assumed that *in vivo* a monocarbonyl complex can't be formed or even a totally CO-depleted molecule through displacement of CO by different triggering agents.

However, for *in vitro* studies CORM-2 is always pre-dissolved in DMSO and this has to be considered when interpreting the results. For example, as DMSO breakes the dimeric structure of CORM-2 the molar concentration of active Ru doubles.

Complexes **1**, **2** and **3** were tested in 2 models where CORM-2 had shown positive results, bacterial infection by *Escherichia coli* and *Staphylococcus aureus* and cerebral malaria infection (unpublished results).

In the bacterial model, **1** was effective at a slightly higher concentration than the one used for CORM-2 (250 μM). In addition, CORM-3 was also effective in this model at the same concentration as **1**.

In a malaria model, CORM-2 was able to rescue infected mice and the same result was replicated by **1**. Neither **2** nor **3** showed any protection in the same model.

Although these results arise only from 2 models, the data collected demonstrates that CORM-2 is actually a pro-drug, since the active molecule is in fact the tricarbonyl complex formed when the dimer is broken with DMSO. Together with the good results demonstrated by CORM-3 in several *in vivo* and *in vitro* models it became obvious that 3 carbonyls are needed to afford a biologically active compound, although as shown by the Mb assay, in principle only one is transferred to the target.

Since the "active ingredient" of CORM-2 is actually the tricarbonyl complex, the use of CORM-2 as a tricarbonyl source is therefore a "waste" from the point of view of atom economy. The loss of active compound due to side-formation of

dicarbonyl species is a drawback that decreases the efficacy. Using **1**, one may assure that only the active species is being administered without losing active compound in formulation. Unfortunately **1** is not totally soluble in water but its efficacy was proven beyond doubt.

This was the starting point for the development of a new group of dichloro ruthenium tricarbonyl complexes prepared in order to get new compounds with better properties like water-solubility, higher activity or efficacy both *in vitro* and *in vivo*.

4.2 Development of new Ruthenium tricarbonyl compounds $Ru(CO)_3Cl_2L$

4.2.1 Synthesis and Characterization

Given the success and widespread use of CORM-2 and CORM-3 for proof-of-concept studies on the viability of the use of CO-RMs as vectors for the delivery of CO to biological systems *in vitro* and *in vivo*, it felt reasonable to extend this family of compounds in order to reach better pharmacological properties and higher therapeutic activities. As shown above, CO release is favored by $Ru(CO)_3$ fragments and, therefore, it seems that the reaction in Equation 1 would be appropriate to obtain the desired complexes in which L imparts biocompatibility, water solubility and eventually targeting ability to the final analogues of **1**.

$$[Ru(CO)_3Cl_2]_2 + 2L \rightleftharpoons 2\ Ru(CO)_3Cl_2L \qquad \textbf{Equation 1}$$

Tuning this type of properties should lead to better complexes in terms of drug-like properties and therapeutic efficacy.

Synthesis of neutral ruthenium tricarbonyl complexes of the type $Ru(CO)_3Cl_2L$ (L=water-solubilizing agent) is not straightforward since it often leads to undesired substitution of another carbonyl. Several pathways can be envisaged as

summarized in Scheme 4. Intermediates of the type $Ru(CO)_3Cl_2S$ with a labile S molecule such as THF, Et_3N or $OPPh_3$[62, 66] can be prepared i*n situ* but the following step (the nucleophilic substitution by the ligand L) may be problematic. Using $Ru(CO)_4X_2$ as starting material is an alternative used with success to prepare the di-halo tricarbonyl complexes of the type $Ru(CO)_3Cl_2(OX)$ with O-donor ligands like Opy or $OPPh_3$,[67] but the use of the readily commercially available $[Ru(CO)_3Cl_2]_2$ starting material is preferable.

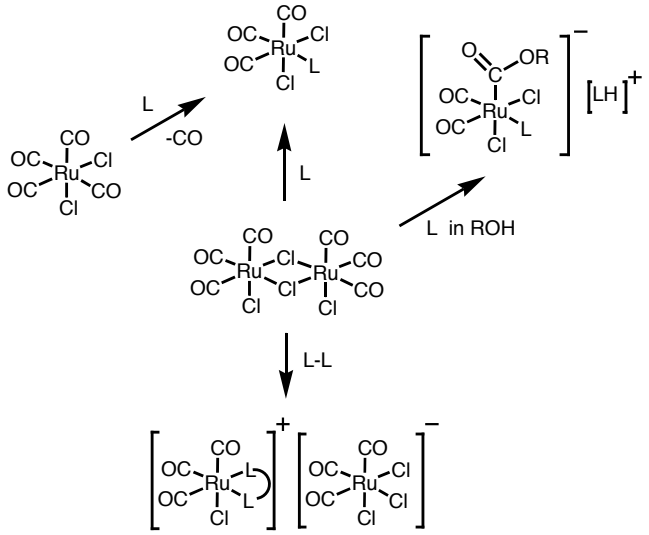

Scheme 4: Possible reaction pathways involving $[Ru(CO)_3Cl_2]_2$ and mono- (L) or bidentate (L-L) ligands in alcoholic media (ROH).

Since the new compounds should be water-soluble in order to facilitate their pharmacological study and application, the L ligand introduced was usually highly hydrophilic. This reduces the number of solvents available to perform the reaction and the solvents used are polar such as alcohols or acetone. Dissolution of the starting material in these solvents results in the cleavage of the halogen bridge with formation of monomeric species[68] of the type $Ru(CO)_3Cl_2(Solv)$.
Reactions of the dimer with N-donors, like N-coordinated nitriles and pyridines[68] results in the desired product but amines, diamines, bipy and phenantrolines, P-

and S- donors[62, 69-71, 77, 78] may also lead to CO replacement forming $RuX_2(CO)_2L_2$ complexes.

Reactions with aromatic nitrogen donor ligands in alcoholic media also proceed through a complicated pathway, dependent on the solvent and the other reagents.[59] For instance $[Ru(CO)_3Cl_2]_2$ reacts with py to give $Ru(CO)_3Cl_2py$ or $Ru(CO)_2Cl_2py_2$ depending on the concentrations; reacts with pz (pyrazine, NC_4H_4N) to give $[Ru(CO)_3Cl_2(pz)Ru(CO)_3Cl_2]$ and reacts with N-N chelating ligands to give $[Ru(CO)_3Cl(N\text{-}N)][Ru(CO)_3Cl_3]$ species.

If we change the solvent to ethylene glycol the reaction with 2,2'-bipyridine may give $Ru(bpy)(CO)_2Cl(C(O)OCH_2CH_2OH)$, $[Ru(bpy)(CO)_2Cl]H$ and $[Ru(bpy)(CO)_2Cl]_2$, which were formed consecutively and isolated by adjusting the reaction conditions.[79] In alcoholic media the same esterification of the third carbonyl occurs at low temperature, giving species of the type $Ru(CO)_2(COOR)Cl_2L$.

Obviously, there's not a standard procedure to perform these reactions. Each reaction is unique and the methodology developed must be determined case-by-case depending on the donor ability and solubility of the ligands.

The reactions with monodentate ligands proceeded without problems, with coordination to the metal center through the donor atom present in the molecule. Reactions with ligands containing more than one donor atom afforded mixtures of compounds, mainly bridged dimers.

With these provisos in mind, the following $Ru(CO)_3Cl_2L$ compounds were synthesized (Table 4):

L = D,L-$H_3CSO(CH_2)_2CH(NH_2)CO_2H$ (**5**); L-$H_3CSO(CH_2)_2CH(NH_2)CO_2H$) (**6**); 3-$NC_5H_4(CH_2)_2SO_3Na$ (**7**); 4-$NC_5H_4(CH_2)_2SO_3Na$ (**8**); 3-$NC_5H_4(CH_2)_2NMe_3I$ (**9**); PTA (**10**); DAPTA (**11**); $H_3CS(CH_2)_2CH(OH)CO_2H$ (**12**); GaL-S-Me (**13**); NAC (**14**). For synthetic details see Experimental Section.

Table 4: Spectroscopic information, solubility data and synthetic information for several $Ru(CO)_3Cl_2L$ complexes.

Entry	*Structure*	*Solubility in H_2O*	*vCO bands*	*Color*	*Yield*
CORM-3	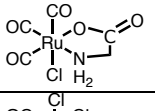	>20 mg/ml	2139(s) 2057(s) 1981(w)	pale yellow	50-90%
1	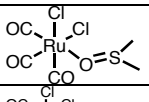	2 mg/ml	2134(s) 2068(s)	white	23%
5	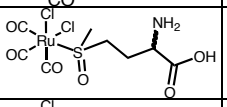	>5 mg/ml	2133(s) 2056(s)	off-white	36%
6	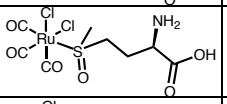	>5 mg/ml	2131(s) 2055(s)	off-white	83%
7	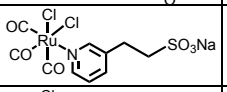	>5 mg/ml	2137(s) 2053(s)	pale yellow	63%
8	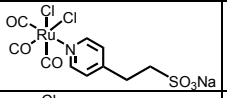	>5 mg/ml	2137(s) 2053(s)	white	53%
9	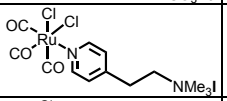	Insoluble	2130(w) 2047(s) 1975(s)	orange	12%
10	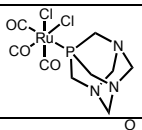	Insoluble	2134(w) 2060(s) 1994(s)	white	56%
11	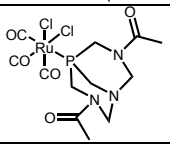	>5 mg/ml	2135(w) 2067(s) 2001(s)	white	75%
12	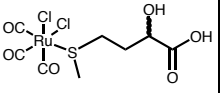	5 mg/ml 10% DMSO/ water	2137(s) 2053(s)	white	85%
13	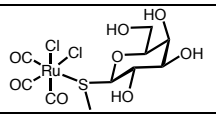	>5 mg/ml	2138(s) 2057(s)	white	73%
14	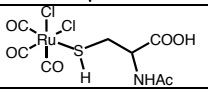	>5 mg/ml	2126(s) 2062(s)	light yellow	53%

Generally, the complexes **5-14** were obtained from reaction of $[Ru(CO)_3Cl_2]_2$ with the ligand in MeOH or acetone, depending on the ligand solubility. The reactions were performed at room temperature according to Equation 2 but the

reaction time varied from case to case, ranging from 15min (**10**), to 2h (**11**), 4h (**14**) or reacting overnight (**8**).

$$[Ru(CO)_3Cl_2]_2 + 2L \underset{\text{MeOH or acetone}}{\overset{\text{RT}}{\rightleftharpoons}} 2\ Ru(CO)_3Cl_2L \qquad \textbf{Equation 2}$$

The long reaction periods were employed to ensure the total solubilization of the ligands in the reaction medium. The solids were isolated in fairly good yields as white to pale yellow solids except **9** that was isolated as an orange solid with only 12% yield.

All the compounds were duly characterized by the usual spectroscopic (IR and NMR) and analytical (EA) methods. Mass spectrometric studies were undertaken and will be mentioned in the next section. The IR spectra of most of the compounds present the usual pattern corresponding to the *fac*-$M(CO)_3$ fragment with two CO stretching bands: a sharp strong vibration at ca. 2135 cm^{-1} and a broader band at ca. 2055 cm^{-1}. Compounds **9**, **10** and **11** have a different IR carbonyl pattern with a weaker band at ca. 2135 cm^{-1}, and two other strong and broader bands at ca. 2060 cm^{-1} and 2000 cm^{-1}. We did not find any explanation for the pattern observed, but some possible causes may be attributed to secondary effects such as Fermi resonance and overtone interactions that alter the "normal" IR spectrum.

From the values collected in table 4 it is clear that there are not major differences in the νCO of the different complexes. This data shows that the different ligands coordinated to the Ru(II) center do not have a major electronic effect on the M-CO bond, although different donor atoms as N, O, S or P are present.

Nevertheless, the high wavenumber at which the carbonyl stretching vibrations are observed reflects the weak coordination of the carbonyls to the Ru center. An important difference is observed between the coordination mode of **1**, **5** and **6**, which isn't shown in table 4. Compound **1** has a band at 903 cm^{-1} which was assigned to a Me_2SO group coordinated through the oxygen atom while

complexes **5** and **6** have bands at 1016 and 1017 cm^{-1}, respectively, assigned to a Ru-S coordination. The versatility of the sulfoxide functionality allows different coordination modes[80] and the unexpected coordination through the sulfur atom was indeed the driving force to use ligands with tioether functional groups leading to the synthesis of **12** and **13**. In these complexes the Ru-S bands are at 1125 and 1090 cm^{-1}, respectively, meaning that they're shifted to higher wavenumber when compared with the sulfoxides, showing evidence of stronger Ru-S bonds.

The ^1H NMR spectra show the ligand protons usually shifted downfield due to the electropositive character of the $Ru(CO)_3Cl_2$ fragment. A special behavior is observed with complexes **5**-**8** in D_2O. In the free ligands, the two CH_2 groups of the linear chain are observed as multiplets but after coordination to the metal they become equivalent, affording one singlet in the same location.

4.2.2 CO release profiles of the new $[Ru(CO)_3Cl_2L]$ complexes

Since all these new compounds were intended to perform as CO-RMs, their CO release profile has to be evaluated as for the other MCCs already discussed in this and previous chapters.

a. CO release to the headspace in aqueous media

Following the behavior already described for CORM-2 and CORM-3 none of the compounds in table 4 released CO to the headspace of their solutions in PBS7.4 at the level of the GC/TCD detection used in macroscopic assays (ca. 10 mg of compound in 2 mL of medium). Instead, like in the cases of **1** and CORM-3**,** large amounts of CO_2 were detected (see table 5).

On the contrary, no CO_2 was generated in the analogous solutions of the dicarbonyl complex **2** or the monocarbonyl **3**.

Table 5: Equiv. CO_2 released by ruthenium tricarbonyl compounds after 24h in H_2O or PBS7.4, at room temperature under N_2.

Compound	Equiv. CO_2
CORM-3	0.68 (PBS7.4) 0.29 (H_2O)
1	0.71 (H_2O)
5	0.98 (H_2O)
6	1.20 (H_2O)
7	0.96 (H_2O)
8	1.00 (H_2O)
9	0.53 (H_2O)
10	0.28 (H_2O)
11	0.19 (H_2O)
12	0.40 (H_2O)
13	0.71 (H_2O)
14	0.65 (H_2O)

The release of CO_2 is the result of the known *water-gas shift reaction* (WGSR) where CO reacts with H_2O to give CO_2 and H_2.

$$CO + H_2O \rightleftharpoons CO_2 + H_2$$ **Water-Gas Shift Reaction**

Since the first report of homogeneous WGSR catalyzed by ruthenium complexes in 1977 by Laine and co-workers,[81] this reaction has been widely studied employing mono- and polynuclear transition metal carbonyl complexes[82-87] of which ruthenium carbonyl clusters were actively studied.[88-93]

The studies performed elicited the general pathway shown in scheme 5.

In one pathway, a nucleophilic attack by OH^- or H_2O on the carbonyl leading to the formation of a metallo-carboxylate[94-97] (i); followed by decarboxylation with hydride formation (iia); the hydride may then react with H^+ from the medium and release H_2 (iiia).

Alternatively, the metal carboxylate may be deprotonated by an incoming base (iib) and then lose CO_2 to give M^{2-} (iiib). This may be protonated to give MH_2 (ivb). The dihydride may reductively eliminate H_2 (vb) to give M. All the equilibria will be dependent on pH and the co-ligands.

These features have been observed in related complexes. The group of Tanaka showed that $[Ru(bipy)_2(CO)Cl]^+$ and $[Ru(bipy)_2(CO)_2]^{2+}$ are good catalysts for WGSR in alkaline medium, and isolated and characterized the species involved in the catalytic cycle.[98]

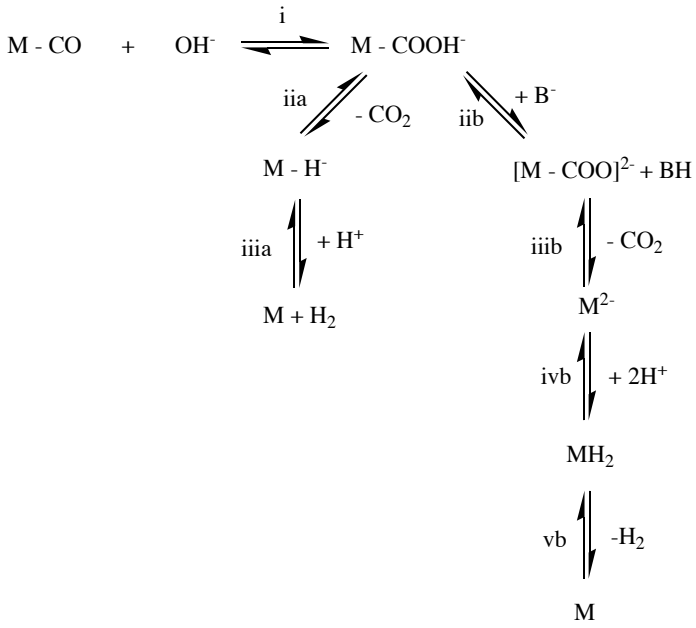

Scheme 5: General WGS reaction pathway leading to CO_2 and H_2 release.

Pakkanen and co-workers showed the activity of $Ru(bipy)_2(CO)_2Cl_2$ and $Ru(bipy)_2(CO)_2ClH$ supported on SiO_2 [99] and the effect of modifying the bipy rings[100] or the influence of the medium[79] with the complexes of the type $Ru(bipy)(CO)_2X_2$. In fact, bipyridine and phenantroline ligands are some of the most used ligands for WGSR Ru catalysts.[101]

Most of these catalysts are active in reactions performed in basic medium[102] but acid catalyzed WGSR is also possible,[103, 104] as well as water attack on tricarbonyl ionic complexes if the carbon atom is highly electrophilic.[105]

Evidence that this mechanism is occurring with these compounds is supported by different observations in aqueous solution. The aqueous chemistry of CORM-3 was extensively studied by Brian Mann's group, who found that a complex set of equilibria were taking place in water.[106]

Several important observations are fundamental and may help explaining the reaction pathway:

1. When the compound was dissolved in pure distilled water the pH of the solution dropped from ca. 5.5 to pH=2-3 depending on the concentration;
2. The typical tricarbonyl pattern of the IR bands changes and a new band appears in the carboxylate region ~1700cm^{-1};
3. At low pH the compound is stable but decomposes rapidly at high pH;

These observations support the WGS reaction detected in the GC assays.

When the compound is dissolved in water one of the carbonyls is immediately attacked by hydroxide anion. The corresponding H^+ becomes free and the pH lowers drastically, similarly to what is reported[105] for $[Ru(CO)_3(H_2O)_3]^{2+}$ which gives a pH 1.6 solution at 0.4 M, with formation of $[Ru(CO)_2(COOH)(H_2O)_3]^+$.

If a decarboxylation occurs, CO_2 is liberated and a hydride is formed (detected by ^{1}H NMR after 24h in D_2O at δ -14.5 ppm). This step is not as fast as with $[Ru(CO)_2(COOH)(H_2O)_3]^+$ that completely loses CO_2 within 3h (cited in reference [106]) .

The hydride $[RuH(CO)_2(H_2O)_3]^+$ preferentially reacts with H^+ from the medium and H_2 is released. Indeed, H_2 release was detected by GC-RCP after 24h in water and PBS7.4. In summary, a dicarbonyl complex is obtained as end-product of the reaction of a $Ru^{II}(CO)_3$ derived complex in water.

In the case of CORM-3, the IR spectrum of the product of this reaction, obtained after evaporation of the water shows the presence of 2 bands of terminal carbonyls. This species was termed in literature "*i-CORM-3*" (from inactivated CORM-3) since it has no biological effect and is used as a negative control for CORM-3 activity.[30]

The aqueous chemistry of the remaining complexes was not so extensively studied but the majority of them showed several aspects common to the chemistry of CORM-3 and $[Ru(CO)_3(H_2O)_3]^+$. Apart from the already mentioned CO_2 release, the formation of acidic solutions in water is common to all the water soluble compounds in Table 4 and the formation of a hydride after 24h in D_2O was also observed for **6** (δ -13.96 ppm), **7** (δ -13.94 ppm), **8** (δ -13.94 ppm), **13** (δ -13.97 ppm) and **14** (δ -15.29 ppm).

The HPLC trace of these water-soluble compounds was acquired in a MeOH/Water gradient. The chromatograms obtained reveal the presence of several species in solution. Typically two main groups of peaks are observed at retention times of ca. 2-3 min and 9-11 min but more peaks are sometimes observed. As exemplified in Figure 12, compound **1**, presents three major peaks at retention times of 3.0, 6.6 and 8.7 min while for compound **5** two major peaks are registered at retention times of 3.0 and 10.0 min.

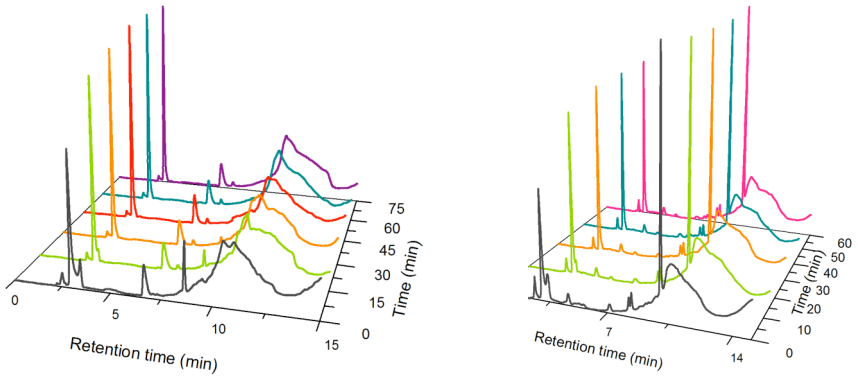

Figure 12: Time evolution of the HPLC trace of compounds **1** (left) and **5** (right).

Analysis and resolution of each peak eluted by LC-MS-ESI in positive ion mode was attempted with compounds **1**, **5** and **13**. The results further revealed that each of the chromatographic peaks contained several species eluting at very close retention times. In most of the cases a mixture of species was detected including

aggregates and oligomers, the identification of which was not pursued. The lability of these compounds in solution has become very clearly demonstrated and certainly will pose problems when it comes to interpret their biological activity.

b. CO transfer to deoxy-Myoglobin

The incubation of the compounds in Table 4 with deoxy-Mb resulted in similar profiles of carbonylation of Mb but with different reaction extensions since the amount of CO transferred is not the same for all compounds.

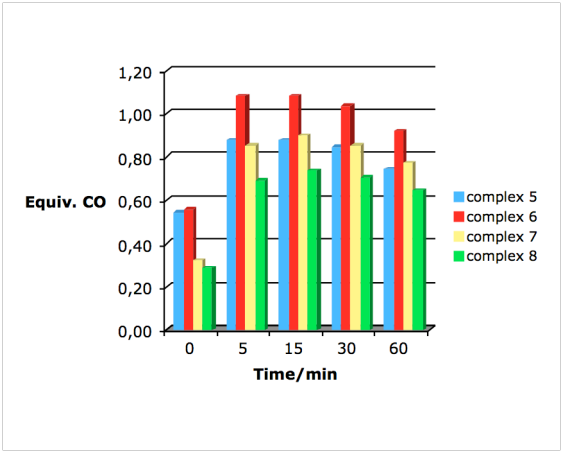

Figure 13: Equivalents of CO transferred from compounds **5**, **6**, **7** and **8** to deoxy-Mb in PBS7.4 at room temperature. Compound **5** was pre-dissolved in PBS7.4 and added to a deoxy-Mb solution (55µM) giving a final concentration of 50µM. Compound **6** was pre-dissolved in PBS7.4 and added to a deoxy-Mb solution (58µM) giving a final concentration of 50µM. Compound **7** was pre-dissolved in PBS7.4 and added to a deoxy-Mb solution (58µM) giving a final concentration of 50µM. Compound **8** was pre-dissolved in PBS7.4 and added to a deoxy-Mb solution (58µM) giving a final concentration of 50µM.

All the compounds shown in Figure 13 are able to complete CO transfer to deoxy-Mb within 5 min of incubation. That maximum reached 0.9 to 1 equivalent for compounds **5**, **6** and **7**, and 0.7 equiv for **8**. Compounds **5** and **6** only differ in the chiral purity of the methionine sulfoxide ligand, therefore, similar results (rate and extension of reaction) are expected and indeed observed both in PBS and H_2O. Compounds **7** and **8** are pyridine derivatives that only differ in the position of the ethyl-sulfonate substituent which is 3 and 4, respectively.

While **7** transferred roughly 1 equiv. CO to Mb very rapidly in both PBS and water (0.9 equiv. donated in PBS and 1.1 equiv. donated in water (data not shown), **8** transferred a slightly lower amount of CO (0.7 equiv.) in the same time span in PBS7.4. It is tempting to assign this difference of CO transfer rates to the difference in the σ-donating ability of both substituted pyridine ligands which is expected to decrease in the order 4-$NC_5H_4(CH_2)_2SO_3Na$ > 3-$NC_5H_4(CH_2)_2SO_3Na$.

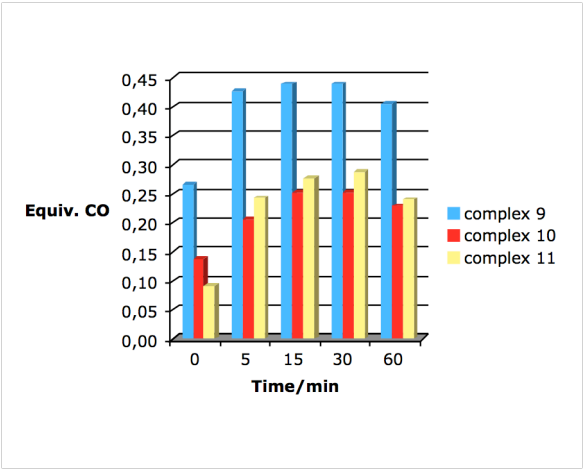

Figure 14: Equivalents of CO transferred from compounds **9**, **10** and **11** to deoxy-Mb in PBS7.4 at room temperature. Compound **9** was pre-dissolved in MeOH and added to a deoxy-Mb solution (58μM) giving a final concentration of 50μM (5.5% MeOH). Compound **10** was pre-dissolved in DMSO and added to a deoxy-Mb solution (58μM) giving a final concentration of 51μM (2.2% DMSO). Compound **11** was pre-dissolved in PBS7.4 and added to a deoxy-Mb solution (61μM) giving a final concentration of 58μM.

Figure 14 depicts the results obtained for compounds **9, 10** and **11**. One would expect that **9** would have a similar result to that of **8**. Experimentally, **9** only transferred ca. 0.4 equiv. CO to deoxy-Mb.

Despite the use of different solvents (**9** was pre-dissolved in MeOH) this shouldn't interfere with their transfer capacity like is demonstrated by **10** and **11**. Although different media were employed to solubilize the compounds, **10** and **11** both transferred 0.3 equiv. CO to deoxy-Mb. This very small amount which contrasts with that of all the other compounds in Table 4, strongly reinforces the suggestion that strong, substitutionally inert Ru-L bonds, hamper the CO transfer process between $Ru(CO)_3Cl_2L$ complexes and myoglobin.

Compounds **12** and **13** transferred, respectively, 0.7 equiv. and 0.8 equiv. CO to deoxy-Mb. Although **12** needed to be solubilized in MeOH, we already observed that the solubilizing medium does not greatly interfere with the donation capacity. In fact, this is confirmed by the similar profile observed with **12** and **13** (Fig. 15)

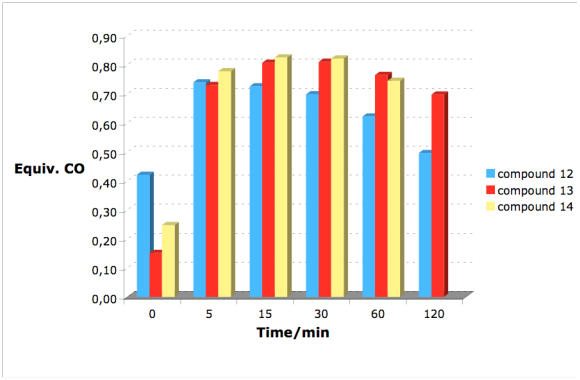

Figure 15: Equivalents of CO transferred from compounds **12**, **13** and **14** to deoxy-Mb in PBS7.4 at room temperature. Compound **12** was pre-dissolved in MeOH and added to a deoxy-Mb solution (68µM) giving a final concentration of 50µM (2% MeOH). Compound **13** was pre-dissolved in PBS7.4 and added to a deoxy-Mb solution (61µM) giving a final concentration of 51µM. Compound **14** was pre-dissolved in PBS7.4 and added to a deoxy-Mb solution (68µM) giving a final concentration of 50µM.

The broad picture of these CO transfer studies is that all the compounds in Table 4 are able to complete their CO transfer to deoxy-Mb within 5 min of incubation. This transfer is > 0.7 equivalents for most compounds and seems to decrease with decreasing donor strength of the ligand L in the following way: $R_2SO > R_2S \sim py >>> PR_3$. Under this light, it seems quite plausible that it is the substitutional stability of the coordination sphere of the $Ru(CO)_3Cl_2L$ complexes and not the electrophilicity of their CO ligands that controls their reactivity towards myoglobin.

c. Deactivation of the CO transfer capacity

Given the high reactivity and lability of these $Ru(CO)_3Cl_2L$ complexes it became important to establish their ability to retain the initial capacity to transfer CO once they are dissolved in pharmacologically or biologically compatible media. The importance of this study derives from the fact that many biological tests are

performed with stock solutions from which aliquots are successively administered to cells or animals along the time or, at least, after some time has passed.

This behavior was first recognized with CORM-3 which was not able to transfer the full CO equivalent to deoxy-Mb if the addition of its solution to the deoxy-Mb preparation wasn't performed immediately after dissolution. To determine if the donating ability of the compound is retained after staying in solution for a determined period of time, a series of studies were conducted with fresh and "aged" solutions (see Experimental Section for details).

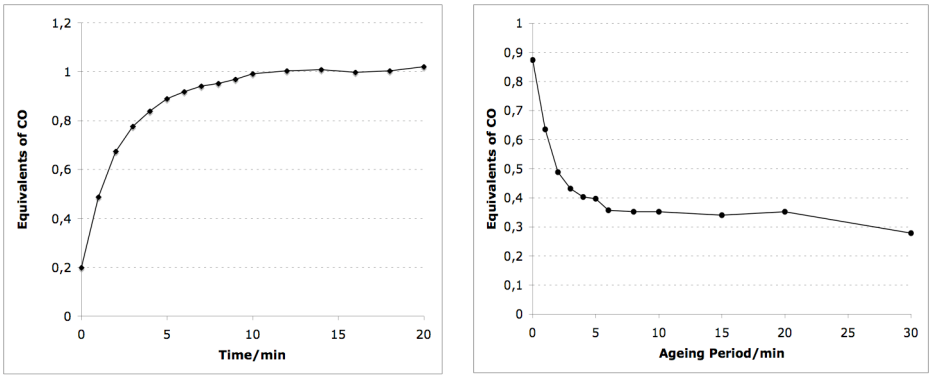

Figure 16: **Left:** Equivalents of CO donated to deoxy-Mb from CORM-3 freshly dissolved solution in PBS7.4. CORM-3 was pre-dissolved in PBS7.4 and added to a deoxy-Mb solution (57μM) giving a final concentration of 50μM; **Right**: Equivalents of CO donated to deoxy-Mb from CORM-3 aged solution in PBS7.4. CORM-3 was pre-dissolved in PBS7.4 and added to a deoxy-Mb solution (57μM) giving a final concentration of 50μM.

When CORM-3 is dissolved in PBS and the solution immediately added to the protein (deoxy-Mb), it rapidly donates 1 equivalent of CO to deoxy-Mb as seen in Figure 16-left. If the compound is left standing in PBS7.4 solution for some time (ageing period) it loses the capacity to transfer one CO ligand to deoxy-Mb as seen in Figure 16-right. If the solution of the compound is added to deoxy-Mb 5 min after being prepared around 50% donation capacity is lost. This very rapid inactivation observed in the first 3 to 4 minutes lowers the donation capacity to

ca. 0.3 equiv. CO, remaining almost constant up to 3h ageing period. After 24 hours ageing time, only 0.2 equiv. of CO are transferred to deoxy-Mb (Table 6).

Table 6: Amount of CO transferred to deoxy-Mb from aged CORM-3 solutions in PBS7.4.

Ageing period	Equiv. CO donated to Mb
0	1
5 min	0.4
15 min	0.4
60 min	0.3
180 min	0.3
24 h	0.2

This decrease in the CO donation capacity is herein called *deactivation*, since it reflects the loss of capacity to deliver the active principle CO. The deactivation of stock solutions in PBS poses a major limitation for biological work since it is difficult to have a control on the CO transferring ability of CORM-3. However, we hypothesized that such deactivation might be dependent on the medium as we know that coordinated CO is attacked by water in aqueous solutions of CORM-3. We therefore studied CO transfer from CORM-3 to deoxy-Mb in different media: distilled water (pH~5.5), DMSO and saline (0.9% NaCl). At the shortest possible ageing time, which we take as zero ageing time, the compound has a very similar behavior in the three media (see Table 7), transferring close to 1 equivalent CO to deoxy-Mb within the first 15 min of incubation. Nevertheless, it is clear that saline somehow increases the CO transfer capacity which actually exceeds 1 equiv. while water and DMSO are essentially the same.

Table 7: Amount of CO transferred from CORM-3 to deoxy-Mb in PBS7.4, H_2O, DMSO and saline 0.9% after 15min incubation.

Medium	Equiv. CO
PBS7.4	1.0
H_2O	0.9
DMSO	0.8
Saline (0.9% NaCl)	1.1

When CORM-3 solutions are aged before being added to deoxy-Mb, the deactivation observed is clearly dependent on the medium. As seen in Figure 17, saline effectively stabilizes the solutions of CORM-3 which lose only a little of their CO transfer ability in the first 4 hours. This strongly contrasts with the very

fast deactivation observed in PBS7.4. Distilled water is also more stabilizing than PBS7.4.

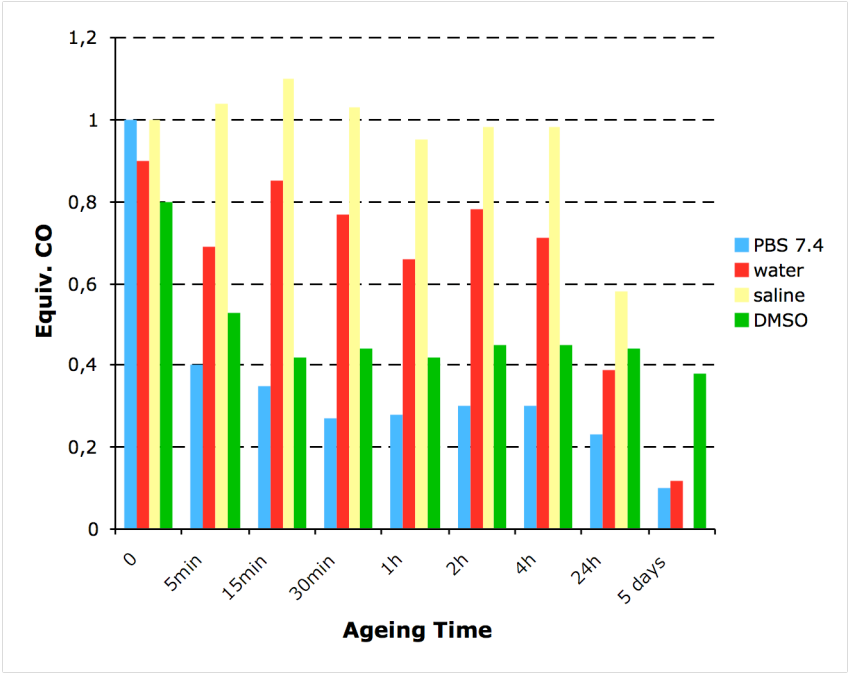

Figure 17: Equivalents of CO donated to deoxy-Mb from CORM-3 aged solutions in different media. The experiments were performed in similar setups as described above, dissolving the compound in the respective medium and adding to the deoxy-Mb preparation samples of the aged solutions, periodically.

Obviously, the high pH of PBS7.4 compared to saline and distilled water leads to a faster inactivation of one CO due to the higher concentration of OH^-. Consistent with this, the fast deactivation in PBS7.4 is accompanied by a high rate of CO_2 release as observed in the GC experiments.

The deactivation profile in DMSO is different. The initial amount of CO donated is slightly lower (0.8 equiv. CO), some deactivation is observed after 15min (to 0.4 equiv. CO) but this value is kept constant up to 24h. The data suggest that a stable species is formed within the first 15min, most probably a dicarbonyl compound since the amount of CO donated to deoxy-Mb is roughly the same of the dicarbonyl complex **2** (0.5 equiv. CO). The dicarbonyl structure was later confirmed by IR studies in DMSO.

Beyond pH influence, the stability in saline parallels that seen when NAMI-A is solubilized in saline: the presence of NaCl stabilizes the complex by preventing loss of chloride ligand. This suggests that such loss accelerates nucleophilic attack at the coordinated CO, which results in deactivation due to consumption of the "transferable" carbonyl. Indeed, aquation of the Ru-Cl bond increases the positive charge of the complex and favors nucleophilic attack by water. However, this is not the only process going on in solution since CORM-3 in isotonic NaCl exchanges glycine and is converted into $[Ru(CO)_3Cl_3]^-$ over a day at room temperature.[106] In summary, CORM-3 has a very labile coordination sphere particularly sensitive to H_2O and pH variations.

The deactivation process was also evaluated with the other ruthenium complexes described above. However, since not all are water soluble, the ageing process was performed in different solvents, which limits the comparison between all the complexes.

Compounds **1**, **9** and **12** that were solubilized and aged in MeOH before addition to deoxy-Mb did not show any important loss of donation capacity within 2h ageing time. This is not entirely unexpected since MeOH is probably unable to replace Cl^- and to esterify the complexes and form "$Ru(CO)_2(COOMe)$" containing species at room temperature, within 1h. Compounds **10** and **1** were also aged in DMSO, the only useful solvent for the former. In the case of **1** in DMSO, the amount of CO donated to deoxy-Mb was roughly 1 equiv. and the donation was completed after 5min. Solutions aged 1h lost ca. 30% CO transfer capacity, a fact that contrasts with the very high rate of deactivation of CORM-3 in DMSO.

Compound **10** was found to transfer as little as ca. 0.3 equiv. CO to deoxy-Mb but retained this capacity up to 1h ageing time. Of course, this is a situation chemically different from the compounds in water since in DMSO solution no attack occurs at CO and CO substitution is the only deactivation process available. However, the same exact profile was observed with **11** which is water soluble. This result shows the influence of the strong phosphine ligand that

produces a slow transfer but doesn't deactivate contrary to the remaining S- and N- bonded ligands.

Table 8: Deactivation of the ruthenium tricarbonyl compounds in the medium used for solubilization.

Compound	Structure	Medium	Equiv. CO donated at t=0	Equiv. CO donated after 1h deactivation
1	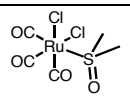	DMSO MeOH	1.1 1.0	0.7 0.8
5	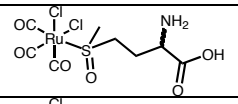	PBS7.4	0.9	0.7
6	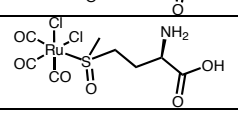	PBS7.4 H_2O	1.1 1.1	0.6 0.7
7	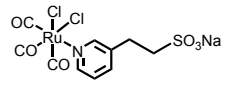	PBS7.4 H_2O	0.9 1.1	0.7 0.2
8	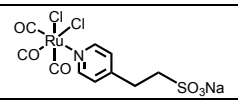	PBS7.4 H_2O	0.7 0.9	0.6 0.2
9	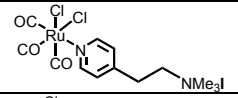	DMSO	0.4	0.3
10	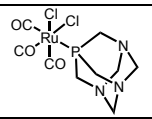	DMSO	0.3	0.2
11	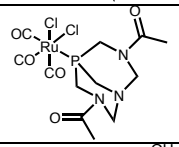	PBS7.4 H_2O	0.3 0.4	0.2 0.2
12	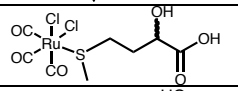	MeOH	0.7	0.8
13	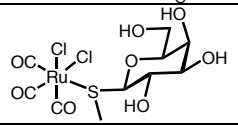	PBS7.4 H_2O	0.8 0.9	0.8 0.3
14	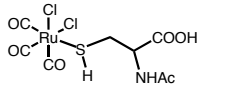	PBS7.4 H_2O	0.7 0.8	0.5 0.6

The water-soluble methionine-oxide complexes **5** and **6** donate roughly 1 equiv. CO to deoxy-Mb at ageing time zero in PBS7.4 but solutions aged for 1h lose the donation capacity by ca. 60% and 40% respectively.

The thioether counterpart **13** shows a different deactivation profile in H_2O and PBS7.4. In water, a 67% decrease in CO donation capacity is observed, from 0.9 equiv. CO in fresh solutions to 0.3 equiv. after 1h in H_2O. In PBS no deactivation is observed and the donation capacity is retained for 1h.

Compound **7** was also tested in PBS7.4 and water and was able to donate 1 CO to deoxy-Mb very rapidly in both solvents (0.9 equiv. donated in PBS and 1.1 equiv. donated in water). Similarly to **13** and in contrast to the case of CORM-3, the compound is more stable in PBS than in water. In PBS the amount of CO donated only decreases from 0.9 equiv. CO to 0.8 equiv. after 10 min and 0.7 equiv. after 2h. In water a very rapid decay is observed with the initial value of 1.1 equiv. CO decreasing to 0.3 equiv. after 20 min, that is a 70% activity loss. **8** also showed a good stability in PBS, decreasing from 0.7 equiv. CO to 0.6 equiv. after 10 min and remaining stable after 1h.

Compound **14** has the same behavior in PBS and H_2O and similar deactivation profiles are observed. In PBS a 29% decrease is observed after ageing 1h while in water the decrease in the donation capacity was 25%.

4.2.3 Conclusions

The studies performed showed very important features regarding the behavior of the Ru^{II} tricarbonyl complexes $[Ru(CO)_3Cl_2L]$ in aqueous systems. It was observed that this class of compounds is able to transfer up to 1 CO to Mb, depending on the nature of the sixth ligand. Similarly to CORM-2 and CORM-3, all the compounds are able to carbonylate deoxy-Mb within 5 to 15 min and if the compounds are left in solution for a large period of time, their donation capacity decreases.

It is observed that stronger σ donating ligands decrease the capacity of CO donation to Mb. We attribute these differences to the substitutionally stability provided by the strong ligands which are harder to displace and, therefore, protect the coordination sphere.

Interestingly, the amount of CO transferred to Mb is roughly the same as the amount of gas detected in the GC experiments and liberated as CO_2 into the headspace of aqueous solutions after 24h (see tables 5 and 8). In the presence of a heme scavenger, the carbonyl group is mobilized and transferred to the heme center as CO. In aqueous solutions, without protein present, the carbonyl is also liberated in the same extent, but at a much slower rate and as CO_2 instead of CO. The HPLC trace didn't show any correlation between the decomposition profile and the rate of gas release. Two major peaks are observed at 2-3 min and 9-11 min and each of them contains several species each one with a specific CO release capacity.

Importantly, however, the profile of Mb carbonylation by the $[Ru(CO)_3Cl_2L]$ complexes can be tuned by the nature of L. Although the differences are not overwhelming they are clear in showing that the stronger Ru-L bond slow down CO transfer to deoxy-Mb. We believe that this finding is crucial to start understanding the mechanism of CO donation from a CO-RM to a heme protein.

4.3 Anti-oxidant activity of Ru^{II} carbonyl complexes

The relevant role of ROS in several pathological processes was highlighted in Chapter III, section 2.1 and includes tissue injury,[107] inflammatory disorders,[108] cardiovascular diseases,[109] pulmonary disease[110] and neurodegenerative diseases.[111] Catalytic decomposition of radical species has often been suggested as a therapeutic approach to several inflammatory diseases.[112, 113] The use of the natural catalytic antioxidant proteins like SOD and catalase as therapeutic agents showed severe limitations such as a short circulating half-life, low cell permeability and antigenicity, all due to their large sizes. A new series of low

molecular weight metal based catalytic antioxidants featuring macrocycles, salens and metalloporphyrin ligands were developed and showed excellent results in several *in vitro*, *ex vivo* and *in vivo* models (see Scheme 6). The successful results were obtained in a large number of rat and mice models of diseases such as lung, renal and liver diseases or cardiovascular and central nervous systems disorders (for a complete review see reference [114]). Successful results were also obtained with higher animals like preterm baboons where catalytic antioxidants were able to suppress lung inflammation and improve lung function in a hyperoxic model of bronchopulmunary dysplasia.[115] M40403[116] improves the analgesic profile of morphine and passed phase II clinical trials for post-surgical pain as an additive to morphine. EUK134 was developed by Eukarion and later licensed by Modex to treat induced skin damage while AEOL10150 is currently under clinical trials to be used as a countermeasure for radiation exposure to the gastrointestinal tract (http://www.aeoluspharma.com/index.html).[113]

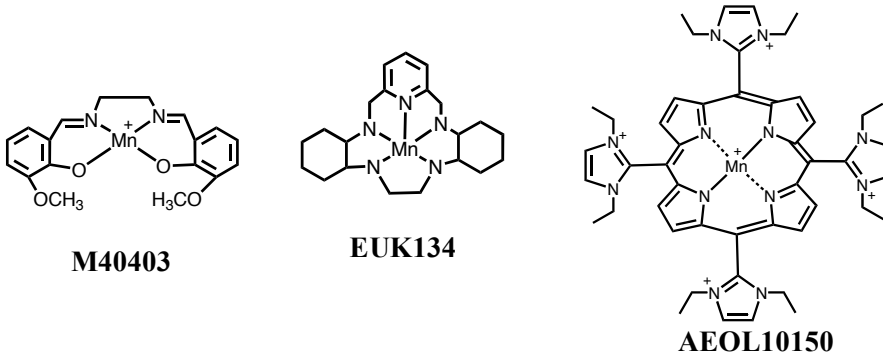

Scheme 6: Catalytic antioxidants macrocycles (M40403), salens (EUK134) and metalloporphyrins (AEOL10150).

One of the most striking observations one makes when looking at the long list of diseases that can be treated with these catalytic antioxidants,[114] is that it is essentially superimposable on the list of indications for the therapeutic use of CO.[117]

The large number of positive biological results obtained with CORM-3 and CORM-2 has always been assumed to be the result of CO release. However, as

Table 9: Equivalents of CO_2 released from CORM-3 to headspace after 1h, 3h, 5h and 24h with 100 molar equivalents of H_2O_2 and TBHP under N_2, at RT.

	1h	3h	5h	24h
H_2O_2	1.0	1.2	1.3	1.5
TBHP	2.1	2.4	3.0	3.7

we have extensively shown above, none of them releases CO spontaneously to the headspace of their solutions in biologically compatible media or conditions. On the contrary, the formation of CO_2 in these solutions implies the "neutralization" of the labile CO in these complexes, leaving a dicarbonyl complex devoid of CO releasing ability (iCORM). Furthermore, reaction of these complexes with H_2O_2 or TBHP (in the standard conditions shown in Experimental Section Chapter II) *do not release CO*. Instead, CO_2 is produced as can be seen in the example of Table 9 obtained for CORM-3. These results show that TBHP completely oxidizes the 3 carbonyls to CO_2 and if the reaction is not stopped it proceeds with the partial oxidation of the aminoacid which is the only other source of carbon in the reaction mixture. With H_2O_2 a smaller amount of CO_2 is liberated, however, a very important observation was made: like some iron compounds, CORM-3 produced high amounts of O_2 from H_2O_2. The O_2 quantification was not performed but the amount of O_2 produced was higher when compared to all other iron compounds tested. Like iron[118, 119] and manganese[120] compounds, catalase-like activity of Ru(II) compounds is not a new subject[121] but the issues that this behavior brought up are relevant. Indeed, these observations raise the hypothesis that both CORM-2 and CORM-3 (and other Ru derivatives) could be exerting their therapeutic action as a result of their antioxidant and ROS scavenging activity.

To look deeper into this behavior a series of experiments were conducted, evaluating the ability of the ruthenium complexes to decompose H_2O_2. An enzymatic assay with horseradish peroxidase (HRP) was performed in order to check the anti-oxidant properties of CO-RMs. These experiments allowed the quantification of H_2O_2 breakdown by CO-RMs measured through the decrease in HRP activity. For details see Experimental Section.

The results obtained are graphically depicted in Figures 18-23 and show that all the compounds are able to decompose H_2O_2 at different rates. However, there are differences which have important consequences in terms of the interpretation of the biological results obtained with these compounds.

Since it is devoid of CO ligands and bears both chloride and DMSO which are unavoidable in tests with CORM-2, the complex $RuCl_2(DMSO)_4$ has been used as a negative control for CO activity in many biological experiments. Figure 18 shows that $RuCl_2(DMSO)_4$ has the highest rate of H_2O_2 decomposition. In 1:1 and 1:10 ratios when the compound is present in 198 μM and 19.8 μM concentrations in a 198 μM H_2O_2 solution, all hydrogen peroxide was decomposed within 15 min; at the 1:50 ratio total H_2O_2 decomposition took 30 min and with 1:100 ratio the H_2O_2 decreased to 87%, 53% and 15% after 15 min, 30 min and 1h respectively. A linear correlation was observed between the compound:H_2O_2 ratio and the rate of H_2O_2 decomposition.

Replacement of one DMSO by one CO ligand, as in $RuCl_2(CO)(DMSO)_3$ (Figure 19), markedly slows the activity of H_2O_2 decomposition. In equimolar and 1:10 complex:H_2O_2 ratios the decomposition of H_2O_2 after 15min decreases respectively to 57% and 64% from the almost quantitative values recorded for $RuCl_2(DMSO)_4$ under the same conditions. An initial induction period without decomposition of H_2O_2 is apparent at the 1:50 and 1:100 ratio. Although different rates are observed roughly the same amount of decomposition is obtained after 60 min for all tested complex:H_2O_2 ratios.

The next compound in the series, $RuCl_2(CO)_2(DMSO)_2$ (Fig. 20), which has one more CO and one less DMSO in the coordination sphere, does not change the reactivity in any marked way and the total H_2O_2 decomposition is essentially the same as that of the previous compound although a little slower at 15 min time point. The main difference is that the 1:1 ratio has a much slower evolution than the ratios where excess H_2O_2 is present.

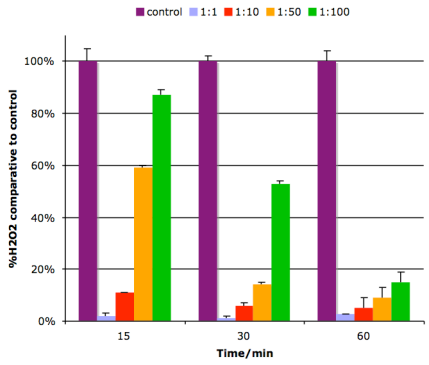

Figure 18: H_2O_2 concentration decrease expressed in percentage of initial concentration, as a function of time for 1:1, 1:10, 1:50 and 1:100 $RuCl_2(DMSO)_4$:H_2O_2 ratios, calculated against a $[H_2O_2]$ = 198 µM control. Data collected after 15min, 30min and 1h incubation of **$RuCl_2(DMSO)_4$** with H_2O_2.

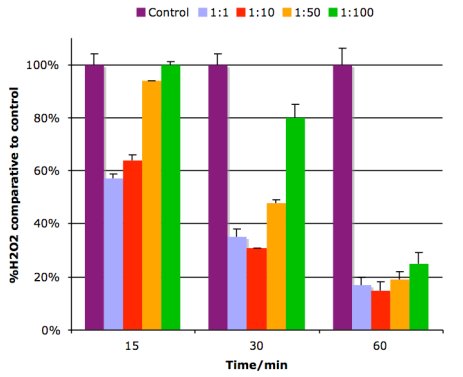

Figure 19: H_2O_2 concentration decrease expressed in percentage of initial concentration, as a function of time for 1:1, 1:10, 1:50 and 1:100 $RuCl_2(CO)(DMSO)_3$:H_2O_2 ratios, calculated against a $[H_2O_2]$ = 198 µM control. Data collected after 15min, 30min and 1h incubation of $RuCl_2(CO)(DMSO)_3$ (**3**) with H_2O_2.

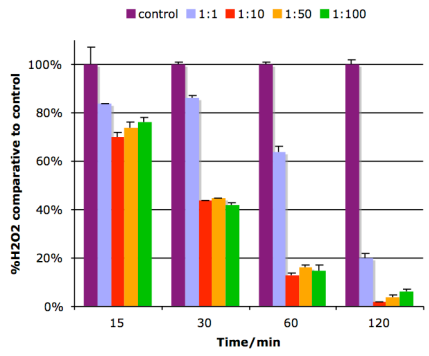

Figure 20: H_2O_2 concentration decrease expressed in percentage of initial concentration, as a function of time for 1:1, 1:10, 1:50 and 1:100 $RuCl_2(CO)_2(DMSO)_2$:H_2O_2 ratios, calculated against a $[H_2O_2]$ = 234 µM control. Data collected after 15min, 30min, 1h and 2h incubation of $RuCl_2(CO)_2(DMSO)_2$ (**2**) with H_2O_2.

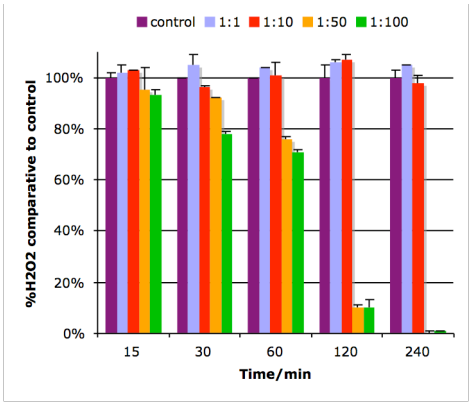

Figure 21: H_2O_2 concentration decrease expressed in percentage of initial concentration, as a function of time for 1:1, 1:10, 1:50 and 1:100 $RuCl_2(CO)_3(DMSO)$:H_2O_2 ratios, calculated against a $[H_2O_2]$ = 234 µM control. Data collected after 15min, 30min, 1h, 2h and 4h incubation of $RuCl_2(CO)_3(DMSO)$ (**1**) with H_2O_2.

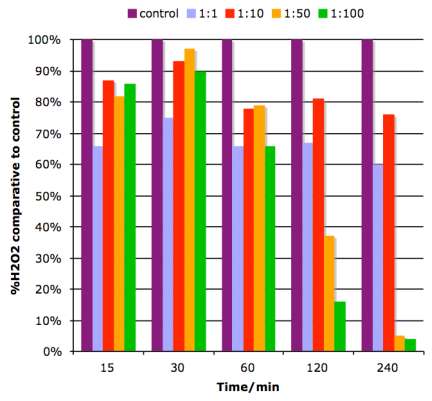

Figure 22: H_2O_2 concentration decrease expressed in percentage of initial concentration, as a function of time for 1:1, 1:10, 1:50 and 1:100 CORM-2:H_2O_2 ratios, calculated against a [H_2O_2] = 198 µM control. Data collected after 15min, 30min, 1h, 2h and 4h incubation of **CORM-2** with H_2O_2.

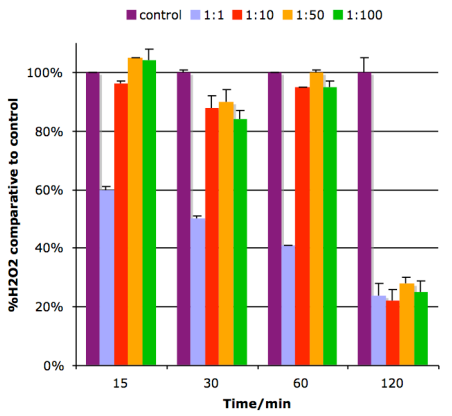

Figure 23: H_2O_2 concentration decrease expressed in percentage of initial concentration, as a function of time for 1:1, 1:10, 1:50 and 1:100 CORM-3:H_2O_2 ratios, calculated against a [H_2O_2] = 220 µM control. Data collected after 15min, 30min, 1h and 2h incubation of **CORM-3** with H_2O_2.

With the tricarbonyl complex $RuCl_2(CO)_3(DMSO)$ (Fig. 21) only the highest excesses of H_2O_2 1:100 and 1:50 lead to H_2O_2 decomposition. No H_2O_2 decomposition is observed with a 1:1 or a 1:10 complex:H_2O_2 ratios, not even after 4h incubation. With 1:50 and 1:100 ratios a longer induction period is observed since after 1h there's still 76% and 71%, respectively, of the initial H_2O_2 amount. After 2h, 90% of H_2O_2 decomposition is observed and the reaction is completed after 4h, showing clearly a slower kinetics than the previous compounds. It is now very clear that the increase in the number of CO ligands significantly stabilizes the Ru(II) complex against H_2O_2.

CORM-2 (Fig. 22) showed a similar profile to $RuCl_2(CO)_3(DMSO)$ which is not surprising in view of the relationship of both compounds in DMSO solvent needed to solubilize CORM-2. A long induction period was observed with stable levels of H_2O_2 between 65% and 80% up to 1h with all the concentration ratios tested. The total decomposition of H_2O_2 is only observed with the more diluted samples 1:50 and 1:100 after 4h. The more diluted sample 1:100 shows the fastest

reaction where only 16% H_2O_2 is left after 2h while with 1:50 ratio 37% H_2O_2 was obtained after 2h. In equimolar conditions and 1:10 dilution more than 60% H_2O_2 is still present after 4h incubation with compound.

CORM-3 (Fig. 23) is different from all other compounds because it showed a time-dependent decomposition profile when incubated with H_2O_2 in equimolar conditions but virtually no reactivity to large excesses of H_2O_2 in incubations up to 1h. After 2h though, all the concentration ratios tested induced a H_2O_2 decomposition of about 80% of the initial concentration.

In order to compare the different reaction profiles more clearly, Figure 24 represents the consumption of H_2O_2 as a function of time at the ratio complex:H_2O_2 = 1:50 for the several complexes tested. It is clear that the derivatives of the "$Ru(CO)_3$" fragment all have long induction periods before they actually start to react with and decompose H_2O_2. A CO saturated solution was also tested at 1 mM concentration and no effect on HRP or H_2O_2 was observed showing that CO doesn't react with H_2O_2 under these conditions. DMSO was also tested in the same concentration as it is present as the solvent of some of the complexes and it also didn't have any effect on H_2O_2.

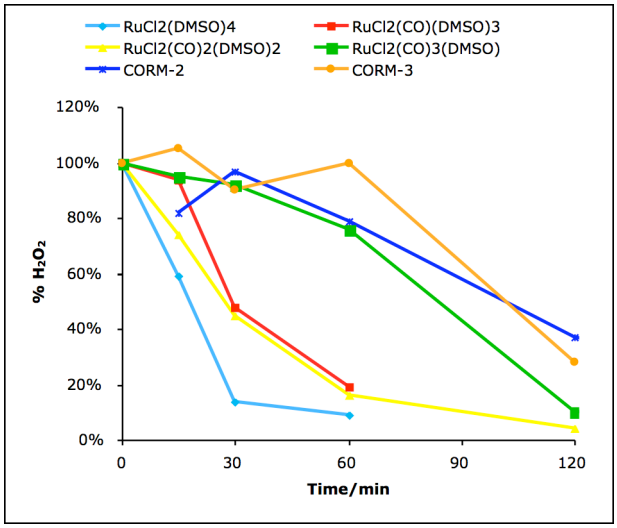

Figure 24: Comparative H_2O_2 concentration decrease expressed in percentage of initial concentration, as a function of for 1:50 dilutions for compounds $RuCl_2(DMSO)_4$, $RuCl_2(CO)(DMSO)_3$, $RuCl_2(CO)_2(DMSO)_2$, $RuCl_2(CO)_3(DMSO)$, CORM-2 and CORM-3.

The data collected is too few to accurately calculate reaction rates and substantiate mechanistic proposals. Nevertheless, some information can be extracted out from the results obtained under fixed conditions.

Quantitative comparison with other catalysts is also difficult since the experimental conditions (pH, buffers, concentrations) are not the same in all the experiments and the observed rate laws are not identical.

In Table 10 are presented data collected by Waldmeier and Sigel[122] that compared the initial reaction rate of several catalysts under standard conditions. These data are the result of direct experimental calculation or calculations from the determined rate laws.

Table 10: Comparison of the initial rates v_0 of hydrogen peroxide decomposition for several catalysts in standard conditions ($[H_2O_2]=10^{-2}$M; [catalyst]=10^{-4} M; pH8; aqueous solution; room temperature).

Catalyst	$v_0(M^{-1}s^{-1})$	Reference
$Cu(bipy)^{2+}$	6.8×10^{-4}	[123]
$TETAFe(OH)_2^{+}$	3.9×10^{-4}	[124]
$Mn(bipy)^{2+}$	3.2×10^{-4}	[125]
L_2(di-μ-oxo)Mn(III/IV)	2.4×10^{-4}	[126]
$McRu(DMSO)_2(H_2O)$	6.0×10^{-5}	[121]
Mn^{III}(saltm)Br	3.4×10^{-5}	[127]
Mn^{2+}	2.0×10^{-4}	[128]
Fe(III)PTS	2×10^{-5}	[122]

TETA = triethylenetetramine
L=[N,N'-bismethyl,bis(2-pyridylmethyl)-1,2-ethanediamine]
Mc is a macrocycle with pyrazole and tertiary amine atoms as donor sites[121,129]
saltm = [N,N' bis (salicylidene) propylenediamine]
PTS = 4,4',4'',4''' - tetrasulfophtalocyanine

Although our experimental conditions are far from the standardized conditions presented in Table 10, the cleanest and fastest decomposition profiles observed (Fig 18 at 1:100 ratio, Fig. 19 and Fig. 20 at both 1:50 and 1:100 ratios) provide information that allows the calculation of the magnitude of the initial rate of H_2O_2 decomposition. These values are given in Table 11.

Table 11: Comparison between the initial rates v_0 of hydrogen peroxide decomposition for $RuCl_2(DMSO)_4$, $RuCl_2(CO)(DMSO)_3$ and $RuCl_2(CO)_2(DMSO)_2$.

Compound	Compound Concentration	$v_0(M^{-1}s^{-1})$
$RuCl_2(DMSO)_4$	1.98 µM	4.9×10^{-8}
	3.96 µM	9.5×10^{-8}
$RuCl_2(CO)(DMSO)_3$	1.98 µM	5.6×10^{-8}
	3.96 µM	4.8×10^{-8}
$RuCl_2(CO)_2(DMSO)_2$	2.34 µM	5.6×10^{-8}
	4.68 µM	5.4×10^{-8}

As could be observed from Figure 24 and corroborated from Table 11 $RuCl_2(DMSO)_4$ is the fastest compound decomposing H_2O_2. However, its ability to decompose hydrogen peroxide is at least three orders of magnitude slower than other catalytic peroxide scavengers, or catalytic anti-oxidants given in table 10.

Ruthenium complexes are known to be good oxidation catalysts. The Ru^{IV} oxides are able to oxidize H_2O_2 to O_2 and these structures resemble the Fe^{IV}=O porphyrin group invoked as the active site in heme catalases.[130, 131] This disproportionation process may occur through two different pathways: the complexes may have a vacant or labile coordination site or it can occur through an outer-sphere reaction.

Given the lability of the ligands for CORM-3 and $RuCl_2(CO)_3(DMSO)$, in the present case an inner-sphere oxidation process is most probably taking place. Of course, the rate of hydrolysis is different depending on the ligands, leading to different oxide-formation time. The identity of the catalyst formed is unknown and probably different catalysts are formed with different complexes.

It has already been shown that other Ru(II) complexes like [*cis*-$Ru(dmp)_2(H_2O)_2]^{2+}$(where dmp is 2,9-dimethyl-1,10-phenantroline)[132] and $(Mc)Ru(DMSO)_2(H_2O)_2]^{2+}$ (where Mc is a bidentate coordinating macrocycle) [121] are oxidized by hydrogen peroxide to give [*cis*-$Ru^{IV}O(dmp)_2(H_2O)_2]^{2+}$ and $(Mc)Ru^{IV}O(DMSO)_2(H_2O)]^{2+}$. $(Mc)Ru(DMSO)_2(H_2O)_2]^{2+}$ (which has the same chloride and DMSO ligands like $Ru(CO)_2(DMSO)_2Cl_2$) is obtained from hydrolysis of $(Mc)Ru(DMSO)_2Cl_2]^{2+}$ in water. Interestingly, the efficiency of

$Ru(CO)_2(DMSO)_2Cl_2$ in degrading H_2O_2 is several orders of magnitude slower, most probably due to the different stability provided by the macrocyclic ligand in comparison to the oxidazible carbonyls (see table 9).

Regardless of the reaction mechanisms involved, which can vary from compound to compound, a number of conclusions may be safely withdrawn from the above data.

1. In all the above compounds Ruthenium is responsible for the decomposition of H_2O_2;
2. Carbonyl ligands seem to slow down this process, that is, seem to stabilize the Ru(II) complexes;
3. The observed overall reaction rate of H_2O_2 decomposition by the compounds tested is not comparable to that of actual biologically active anti-oxidant catalysts (peroxide scavengers) let alone catalase;
4. These results strongly disfavor the hypothesis that the biological effects of CORM-2 and CORM-3 result from their anti-oxidant (peroxide scavenging) properties due to the prolonged induction periods needed to trigger this kind of reactivity and to its relatively slow rate.

5. Final Remarks and Conclusions

CORM-2 is undoubtedly the CO releasing compound to which scientists working on the CO field have devoted more attention, since it is a commercially available CO source. However, the activity observed with CORM-2 arises from one of the several species obtained when the compound is dissolved in DMSO. The identification of this species was performed and several analogues of this compound were prepared in order to get more drug-like water-soluble molecules. A simple, efficient and clean methodology was developed to prepare these compounds from commercially available CORM-2 and the activity in several *in*

vitro and *in vivo* models is currently under evaluation. Some insights over the specific reactivity of these molecules revealed the capacity to decompose H_2O_2 into O_2. However, the low rates of these reactions seems to rule out the possibility that the anti-inflammatory activity of $Ru(CO)_3Cl_2L$ complexes, including CORM-2 and CORM-3, originates from their anti-oxidant activity.

6. References

1. Clarke, M.J., *Coord. Chem. Rev.* **2002**, 232, 69.
2. Sava, G., Pacor, S., Coluccia, M., Mariggio, M., Cocchietto, M., Alessio, E., Mestroni, G., *Drug Investigation* **1994**, 8, 150.
3. Sava, G., Pacor, S., Mestroni, G., Alessio, E., *Clin. Exp. Metastasis* **1992**, 10, 273.
4. Sava, G., Pacor, S., Bergamo, A., Cocchietto, M., Mestroni, G., Alessio, E., *Chem.-Biol. Interact.* **1995**, 95, 109.
5. Capozzi, I., Clerici, K., Cocchietto, M., Salerno, G., Bergamo, A., Sava, G., *Chem.-Biol. Interact.* **1998**, 113, 51.
6. Sava, G., Pacor, S., Mestroni, G., Alessio, E., *Anti-Cancer Drugs* **1992**, 3, 25.
7. Bergamo, A., Cocchietto, M., Capozzi, I., Mestroni, G., Alessio, E., Sava, G., *Anti-Cancer Drugs* **1996**, 7, 697.
8. Sava, G., Gagliardi, R., Cocchietto, M., Clerici, K., Capozzi, I., Marrella, M., Alessio, E., Mestroni, G., Milanino, R., *Pathol. Oncol. Res.* **1998**, 4, 30.
9. Zorzet, S., Sorc, A., Casarsa, C., Cocchietto, M., Sava, G., *Metal-based drugs* **2001**, 8, 1.
10. Geremia, S., Alessio, E., Todone, F., *Inorg. Chim. Acta* **1996**, 253, 87.
11. Bouma, M., Nuijen, B., Challa, E.E., Sava, G., Flaibani, A., Bult, A., Beijnen, J.H., *J. Oncol. Pharm. Pract.* **2004**, 10, 7.
12. Keppler, B.K., Rupp, W., Juhl, U.M., Endres, H., Niebl, R., Balzer, W., *Inorg. Chem.* **1987**, 26, 4366.
13. Pieper, T., Keppler, B.K., *Analusis Magazine* **1998**, 26, M84.
14. Kuehn, C.G., Taube, H., *J. Am. Chem. Soc.* **1976**, 98, 689.
15. Clarke, M.J., Dowling, M.G., *Inorg. Chem.* **1981**, 20, 3506.
16. Abelleira, A., Galang, R.D., Clarke, M.J., *Inorg. Chem.* **1990**, 29, 633.
17. Yan, Y.K., Melchart, M., Habtemariam, A., Sadler, P.J., *Chem. Commun.* **2005**, 4764.
18. Peacock, A.F.A., Sadler, P.J., *Chem.- Asian J.* **2008**, 3, 1890.
19. Allardyce, C.S., Dyson, P.J., Ellis, D.J., Salter, P.A., Scopelliti, R., *J. Organomet. Chem.* **2003**, 668, 35.
20. Belshaw, P.J., Schreiber, S.L., *J. Am. Chem. Soc.* **1997**, 119, 1805.
21. Charuk, J.H.M., Pirraglia, C.A., Reithmeier, R.A.F., *Anal. Biochem.* **1990**, 188, 123.
22. Reed, K.C., Bygrave, F.L., *Biochem. J.* **1974**, 140, 143.
23. Smaili, S.S., Russell, J.T., *Cell Calcium* **1999**, 26, 121.
24. Clarke, M.J., Bailey, V.M., Doan, P.E., Hiller, C.D., LaChanceGalang, K.J., Daghlian, H., Mandal, S., Bastos, C.M., *Inorg. Chem.* **1996**, 35, 4896.

25. Ocain, T.D., Bastos, C.M., Gordon, K.A., Granstein, R.D., Jenson, J.C., Jones, B., McAuliffe, D.J., Newcomb, J.R., *Transplant. Proc.* **1996**, 28, 3032.
26. Bastos, C.M., Gordon, K.A., Ocain, T.D., *Bioorg. Med. Chem. Lett.* **1998**, 8, 147.
27. Johnson, T.R., Mann, B.E., Clark, J.E., Foresti, R., Green, C.J., Motterlini, R., *Angew. Chem. Int. Ed. Engl.* **2003**, 42, 3722.
28. Motterlini, R., Mann, B.E., Foresti, R., *Expert Opin. Investig. Drugs* **2005**, 14, 1305.
29. Foresti, R., Hammad, J., Clark, J.E., Johnson, T.R., Mann, B.E., Friebe, A., Green, C.J., Motterlini, R., *Br. J. Pharmacol.* **2004**, 142, 453.
30. Clark, J.E., Naughton, P., Shurey, S., Green, C.J., Johnson, T.R., Mann, B.E., Foresti, R., Motterlini, R., *Circ. Res.* **2003**, 93, e2.
31. Varadi, J., Lekli, I., Juhasz, B., Bacskay, I., Szabo, G., Gesztelyi, R., Szendrei, L., Varga, E., Bak, I., Foresti, R., Motterlini, R., Tosaki, A., *Life Sci* **2007**, 80, 1619.
32. Guo, Y., Stein, A.B., Wu, W.J., Tan, W., Zhu, X., Li, Q.H., Dawn, B., Motterlini, R., Bolli, R., *Am. J. Physiol. Heart Circ. Physiol.* **2004**, 286, H1649.
33. Vera, T., Henegar, J.R., Drummond, H.A., Rimoldi, J.M., Stec, D.E., *J. Am. Soc. Nephrol.* **2005**, 16, 950.
34. Tayem, Y., Johnson, T.R., Mann, B.E., Green, C.J., Motterlini, R., *Am. J. Physiol. Renal Physiol.* **2006**, 290, F789.
35. Sandouka, A., Fuller, B.J., Mann, B.E., Green, C.J., Foresti, R., Motterlini, R., *Kidney international* **2006**, 69, 239.
36. Sawle, P., Foresti, R., Mann, B.E., Johnson, T.R., Green, C.J., Motterlini, R., *Br. J. Pharmacol.* **2005**, 145, 800.
37. Bani-Hani, M.G., Greenstein, D., Mann, B.E., Green, C.J., Motterlini, R., *J. Pharmacol. Exp. Ther.* **2006**, 318, 1315.
38. Bani-Hani, M.G., Greenstein, D., Mann, B.E., Green, C.J., Motterlini, R., *Pharmacol. Rep.* **2006**, 58 Suppl, 132.
39. Urquhart, P., Rosignoli, G., Cooper, D., Motterlini, R., Perretti, M., *J. Pharmacol. Exp. Ther.* **2007**, 321, 656.
40. Vannacci, A., Giannini, L., Fabrizi, F., Uliva, C., Mastroianni, R., Masini, E., Motterlini, R., Mannaioni, P.F., *Inflamm. Res.* **2007**, 56 Suppl 1, S13.
41. Bagul, A., Hosgood, S.A., Kaushik, M., Nicholson, M.L., *Transplantation* **2008**, 85, 576.
42. Davidge, K.S., Sanguinetti, G., Yee, C.H., Cox, A.G., McLeod, C.W., Monk, C.E., Mann, B.E., Motterlini, R., Poole, R.K., *J. Biol. Chem.* **2009**, 284, 4516.
43. Desmard, M., Davidge, K.S., Bouvet, O., Morin, D., Roux, D., Foresti, R., Ricard, J.D., Denamur, E., Poole, R.K., Montravers, P., Motterlini, R., Boczkowski, J., *FASEB J.* **2008**.
44. Boissiere, J., Lemaire, M.C., Antier, D., Courteix, D., Bonnet, P., *Med. Sci. Sports Exerc.* **2006**, 38, 652.
45. Stanford, S.J., Walters, M.J., Mitchell, J.A., *Eur. J. Pharmacol.* **2004**, 486, 349.
46. Motterlini, R., Clark, J.E., Foresti, R., Sarathchandra, P., Mann, B.E., Green, C.J., *Circ. Res.* **2002**, 90, E17.
47. Botros, F.T., Navar, L.G., *Am. J. Physiol. Heart Circ. Physiol.* **2006**, 291, H2772.
48. Rattan, S., Al Haj, R., De Godoy, M.A., *Am J Physiol Gastrointest Liver Physiol* **2004**, 287, G605.
49. Matsuda, N.M., Miller, S.M., Sha, L., Farrugia, G., Szurszewski, J.H., *Neurogastroenterol. Motil.* **2004**, 16, 605.

50. Allanson, M., Reeve, V.E., *J. Invest. Dermatol.* **2005**, 124, 644.
51. Uc, A., Husted, R.F., Giriyappa, R.L., Britigan, B.E., Stokes, J.B., *Am J Physiol Gastrointest Liver Physiol* **2005**, 289, G202.
52. Orozco-Ibarra, M., Estrada-Sanchez, A.M., Massieu, L., Pedraza-Chaverri, J., *Int. J. Biochem. Cell Biol.* **2009**, 41, 1304.
53. Zhou, J.L., Li, G., Hai, Y., Guan, L., Huang, X.L., Sun, P., *Chin. J. Traumatol.* **2009**, 12, 71.
54. Sun, B.W., Sun, Y., Sun, Z.W., Chen, X., *World J. Gastroenterol.* **2008**, 14, 547.
55. Sun, B., Sun, H., Liu, C., Shen, J., Chen, Z., Chen, X., *J. Surg. Res.* **2007**, 139, 128.
56. Nobre, L.S., Seixas, J.D., Romao, C.C., Saraiva, L.M., *Antimicrob. Agents Chemother.* **2007**, 51, 4303.
57. Davidge, K.S., Sanguinetti, G., Yee, C.H., Cox, A.G., McLeod, C.W., Monk, C.E., Mann, B.E., Motterlini, R., Poole, R.K., *J. Biol. Chem.* **2008**.
58. Alessio, E., Milani, B., Bolle, M., Mestroni, G., Faleschini, P., Todone, F., Geremia, S., Calligaris, M., *Inorg. Chem.* **1995**, 34, 4722.
59. Moreno, M.A., Haukka, M., Kallinen, M., Pakkanen, T.A., *Appl. Organomet. Chem.* **2006**, 20, 51.
60. Collman, J.P., Roper, W.R., *J. Am. Chem. Soc.* **1965**, 87, 4008.
61. Johnson, B.F.G., Johnston, R.D., Josty, P.L., Lewis, J., Williams, I.G., *Nature* **1967**, 213, 901.
62. Bruce, M.I., Stone, F.G.A., *J. Chem. Soc. A* **1967**, 1238.
63. Braca, G., Sbrana, G., Pino, P., Benedetti, E., *Chimica & L Industria* **1967**, 49, 1381.
64. Cotton, J.D., Bruce, M.I., Stone, F.G.A., *J. Chem. Soc. A* **1968**, 2162.
65. Johnson, B.F.G., Johnston, R.D., Lewis, J., *J. Chem. Soc. A* **1969**, 792.
66. Trovati, A., Araneo, A., Uguagliati, P., Zingales, F., *Inorg. Chem.* **1970**, 9, 671.
67. Araneo, A., Trovati, A., *Inorg. Chim. Acta* **1969**, 3, 471.
68. Benedetti, E., Braca, G., Sbrana, G., Salvetti, F., Grassi, B., *J. Organomet. Chem.* **1972**, 37, 361.
69. Hieber, W., Heusinger, H., *J. Inorg. Nucl. Chem.* **1957**, 4, 179.
70. Kingston, J.V., Jamieson, J.W., Wilkinso.G, *J. Inorg. Nucl. Chem.* **1967**, 29, 133.
71. Irving, R.J., *J. Chem. Soc.* **1956**, 2879.
72. Alessio, E., Bolle, M., Milani, B., Mestroni, G., Faleschini, P., Geremia, S., Calligaris, M., *Inorg. Chem.* **1995**, 34, 4716.
73. Calligaris, M., Panina, N.S., *J. Mol. Struct.* **2003**, 646, 61.
74. Alessio, E., Iengo, E., Geremia, S., Calligaris, M., *Inorg. Chim. Acta* **2003**, 344, 183.
75. Evans, I.P., Spencer, A., Wilkinso.G, *J. Chem. Soc.-Dalton Trans.* **1973**, 204.
76. Alessio, E., Mestroni, G., Nardin, G., Attia, W.M., Calligaris, M., Sava, G., Zorzet, S., *Inorg. Chem.* **1988**, 27, 4099.
77. Cenini, S., Pizzotti, M., Porta, F., Lamonica, G., *J. Organomet. Chem.* **1977**, 125, 95.
78. Kingston, J.V., Mahmoud, F.T., Scollary, G.R., *J. Inorg. Nucl. Chem.* **1972**, 34, 3197.
79. Haukka, M., Hirva, P., Luukkanen, S., Kallinen, M., Ahlgren, M., Pakkanen, T.A., *Inorg. Chem.* **1999**, 38, 3182.
80. Calligaris, M., Carugo, O., *Coord. Chem. Rev.* **1996**, 153, 83.
81. Laine, R.M., Rinker, R.G., Ford, P.C., *J. Am. Chem. Soc.* **1977**, 99, 252.
82. Darensbourg, D.J., Rokicki, A., *Organometallics* **1982**, 1, 1685.

83. Pearson, R.G., Mauermann, H., *J. Am. Chem. Soc.* **1982**, 104, 500.
84. Yoshida, T., Okano, T., Ueda, Y., Otsuka, S., *J. Am. Chem. Soc.* **1981**, 103, 3411.
85. Baker, E.C., Hendriksen, D.E., Eisenberg, R., *J. Am. Chem. Soc.* **1980**, 102, 1020.
86. Sato, S., White, J.M., *J. Am. Chem. Soc.* **1980**, 102, 7206.
87. Ford, P.C., *Acc. Chem. Res.* **1981**, 14, 31.
88. Inkrott, K.E., Shore, S.G., *J. Am. Chem. Soc.* **1978**, 100, 3954.
89. Inkrott, K.E., Shore, S.G., *Inorg. Chem.* **1979**, 18, 2817.
90. Ford, P.C., Rinker, R.G., Ungermann, C., Laine, R.M., Landis, V., Moya, S.A., *J. Am. Chem. Soc.* **1978**, 100, 4595.
91. Laine, R.M., *J. Am. Chem. Soc.* **1978**, 100, 6451.
92. Nagel, C.C., Bricker, J.C., Alway, D.G., Shore, S.G., *J. Organomet. Chem.* **1981**, 219, C9.
93. Bricker, J.C., Nagel, C.C., Bhattacharyya, A.A., Shore, S.G., *J. Am. Chem. Soc.* **1985**, 107, 377.
94. Darensbourg, D.J., Froelich, J.A., *J. Am. Chem. Soc.* **1977**, 99, 5940.
95. Lane, K.R., Lee, R.E., Sallans, L., Squires, R.R., *J. Am. Chem. Soc.* **1984**, 106, 5767.
96. Lane, K.R., Sallans, L., Squires, R.R., *Inorg. Chem.* **1984**, 23, 1999.
97. Trautman, R.J., Gross, D.C., Ford, P.C., *J. Am. Chem. Soc.* **1985**, 107, 2355.
98. Ishida, H., Tanaka, K., Morimoto, M., Tanaka, T., *Organometallics* **1986**, 5, 724.
99. Haukka, M., Venalainen, T., Kallinen, M., Pakkanen, T.A., *J. Mol. Catal. A: Chem.* **1998**, 136, 127.
100. Luukkanen, S., Homanen, P., Haukka, M., Pakkanen, T.A., Deronzier, A., Chardon-Noblat, S., Zsoldos, D., Ziessel, R., *Appl. Catal., A* **1999**, 185, 157.
101. Aguirre, P., Lopez, R., Villagra, D., Azocar-Guzman, I., Pardey, A.J., Moya, S.A., *Appl. Organomet. Chem.* **2003**, 17, 36.
102. Frediani, P., Faggi, C., Salvini, A., Bianchi, M., Piacenti, F., *Inorg. Chim. Acta* **1998**, 272, 141.
103. Fachinetti, G., Funaioli, T., Lecci, L., Marchetti, F., *Inorg. Chem.* **1996**, 35, 7217.
104. Ford, P.C., Yarrow, P., Cohen, H., Musto, J., Rinker, R.G., *Abstr. Pap. Am. Chem. Soc.* **1980**, 180, 93.
105. Funaioli, T., Cavazza, C., Marchetti, F., Fachinetti, G., *Inorg. Chem.* **1999**, 38, 3361.
106. Johnson, T.R., Mann, B.E., Teasdale, I.P., Adams, H., Foresti, R., Green, C.J., Motterlini, R., *Dalton Trans.* **2007**, 1500.
107. Freeman, B.A., Crapo, J.D., *Lab. Invest.* **1982**, 47, 412.
108. McCord, J.M., Fridovich, I., *Ann. Intern. Med.* **1978**, 89, 122.
109. Maxwell, S.R., Lip, G.Y., *Br. J. Clin. Pharmacol.* **1997**, 44, 307.
110. Kinnula, V.L., Chang, L.Y., Ho, Y.S., Crapo, J.D., *Exp. Lung Res.* **1992**, 18, 655.
111. Halliwell, B., *J. Neurochem.* **1992**, 59, 1609.
112. Fisher, A.E.O., Maxwell, S.C., Naughton, D.P., *Inorg. Chem. Commun.* **2003**, 6, 1205.
113. Golden, T.R., Patel, M., *Antioxid. Redox Signal.* **2009**, 11, 555.
114. Day, B.J., *Drug Discov Today* **2004**, 9, 557.
115. Chang, L.Y., Subramaniam, M., Yoder, B.A., Day, B.J., Ellison, M.C., Sunday, M.E., Crapo, J.D., *Am. J. Respir. Crit. Care Med.* **2003**, 167, 57.
116. Di Napoli, M., Papa, F., *IDrugs* **2005**, 8, 67.

117. Ryter, S.W., Otterbein, L.E., *BioEssays* **2004**, 26, 270.
118. Autzen, S., Korth, H.G., de Groot, H., Sustmann, R., *Eur. J. Org. Chem.* **2001**, 3119.
119. Sustmann, R., Korth, H.G., Kobus, D., Baute, J., Seiffert, K.H., Verheggen, E., Bill, E., Kirsch, M., de Groot, H., *Inorg. Chem.* **2007**, 46, 11416.
120. Kurz, P., Berggren, G., Anderlund, M.F., Styring, S., *Dalton Trans.* **2007**, 4258.
121. Choua, S., Pacheco, P., Coquelet, C., Bienvenue, E., *J. Inorg. Biochem.* **1997**, 65, 79.
122. Waldmeier, P., Sigel, H., *Inorg. Chem.* **1972**, 11, 2174.
123. Sigel, H., Flierl, C., Griesser, R., *J. Am. Chem. Soc.* **1969**, 91, 1061.
124. Wang, J.H., *J. Am. Chem. Soc.* **1955**, 77, 4715.
125. Tiginyanu, Y.D., Sychev, A.Y., Berdnikov, V.M., *Russ. J. Phys. Chem.* **1971**, 45, 975.
126. Delroisse, M., Rabion, A., Chardac, F., Tetard, D., Verlhac, J.B., Fraisse, L., Seris, J.L., *J. Chem. Soc.-Chem. Commun.* **1995**, 949.
127. Salem, I.A., *Polyhedron* **1994**, 13, 1547.
128. Stadtman, E.R., Berlett, B.S., Chock, P.B., *Proc. Natl. Acad. Sci. U. S. A.* **1990**, 87, 384.
129. Bienvenue, E., Choua, S., Loborecio, M.A., Marzin, C., Pacheco, P., Seta, P., Tarrago, G., *J. Inorg. Biochem.* **1995**, 57, 157.
130. Gilbert, J., Roecker, L., Meyer, T.J., *Inorg. Chem.* **1987**, 26, 1126.
131. Gilbert, J.A., Gersten, S.W., Meyer, T.J., *J. Am. Chem. Soc.* **1982**, 104, 6872.
132. Goldstein, A.S., Beer, R.H., Drago, R.S., *J. Am. Chem. Soc.* **1994**, 116, 2424.

7. Acknowledgments

Ana Rita Marques is acknowledged for performing the Horseradish Peroxidase assays and helpful contribution for rationalizing the data obtained.

Ana Margarida Gonçalves is acknowledged for measurements of CO_2 release through GC.

Gonçalo Bernardes is acknowledged for the preparation of complexes $Ru(CO)_3Cl_2$(DAPTA) and $Ru(CO)_3Cl_2$(NAC).

Chapter VI: Interaction of Metal Carbonyl Complexes with serum proteins

1. Summary

The interaction between several types of MCCs and both Bovine Serum Albumin (BSA) and human *Apo*-Transferrin (h-Tf) was investigated with Circular Dichroism and UV/Vis absorbance spectrophotometry techniques.

Mo^0 complexes $[Et_4N][Mo(CO)_5Br]$ and $Na_3[Mo(CO)_3(cit)]$ showed a high degree of association with BSA, while the Mo^{II} and Ru^{II} complexes $CpMo(CO)_3CH_2CONH_2$ and $Ru(CO)_3Cl(glycinate)$ showed minor or no interaction with the carrier protein.

With h-Tf only $Ru(CO)_3Cl(glycinate)$ showed some binding activity after 24h incubation.

2. Introduction

The interaction of MCCs with myoglobin, a simple and yet very important hemeprotein, was studied in Chapter IV. In these studies it was shown that many MCCs are able to transfer CO to the heme of reduced deoxy-myoglobin, therefore carbonylating it. This kind of transfer of CO from the MCC or CO-RM to a hemeprotein, namely NADPH,[1] cytochrome c oxidase and mithocondrial complexes[2-4] has been considered as the decisive event in the mechanism of therapeutic CO delivery from CO-RMs to biological targets.

However, CO also activates/inhibits several signaling pathways that are not directly related to heme binding. CO appears to modulate mitogen activated protein kinases (MAPK)-related pathways through down-regulation of ERK1-2[5] and suppression of inflammatory cytokine production by CO appears to involve the JNK pathway.[6] These proteins do not have a metal center so the CO

signaling process is necessarily different. It had already been suggested that it may arise from different interactions like non-covalent bonding to sites within protein.[7]

In any case, the use of CO-RMs as CO delivering devices raises new questions in regard to how CO is carried and reaches the targets. Although CO-RMs are in fact pro-drugs which transport and liberate the active principle CO, they must interact with biological entities on their way to the targets just like any other drug. In this respect, interaction of drug molecules with serum proteins plays an important role in the distribution of the drug in the body and affects properties like toxicity and biological activity.

The results presented in Chapter IV regarding the release of CO from several MCCs to whole blood clearly suggest that plasma proteins have a decisive effect on the rate of release of CO from a CO-RM to the circulating blood.

Albumin is the most abundant protein in blood plasma (60% of the total plasma protein) and functions as a transporter both to endogenous and exogenous compounds. Binding to Human Serum Albumin (HSA) is one of the most determinant aspects of the pharmacokinetics of drugs.[8-11] Especially for highly albumin bound drugs (e.g. NSAIDs) the equilibrium between bound and free drug is many times determinant for changes in drug effects[12-14] since it reduces free drug in solution for penetration into tissue to reach the therapeutic target or to the liver and kidneys for elimination. In addition, binding affinities allow a better understanding of the pharmacological profile of the drug and may also help determining a better dosage regimen.[15, 16]

Another serum protein, human Transferrin (Tf), is mainly an iron transport protein but with a very important role in delivering drugs to the cells. Apart from the natural iron binding properties Tf also exhibited binding affinities for several metals with different biological effects. Tf has an important role in transport and delivery of $^{67}Ga^{3+}$[17-20] and $^{111}In^{3+}$[21, 22] for diagnostics, it binds vanadium[23] and other trivalent ions such as Al^{3+}[24, 25] and Bi^{3+}[26, 27] interfering with iron uptake, and delivers Ru^{3+}[28, 29] and Ti^{4+}[30] to cells through specific Tf receptors. Tf

receptors are a major target for site-specific metallodrug delivery and also allow cellular uptake via the receptors mediated endocytosis.

The association between drugs and these proteins has been extensively studied and typically the interaction of drug molecules with plasma proteins is electrostatic and hydrophobic, the binding is usually rapid and reversible with an average equilibrium time of 20 ms. Not only the binding capacity is an important factor, but also the on/off rate of binding can act as a major determining step. However, since CO-RMs are organometallic compounds their interaction with serum proteins is expected to be quite different from that of other drugs. Indeed, the tridimensional bulk of MCCs is rather different from the relatively "flat" shape of most drug molecules, and the intermolecular interactions between hydrophobic CO ligands and the mostly polar surface of proteins in aqueous solution has not been studied in any detail. The possibility of reactions occuring between proteins and MCCs has only been barely tested in cases where MCCs were deliberately designed to enhance such reactivity in order to enable their use as protein markers. [31, 32]

In this chapter the interaction between several types of MCCs and both BSA and h-Tf was investigated with Circular Dichroism and UV/VIS absorbance spectrophotometry techniques. A short number of compounds was studied but the complexes selected present specific properties common to a wide variety of other complexes which allows them to be classified as prototypes of a determined family of possible CO-RMs with biological activity. Their structures are represented in Scheme 1.

Circular Dichroism[33] (CD) has long been used to provide information on protein structure, and also as a simple way to probe the interaction between metal ions and proteins, the formation of adducts and analysis of the protein secondary and tertiary structure and how it is affected upon drug binding.

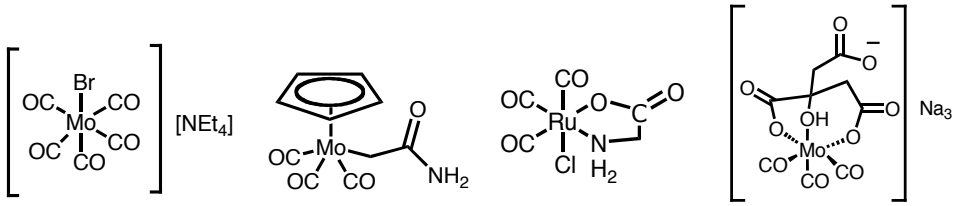

1 **2** **3** **4**

Scheme 1: Structure of the complexes $[Et_4N][Mo(CO)_5Br]$ (**1**), $CpMo(CO)_3CH_2CONH_2$ (**2**), $Ru(CO)_3Cl(glycinate)$ (**3**) and $Na_3[Mo(CO)_3(cit)]$ (**4**).

3. Experimental Section

3.1 Methodological remarks on the Circular Dichroism and UV-Vis studies with Bovine Serum Albumin and human Apo-Transferrin

The CD studies were performed in the laboratory of Prof. João Costa Pessoa in Instituto Superior Técnico, Lisboa, with the help and guidance of Dr. Isabel Tomaz and Dr. Isabel Correia.

In the CD study, the compounds were incubated with the proteins at different complex:protein ratios and the CD spectra were typically recorded in the 205-230 nm and 250-800 nm spectral range with BSA and from 195-260 nm and 250-800 nm spectral range with h-Tf.

The characteristic CD α-helix signal obtained in the far UV region arises from the chiral amide chromofore transitions which have a negative ($n \Rightarrow \pi^*$) band at 222 nm, parallel negative ($\pi \Rightarrow \pi^*$) at 206 nm and perpendicular positive ($\pi \Rightarrow \pi^*$) at 190 nm.[34] The near UV region (250-350 nm) of CD spectra may give information on tertiary structure and in the visible region the induced CD signal obtained arises from the metal complex d electrons.

The characteristic CD signals are coming from tryptophan (290 nm), tyrosine (284 nm) and phenylalanine residues (254 nm) as well as broad band disulfide

bonds (near-UV). The protein is CD-silent in the visible region and any induced signal arises from the metal complex d electrons.

The optimal concentrations of BSA are: 30–50 μM for the near UV and visible range with the spectra recorded with a 1 cm pathlength cell; 3 μM for the far UV region, using a 1 mm pathlength cell. The spectra were acquired immediately after incubation with BSA. Incubation of **2** with BSA in the near UV-VIS region was performed with a 2 cm pathlength cell.

The optimal concentration of h-Tf is 30 μM in the near UV and visible range, recorded with a 1 cm pathlength cell, and 5 μM in the far UV region, using a 1 mm pathlength cell. The spectra were acquired immediately after incubation with h-Tf and also after 24h.

The CD spectrum of all the complexes was recorded at the maximum concentration used and no CD signal was obtained with the complex alone.

The CD signal (in mdeg) was converted to mean residual ellipticity ([θ] in $deg.cm^2.dmol^{-1}$) defined as

$$[\Theta] = \frac{\Theta_{obs}}{10.c.l.n} \qquad \textbf{Equation 1}$$

where θ_{obs} (mdeg) is the experimental ellipticity, c ($mol.dm^{-3}$) is the protein concentration, l (cm) is the cell pathlength, and n is the number of residues in the protein - 583 aminoacids for BSA[35] and 678 for h-Tf.[36]

Isotropic UV-VIS absorbance spectra of the complexes and of the complexes with protein were recorded in PBS7.4 at room temperature in the dark, under normal air. The spectra were collected over 4h, in 10 min intervals, from 250 nm to 800 nm in Quartz cells.

Circular Dichroism:

Method description:

The experiments were performed in a spectropolarimeter Jasco J-720, either with a red-sensitive photomultiplier (EXEL-308) suitable for the 400-1000 nm range or a photomultiplier suitable for the 200-700 nm range. The parameters used were the following:

Band width: 2.0 nm; response: 4 sec; measurement range: 450-250 nm (near UV) - cells with l = 1 cm and 260-190 nm (far UV) - cells with l = 1 mm ; data pitch: 0.2 nm; scan speed: 20 nm/min; accumulation: 1; temperature: RT (23-25ºC).

The compounds were dissolved in PBS7.4 and added to a previously prepared BSA or h-Tf solution in PBS7.4. $[Et_4N][Mo(CO)_5Br]$ was dissolved in MeOH due to its insolubility in PBS giving a final concentration of 5% MeOH in the cuvette.

Material:

Bovine Serum Albumin – fraction V – and Human *Apo*-Transferrin were acquired from *Roche*; Circular dichroism 1 mm, 1cm and 2 cm pathlength quartz cuvettes; PBS7.4 was prepared by dissolving PBS tablets from *Gibco* in 500 mL of distilled water giving a final concentration of 0.14 M NaCl, 0.01 M PO_4^{2-} buffer and 0.003 M KCl.

UV/Vis absorbance spectrophotometry:

Method description:

The experiments were performed in Perkin Elmer Lambda35 spectrophotometer as follows:

A stock solution of the complex was prepared in PBS7.4 or MeOH in the case of $[Et_4N][Mo(CO)_5Br]$. A calculated amount from this solution was added to the cuvette in order to obtain the desired final concentration and PBS7.4 added to perform 1 ml total volume. In the case of $[Et_4N][Mo(CO)_5Br]$ a 4% final concentration of MeOH was obtained. The absorbance spectrum was recorded from 250 nm to 800 nm with 10 min interval.

A similar experiment was performed but in addition to the complex, a calculated amount of protein was added in PBS7.4. This was taken from a previously prepared stock solution in order to give a final concentration of typically 30 μM h-Tf and 50 μM BSA in the cuvette. The absorbance spectrum was recorded from 250 nm to 800 nm with 10 min interval.

Material:

Bovine Serum Albumin – fraction V – and Human *Apo*-Transferrin were acquired from *Roche*; Quartz SUPRASIL® cuvettes with 10 mm pathlength from *Hellma*; PBS7.4 was prepared by dissolving PBS tablets from *Gibco* in 500mL of distilled water giving a final concentration of 0.14 M NaCl, 0.01 M PO_4^{2-} buffer and 0.003 M KCl.

3.2 Technical Details

Synthetic Work:

All the compounds were prepared as described in Chapter II or table A1 in Annex I.

4. Results and Discussion

4.1 Interactions with Bovine Serum Albumin

Human serum albumin (HSA) is a largely α-helical single-chain 66 kDa protein, consisting of three structurally homologous domains that assemble to form a heart-shaped molecule. Each domain has two sub-domains, which are predominantly helical (67% of the protein is helical with a total of 28 helices) and extensively cross-linked by several disulfide bridges.[37] From a total of 585 aminoacids its sequence contains a total of 17 disulphide bridges, one free thiol (Cys 34) and a single tryptophan (Trp 214). This configuration was shown to possess at least 6 primary binding sites of high specificity. HSA primarily binds

strongly to organic anions (e.g. carboxilates, phenolates) but it can also bind basic and neutral drugs.

The hydrophobic cavities of the protein exhibit similar chemistry and are the main regions of ligand binding sites. The binding sites are located in sub-domains IIA and IIIA and have been determined crystallographically for several ligands. There is a large number of secondary binding sites with low affinity that allows binding of a high number of ligands, mainly by hydrophobic interactions. Imipramine, that binds up to 30 molecules per albumin unit is one such ligand.

The IIIA sub-domain is the preferential receptor for several molecules such as digitoxin, ibuprofen and tryptophan. On the other hand, warfarin prefers binding to the IIA[38] sub-domain while aspirin shows nearly equal distributions between binding sites located in IIA and IIIA sub-domains. The high-affinity site for bilirubin has been isolated in domain II[39] and the main binding site for long-chain fatty acids has been shown to occupy the domain III.[40] The likely location of the multi-metal site in human albumins is thus the area of contact of domains I and II.[41, 42] Ligand binding to one domain induces distinct conformational changes in the other domain, as both sub-domains share a common interface. Thus, the binding of a particular drug molecule to serum albumin may change considerably the binding abilities of HSA towards other molecules. BSA is quite often used as an *in vitro* mimic of HSA due to the similarities of properties between both proteins. In the present study, BSA was used as a model of HSA since their drug-binding capacities are very similar.

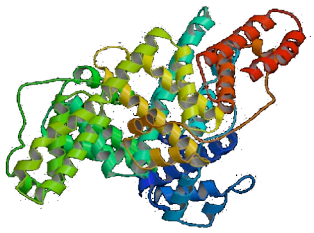

Figure 1: BSA structure

4.1.1 Study of the interaction of $[Et_4N][Mo(CO)_5Br]$ (1) and BSA

Circular Dichroism

BSA (30 μM) and **1** were incubated in 1:1, 1:2, 1:15 and 1:20 protein:complex ratio and the CD spectra recorded from 300 to 600 nm (see Fig. 2 left).

Assays at 50 μM protein concentration were performed with 1:5 and 1:10 ratio between 300 and 500 nm. These showed the same bands observed at 1:2 ratio but not the broad negative band at 480 nm (see Fig. 2 right).

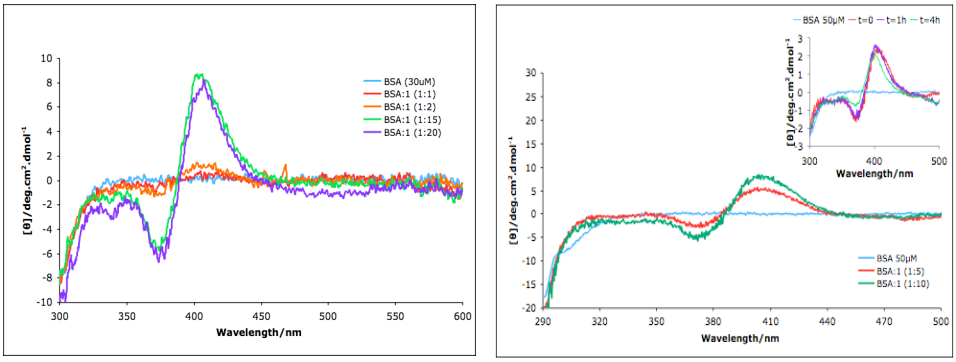

Figure 2: **Left:** CD spectra of BSA (30μM) incubated with **1** at RT, in PBS7.4 at 1:1, 1:2, 1:15 and 1:20 protein:complex ratio. The spectra were recorded from 300 to 600 nm. **Right:** CD spectra of BSA (50 μM) incubated with **1** at RT, in PBS7.4 at 1:5 and 1:10 protein:complex ratio. The spectra were recorded from 300 to 500 nm. Insert – Time stability of 1:10 sample at t=0, t=1h and t=4h.

Different ratios gave very distinct spectra. At low BSA/compound ratio (1:1 and 1:2) a low intensity positive band is observed at 408 nm and a negative band is observed at 374 nm. These bands increase in intensity and at a 1:15 ratio are very intense.

The fact that a CD signal is observed in this region shows undoubtedly the binding of a metallic fragment (or the whole complex) to a chiral environment of the protein since neither the protein nor the metal complex alone have a CD signal in this wavelength range. The CD spectra obtained correspond to an induced CD signal at the same wavelength where the compound absorbs (Fig.5A). A slight deviation from protein's baseline CD signal is observed at 480 nm when the ratio

increases to 1:20.

The interactions observed are stable up to 4h (see insert Fig. 2), however, this only occurs if both species are incubated at the same time. If the compound is left in solution alone for 2h and then incubated with BSA no induced CD signal is observed. As shown in Fig. 5A, the compound rapidly decomposes in PBS7.4 and the product of decomposition no longer binds to BSA.

The highest ratios used allowed the identification of new bands, not observed on the remaining spectra. This signal arises from some changes in the protein structure that allowed the interaction of the protein with the metal, most probably from some metal-to-ligand charge-transfer, MLCT. In order to get a CD signal at a certain wavelength the sample must be active and absorb light at that wavelength. Therefore, CD spectra are observed at the same wavelengths as the absorption spectra of the sample. In some cases, when high complex:protein ratios are used very high absorbance values are obtained and the CD signal becomes saturated. **1** has a strong absorbance band centered at 401 nm and another shoulder in the 288 nm region (Fig. 5A) and therefore to study the 250-350 nm region with a protein concentration of 30 μM, only 1:1 and 1:2 samples could be used due to the aforementioned absorbance limitation.

The spectra only show a minor influence on a positive band centered at 258 nm, arising from the phenylalanine residues showing that the tertiary structure of the protein isn't strongly affected (see Fig. 3).

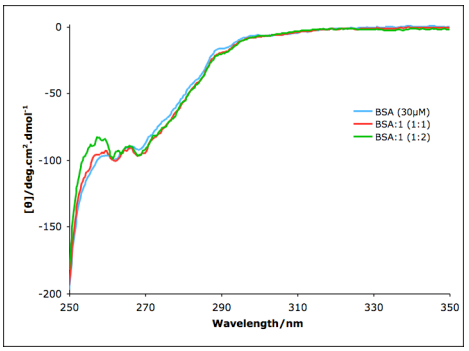

Figure 3: CD spectra of BSA (30µM) incubated with **1** at RT, in PBS7.4 at 1:1 and 1:2 protein:complex ratio. The spectra were recorded from 250 to 350 nm.

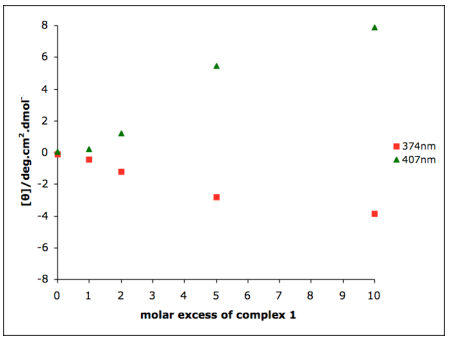

Figure 4: Variation of the mean residual ellipticity ([θ]) with the molar excess of **1**, followed at $\lambda_{max}^{(+)}$ (407 nm) and $\lambda_{max}^{(-)}$ (374 nm).

In Fig. 4 is possible to observe that the variation of the mean residual ellipticity ([θ]) with different ratios of **1**, followed at $\lambda_{max}^{(+)}$ (407 nm) and $\lambda_{max}^{(-)}$ (374 nm) shows an increase of [θ] up to 10 molar excess of **1** over BSA. This shows the high binding capacity of this transport protein and supports the strong affinity between the protein and the compound with a high degree of association.

UV-VIS absorbance

The UV-VIS absorption spectrum of **1** was recorded with and without BSA. The spectrum of the complex alone was followed over time and the same procedure was followed with a BSA:complex sample with 1:20 ratio. This ratio was the highest used in the CD study (Fig. 2) and gave a strong induced CD signal. The spectrum of BSA alone shows a very well defined absorption peak at 278 nm.

1 has 2 major absorption bands, one centered at 401 nm and another broad shoulder at 288 nm and both rapidly decay over time (Fig.5 A and C).

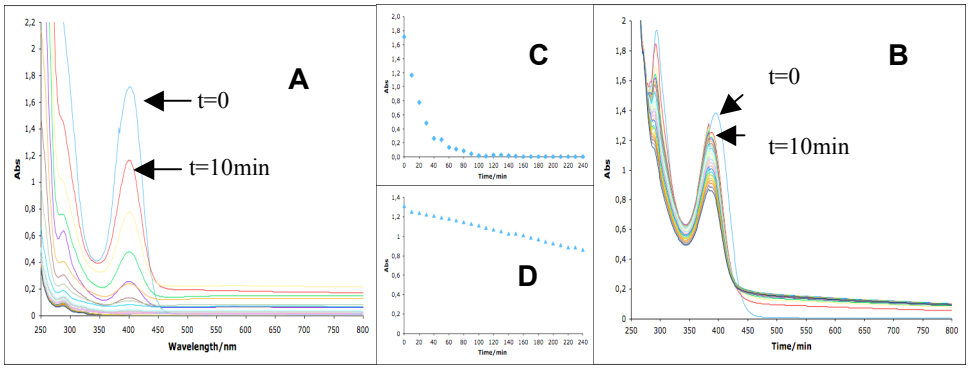

Figure 5: Time evolution of UV-VIS absorption spectrum of **1** (600 μM) in PBS7.4 (4%MeOH) at RT. A – **1** alone; B – **1** and BSA (30 μM; BSA spectrum subtracted); C – Decay in absorbance measured at 401 nm with **1** alone; D – Decay in absorbance measured at 387 nm with **1** and BSA (30 μM).

It had been already demonstrated in Chapter II through CO release experiments that the parent compound is unstable in solution and this behavior is supported by this absorption profile. Within 2h virtually no absorption is observed at 401 nm and the band at 286 nm has very low intensity (Fig.5 C).

When incubated with BSA, a major band is observed at 395 nm and another at 294 nm. The highest wavelength band slightly shifts within the first 10 min to 387 nm without a rapid decay in intensity. The band at 294 nm shifts to 292 nm after 10 min and 291 nm after 20 min. Notably, the 2 bands are quite stable over 4h (Fig.5 D)

These results strongly support the data obtained from the CD study, showing a clear and strong interaction between **1** and BSA, which completely alters the decomposition profile of the compound in solution. The decrease in the absorbance is much less pronounced suggesting that BSA partially prevents the decomposition of the complex.

4.1.2 Study of the interaction of $CpMo(CO)_3CH_2CONH_2$ (2) and BSA

Circular Dichroism

Interaction between **2** and BSA was studied in the far-UV and near UV-VIS region using 1:1 and 1:10 protein:complex ratios.

An exploratory fast scan was recorded from 250 to 800 nm with a 1:10 (50 µM BSA:**2**) sample and no signal was obtained so it was decided to decrease the scanning range.

2 and BSA (50 µM) were incubated in 1:1 and 1:10 protein:complex ratio and the spectrum recorded from 250 to 450 nm with a 2 cm pathlength cell (Fig. 6 left). In the far-UV region the compound was incubated with BSA (3 µM) at 1:1, 1:3, 1:5, 1:10 and 1:25 protein:complex ratio and the spectra recorded from 190 to 250 nm (see Fig. 6 right).

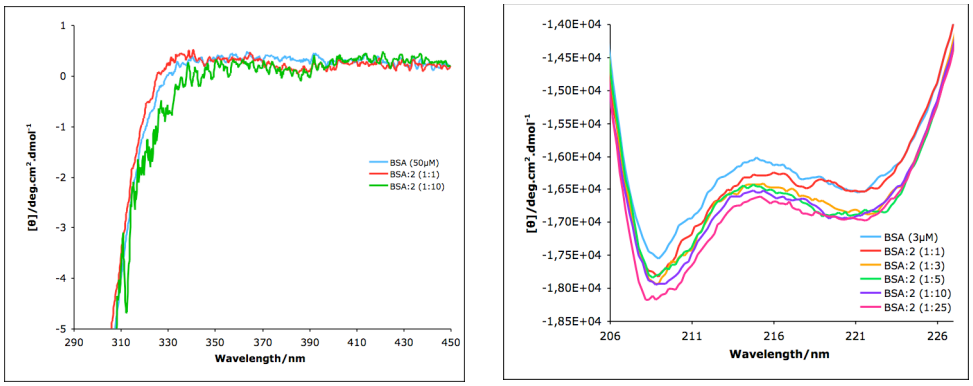

Figure 6: **Left:** CD spectra BSA (50 µM) incubated with **2** at RT, in PBS7.4 at 1:1 and 1:10 protein:complex ratio. The spectra were recorded from 250 to 450 nm. **Right**: CD spectra of BSA (3 µM) incubated with **2** at RT, in PBS7.4 at 1:1, 1:3, 1:5, 1:10 and 1:25 protein:complex ratio. The spectra were recorded from 190 to 250 nm.

Incubation of **2** with BSA did not produce any effects on the CD signal of protein either at low (1:1) or high (1:10) ratios in the near UV and visible range. No binding activity is detected since the spectrum didn't change. In the far UV region

a consistent signal is observed that changes with concentration. These small changes are due to some interference of the compound in the protein secondary structure. Possibly, the amide group of the complex is able to interact through hydrogen bonding with some protein sites and these oscillations may be reflected in the helical arrangement of the protein. Also the Cp ring may account for some spatial disorder that is reflected in the CD signal changes in the far UV range.

To determine the degree of influence in the helical arrangement of the protein, the α-helical content was estimated from the mean residue ellipticity at 222 nm[43] taking into account a helix length-dependent factor according to equation 2 where *n* represents the number of residues in the protein.[34]

$$\% \alpha\text{- helix} = \frac{(\theta)_{222nm}}{-39500 \times (1 - 2.57/n)} \times 100$$

Equation 2

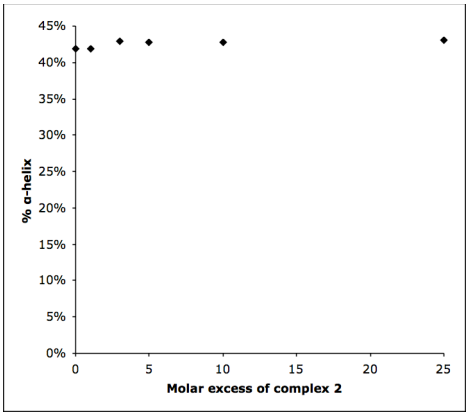

Figure 7: % α-helix obtained using Eq. 2 for BSA in the presence of 0, 1, 3, 5, 10 and 25 molar excess of **2**.

From Figure 7 one can see that the % of α-helical content does not change upon incubation with up to 25-fold excess of **2**. These observations show that contrary to what was observed with **1**, this complex doesn't covalently bind BSA. Only minor electrostatic interactions are observed but these don't affect the protein secondary structure.

UV-VIS absorbance

The absorbance spectrum of **2** was recorded in the presence and absence of BSA. The incubation with the protein was performed with a 10-fold excess of complex over protein, since this was the highest ratio used in the CD assays.

The absorption spectrum of **2** shows two bands with maxima located at 314 nm and 382 nm (Fig. 8A). The lowest wavelength maximum has higher intensity than the highest wavelength one and a highly stable profile is observed, with no changes in absorption during 4h (Fig. 8C). When incubated with BSA a similar spectrum is observed, with both maxima at the same wavelength together with another maximum at 290 nm obtained after subtraction of the BSA spectrum which has a maximum absorption at 279 nm (Fig. 8B). All the maxima are highly stable over 4h (Fig. 8D) and no changes on the absorption profile are observed thus not showing any kind of interaction between the complex and BSA, supporting the CD observations.

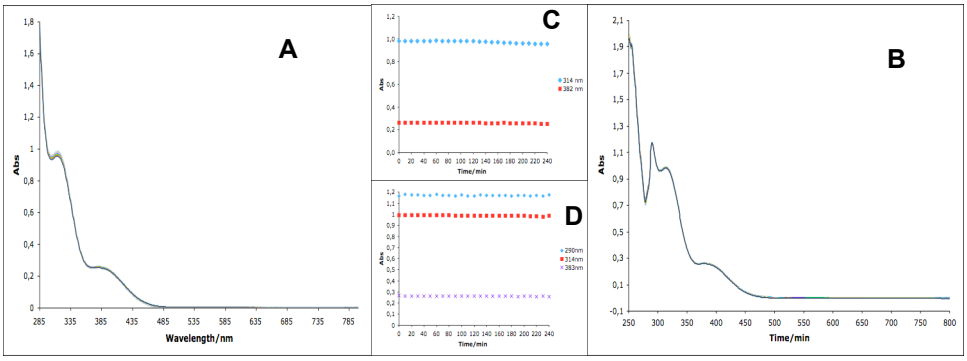

Figure 8: Time evolution of UV-VIS absorption spectrum of **2** (500 μM) in PBS7.4 at RT. A – **2** alone; B – **2** and BSA (50 μM; BSA spectrum subtracted); C – Decay in absorbance measured at 314 nm and 382 nm with **2** alone; D – Decay in absorbance measured at 290 nm, 314 nm and 383 nm with **2** and BSA (50 μM; BSA spectrum subtracted).

4.1.3 Study of the interaction of $Ru(CO)_3Cl$(glycinate) (3) and BSA

Circular Dichroism

Compound **3** was incubated with BSA (50 µM) in 1:3, 1:10, 1:15 and 1:25 protein:complex ratios and the spectra recorded from 250 to 800 nm (see Fig. 9 left). In the far UV range the compound and BSA (3 µM) were incubated in 1:1, 1:3, 1:5, 1:10, 1:25 and 1:50 protein:complex ratios and the spectrum recorded from 194 to 260 nm (see Fig. 9 right).

The results obtained suggest that the complex is not covalently bound to albumin. The spectrum doesn't show any differences in the visible range and some interaction is observed in the far and near UV region. A positive band appears around 336 nm and increases consistently with increasing complex:BSA ratios.

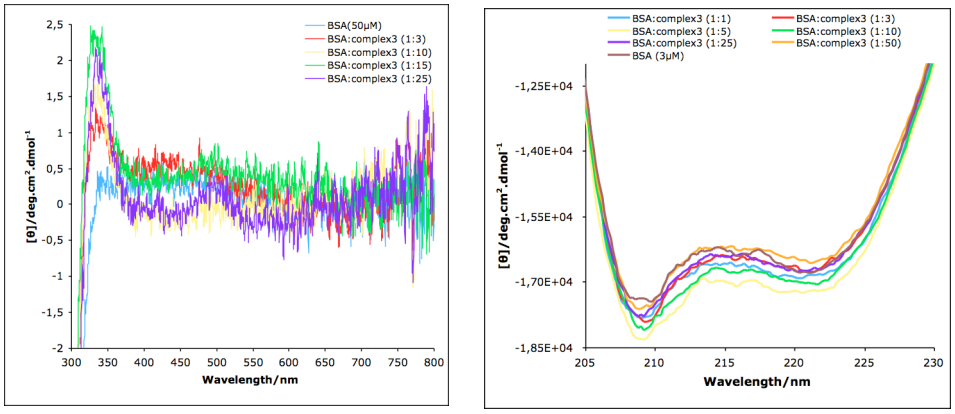

Figure 9: **Left:** CD spectra of BSA (50 µM) incubated with **3** at RT, in PBS7.4 at 1:3, 1:10, 1:15 and 1:25 protein:complex ratio. The spectra were recorded from 250 to 800 nm. **Right**: CD spectra of BSA (3 µM) incubated with **3** at RT, in PBS7.4 at 1:1, 1:3, 1:5, 1:10, 1:25 and 1:50 protein:complex ratio. The spectra were recorded from 194 to 260 nm.

This signal clearly shows an interaction between the protein and the compound although this is not a strong binding effect. In the far UV-region no clear pattern is detected but some deviations to the native protein CD signal are observed. These most probably arise from the same interactions which do not influence the overall protein structure but exert some local electrostatic forces that induce the

CD signal. As explained in the previous Chapter this compound undergoes a WGS reaction with the formation of a metalo-carboxylate group, which may be responsible for H bonding with other residues from the protein.

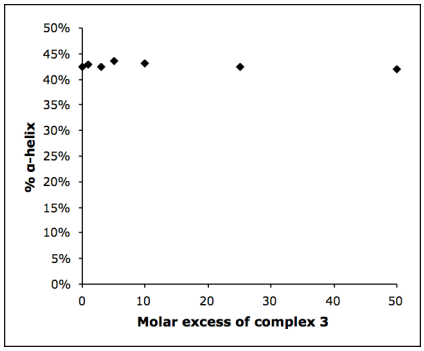

Figure 10: % α-helix obtained using Equation 2 for BSA in the presence of 0, 1, 3, 5, 10, 25 and 50 molar excess of **3**.

The α-helical content was calculated from the mean residue ellipticity at 222 nm and no significant changes were observed even when a 50-fold molar excess of complex was incubated with the protein (see Fig. 10). These results show that the secondary structure of the protein isn't affected even in the presence of a large excess of complex.

UV-VIS absorbance

The UV-VIS absorption spectrum of **3** was recorded with and without BSA. The incubation with the protein was performed with 1:15 protein:**3** ratio, since this was the highest ratio used in the CD assays.

Compound **3** has no absorbance peak but rather a broad band from 250 nm to 350 nm (Fig. 11A). This band shows a quick decay in absorbance after the first 10 min but then maintains a complete stability up to 4h in solution (Fig. 11C). With BSA an identical spectrum is obtained (Fig. 11B), with the maximum at 292 nm (obtained after subtraction of BSA spectrum) and also a rapid decay in absorbance is observed within the first 10 min followed by a high stability profile up to 4h (Fig. 11D).

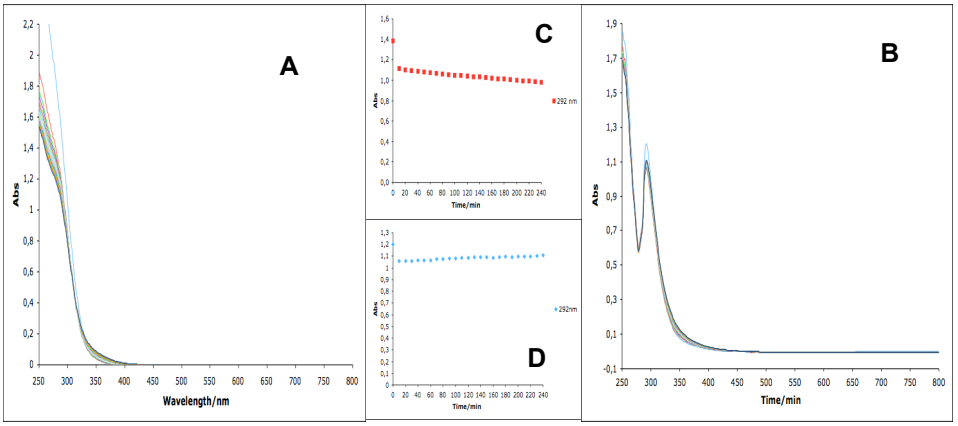

Figure 11: Time evolution of UV-VIS absorption spectrum of **3** (750 µM) in PBS7.4 at RT. A – **3** alone; B – **3** and BSA (50 µM; BSA spectrum subtracted); C – Decay in absorbance measured at 292 nm with **3** alone; D – Decay in absorbance measured at 292 nm with **3** and BSA (50 µM; BSA spectrum subtracted).

From the observed profile it isn't possible to infer if any kind of interaction is established between the protein and the complex since no changes are observed in the absorption spectra. However, the absence of differences suggests that no interaction is taking place between both species.

4.1.4 Study of the interaction of $Na_3[Mo(CO)_3(cit)]$ (4) and BSA

Circular Dichroism

Compound **4** and BSA (50 µM) were incubated in 1:5, 1:10, 1:25 and 1:50 protein:complex ratio and the spectrum recorded from 250 to 800 nm (see Fig. 12).

In the far-UV region the compound was incubated with BSA (3 µM) in 1:1, 1:10, 1:25 and 1:50 protein:complex ratio and the spectrum recorded from 190 to 300 nm. Neither the complex **4** (2.5 mM) nor the sodium citrate ligand (2.5 mM) alone are CD active. In addition sodium citrate (2.5 mM) was also incubated with BSA (50 µM) and no induced CD signal was obtained in the whole spectrum.

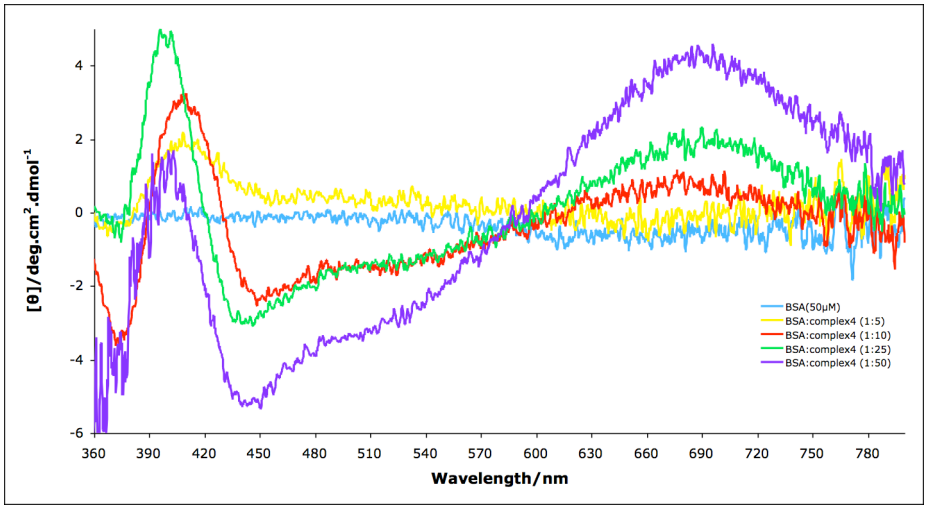

Figure 12: CD spectra of BSA (50 μM) incubated with **4** at RT, in PBS7.4 at 1:5, 1:10, 1:25 and 1:50 protein:complex ratio. The spectra were recorded from 250 to 800 nm.

A clear induced CD signal is observed in the near UV-VIS range. At 1:5 BSA/compound ratio a low intensity positive band is observed at 408 nm. When the ratio is increased to 1:10 two new negative bands are observed at 374 nm and 450 nm together with a positive broad band centered at 690 nm. When the BSA/complex ratio is increased to 1:25 and 1:50 all the bands increase accordingly except the negative band at 374 nm. This is due to signal saturation that doesn't allow the identification of bands in the near UV region.

Like in the case of **1** the extremely high ratios used allowed the identification of new bands not observed on the remaining spectra. The CD signal observed in the visible region shows the covalent binding of a metallic core to the protein in a chiral environment.

The very high concentrations used (1:50) distorted the signal in the near UV region of the spectrum due to a high absorbance of the complex in this range. Decreasing the amount of complex to a lower ratio (1:10) made it possible to clearly identify the different bands formed as well as their stability.

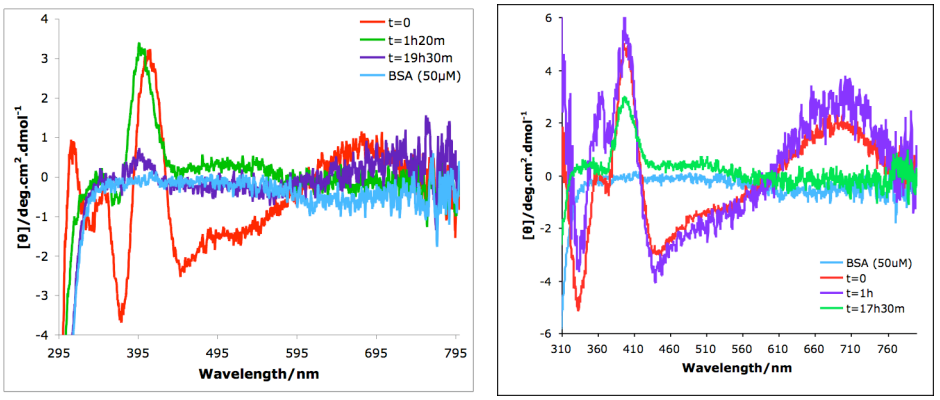

Figure 13: Time evolution of the CD spectra of BSA (50 µM) incubated with **4** at RT, in PBS7.4 at 1:10 (**left**) and 1:25 (**right**) protein:complex ratio. The spectra were recorded from 250 to 800 nm.

With 1:10 ratio after 1h incubation, all the bands disappear except the positive loop at 408 nm (see Fig. 13 left). With higher ratios, like 1:25 the other bands are kept during the first hour but also disappear after 17h30min (see Fig. 13 right). Nevertheless, the positive band at 408 nm is kept up without significant modifications. The same behavior is observed when aged solutions of **4** are added to BSA. If **4** is aged, standing in PBS7.4 solution for 80 min (same procedure like in Chapter V) and added to BSA in 1:10 ratio only the 408 nm band is observed (see Fig. 14).

This result shows that the changes in the visible CD spectra are due to some transient bands arising from weak interactions established at earlier times and not effective strong binding that stabilizes the complex like the band at 408 nm.

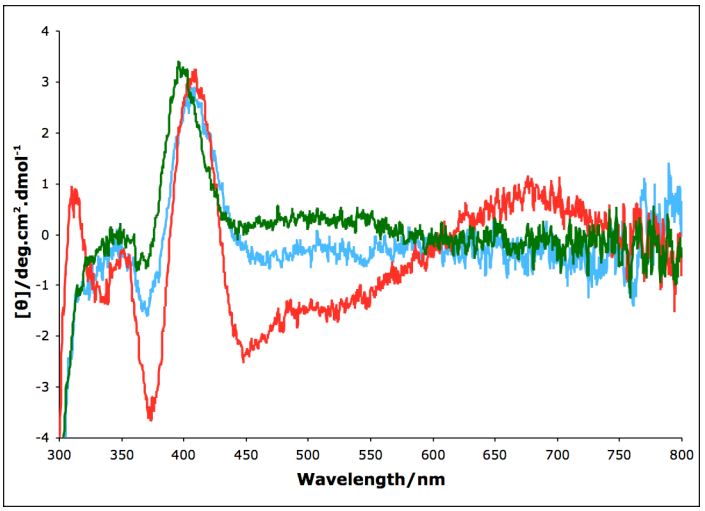

Figure 14: CD spectra of BSA(50 μM) incubated with **4** at RT, in PBS7.4 at 1:10 protein:complex ratio. Red – Spectrum acquired immediately after mixing a fresh complex solution and protein. Green – Spectrum acquired after 80 min incubation of complex with protein. Blue – Spectrum acquired after mixing an aged solution of complex (aged for 80 min in PBS7.4) and protein. The spectra were recorded from 250 to 800 nm.

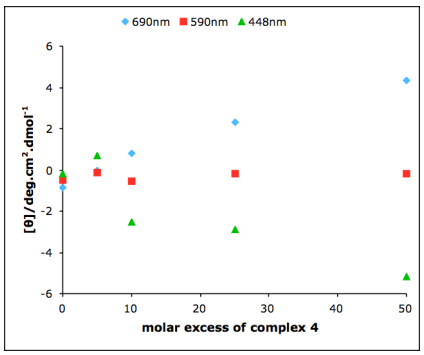

Figure 15: Variation of the mean residual ellipticity ([θ]) with the molar excess of **4**, followed at λ_1^+(690 nm), λ_2 (590 nm) and λ_3^- (448 nm).

From Fig.15 it is possible to observe the variation of the mean residual ellipticity ([θ]) with the molar excess of **4**, followed at three different λ values (690, 590 and 448 nm) which correspond to a positive band, neutral and negative band, respectively. Increasing the molar excess of **4** over BSA leads to a continuous increase of the mean residual ellipticity according with the sign of the band. Once again, this shows the high binding capacity of this transport protein and evidentiates the strong affinity between the protein and the compound with a high degree of association.

In the far-UV region once more some changes are observed but not a consistent concentration-dependent signal change (see Fig. 16).

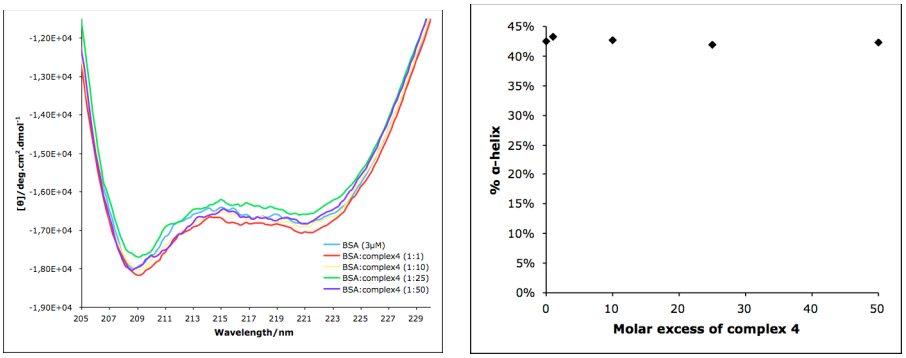

Figure 16: **Left**: CD spectra of BSA (3 μM) incubated with **4** at RT, in PBS7.4 at 1:1, 1:10, 1:25 and 1:50 protein:complex ratio. The spectra were recorded from 190 to 300 nm. **Right**: % α-helix obtained using Equation 2 for BSA in the presence of 0, 1, 10, 25 and 50 molar excess of **4**.

These results indicate that the binding observed is not strongly influencing the protein secondary structure. The compound is bound to the protein and the overall spatial arrangement of the protein remains intact with the adduct. This observation is reflected in the percentage of α-helical content that was calculated and showed a stable amount independently of the high concentrations of complex used (see Fig. 16).

The data show that in spite of the strong binding observed, the secondary structure of the protein is not affected.

UV-VIS absorbance

The absorbance spectrum of **4** was recorded in the presence and absence of BSA. The incubation with the protein was performed with a 10-fold excess of complex over protein. This ratio was selected since in the CD assays it induced a strong CD signal that showed variability along time (see Fig. 17).

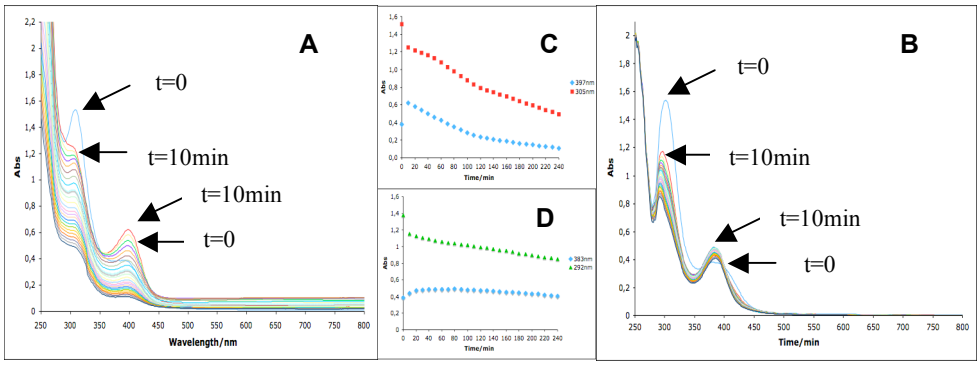

Figure 17: Time evolution of UV-VIS absorption spectrum of **4** (500 µM) in PBS7.4 at RT. A – **4** alone; B – **4** and BSA (50 µM; BSA spectrum subtracted); C – Decay in absorbance measured at 397 nm and 305 nm with **4** alone; D – Decay in absorbance measured at 383 nm and 292 nm with **4** and BSA (50 µM; BSA spectrum subtracted).

Compound **4** shows a distinct behavior from the previous compounds. As detected by the CO release experiments, the compound gradually decomposes in PBS. At the time of dissolution it has one major band absorption at 308 nm and another small and broad band centered at 395 nm (Fig. 17A). During the following 10 min the absolute maximum rapidly decreases in intensity and the highest wavelength peak increases intensity. After this initial "rearrangement" both bands slightly shift the maxima and decrease over time (Fig. 17C). Incubation with BSA also affords a slight shift of the maximum at 302 nm (observed at t=0) to 296 nm (at t=10 min) and lately to 292 nm (at t=30 min). The broad band observed at the initial time in the 350-400 nm region gives rise to a local maximum at 383 nm (Fig. 17B) after 10 min, but a higher degree of stability is achieved (Fig. 17D). This suggests that a protein-complex adduct is formed and the molecular rearrangement leads to the formation of a new species stable over time.

Also, the absorbance baseline level of **4** increases with time due to an increased turbidity of the sample (Fig. 17A) and BSA is able to keep the complex in solution (Fig. 17B) giving evidence, once more, of the interaction between the two species.

4.2 Interactions with Human Apo-Transferrin

The transferrins are a family of non-heme iron-binding glycoproteins containing ca. 700 aminoacids (Human *apo* transferrin has 678 residues)[36, 44] with molecular mass ca. 80 kDa. These are single-chain glycoproteins of which three major types were characterized: ovotransferrin,[45, 46] lactoferrin[47-49] and serum transferrin which occurs in blood and other mammalian fluids like bile, amniotic fluid, cerebrospinal fluid, lymph and milk.

There is a high sequence identity between different species and different members of the same family and the high levels of conservation in their primary structures are also reflected in their three-dimensional structures. Many crystal structures of transferrins (different species and some fragments) are available and have been reviewed previously.[50] Briefly, the polypeptide chain is folded into two structurally similar but functionally different lobes, referred to as N- and C-lobe, respectively. The two lobes are connected by a short peptide and each lobe can be further divided into two domains enclosing a deep hydrophilic cleft where the iron-binding site is located. Here, Fe^{3+} (and other metals) coordinates with distorted octahedral geometry to two oxygens from Tyrosine, one nitrogen from Histidine, one oxygen from Aspartate, and two oxygens from a bidentate carbonate that acts as synergistic anion. The ligands are from two domains and two polypeptide strands, which cross over between the two domains at the back of the iron site. This kind of arrangement is crucial to ensure that the domains are able to move apart to form an open conformation, hinged by the backbone strands, which leads to iron release. An important feature is the conformational changes that the protein suffers during iron uptake and release, which is also important for the Tf receptor recognition.

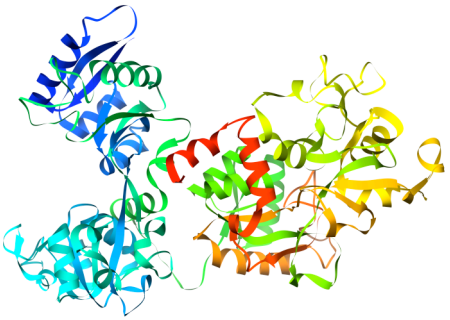

Figure 18: Human *apo*-Transferrin structure exhibiting the N and C lobe

4.2.1 Study of the interaction of $[Et_4N][Mo(CO)_5Br]$ (1) and h-Tf

Circular Dichroism

Compound **1** and h-Tf (30 μM) were incubated in 1:1, 1:3, 1:5, 1:10 and 1:20 protein:complex ratio and the spectrum was recorded from 250 to 800 nm (see Fig. 19).

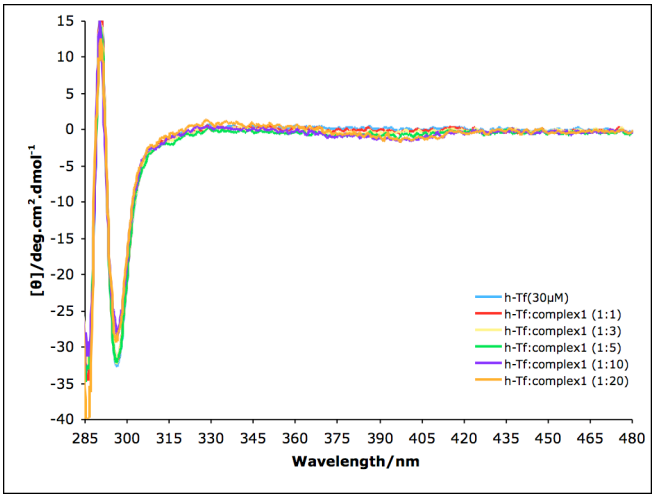

Figure 19: CD spectra of h-Tf (30 μM) incubated with **1** at RT, in PBS7.4 at 1:1, 1:3, 1:5, 1:10 and 1:20 protein:complex ratio. The spectra were recorded from 250 to 800 nm.

The presence of the complex doesn't change either the intensity or the shape of the CD spectrum of the protein. In the visible range no induced CD signal is detected and in the near UV region only minor differences are detected in the

negative loop centered at 297 nm. However, the CD spectrum of h-Tf is not significantly changed by the presence of the complex, even for very high complex excess like 1:10 and 1:20 ratios. Also, no differences were observed in the CD spectra over a 24h incubation period, therefore, CD data does not suggest an interaction between complex and protein.

UV-VIS absorbance

The UV-VIS absorption spectrum of **1** was recorded alone and with h-Tf (see Fig. 20). The spectrum of complex alone was followed over time and the same procedure was followed with a h-Tf:complex sample with 1:20 ratio which was the highest ratio used in the CD assays. h-Tf spectrum alone was also recorded and the protein has a very well defined absorption peak at 279 nm.

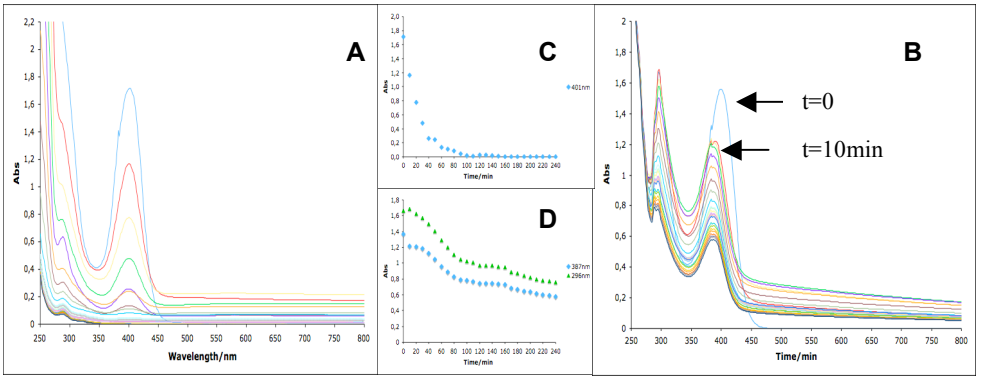

Figure 20: Time evolution of UV-VIS absorption spectrum of **1** (600 µM; 4%MeOH) in PBS7.4 at RT. A – **1** alone; B – **1** and h-Tf (30 µM; h-Tf spectrum subtracted); C – Decay in absorbance measured at 401 nm with **1** alone; D – Decay in absorbance measured at 387 nm and 296 nm with **1** and h-Tf (30 µM; h-Tf spectrum subtracted).

Like previously shown in Fig. 5, **1** has 2 major absorption bands, one centered at 401 nm and another broad shoulder at 288 nm and both rapidly decay over time, also in 600 µM concentration (Fig. 20A and C). Again, after 2h virtually no absorption is observed at 401 nm and the band at 286 nm has very low intensity

(Fig. 20C). When incubated with h-Tf the maximum at 400 nm is only observed immediately after addition and shifts to 387 nm after 10 min. Another maximum is observed at 296 nm and doesn't shift position along time (Fig. 20B). A similar profile is observed in both peaks, with a rapid decay within the first 80 min to 90 min of reaction, followed by a slightly stable plateau between 90 min to 160 min and then again another less pronounced decay in absorbance (Fig. 20D).

The behavior observed in the presence of h-Tf is different from the decomposition profile of the complex alone. The absorbance decrease is less pronounced and suggests a 2-step decomposition. This may indicate a slower decomposition process, first, corresponding to the bromide loss and which is followed by a second step. This decay is in agreement with the profile observed by Lynam and co-workers[51] who identified the formation of an intermediate species on the decomposition of the Cr analogue $[Cr(CO)_5Cl]^-$.

Although there's no evidence of association between the two species, the presence of the protein clearly interferes with the decomposition pathway of the complex.

4.2.2 Study of the interaction of $CpMo(CO)_3CH_2CONH_2$ (2) and h-Tf

Circular Dichroism

The CD signal was recorded in the UV-VIS range (280 nm - 800 nm) for 1:1, 1:2, 1:3, 1:5 and 1:10 protein(30 μM)/complex ratios and in the far UV range (198 nm – 260 nm) for 1:1, 1:3, 1:5, 1:10 and 1:15 protein (5 μM)/complex ratios and no interaction was observed (see Fig. 21).

No measurable differences were detected in the protein spectrum in the presence of the metal complex at any ratio studied even after a 24h incubation period. CD data thus suggests that there is no measurable interaction between h-Tf and **2**.

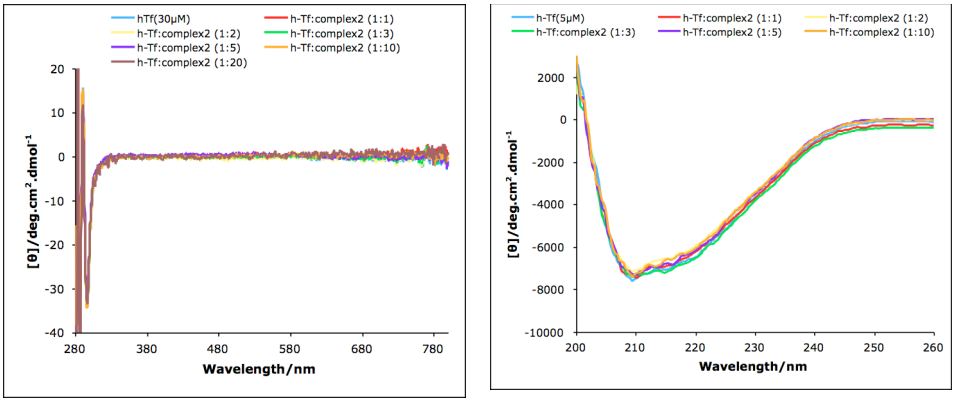

Figure 21: **Left:** CD spectra of h-Tf (30 μM) incubated with **2** at RT, in PBS7.4 at 1:1, 1:2, 1:3, 1:5, 1:10 and 1:20 protein:complex ratio. The spectra were recorded from 250 to 800 nm. **Right:** CD spectra of h-Tf (5 μM) incubated with **2** at RT, in PBS7.4 at 1:1, 1:2, 1:3, 1:5 and 1:10 protein:complex ratio. The spectra were recorded from 198 to 260 nm.

UV-VIS absorbance

The absorbance spectrum of **2** was recorded in the presence and absence h-Tf. The incubation with the protein was performed with a 20-fold excess of complex over protein, since this was the highest ratio used in the CD assays.

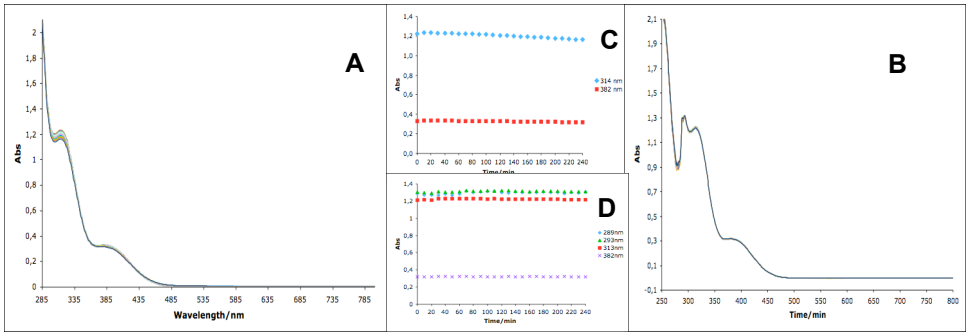

Figure 22: Time evolution of UV-VIS absorption spectrum of **2** (600 μM) in PBS7.4 at RT. A – **2** alone; B – **2** and h-Tf (30 μM; h-Tf spectrum subtracted); C – Decay in absorbance measured at 314 nm and 382 nm with **2** alone; D – Decay in absorbance measured at 289 nm, 293 nm, 313 nm and 382 nm with **2** and h-Tf (30 μM; h-Tf spectrum subtracted).

2 has a highly stable profile in PBS7.4. It has two bands with maxima at 314 nm and 382 nm that do not change absorption during 4h (Fig. 22A). When incubated with h-Tf two new maxima are obtained at 289 nm and 293 nm resulting from the

subtraction of the h-Tf spectrum which has the maximum absorption at 279 nm (Fig. 22B). A completely stable profile is observed over a period of 4h (Fig. 22C and D) which doesn't suggest any kind of interaction between **2** and h-Tf thus supporting the CD observations.

4.2.3 Study of the interaction of $Ru(CO)_3Cl$(glycinate) (3) and h-Tf

Circular Dichroism

The interaction of **3** with h-Tf was studied in the near-UV and visible range with protein/complex ratios of 1:1, 1:3, 1:5, 1:10 and 1:15. CD spectra were recorded immediately after mixing and after a 24h incubation period. Although no interactions were observed immediately after incubation (see Fig. 23 - left), significant changes are detected in the near UV region of the spectrum after a 24h incubation period (see Fig. 23 - right). However, in the visible range no induced CD signal is detected, not even after a 24h incubation period (see Fig. 23 - right).
The native protein has two negative bands centered at 297 nm and 286 nm and a positive band at 291 nm. Low protein/complex ratios (1:1 and 1:3) seem not to disturb the protein's tertiary structure since similar CD spectra are obtained. However, when the ratio increases to 1:5 a consistent change is observed, decreasing the intensity of both negative and positive bands. This tendency is confirmed at even higher ratios (1:10 and 1:25).

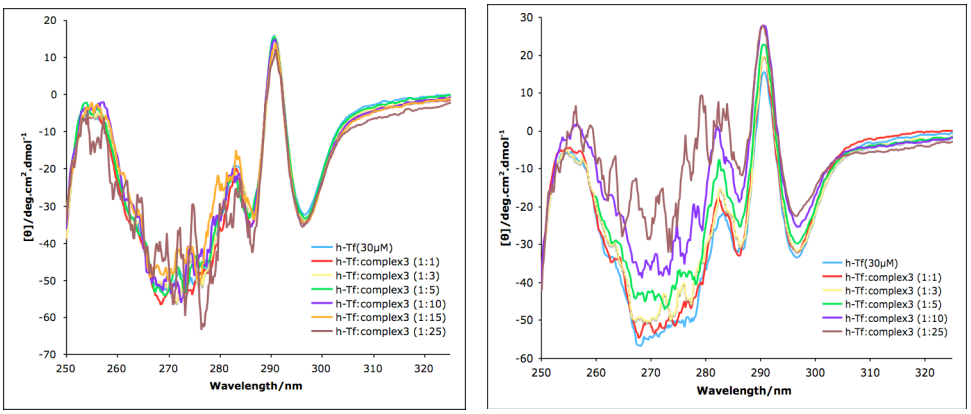

Figure 23: **Left**:CD spectra of h-Tf (30 μM) incubated with **3** at RT, in PBS7.4 at 1:1, 1:3, 1:5, 1:10 and 1:15 protein:complex ratio. The spectra were recorded from 250 to 800 nm immediately after mixing both species. **Right**: CD spectra of h-Tf (30 μM) after 24h incubation with **3** at RT, in PBS7.4 at 1:1, 1:3, 1:5, 1:10 and 1:15 protein:complex ratio. The spectra were recorded from 250 to 800 nm.

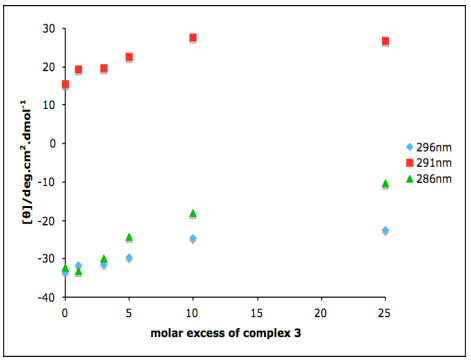

Figure 24: Variation of the mean residual ellipticity ([θ]) with the molar excess of **3**, followed at λ_1^- (296 nm), λ_2^+ (291 nm) and λ_3^- (286 nm).

Plotting the mean residual ellipticity *vs* the molar excess (Fig. 24) at the minima (286 nm and 296 nm) and maximum (291 nm) we can see a continuous increase of [Θ] up to 10-fold excess of **3**. The slope of [Θ] variation decreases when increasing from 10 to 25 molar excess of complex. This suggests that at 10 fold excess the maximum binding interaction was already achieved.

In the far UV region no changes are observed, not even after 24h. This data strongly suggest that the protein's secondary structure is not altered upon metal binding. The lack of changes in the secondary structure of h-Tf upon metal binding has been previously observed with Bi^{3+}, In^{3+} and even Fe^{3+} that bind transferrin in an open state and even after metal coordination the protein stays in the same configuration, which is energetically favored.[27]

The CD data thus suggest a weak interaction between protein and metal complex, which isn't covalent but most probably electrostatic.

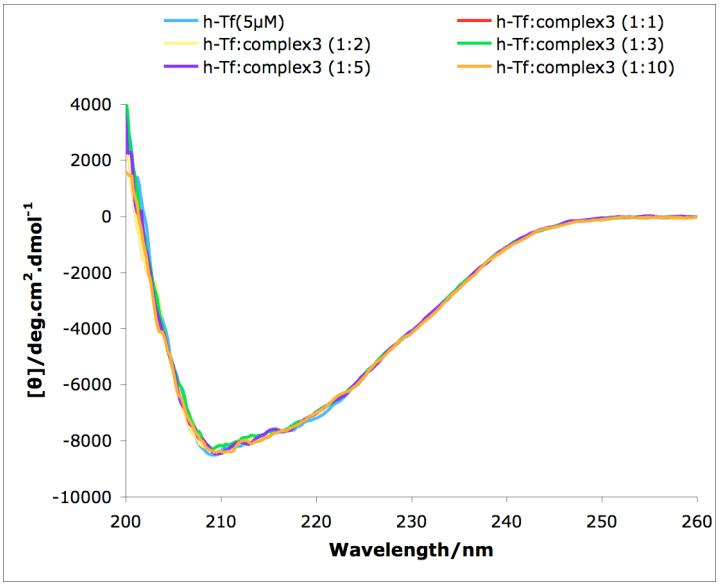

Figure 25: CD spectra of h-Tf (5 μM) after 24h incubation with 3 at RT, in PBS7.4 at 1:1, 1:2, 1:3, 1:5 and 1:10 protein:complex ratio. The spectra were recorded from 250 to 800 nm.

UV-VIS absorbance

The UV-VIS absorption spectrum of **3** was recorded with and without h-Tf. The incubation with the protein was performed with 1:25 protein:**3** ratio, since this was the highest ratio used in the CD assays and showed some interaction after 24h.

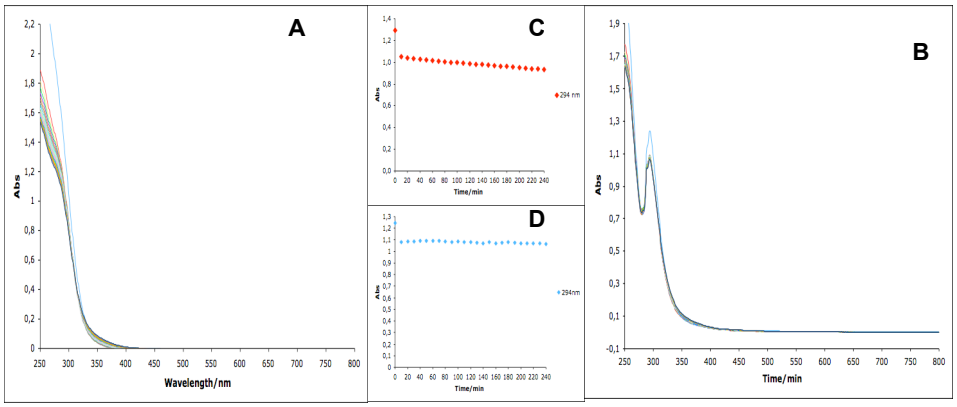

Figure 26: Time evolution of UV-VIS absorption spectrum of **3** (750 μM) in PBS7.4 at RT. A – **3** alone; B – **3** and h-Tf (30 μM; h-Tf spectrum subtracted); C – Decay in absorbance measured at 294 nm with **3** alone; D – Decay in absorbance measured at 294 nm with **3** and h-Tf (30 μM; h-Tf spectrum subtracted).

As previously shown in Fig. 11, **3** has a broad band from 250 nm to 350nm (Fig. 26A) that quickly decays in absorbance after the first 10 min but then maintains a complete stability up to 4h in solution (Fig. 26C). With h-Tf an identical spectrum is obtained (Fig. 26B), with the maximum at the same wavelength and totally stable over 4h (Fig. 26D). These results do not show if any kind of interaction is taking place between both species, and like we have seen in the incubation with BSA the UV-VIS absorbance profile is not a useful tool to determine protein binding in this case.

4.2.4 Study of the interaction of $Na_3[Mo(CO)_3(cit)]$ (4) and h-Tf

Circular Dichroism

The CD spectra of h-Tf with **4** were recorded between 250 nm and 400 nm with protein/complex ratios of 1:1, 1:5, 1:7.5 and 1:15. A sample with 1:25 ratio was recorded up to 800 nm and no induced CD signal was observed in the visible range.

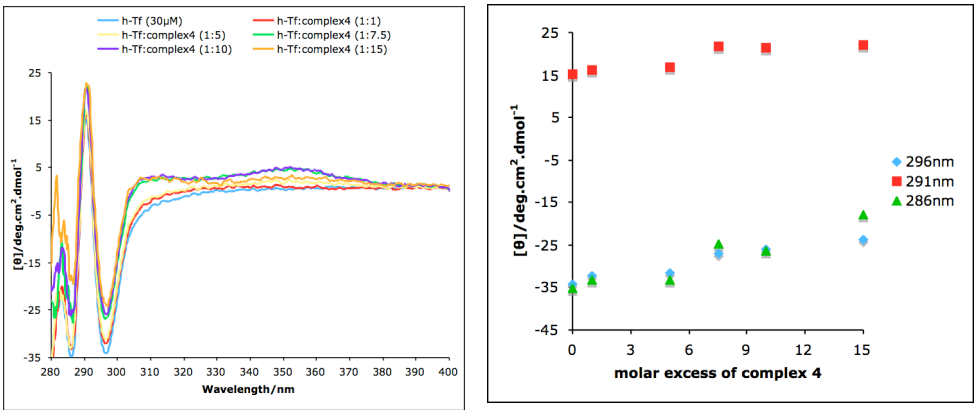

Figure 27: **Left**: CD spectra of h-Tf (30µM) after incubation with **4** at RT, in PBS7.4 at 1:1, 1:5, 1:7.5 , 1:10 and 1:15 protein:complex ratio. The spectra were recorded from 250 to 400 nm. **Right**: Variation of the mean residual ellipticity ([θ]) with the molar excess of **4**, followed at λ_1^- (296 nm), λ_2^+ (291 nm) and λ_3^- (286 nm).

The 1:1 and 1:5 samples do not exhibit changes in the CD spectra but at higher ratios such as 1:7.5 and 1:10, some changes are observed starting from 385 nm to lower wavelengths. A clear shift is observed from the original spectrum and both negative (297 nm and 286 nm) and positive bands (at 291 nm) show interference of the metal complexes with the CD signal.

Plotting the mean residual ellipticity *vs* the molar excess (Fig. 27 right) at the minima (286 nm and 296 nm) and maximum (291 nm) it is clear that two different profiles are observed. The same variance is obtained with 1- and 5- fold excess and a different one with 7.5-, 10- and 15-fold excess.

There's not a continuous increase of [Θ] but a gap, between lower and higher concentrations, but not in a clear direction.

The induced signal differences are not long-lasting like observed with BSA, and also depend on the concentration. With 1:5 ratio the differences observed in the CD signal remain unchanged up to 24h (Fig. 28 left) and with higher metal complex excess (1:10 ratio) the initial changes in the CD signal tend to decrease over time and after 4h30m the differences to the protein signal are less pronounced (Fig. 28 right). Nevertheless, this CD spectrum is kept up to 24h.

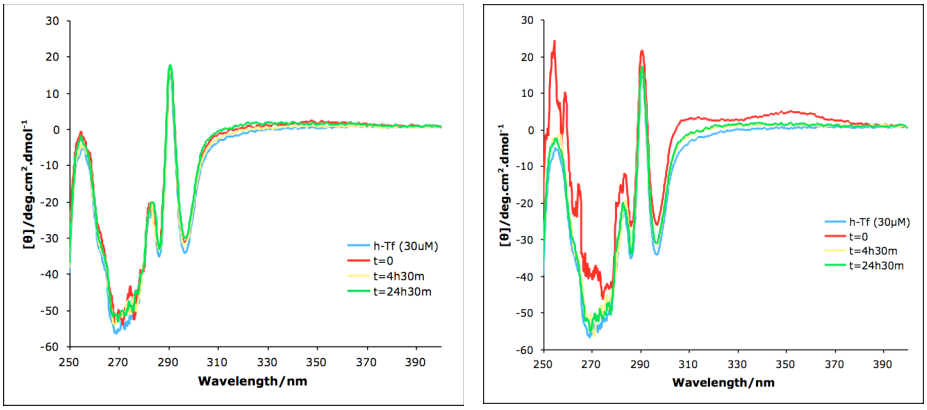

Figure 28: Time evolution of the CD spectra of h-Tf (30 µM) incubation with **4** at RT, in PBS7.4 at 1:5 (**left)** and 1:10 (**right**) protein:complex ratio. The spectra were recorded from 250 to 400 nm.

In the far UV region, a clear difference is observed between the native protein and the complex adducts. These differences are detected immediately after incubation with protein and remain up to 4h.

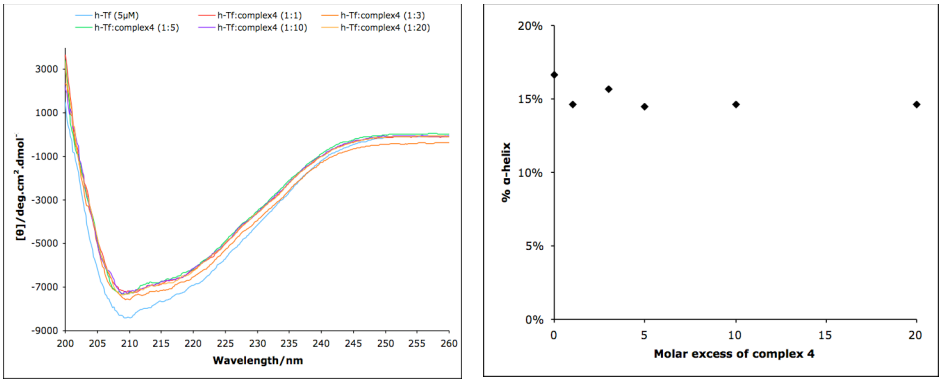

Figure 29: **Left**:CD spectra of **4** and h-Tf (5 µM) after 24h incubation at RT, in PBS7.4 at 1:1, 1:3, 1:5, 1:10 and 1:20 protein:complex ratio. The spectra were recorded from 198 to 260 nm. **Right**: % α-helix obtained using Equation 2 for h-Tf in the presence of 0, 1, 3, 5, 10 and 20 molar excess of **4**.

In the far UV range a sudden change is observed in the h-Tf spectrum in the presence of equimolar ratio of protein to complex that is not sensitive to excess of

complex (up to 20-fold excess). The α helical content was calculated and showed a decrease of 3% of α helice. CD data suggests an interaction between the complex and the protein by the observation of a weak induced CD signal and a change of its secondary structure upon binding (see Figure 29 right).

UV-VIS absorbance

The absorbance spectrum of **4** was recorded in the presence and absence of h-Tf. The incubation with the protein was performed with a 10-fold excess of complex over protein. This ratio induced some changes in the CD signal and was also followed along the time (Fig. 30).

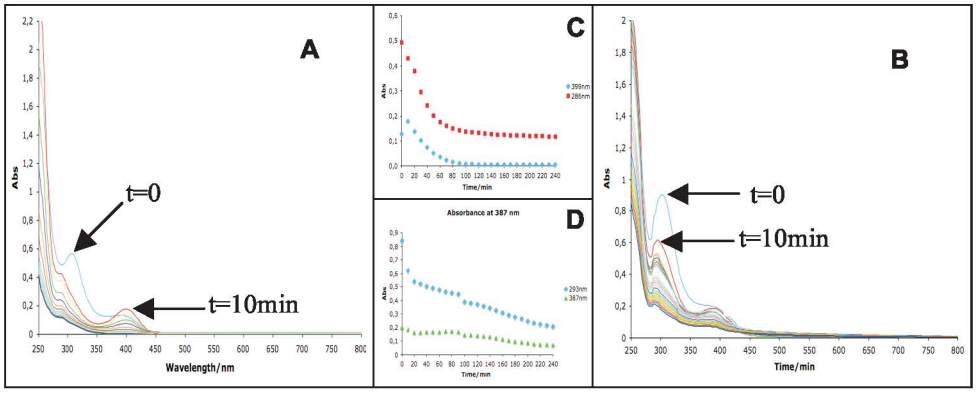

Figure 30: Time evolution of UV-VIS absorption spectrum of **4** (300 μM) in PBS7.4 at RT. A – **4** alone; B – **4** and h-Tf (30 μM; h-Tf spectrum subtracted); C – Decay in absorbance measured at 399 nm and 286 nm with **4** alone; D – Decay in absorbance measured at 387 nm and 293 nm with **4** and h-Tf (30 μM; h-Tf spectrum subtracted). t=0 blue line; t=10min red line

The UV-VIS absorbance spectra of **4** shows a slightly different profile than the one previously observed at 500 μM (Fig. 17).

At the time of dissolution it has one major absorption peak with maximum located at 307 nm and another small broad band from 370 to 400 nm (Fig. 30A). After 10 min, the absolute maximum decreases intensity and a lower intensity band (shoulder) is observed centered around 285 nm. At the highest wavelength

band the intensity slightly increases and a local maximum is observed at 400 nm. Both maxima then decrease over time (Fig. 30C). Incubation with h-Tf also affords a slight shift of the maximum at 303 nm (observed at t=0) to 295 nm (at t=10 min) and lately to 293 nm (at t=30 min), similarly to what is observed with BSA. The broad band observed at the initial time in the 350-400 nm region slightly decreases in intensity but a local maximum is observed at 387 nm (Fig. 30B) after 10 min. Contrary to what was observed with BSA a stable adduct is not achieved, but a slower decay in absorbance is observed (Fig. 30D). The time evolution spectrum of **4** alone is slightly different when followed at 300 μM or 500 μM, giving different absorption profiles in the 300 nm region. Since a new spectrum is obtained after 10 min, with new maxima located at different wavelengths (and higher absorbance values) this suggests different decomposition profiles, dependent on the formation of some intermediates, and therefore, possibly concentration-dependent. Interaction with h-Tf clearly interferes with the decomposition profile of **4**, however, the data doesn't suggest any kind of covalent interaction between the protein and the complex.

4.3 Discussion

The incubation of CO-RMs with BSA revealed a tendency of interaction between the carrier protein and the complexes.

Complexes **1** and **4** were already previously characterized as spontaneous CO releasers due to their low stability in aerobic aqueous solutions. The time evolution of the UV-VIS absorbance spectra of these species in PBS7.4 showed that the complexes decompose rapidly and in the case of **4** giving intermediate species with different absorption maxima. Moreover, the decomposition profile of **4** is concentration dependent as different concentrations lead to different absorbance peaks. Addition of BSA in a 1:20 (protein:complex) ratio leads to the formation of a new species highly stable up to 4h with both compounds. The new protein-associated complexes are clearly observed in the CD spectra recorded. Incubation of **1** with BSA afforded very intense circular dichroic changes in the

350 to 550 nm region owed to the binding of metal complexes to the protein. The same behavior is observed with **4** in the 360 to 800 nm region showing effective binding between protein and metal complex. Interestingly, these two complexes also share another common feature, which is the lack of interaction of aged solutions with BSA. The binding is only observed when the fresh compound is added to BSA and if the compound is left in solution for 2h (in the case of **1**) or 80 min (in the case of **4**) no interactions are observed at low complex:protein ratios. This data shows that BSA is an effective carrier of these two compounds and the integrity of the protein-metal complex adduct is maintained for a large period of time, therefore increasing their half-life in circulation. On the other hand, when the compound decomposes, the metabolites are no longer transported by BSA since no evidence of association was found with aged solutions.

Incubation with h-Tf gave different interaction profiles. **1** does not interact with h-Tf, in the several protein:complex ratios tested (ranging from 1:1 to 1:20), not even after 24h incubation. However, binding to h-Tf is not as fast as it is observed with BSA and since the complex is not stable in PBS solution it is possible that a larger period of time would be needed for some binding to occur but after which no more compound is present in solution. The decomposition of the complex was clearly observed due to a high degree of turbidity in solution.

With **4** no binding to h-Tf is observed and only minor changes in the CD spectrum are observed. With 1:7.5 and 1:10 ratios a small interaction is observed between the metal complex and the protein and this interaction may induce some changes in the secondary structure of the protein. This explains why in the far UV region, a clear difference is observed between the native protein and the complex adducts. These differences are immediate after incubation with protein and the induced CD signal is maintained after 4h.

It is known that binding does not specifically occur at the C- and N-lobe iron-binding cleft of the protein, but can also occur at histidine residues on the surface of the protein. Binding to the binding site is usually accompanied with major changes since the protein can balance between two configurations, open and

closed.[52] Binding of metal ions to the phenolic groups of the tyrosine residues in the specific metal binding sites of apo-Tf leads to the production of two new absorption bands centered at ca. 240 nm and ca. 295 nm in the UV-difference spectra. When metals bind to Tf usually intense tyrosinate–to-metal charge transfer bands (LMCT) are observed in the visible region (400-500 cm^{-1}) which could originate CD signal in the visible range. Therefore, the results obtained with **4** may be due to surface binding instead of specifically to the binding site.

The h-Tf binding cleft is designed to accommodate Fe^{3+} atoms which have an ionic radius of 0.65 Å[53] and previous studies[54] suggest that neither N- nor C-lobe are able to accommodate metals with radii larger than 0.95 Å. The strength of the metal binding strongly depends on the metal[55] so in the present case both compounds would require total CO depletion, ligand dissociation and oxidation in order to coordinate the metal ion in the binding cleft and with the residues in the vicinity.

Compound **2** is a completely different complex from the two discussed above. It is very stable in aqueous solution, as reflected by the absence of changes in the UV-VIS spectra observed over 4h (Fig. 12). Incubation with BSA does not produce any differences in the absorption spectrum, but since it has very weak absorbance bands these differences would hardly be noted unless a totally different association complex would be formed. This clearly isn't the case as the CD spectra reinforce the idea of a very weak interaction between the complex and BSA. A consistent signal variation is observed in the far UV region, probably arising from some weak interaction with the complex, since a strong binding is clearly not present.

Incubation with h-Tf didn't afford any type of association between both species. The CD spectra recorded do not detect any kind of interaction between the metal complex and the protein not even after 24h. Apart from the natural low affinity of h-Tf for Mo complexes also the piano stool geometry may account for some steric hindrance. As already explained, the approach to the binding cavity of the protein requires labile ligands that allow an easy exchange or hydrolysis and with **2** the

hydrolysis or ligand substitution doesn't occur as confirmed by the CO release rate and UV-VIS spectrum in PBS7.4. The amide functionality and Cp ring may still be responsible for some electrostatic interactions between the compound and some residues in the protein, but not a strong binding.

Compound **3** showed a distinct interaction with both proteins. With BSA only minor interactions were observed probably due to some surface reactivity and not effective binding. Incubation with h-Tf gave different results with a clear binding being observed. The changes in the CD spectra are only observed after 24h showing that the reaction between both species is not immediate. The changes observed in the CD spectra show the increase of intensity of the aromatic residues but in the far UV region no changes are observed suggesting that the protein secondary structure is not altered upon metal binding.

A possible explanation for the fact that binding only occurs after 24h incubation may lie on a possible conversion or decomposition of the initial compound. **3** is a Ru(II) species but oxidation may lead to Ru(III) species which like Fe(III) have high affinity for phenolate ligands[56] which are involved in the Tyr residues of transferrin-binding site.[57] Ru(III) ions are relatively hard and therefore have high attraction for halides and anionic oxygen ligands, all of which are retained for fairly long periods. Conversely, Ru(II) ions are relatively soft and have little affinity for these ligands so it is not surprising that binding activity could only be observed after 24h, increasing the affinity for this plasma protein. However, at this stage, this is only a speculative interpretation, as we don't have any experimental evidence to support this possibility.

As stated in the beginning of the Chapter, the compounds studied were selected because each of them possesses a set of properties that exemplify several families of compounds which actually produced therapeutically positive results *in vivo*.

2 is the prototype of a large family of very stable organometallic carbonyl compounds, activated by oxidation or light, with a Cp ring as ligand in a piano stool geometry around a Mo(II) metal center. One can extrapolate that $CpM(CO)_xL$ compounds behave similarly and will be poorly transported by

albumin in blood. Interaction with h-Tf doesn't occur either. Therefore other specific receptor-mediated transport mechanisms to tissues are required for CO to reach the targets if these compounds are to be actively transported as CO-RMs.

1 and **4** are Mo(0) compounds that liberate CO at high rates but have different coordination spheres. With 5 and 3 carbonyl groups *per* molecule, respectively, **1** and **4** are negatively charged, have hard labile ligands (bromide or citrate) but interestingly behave similarly in albumin binding. In both cases the labile ligands are most probably removed and a protein-metal complex adduct is formed. Contrary to substitutionally inert **2** there is evidence of strong binding which is most likely made possible by the lability of the ligands. With h-Tf no interaction was observed. Indeed, a low valent metal complex is not fit to coordinate the h-Tf binding site. Higher oxidation products of Mo are likely to have Mo=O bonds and will have small negative charges inappropriate to bind a site designed for hard Fe(III) cations.

Compound **3** shows a very weak interaction with albumin which indicates that the compound circulates with a low degree of association with this carrier. Several studies[58, 59] have shown that albumin can specifically bind Ru(III) complexes like $HInd[RuInd_2Cl_4]$ (Ind=indazole) or $Na[RuImCl_4Me_2SO]$ (Im=Imidazole). Initial results suggested that the kinetics of association is very slow and takes several hours to obtain the final adducts. However, a very recent study showed that $Na[RuImCl_4Me_2SO]$ (NAMI-A) reacts very fast with BSA with total replacement of the coordination sphere of Ru(III) by albumin based ligands! The most interesting fact is that this binding of the Ru(III) to albumin is responsible for the biological anti-metastic activity formerly attributed to the precursor complex NAMI-A.[60]

The transferrins are primarily iron binding proteins but in serum only about 30% is saturated with iron, leaving a high potential to other metal ions in circulation. Given the similarities between Ruthenium and Iron it was expected that this compound could actually bind transferrin. The data collected shows that it's

plausible to think that delivery of ruthenium complexes similar to **3** to cells may be mediated by transferrin receptors.[29, 61, 62]

Furthermore, the results obtained from the incubation of compounds **1** and **4** with BSA suggest an extrapolation to what has been observed both *in vivo* and *in vitro* in blood.

The data presented in Chapter IV showed that compound **1** undergoes a steady and continuous liberation of CO in blood while compound **4** readily liberates 1 CO to Hb and doesn't increase CO-Hb levels over the next 30 min. From Fig. 5D one can see that **1** has a slow and continuous decay over time since is stabilized by the carrier protein. On the other hand, **4** shows a very rapid decay in Abs during the first 10 min with the formation of a new species which then shows a highly stable profile over time (Fig. 17B). Although only CO release experiments performed under the same conditions could explain if the adducts formed promote or prevent CO release, all the spectroscopic data suggests that CO-RM-protein association could be responsible for the profile observed in blood.

5. Final Remarks and Conclusion

The distribution of a drug through the bloodstream following its administration is largely dependent on plasma protein binding which conditions the pharmacological profile of the drug, the dosing regimen and even the clearance process. Only unbound drug is able to permeate the blood vessels and enter the tissues.

In the case of CO-RMs, where the active drug is in fact CO, this association may accelerate the release of the active principle, which is then trapped by hemoglobin losing its therapeutic effect and increasing toxicity. Understanding the nature of these associations is therefore relevant for the design of better CO-RMs, in order to either prevent destructive interaction with these carriers or conversely to make stable adducts that interact without decomposition and enhance the stability of the CO-RM in circulation and its half-life *in vivo*. The few compounds studied

provided different examples of behaviors that may be helpful for the design of future molecules.

6. References

1. Taille, C., El-Benna, J., Lanone, S., Boczkowski, J., Motterlini, R., *J. Biol. Chem.* **2005**, 280, 25350.
2. Suliman, H.B., Carraway, M.S., Tatro, L.G., Piantadosi, C.A., *J. Cell Sci.* **2007**, 120, 299.
3. Sandouka, A., Balogun, E., Foresti, R., Mann, B.E., Johnson, T.R., Tayem, Y., Green, C.J., Fuller, B., Motterlini, R., *Cell. Mol. Biol.* **2005**, 51, 425.
4. Sandouka, A., Fuller, B.J., Mann, B.E., Green, C.J., Foresti, R., Motterlini, R., *Kidney international* **2006**, 69, 239.
5. Kim, H.P., Ryter, S.W., Choi, A.M.K., *Annu. Rev. Pharmacol. Toxicol.* **2006**, 46, 411.
6. Morse, D., Pischke, S.E., Zhou, Z.H., Davis, R.J., Flavell, R.A., Loop, T., Otterbein, S.L., Otterbein, L.E., Choi, A.M.K., *J. Biol. Chem.* **2003**, 278, 36993.
7. Sampath, V., Zhao, X.J., Caughey, W.S., *J. Biol. Chem.* **2001**, 276, 13635.
8. Kober, A., Sjoholm, I., *Mol. Pharmacol.* **1980**, 18, 421.
9. Kragh-Hansen, U., *Pharmacol. Rev.* **1981**, 33, 17.
10. Fehske, K.J., Muller, W.E., Wollert, U., *Biochem. Pharmacol.* **1981**, 30, 687.
11. Theodore Peters, J., *All About Albumin: Biochemistry, Genetics, and Medical Applications* Elsevier Science & Technology Books, San Diego, **1996**.
12. Zhang, Y., Wilcox, D.E., *J. Biol. Inorg. Chem.* **2002**, 7, 327.
13. Zlotos, G., Bucker, A., Jurgens, J., Holzgrabe, U., *Int. J. Pharm.* **1998**, 169, 229.
14. Seedher, N., Singh, B., Singh, P., *Indian J. Pharm. Sci.* **1999**, 61, 143.
15. Borga, O., Borga, B., *J. Pharmacokinet. Biopharm.* **1997**, 25, 63.
16. Rieutord, A., Bourget, P., Troche, G., Zazzo, J.F., *Int. J. Pharm.* **1995**, 119, 57.
17. Harris, W.R., Pecoraro, V.L., *Biochemistry* **1983**, 22, 292.
18. Chitambar, C.R., Massey, E.J., Seligman, P.A., *J. Clin. Invest.* **1983**, 72, 1314.
19. Winsper, S.J., Armstrong, R.A., Hodgkins, P.S., Blair, J.A., *Neuroreport* **1997**, 8, 709.
20. Clausen, J., Edeling, C.J., Fogh, J., *Cancer Res.* **1974**, 34, 1931.
21. Harris, W.R., Chen, Y., Wein, K., *Inorg. Chem.* **1994**, 33, 4991.
22. Battistuzzi, G., Calzolai, L., Messori, L., Sola, M., *Biochem. Biophys. Res. Commun.* **1995**, 206, 161.
23. Fernandes, K.G., Montes-Bayon, M., Gonzalez, E.B., Del Castillo-Busto, E., Nobrega, J.A., Sanz-Medel, A., *J. Anal. At. Spectrom.* **2005**, 20, 210.
24. Harris, W.R., Sheldon, J., *Inorg. Chem.* **1990**, 29, 119.
25. Tang, S., Maccoll, R., Parsons, P.J., *J. Inorg. Biochem.* **1995**, 60, 175.
26. Li, H., Sadler, P.J., Sun, H., *J. Biol. Chem.* **1996**, 271, 9483.
27. Zhang, M.X., Gumerov, D.R., Kaltashov, I.A., Mason, A.B., *J. Am. Soc. Mass Spectrom.* **2004**, 15, 1658.
28. Kratz, F., Hartmann, M., Keppler, B., Messori, L., *J. Biol. Chem.* **1994**, 269, 2581.

29. Pongratz, M., Schluga, P., Jakupec, M.A., Arion, V.B., Hartinger, C.G., Allmaier, G., Keppler, B.K., *J. Anal. At. Spectrom.* **2004**, 19, 46.
30. Guo, M.L., Sun, H.Z., McArdle, H.J., Gambling, L., Sadler, P.J., *Biochemistry* **2000**, 39, 10023.
31. Salmain, M., Licandro, E., Baldoli, C., Maiorana, S., Tran-Huy, H., Jaouen, G., *J. Organomet. Chem*. **2001**, 617, 376.
32. Hromadova, M., Salmain, M., Sokolova, R., Pospisil, L., Jaouen, G., *J. Organomet. Chem.* **2003**, 668, 17.
33. Zsila, F., Bikadi, Z., Fitos, I., Simonyi, M., *Curr. Drug Discov. Technol.* **2004**, 1, 133.
34. Chen, Y.H., Yang, J.T., Chau, K.H., *Biochemistry* **1974**, 13, 3350.
35. Bychkova, V.E., Berni, R., Rossi, G.L., Kutyshenko, V.P., Ptitsyn, O.B., *Biochemistry* **1992**, 31, 7566.
36. Rezaei Tavirani, M., Moosavi-Movahedi, A.A., Moosavi-Nejad, S.Z., Chamani, J., Ajloo, D., *Thermochim. Acta* **2003**, 408, 9.
37. Carter, D.C., Ho, J.X., *Adv. Protein Chem*. **1994**, 45, 153.
38. He, X.M., Carter, D.C., *Nature* **1992**, 358, 209.
39. Sudlow, G., Birkett, D.J., Wade, D.N., *Mol. Pharmacol.* **1976**, 12, 1052.
40. Soltys, B.J., Hsia, J.C., *J. Biol. Chem*. **1978**, 253, 3023.
41. Sadler, P.J., Viles, J.H., *Inorg. Chem*. **1996**, 35, 4490.
42. Taylor, R.T., Hanna, M.L., *Arch. Biochem. Biophys*. **1970**, 141, 247.
43. Andrade, S.M., Costa, S.M.B., Borst, J.W., van Hoek, A., Visser, A.J.W.G., *J. Fluorescence* **2008**, 18, 601.
44. Harris, D.C., Aisen, P. in *Iron Carriers and Iron Proteins*.in VCH, New York, **1989**; p 239.
45. Jeltsch, J.M., Chambon, P., *Eur. J. Biochem.* **1982**, 122, 291.
46. Williams, J., Elleman, T.C., Kingston, I.B., Wilkins, A.G., Kuhn, K.A., *Eur. J. Biochem.* **1982**, 122, 297.
47. Baggiolini, M., De Duve, C., Masson, P.L., Heremans, J.F., *J. Exp. Med.* **1970**, 131, 559.
48. Legrand, D., Mazurier, J., Metzboutigue, M.H., Jolles, J., Jolles, P., Montreuil, J., Spik, G., *Biochim. Biophys. Acta* **1984**, 787, 90.
49. MetzBoutigue, M.-H., Jolles, J., Mazurier, J., Schoentgen, F., Legrand, D., Spik, G., Montreuil, J., Jolles, P., *Eur. J. Biochem.* **1984**, 145, 659.
50. Sun, H.Z., Li, H.Y., Sadler, P.J., *Chem. Rev.* **1999**, 99, 2817.
51. Zhang, W.Q., Atkin, A.J., Thatcher, R.J., Whitwood, A.C., Fairlamb, I.J.S., Lynam, J.M., *Dalton Trans.* **2009**, 4351.
52. Baker, H.M., Anderson, B.F., Baker, E.N., *Proc. Natl. Acad. Sci. U. S. A.* **2003**, 100, 3579.
53. Shannon, R.D., *Acta Cristallogr., Sect. A* **1976**, 32, 751.
54. Harris, W.R., Yang, B., Abdollahi, S., Hamada, Y., *J Inorg Biochem* **1999**, 76, 231.
55. Li, H., Sadler, P.J., Sun, H., *Eur. J. Biochem.* **1996**, 242, 387.
56. Pell, S.D., Salmonsen, R.B., Abelleira, A., Clarke, M.J., *Inorg. Chem.* **1984**, 23, 385.
57. Que, L., *Coord. Chem. Rev.* **1983**, 50, 73.
58. Trynda-Lemiesz, L., Karaczyn, A., Keppler, B.K., Kozlowski, H., *J. Inorg. Biochem.* **2000**, 78, 341.
59. Messori, L., Orioli, P., Vullo, D., Alessio, E., Iengo, E., *Eur. J. Biochem*. **2000**, 267, 1206.

60. Liu, M.M., Lim, Z.J., Gwee, Y.Y., Levina, A., Lay, P.A., *Angew. Chem. Int. Edit.* **2010**, 49, 1661.
61. Qian, Z.M., Li, H.Y., Sun, H.Z., Ho, K., *Pharmacol. Rev.* **2002**, 54, 561.
62. Li, H., Sun, H., Qian, Z.M., *Trends Pharmacol. Sci.* **2002**, 23, 206.

7. Acknowledgments

Dr. Isabel Tomaz and Dr. Isabel Correia are acknowledged for their help performing the CD experiments.

Prof. João Costa Pessoa and Dr. Isabel Tomaz are also acknowledged for their help in the interpretation of the results and fruitful suggestions and discussions.

Chapter VII: Conclusions and Prospects

The main purpose of the work presented in this Thesis was the ***development of CO-releasing molecules for the treatment of inflammatory diseases***. In this quest, a large variety of molecules, with different metals, number of carbonyl groups and co-ligands were studied for the first time in aqueous environments. A large number of existing metal carbonyl complexes could eventually be used as CO-RMs, however, very few (if any) exhibit pharmacological profiles that allowed them to be developed as drugs. In this sense, the thorough study presented in Chapter II set the basis for a better understanding of which families of compounds could possibly be used for further drug development and elicited the viability of using MCCs to deliver CO in biological media. Furthermore, it also demonstrated the effect of different biological relevant parameters such as pH or pO_2.

Although this first screening did not intent to draw any structure-activity relationships it allowed the determinations of a structure-properties relationships, helping to understand the main molecular properties that contribute to the profile of CO release of MCCs. Indeed, the fastest and more extensive CO releasers were identified among the Mo^0 octahedral derivatives $[Mo^0(CO)_3L_3]^{0/z-}$ bearing hard donor ligands mainly those of biological relevance, e.g. amines, carboxylates, aminoacids. From these, CO release can be regulated *via* appropriate π-acceptor ligands. On the contrary, cyclopentadienyl complexes of Mo^{II}, Fe^{II}, Ru^{II} and Mn^{I} are very weak CO releasers.

A different profile is exhibited by the $Mn^{I}(CO)_5L$ and $Mn^{I}(CO)_4L_2$ complexes which lose CO dissociatively to form stable, inert $[Mn(CO)_3X_3]^+$ products. A totally unexpected behavior was observed with $[Ru^{II}(CO)_3L_3]$ complexes that do not release CO to the headspace of their aqueous solutions.

One of the main advantages of using CO-RMs over CO inhalation is the possibility of delivering CO locally to the diseased tissues, without loading hemoglobin with CO. In pathophysiological scenarios some of the injury

mediators expressed may become advantageous in order to promote an increased CO delivery. In Chapter III, an extensive study was presented where it was shown that in the presence of oxidants such as H_2O_2 or TBHP, the CO release rate is accelerated. The nature of the gases evolved from the oxidation of these carbonyl complexes was undoubtedly established, contrary to most of the studies reported in the literature concerning oxidation of metal carbonyls and where the nature of the gases evolved is missing or is contradictory. In the studies presented, it was shown that very few compounds resist oxidation under the standard conditions and proved that this could be an advantageous strategy to increase the amount of CO released to inflamed tissues, where large amounts of ROS are present.

The exceptions were the derivatives of $Mn^{I}(CO)_3$ and $Ru^{II}(CO)_3$ that do not respond to the ROS used since the former do not react whereas the latter rapidly decompose the ROS reagent to release O_2 and/or induce strong catalytic oxidation with formation of CO_2.

It was observed that most MCCs tested react preferentially with one of the two ROS used depending on their ancillary ligands and oxidation state. The $CpFe(CO)_2X$ complexes do not react with TBHP and react with H_2O_2 to produce more CO_2 than CO ($CO:CO_2 < 1$); a weak catalytic oxidation activity is observed in these systems contrary to those of Mn and Mo where $CO:CO_2$ is usually > 2.

In summary, the main goal was to evaluate the possibility of using the naturally occurring oxidizing ROS as a means of inducing or triggering release of CO from MCCs at the places of inflammation or oxidative stress and it it was demonstrated that it is a viable possibility.

In Chapter IV, the CO release rate of MCCs was evaluated using a different method, spectrophotometric measurement of CO-Mb formation. This method has some *pros* and *cons* when compared with the gas chromatography measurements performed in Chapter II, however, it allowed the identification of a new feature, only detected in this assay – *CO donation*. This is a specific property of the $Ru^{II}(CO)_3$ complexes, which do not liberate CO to the headspace of aqueous solutions as observed in Chapter V, but are able to transfer CO directly to the

heme center of Mb. This unique property of this family of compounds may be responsible for their pharmacological activity, which has been observed in several different models of disease. Among other factors, this lead us to develop a series of $Ru(CO)_3Cl_2L$ complexes, which were studied and evaluated for their capacity to release CO and become useful drugs (Chapter V). Furthermore, some ruthenium carbonyls exhibited the capacity to decompose H_2O_2, liberating O_2. The catalytic decomposition of H_2O_2 by these compounds was also evaluated and found to be very weak, when compared with other existing peroxide scavengers.

Another study presented in Chapter IV, shows the CO release profile of different compounds in blood. The most striking feature is that most of the compounds tested showed a very rapid (in some cases almost instantaneous and quantitative!) CO release burst. Indeed, blood is somehow different from the biological relevant medium used for the assays presented in Chapter II and strongly labilizes the compounds with amino or hydroxyl ligands in Mo(0) carbonyl complexes. Possibly in a medium rich in proteins the amine ligands of the complex exchange with amines from proteins and during these rapid exchanges, more thermodynamically labile complexes may form, or oxidation may happen leading to CO release.

The interaction between some model complexes and the plasma proteins Albumin and Transferrin is presented in Chapter VI. The interaction between drugs and plasma proteins is one fundamental aspect ruling pharmacological activity so some Circular Dichroism and UV-VIS absorbance spectroscopy studies were undertaken to study this interaction. It was demonstrated that some compounds could easily bind to Albumin in a small period of time while others with strong or labile ligands showed a minor degree of interaction. With Transferrin, only a ruthenium complex (CORM-3) showed some degree of interaction after 24h. Binding of MCCs to these proteins is therefore difficult to predict at this stage.

Taken altogether, the studies presented in this Thesis showed undoubtedly the potential of MCCs to be used as CO-RMs. Their modulation through different substitution degrees and the use of diverse ancillary ligands, strongly influences their ability to release CO. This versatility gives to CO-RMs the possibility of being used in different pathological scenarios, where the need for CO varies according with the disease.

Understanding the chemical behavior of these molecules under biological conditions allowed the development of new compounds, with improved pharmacological profiles.

Given the high number of unmet needs in Medicine, hopefully, in a near future these molecules may be used as drugs for the treatment of diseases which haven't been addressed so far.

ANNEX I

Table A1: List of MCCs synthesized and evaluated for CO release in RPMI (10%FBS) under CO_2 free reconstituted air, at 37ºC and in the dark.

Formula	Structure	Reference
$Mn_2(CO)_{10}$	Commercial	
$CpMn(CO)_3$		
$Mo(CO)_6$		
$Cr(CO)_6$		
$Fe_2(CO)_9$		
$[Ru(CO)_3Cl_2]_2$		
$CpRu(CO)_2I$		
$Mn(CO)_5Br$@TRIMEB	Prepared in the group of Prof. Isabel S. Gonçalves in Universidade de Aveiro, Portugal. The "free" complexes were prepared as stated next.	
$[Et_4N][Mo(CO)_5Br]$@TRIMEB		
$CpMo(CO)_3Cl$@TRIMEB		
$(\eta^5\text{-}C_5H_4COOMe)Mo(CO)_3Cl$@TRIMEB		
$CpMo(CO)_3Cl$@TRIMEB		
$CpFe(CO)_2Cl$@TRIMEB		
$CpFe(CO)_2Cl$@β-CD		
$Mn(CO)_5CH_3$	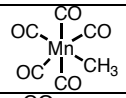	[1]
$Mn(CO)_5CH_2CONH_2$	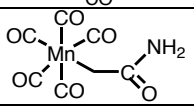	[2]
$Mn(CO)_5OSO_2CF_3$	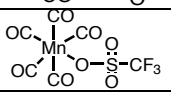	[3]
$Mn(CO)_5Cl$	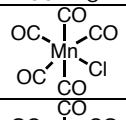	[4]
$Mn(CO)_5Br$	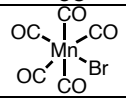	[4]
$[Et_4N][Mn(CO)_4Br_2]$	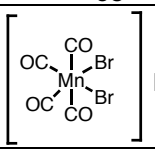	[5]
$Mn(CO)_4S_2CPh$	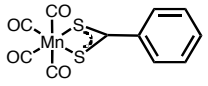	Provided by Prof. Brian Mann from hemoCORM
$[Mn(CO)_3(TACN)]Br$	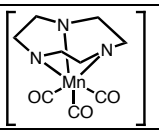	[6]
$[Et_4N][Mn_2(CO)_6Br_3]$	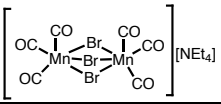	[7]

$Mo(CO)_5PTA$	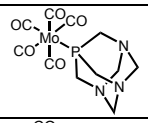	[8] AIP
$Mo(CO)_5PTA.HCl$	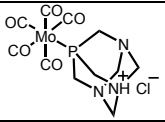	AIP
$Mo(CO)_5P(4\text{-}SO_3Na\text{-}C_6H_4)_3$	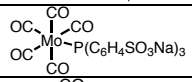	[9]
$Mo(CO)_5P(CH_2OH)_3$	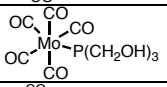	AIP
$Mo(CO)_5P(CH_2CH_2CH_2OH)_3$	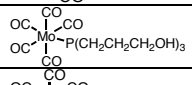	AIP
$Mo(CO)_5P(CH_2CH_2COOH)_3$	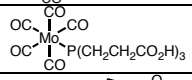	AIP
$Mo(CO)_5(HN(CH_2CH_2)_2O)$	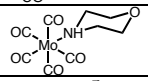	AIP
$[Bu_4N][Mo(CO)_5I]$	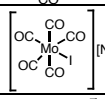	[10, 11]
$[Et_4N][Mo(CO)_5I]$	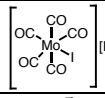	[10, 11]
$[Na(15\text{-crown-5-ether})][Mo(CO)_5I]$	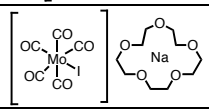	AIP
$[Na(diglyme)_2][Mo(CO)_5I]$	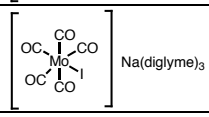	AIP
$[K(diglyme)_3][Mo(CO)_5I]$	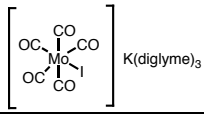	[10]
$[NH_4(diglyme)_3][Mo(CO)_5I]$	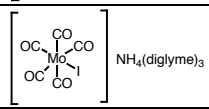	AIP
$[Ca_{1/2}(diglyme)_2][Mo(CO)_5I]$	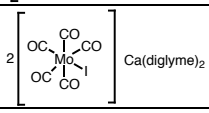	AIP
$[Mg_{1/2}(diglyme)_2][Mo(CO)_5I]$	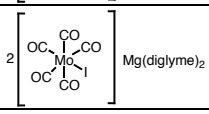	AIP

$[Et_4N][Mo(CO)_5Br]$	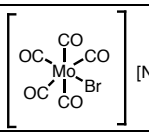	[10, 11]
$[Na][Mo(CO)_5CN]$	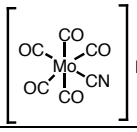	[12]
$Mo(CO)_4(bipy)$	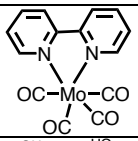	[13]
$Mo(CO)_4(4,4'\text{-}HOOC\text{-}bipy)$	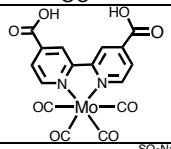	AIP
$Mo(CO)_4(4,4'\text{-}NaO_3SCH_2CH_2OOC\text{-}bipy)$	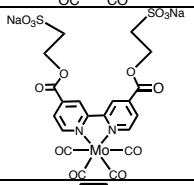	AIP
$Mo(CO)_4(Me\text{-}DAB)$	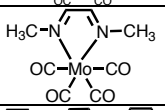	AIP
$Mo(CO)_4(p\text{-}tolil\text{-}DAB)$	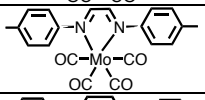	[14]
$Mo(CO)_4(Cy\text{-}DAB)$	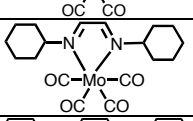	[14, 15]
$Mo(CO)_4(Me\text{-}pip\text{-}DAB)$	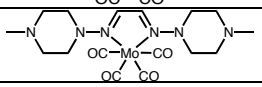	AIP
$Mo(CO)_4(3\text{-}COOH\text{-}py)_2$	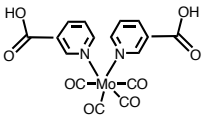	adapted from [16] see Chapter II Experimental Section
$Mo(CO)_4(Me\text{-}pip)_2$	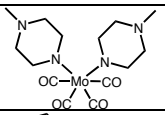	AIP
$Mo(CO)_4(morph)_2$	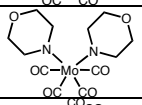	AIP
$Mo(CO)_4(PTA)_2$	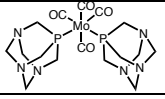	AIP

$Mo(CO)_4(PTA)_2.2HCl$	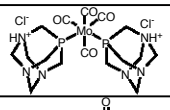	AIP
$Mo(CO)_4(DAPTA)_2$	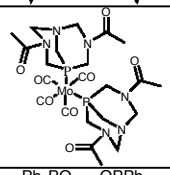	adapted from [17] see Chapter II Experimental Section
$Mo(CO)_4(OPPh_3)_2$	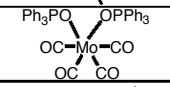	[18]
$[Me_4N]_2[(Mo(CO)_4(SPh)_2]$	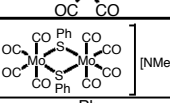	[19]
$[(Mo(CO)_4(SPh)_2]$	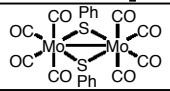	[19]
$[Et_4N][(Mo(CO)_4(Me\text{-}acac)]$	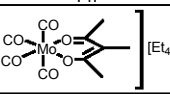	AIP
$[Et_4N][(Mo(CO)_4(glycinate)]$	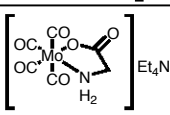	adapted from [20] AIP
$Mo(CO)_3(TACN)$	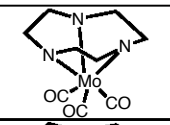	[21]
$Mo(CO)_3(TTCN)$	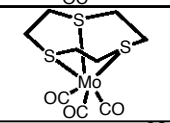	[22]
$Mo(CO)_3(bpa)$	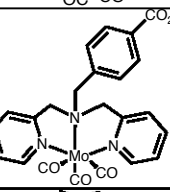	adapted from [23] see Chapter II Experimental Section
$Mo(CO)_3(PTA)_3$	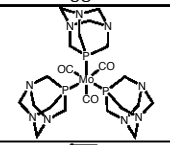	[24] AIP
$Mo(CO)_3(\eta^6\text{-}C_7H_8)$	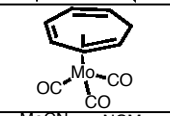	[25]
$Mo(CO)_3I_2(CH_3CN)_2$	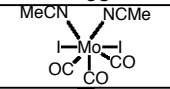	[26]
$Mo(CO)_3I_2(p\text{-tolil-DAB})$	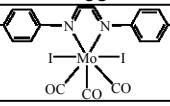	[27]

$Mo(CO)_3I_2$(Cy-DAB)	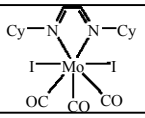	[27]
DAB ligands		[28, 29]
$CpMo(CO)_3I$	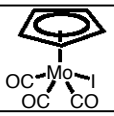	[30]
$CpMo(CO)_3Cl$	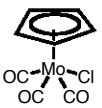	adapted from [30] using CCl_4 instead of $CHCl_3$.
$Cp^*Mo(CO)_3Cl$	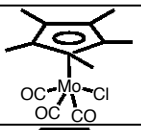	[31]
$CpMo(CO)_3CH_3$	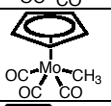	[32]
$CpMo(CO)_3CH_2CONH_2$	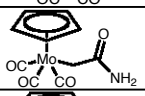	[2]
$CpMo(CO)_3CH_2COOH$	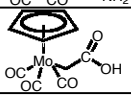	[2]
$CpMo(CO)_3CH_2CONHCH_2OH$	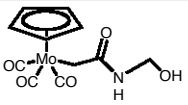	adapted from [33] AIP
$CpMo(CO)_3CH_2COOC(CH_3)_2Ph$	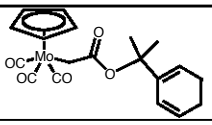	adapted from [33] AIP
$CpMo(CO)_3CH_2CONHCH_2COOCH_3$	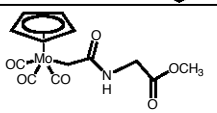	adapted from [33] AIP
$CpMo(CO)_3OC_8H_6OBF_2$	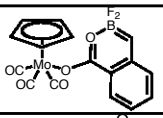	AIP
$(\eta^5\text{-}C_5H_4COOMe)Mo(CO)_3Cl$	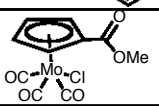	[34]
$(\eta^5\text{-}C_5Ph_4OH)Mo(CO)_3Cl$	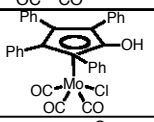	AIP
$(\eta^5\text{-}C_5H_4COOH)Mo(CO)_3I$	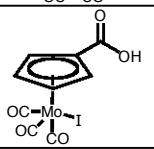	AIP

$(\eta^5\text{-}C_5H_4CH_2CH_3)Mo(CO)_3CH_3$	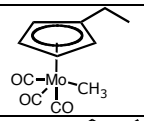	AIP
$(\eta^5\text{-}C_5H_4CH_2CH_2CH_3)Mo(CO)_3CH_3$	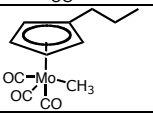	AIP
$(\eta^5\text{-}C_5H_4CH_2CH_2CH_2CH_3)Mo(CO)_3CH_3$	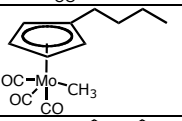	AIP
$(\eta^5\text{-}C_5H_4CH_2Ph)Mo(CO)_3CH_3$	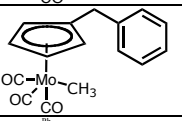	AIP
$[(\eta^5\text{-}C_5Ph_4O)Mo(CO)_3]_2$	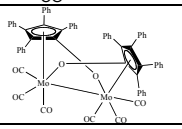	[35]
$[Na][Mo(CO)_3(hist)]$	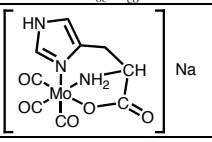	[36]
$[Et_4N][Mo(CO)_3(hist)]$	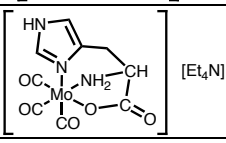	[36]
$[K][Mo(CO)_3(hist)]$	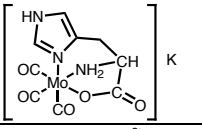	[36]
$[Et_4N]_3[Mo(CO)_3(cit)]$	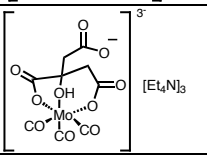	[37]
$[Na]_3[Mo(CO)_3(cit)]$	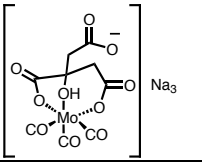	adapted from [37] see Chapter II Experimental Section
$[choline]_3[Mo(CO)_3(cit)]$	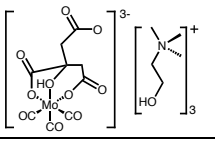	adapted from [37] see Chapter II Experimental Section

$[Na]_3[Mo(CO)_3(nita)]$	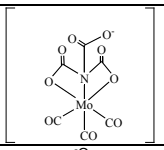	adapted from [37] see Chapter II Experimental Section
$[Et_4N]_3[Mo(CO)_3(nita)]$	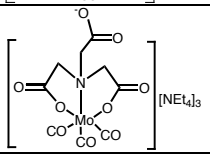	adapted from [37] see Chapter II Experimental Section
$[Na]_5[Mo(CO)_3(detpa)]$	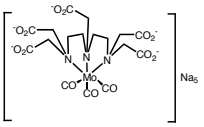	adapted from [37] see Chapter II Experimental Section
$Mo(CO)_2(S_2CNMe_2)_2$	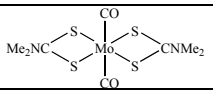	[38]
$Fe(CO)_4I_2$	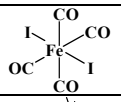	[39]
$(\eta^1\text{-}C_3H_5)Fe(CO)_3Br$	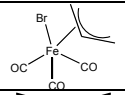	[40]
$Cp^*Fe(CO)_2Cl$	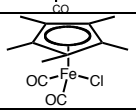	
$CpFe(CO)_2Cl$	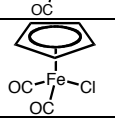	[41, 42]
$CpFe(CO)_2Br$	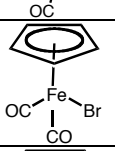	[41, 42]
$CpFe(CO)_2I$	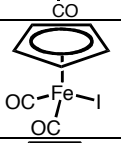	[42]
$CpFe(CO)_2CH_3$	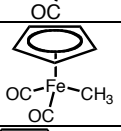	[43]
$CpFe(CO)_2CH_2Ph$	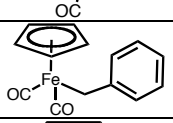	adapted from [43]
$CpFe(CO)_2(\eta^1\text{-}C_3H_5)$	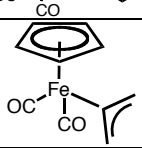	[44]

$CpFe(CO)_2CH_2CH_2CH_2Cl$	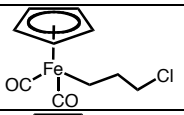	[45]
$CpFe(CO)_2CH_2CONH_2$	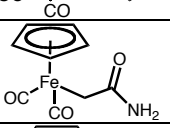	[2]
$CpFe(CO)_2CH_2COOH$	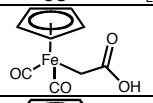	[2]
$CpFe(CO)_2COMe$	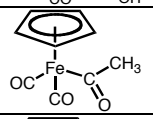	[46]
$CpFe(CO)_2COPh$	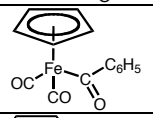	[47]
$CpFe(CO)_2(OCOC_6H_4OCOCH_3)$	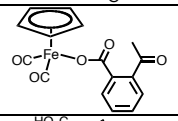	AIP
$Fe(CO)_2(cysteine)_2$	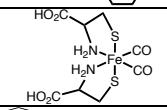	[48]
$CpFe(CO)_2OCOC_5H_4NFe(CO)_2Cp$	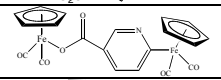	AIP
$[CpFe(CO)_2]_2$	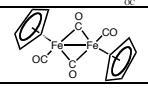	[49]
$Ru(CO)_3Cl(glycinate)$	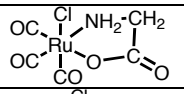	[50]
$Ru(CO)_3Cl_2(DMSO)$	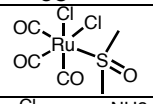	see Chapter V Experimental Section
$Ru(CO)_3Cl_2(methionine)$	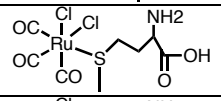	see Chapter V Experimental Section
$Ru(CO)_3Cl_2(methionine\ oxide)$	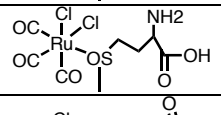	see Chapter V Experimental Section
$Ru(CO)_3Cl_2(DAPTA)$	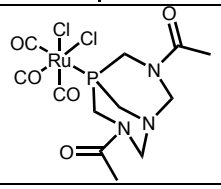	see Chapter V Experimental Section

$CpRu(CO)_2Cl$	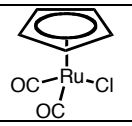	[51]
$[Co(CO)_3]_2(PhC{\equiv}CPh)$	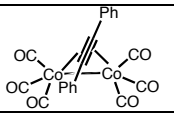	[52, 53]

AIP – ***A**lfama's **I**ntelectual **P**roperty* - Compounds prepared by other colleagues from Alfama's Chemistry Department and that are part of Alfama's portfolio of compounds.
The compounds labeled with AIP and references were prepared using a different procedure from the literature.

References:

1. *Synthetic Methods of Organometallic and Inorganic Chemistry,* (Eds.:W. A. Herrmann) Georg Thieme Verlag, New York, **1997**; Vol. 7, p 92.
2. Ariyaratne, J.K.P., Bierrum, A.M., Green, M.L.H., Ishaq, M., Prout, C.K., Swanwick, M.G., *J. Chem. Soc. A* **1969**, 1309.
3. Nitschke, J., Schmidt, S.P., Trogler, W.C., *Inorg. Chem.* **1985**, 24, 1972.
4. Abel, E.W., Wilkinson, G., *J. Chem. Soc.* **1959**, 1501.
5. Angelici, R.J., *Inorg. Chem.* **1964**, 3, 1099.
6. Pomp, C., Drueke, S., Kuppers, H.J., Wieghardt, K., Kruger, C., Nuber, B., Weiss, J., *Zeit. Naturforsch. B* **1988**, 43, 299.
7. Brisdon, B.J., Edwards, D.A., White, J.W., *J. Organomet. Chem.* **1978**, 161, 233.
8. Alyea, E.C., Fisher, K.J., Foo, S., Philip, B., *Polyhedron* **1993**, 12, 489.
9. Darensbourg, D.J., Bischoff, C.J., *Inorg. Chem.* **1993**, 32, 47.
10. Abel, E.W., Bennett, M.A., Wilkinson, G., *Chem. Ind.* **1960**, 442.
11. Abel, E.W., Reid, J.G., Butler, I.S., *J. Chem. Soc.* **1963**, 2068.
12. King, R.B., *Inorg. Chem.* **1967**, 6, 25.
13. Stiddard, M.H., *J. Chem. Soc.* **1962**, 4712.
14. tom Dieck, H., Renk, I.W., *Chem. Ber.-Recl.* **1971**, 104, 110.
15. Bayer, E., Breitmai.E, Schurig, V., *Chem. Ber.-Recl.* **1968**, 101, 1594.
16. Baker, P.K., Jenkins, A.E., *Polyhedron* **1997**, 16, 2279.
17. Darensbourg, D.J., Kump, R.L., *Inorg. Chem.* **1978**, 17, 2680.
18. Bock, H., Dieck, H.T., *Z. Naturforsch., B.* **1966**, B 21, 739.
19. Smith, D.A., Zhuang, B., Newton, W.E., Mcdonald, J.W., Schultz, F.A., *Inorg. Chem.* **1987**, 26, 2524.
20. Darensbourg, D.J., Draper, J.D., Reibenspies, J.H., *Inorg. Chem.* **1997**, 36, 3648.
21. Chaudhuri, P., Wieghardt, K., Tsai, Y.H., Kruger, C., *Inorg. Chem.* **1984**, 23, 427.
22. Ashby, M.T., Lichtenberger, D.L., *Inorg. Chem.* **1985**, 24, 636.
23. van Staveren, D.R., Bothe, E., Weyhermuller, T., Metzler-Nolte, N., *Eur. J. Inorg. Chem.* **2002**, 1518.
24. Alyea, E.C., Ferguson, G., Kannan, S., *Polyhedron* **1997**, 16, 3533.
25. Abel, E.W., Bennett, M.A., Burton, R., Wilkinson, G., *J. Chem. Soc.* **1958**, 4559.
26. Baker, P.K., Fraser, S.G., Keys, E.M., *J. Organomet. Chem.* **1986**, 309, 319.
27. Baker, P.K., Barfield, J., Vankampen, M., *Inorg. Chim. Acta* **1989**, 156, 179.

28. Tomdieck, H., Renk, I.W., *Chem. Ber.-Recl.* **1971**, 104, 92.
29. Hsieh, A.T.T., West, B.O., *J. Organomet. Chem.* **1976**, 112, 285.
30. White, C., Mawby, R.J., *Inorg. Chim. Acta* **1970**, 4, 261.
31. Abrantes, M., Santos, A.M., Mink, J., Kuhn, F.E., Romao, C.C., *Organometallics* **2003**, 22, 2112.
32. Gladysz, J.A., Williams, G.M., Tam, W., Johnson, D.L., Parker, D.W., Selover, J.C., *Inorg. Chem.* **1979**, 18, 553.
33. Burkhardt, E.R., Doney, J.J., Bergman, R.G., Heathcock, C.H., *J. Am. Chem. Soc.* **1987**, 109, 2022.
34. Abrantes, M., Gago, S., Valente, A.A., Pillinger, M., Goncalves, I.S., Santos, T.M., Rocha, J., Romao, C.C., *Eur. J. Inorg. Chem.* **2004**, 4914.
35. Adams, H., Bailey, N.A., Hempstead, P.D., Morris, M.J., Riley, S., Beddoes, R.L., Cook, E.S., *J. Chem. Soc.-Dalton Trans.* **1993**, 91.
36. Beck, W., Petri, W., Meder, J., *J. Organomet. Chem.* **1980**, 191, 73.
37. Takuma, M., Ohki, Y., Tatsumi, K., *Organometallics* **2005**, 24, 1344.
38. Burgmayer, S.J.N., Templeton, J.L., *Inorg. Chem.* **1985**, 24, 2224.
39. *Synthetic Methods of Organometallic and Inorganic Chemistry,* (Eds.:W. A. Herrmann) Georg Thieme Verlag, New York, **1997**; Vol. 7, p 41.
40. Mocellin, E., Russell, R., Ravera, M., *J. Chem. Educ.* **1998**, 75, 773.
41. Dombek, B.D., Angelici, R.J., *Inorg. Chim. Acta* **1973**, 7, 345.
42. *Synthetic Methods of Organometallic and Inorganic Chemistry,* (Eds.:W. A. Herrmann) Georg Thieme Verlag, New York, **1996**; Vol. 8, p 107.
43. *Synthetic Methods of Organometallic and Inorganic Chemistry,* (Eds.:W. A. Herrmann) Georg Thieme Verlag, New York, **1997**; Vol. 7, p 119.
44. Green, M.L.H., Nagy, P.L.I., *J. Chem. Soc.* **1963**, 189.
45. Casey, C.P., Vosejpka, L.J.S., *Organometallics* **1992**, 11, 738.
46. King, R.B., *J. Am. Chem. Soc.* **1963**, 85, 1918.
47. Brookhart, M., Studabaker, W.B., Humphrey, M.B., Husk, G.R., *Organometallics* **1989**, 8, 132.
48. Schubert, M.P., *J. Am. Chem. Soc.* **1933**, 55, 4563.
49. Herrmann, Brauer, *Synthetic Methods of Organometallic and Inorganic Chemistry,* (Eds.:W. A. Herrmann) Georg Thieme Verlag, New York, **1996**; Vol. 1, p 137.
50. Clark, J.E., Naughton, P., Shurey, S., Green, C.J., Johnson, T.R., Mann, B.E., Foresti, R., Motterlini, R., *Circ. Res.* **2003**, 93, e2.
51. *Synthetic Methods of Organometallic and Inorganic Chemistry,* (Eds.:W. A. Herrmann) Georg Thieme Verlag, New York, **1996**; Vol. 8, p 110.
52. *Synthetic Methods of Organometallic and Inorganic Chemistry,* (Eds.:W. A. Herrmann) Georg Thieme Verlag, New York, **1997**; Vol. 7, p 255.
53. Greenfield, H., Sternberg, H.W., Friedel, R.A., Wotiz, J.H., Markby, R., Wender, I., *J. Am. Chem. Soc.* **1956**, 78, 120.